HYDRODYNAMIC STUDY OF GAS-LIQUID CO-CURRENT BUBBLE COLUMN REACTORS AT LOW SUPERFICIAL GAS VELOCITIES

Viran Pillay

University of KwaZulu-Natal: Howard College Campus

2005

Submitted in fulfillment of the academic requirements for the degree Master of Science in Chemical engineering. All the work presented in this dissertation is original unless otherwise stated and has not (in whole or part) been submitted previously to any tertiary institute as part of a degree.

As the candidate's supervisor, I approve this dissertation for submission

_____

Prof. D Ramjugernath

As the candidate's co-supervisor, I approve this dissertation for submission

_____

Prof. M Carsky

ABSTRACT

Sasol's Research and Development Division has identified several proprietary gas-liquid reactions where very low superficial gas velocities (< 0.8 cm/s) are required to obtain desired conversions in a bubble column reactor.

A review of existing literature has shown that research in bubble column reactors is typically conducted in the superficial gas velocity range of 1 – 40 cm/s. Traditionally bubble column reactors are designed via the application of empirical correlations which are only valid under specific conditions. There is a danger of under or over design if incorrect nonadjustable parameters such as liquid dispersion coefficients, mass transfer coefficients and gas hold-up values are used.

To this extent, a hydrodynamic study was undertaken at superficial gas velocities lower than 0.8 cm/s, to determine whether existing correlations are valid in this little investigated superficial gas velocity regime.

Three bubble column reactors were designed and set up to perform hydrodynamic studies:

- 22 cm inner diameter QVF glass column, 190 cm tall
- 30 cm inner diameter 304 stainless-steel column, 200 cm tall
- 30 cm inner diameter QVF glass column, 80 cm tall

All measurements were undertaken in an air/water system.

Gas hold-up measurements revealed that at the investigated gas flow rates, the gas hold-up was less than 1 % and as such was not investigated extensively.

Partition plates were installed into the bubble columns and residence time distribution measurements were undertaken. The bubble columns were found to behave identically to the well known tanks in series model (Levenspiel, 1962).

Liquid dispersion coefficients were measured via two methods. Batch liquid measurements were undertaken via the method of Ohki and Inoue (1970) and continuous liquid residence time distribution measurements were also undertaken. Data reduction was performed for both methods using the axial dispersion model to regress the liquid dispersion coefficient E_L. Both methods yielded equivalent results. The effect of distributor plate geometry on E_L was also investigated and proved not to affect E_L.

It was found that existing literature correlations developed at higher superficial gas velocities failed to accurately predict the measured dispersion coefficients obtained in this study.

Correlation of the E_L values with column diameter and superficial gas velocity showed E_L to be a weak function of diameter as compared to existing correlations. This will have a significant effect on scale-up to larger column diameters.

ACKNOWLEDGEMENTS

I wish to thank the following people for their contribution to my work:

- My supervisor, Professor Deresh Ramjugernath, for his commitment to both project and student alike.
- My co-supervisor, Professor Milan Carsky, for contributing his time and expertise at a late stage of this project. His input was most appreciated.
- My original co-supervisor, Doctor Randhir Rawatlal, for his enthusiasm and sharing of ideas.
- My colleague, Minal Soni, for providing drive and initiative to the project. More importantly the friendship he afforded me will never be forgotten.
- Doctor Craig McGregor from Sasol for providing valuable insight and perspective from an industrial point of view.
- The lecturing staff and technical staff at the School of Chemical Engineering for always accommodating and assisting in the various queries and tasks posed to them.
- Kumaran Naicker, for his invaluable assistance in developing the logging software.
- My family and friends for their support and encouragement.
- Sasol for financial assistance and affording me the opportunity to pursue a post-graduate degree.

TABLE OF CONTENTS

LIST OF FIGURES

LIST OF TABLES

NOMENCLATURE

Units are SI unless otherwise stated.

Letters

A	gas reactant component
a	interfacial area for mass transfer
a^*	interfacial area per unit volume at gas flow of 1 cm/s
B	liquid reactant component
Bo	dimensionless Bodenstein number
c	concentration profile response to tracer stimulus
C_0	batch reactor concentration at $t = \infty$
C_L	concentration at reactor exit
D_A	diffusivity of A in the liquid phase
D_B	mean bubble diameter
D_c	column diameter
d_h	hole diameter for distributor plates
D_m	molecular diffusion coefficient
E	exit age distribution
E_d	energy dissipated in liquid motion
E_i	energy input into column due to gas dispersion
E_L	lumped liquid dispersion coefficient
f	perforated area of distributor plate
Fr	dimensionless Froude number
g	gravitational constant
Ha	dimensionless Hatta number
H_D	dispersion height
H_L	clear liquid height
I	reverse flow from stage i to i-1
I	index of fitting parameter for curve fitting regression
k_2	second order reaction constant
k_L	liquid mass transfer coefficient
k_r	first order reaction rate constant
L	dispersion height

M	mass of tracer input into system
N	number of stages in cascaded bubble column
N_{ch}	dimensionless chamber volume
Pe_L	liquid Peclet number
Pe_{Lm}	modified liquid Peclet number
P_T	pressure at top of column
Q	liquid volumetric flow-rate
r_d	rate of energy dissipation of small eddies in turbulent flow
t	distributor plate thickness
t	elapsed time for RTD experiment
t_{inj}	time taken to complete tracer injection for RTD experiments
u_b	rise velocity of a single bubble
u_g	superficial gas velocity
u_h	velocity of gas through hole of distributor plate
u_L	superficial liquid velocity
u_o	maximum liquid velocity at centre of column
u_r	relative velocity between gas and liquid phases
V	volume of vessel
V_{ch}	volume of gas chamber for gas distribution
V_G	volume of gas in reactor
V_L	volume of liquid in reactor
$V_L(0)$	centre-line liquid velocity
X	conversion of reactant

Greek symbols

α	ratio of hydrostatic head to pressure at top of column
β	liquid hold-up
δ	distance between injection point and measuring point
ϵ^*	average gas hold-up at a gas velocity of 1 cm/s
ϵ_g	average gas hold-up
ϵ_L	average liquid hold-up
η	length of smallest eddy scale in turbulent flow
θ	reduced time for RTD measurements
κ	electrical conductivity

λ	height filled with tracer
μ	mean value for a residence time distribution
μ_L	liquid viscosity
π	mixing time for batch liquid mixing experiments
ρ_g	gas density
ρ_L	liquid density
ρ_m	density of manometer fluid
σ	liquid surface tension
σ^2	variance of a distribution about its mean value
τ	mean residence time of fluid elements in reactor vessel
υ_L	liquid kinematic viscosity
v_b	mean velocity of rise of bubbles
v_c	circulation velocity of liquid
Ψ	change in electrical conductivity per degree rise in temperature
ω	area above batch mixing curve and line of homogeneous concentration

Abbreviations

ADM	axial dispersion model
BC1	22 cm diameter glass bubble column
BC2	30 cm diameter stainless steel bubble column
BC3	30 cm glass bubble column
CFD	computational fluid dynamics
CSTR	continuously stirred tank reactor
LDA	Laser Doppler Anemometry
PIV	Particle Image Velocimetry
RTD	residence time distribution

CHAPTER ONE

INTRODUCTION

In the field of chemical reactor engineering, the study of multi-phase sparged reactors is of prime interest to chemical engineers. Although there have been extensive modeling and experimental efforts focused on understanding the behaviour of these reactors, there has still been a slow development of fundamental theories for their behaviour due to the complex physical phenomena occurring in these reactors.

Complete and well defined reactor models are required for the prediction of the fluid mechanics of these reactors. These models are needed for reliable designing and scale-up of sparged reactors. Due to the slow development of fundamental theories for multi-phase reactors, the design of these reactors is currently an art rather than a science. This present "state of art" requires that model parameters be obtained from experimental data. This method of design requires accurate experimental data for confident and optimum design.

In general, the following parameters are required for design of multi-phase sparged reactors:

- hydrodynamics and flow regime
- phase hold-ups
- dispersion and back-mixing phenomena
- interfacial area, mass and heat transfer resistances
- residence time distribution data

Sasol's Research and Development division have identified several gas-liquid reactions which they would like to perform on an industrial scale. Some of these reactions involve the use of a homogeneous liquid catalyst. The problem that Sasol is faced with is that the reacting component in the liquid phase is present in trace quantities, and as they would like to perform their reactions with a stoichiometric quantity of gas, this results in very low quantities of gas being required to obtain target conversions.

Bubble column reactors are effective vessels for contacting gas-liquid systems. The gas is sparged into the reactor and the equipment falls into the family of multi-phase sparged reactors. Traditionally bubble column reactors are operated at high gas throughputs ($u_g > 5$ cm/s) to ensure that there is adequate mass transfer and effective heat transfer due to the well mixed nature of bubble columns. Sasol have conducted kinetic studies and mass transfer studies for their systems and found the reactions to be reaction rate limited. An extensive literature review has shown that there is a dearth in the literature on information for the hydrodynamic behaviour of bubble column reactors in the superficial gas velocity range of Sasol's interest ($u_g < 0.8$ cm/s).

At high gas throughputs it is easy to understand that the liquid phase will be well mixed, however at such low gas flow-rates the possibility of a deviation from normal bubble column behaviour could exist. There is also the danger that extrapolation of correlations developed with data for higher gas flow-rates could yield erroneous design parameters at much lower flow-rates.

Furthermore, there is limited knowledge on the behaviour of bubble column reactors in South Africa. Hence the purpose of this study was two-fold. Firstly to address the issue of the measurement of hydrodynamic parameters at superficial gas velocities less than 0.8 cm/s and secondly to develop a bubble column research group at the University of KwaZulu-Natal – Howard College Campus.

With the advent of Sasol moving from coal based technology to that of natural gas, there will be continual interest in the behaviour of gas-liquid systems and the equipment could be used for further research at the University of KwaZulu-Natal as more questions and problems concerning bubble column reactors arise.

This dissertation serves as an introductory study on the hydrodynamic behaviour of two-phase gas-liquid co-current bubble column reactors. The format of the dissertation diverts from the traditional one. The chapters are presented in a manner such that the reader is always provided with the pertinent information that is required for the subsequent chapters to become more meaningful. The chapters are ordered in a manner such that there is always a smooth transition from one topic to the next.

CHAPTER TWO

BUBBLE COLUMN REACTORS – AN OVERVIEW

This chapter will provide a brief description of bubble columns and their applications in industry. A bubble column reactor is a vertical vessel in which a gas is bubbled through either a moving liquid or in a batch liquid. Prior to 1980 very little research was conducted in bubble column reactors. Interest in bubble column reactors grew quickly with the revival in interest of coal liquefaction and slurry phase Fisher-Tropsch synthesis. Bubble column reactors have also found extensive use in biotechnological applications.

Bubble column reactors are favoured for the following reasons:

- very simple structure resulting in low cost
- lack of moving parts
- good heat and mass transfer properties
- high thermal stability (uniform temperature profile)
- low energy input (only gas compression)
- high circulation rate resulting in excellent mixing
- high liquid phase residence time

The disadvantages of bubble columns are:

- complicated hydrodynamic flow patterns
- uncertainties in scale-up
- short residence time of gas (determined by bubble rise velocity)
- volume demand increased due to back-mixing

2.1) Industrial applications of bubble columns

Bubble columns have found diverse applications in chemical industries. Table 2-1 gives a list of two-phase gas-liquid reactions carried out in bubble columns.

Table 2-1: Industrial scale reactions in gas-liquid systems (Deckwer, 1992)

Reaction	Main Product
Partial oxidation of ethylene	Acetaldehyde
Cumene oxidation	Cumene hydroperoxide
Chlorination of aliphatic and aromatic compounds	Chloroparaffin
Ethylation of benzene	Ethylbenzene
Hydroformulation of ethylene	Aldehydes and Alcohols
Hydrogenation reactions	

2.2) Modes and range of operation

Bubble columns may by operated without any internals or they may be staged, packed or operated as a loop reactor.

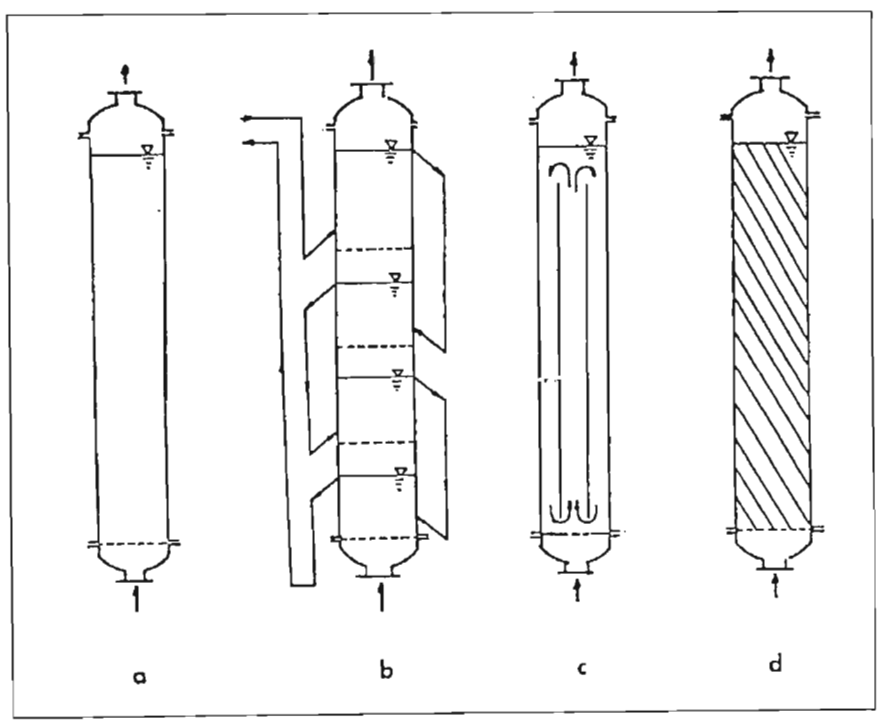

Figure 2-1: Types of gas-liquid bubble columns (Chen, 1986)

(a) simple (b) staged (c) loop-reactor (d) packed

The liquid phase has a much higher density than the gas phase, hence the liquid flow rate passing through a bubble column is low. The superficial gas velocity u_g based on empty reactor volume is typically in the range of 3-12 cm/s. The liquid and gas may be contacted in either a counter or co-current manner.

Table 2-2 summarizes the range of operating variables for bubble columns

Table 2-2: Range of operating variables for bubble columns (Shah and Deckwer, 1983)

Operating Variable	Size	Units
Volume: Chemical Process Industry	< 200	m^3
Volume: Biochemical Processes	< 3000	m^3
Diameter	0.2 – 20	m
Length to Diameter Ratio	3 – 10	
Superficial Gas Velocity	< 100	cm/s
Superficial liquid velocity	< 10	cm/s
Liquid Viscosities	0.5 – 100	mPa.s
Liquid Densities	0.6 – 2	g/cm^3
Liquid Surface Tensions	20 – 73	dyne/cm

2.3) Flow regimes and flow patterns

The phase hold-up, mixing and transport characteristics of a bubble column depend significantly on the prevailing flow regime in the column. Figure 2-2 shows the three observed flow regimes in bubble column reactors.

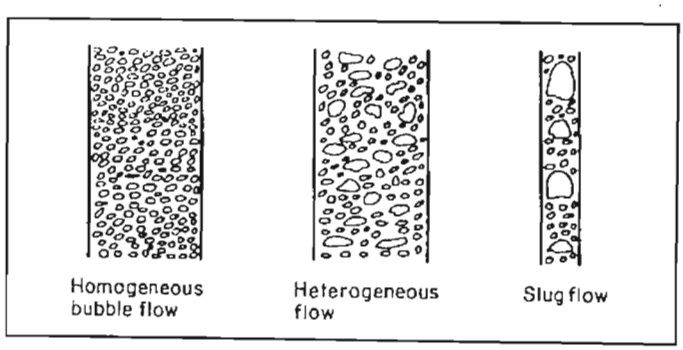

Figure 2-2: Flow regimes in bubble columns (Deckwer, 1992)

The three flow regimes shown above are normally observed as the gas flow rate increases (increasing flow rate from left to right in Figure 2-2).

The bubble flow regime occurs at low gas flows and is characterised by ordered chain bubbling. The churn-turbulent or heterogeneous regime is characterised by the onset of significant bubble coalescence and liquid circulation in the column. At very high gas flow rates, the gas bubbles coalesce to form large slugs.

The transition from one flow regime to another is not well defined. An approximate estimate of the boundaries can be obtained from Figure 2-3 for water and dilute aqueous solutions.

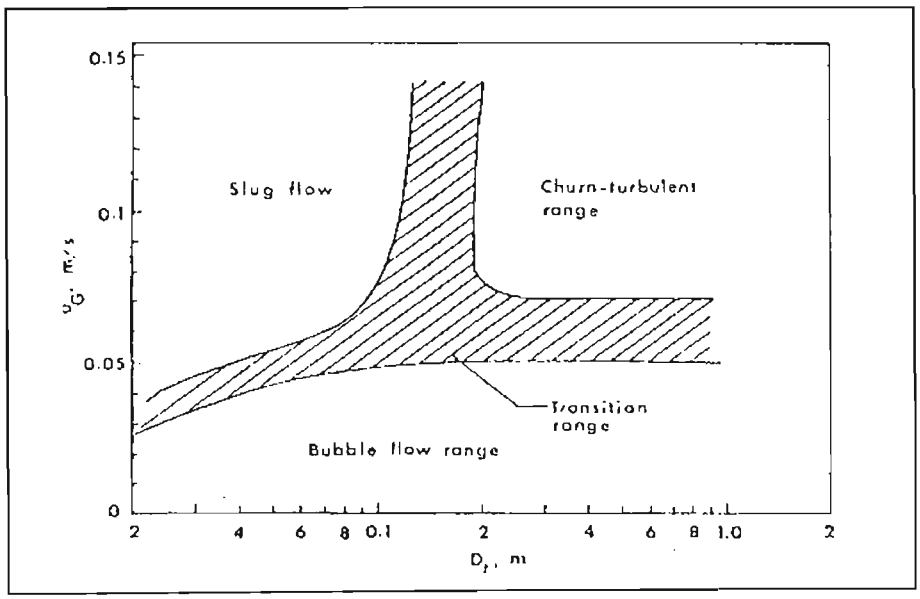

Figure 2-3: Approximate boundaries for flow regimes in gas-liquid bubble columns (Chen, 1986)

The detection of regime transition from homogeneous to churn-turbulent flow and the investigation of the transition regime are important. As the transition takes place, significant changes are observed in the hydrodynamic behaviour of the system.

The liquid flow patterns in bubble column reactors are complex. It is often assumed that large scale eddies with well defined circulation patterns are formed. The mechanism of liquid circulation is explained via the rising gas bubbles which entrain liquid with them, this amount of liquid being considerably greater in bubble column reactors than that corresponding to the liquid throughput (Deckwer, 1992). Continuity ensures that fluid returns down the column, producing a pronounced circulation pattern in which the central liquid is moving upwards and that next to the walls moves downwards (Figure 2-4).

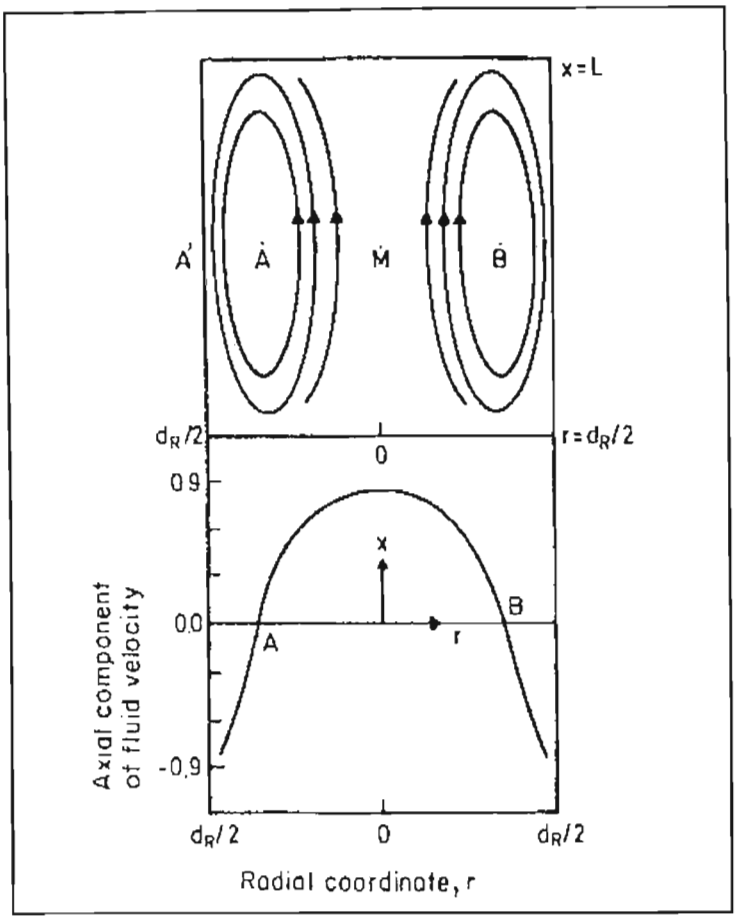

Figure 2-4: Liquid circulation velocity profile in an axial-symmetrical bubble column (Joshi and Sharma, 1979)

This circulatory flux is a function of gas flow-rate, column diameter, cross-sectional shape, gas hold-up, bubble diameter, bubble rise velocity and liquid viscosity (Deckwer, 1992). The zero-velocity point usually occurs at 0.7 of the column radius (Hills, 1974). Nottemkamper et al. (1983) performed velocity profile measurements which supported the findings of Hills (1974).

2.4) Gas distribution

The choice and design of the gas distributor influences the characteristics of the gas dispersion within the reactor. The gas distributor affects the hold-up, interfacial area and the mass transfer in bubble columns.

The gas may be dispersed through pores, holes, sintered plates, nozzles and perforated plates. Perforated plates and sieve plates are particularly useful for gas re-dispersion in cascade bubble columns. These dispersion methods are known as static gas distributors.

In contrast the dynamic twin jet variety of distributors such as an ejector jet, injector jet, venture jets and slit jets cause gas distribution by the kinetic energy generated by the liquid force.

Flexible spargers may also be used (Rice et al. 1980). For example a rubber plate will undergo a periodic deformation which aids in a uniform distribution of gas.

Deckwer (1992) asserts that there is no disadvantage in the gas distribution method used when the process taking place in the column is limited by the chemical reaction rate in the liquid phase. This is also indicative in the literature as the gas dispersion method has a very profound effect on the levels of mass transfer occurring in the column rather than on the dispersion levels.

Depending on the choice of distributor, gas distribution may occur in one of two ways. There may be even distribution of the gas across the reactor or distribution such that three easily identifiable zones may be observed as shown in Figure 2-5(b).

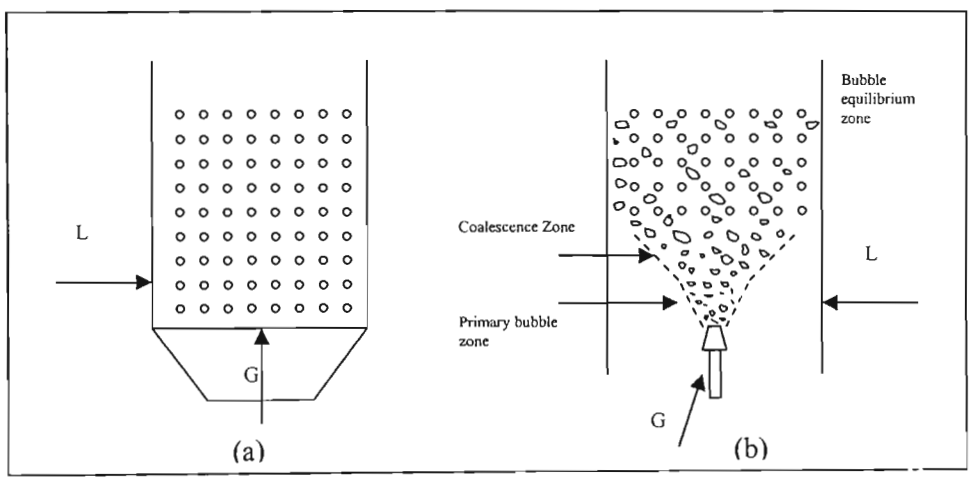

Figure 2-5: Gas distribution in bubble columns

(a) uniform distribution (b) distribution zones

2.5) Design parameters for bubble column reactors

The design, sizing and performance of bubble column reactors depend on the hydrodynamics, axial dispersion, mass and heat transfer and reaction kinetics.

Given the wide variety of gas-liquid reactions utilised in industry (Table 2-1) it becomes necessary to determine when a bubble column reactor will be the most effective means of contacting a gas with a liquid phase.

Other reactors in which a gas may be contacted with a liquid include:

- wetted or packed columns
- mechanically stirred vessels
- spray columns

Charpentier (1981) provides criteria for when the various reactors are suitable. To illustrate the choice of reactor consider a reaction in which a dissolved gas (component A) undergoes an irreversible second-order reaction with a reactant (component B) dissolved in the liquid. The stoichiometry of the reaction is given by

$$A + zB \xrightarrow{k_2} products$$

with the rate equation

$$r_A = k_2 C_A C_B = \frac{r_B}{z} \tag{2-1}$$

The ratio of the reaction rate to the mass transfer rate is represented by the dimensionless Hatta number:

$$Ha = \frac{\left(D_A k_2 C_{B0}\right)^{1/2}}{k_L} \tag{2-2}$$

with D_A, the diffusivity of A in the liquid, C_{B0}, the initial concentration of component B and k_L, the liquid mass transfer coefficient.

The value of the Hatta number provides an important indication of whether a large interfacial area a or a large liquid hold-up β is required for a particular reaction rate constant k_2. Table 2-3 summarises the criteria for selection of a gas-liquid reactor type.

Table 2-3: Selection of reactor for gas-liquid reactions

Reaction type	Ha range	Liquid hold-up	Reactor
Very slow reaction in liquid	Ha < 0.02	$\beta k_2 C_{B0}/k_L a$ <<1	Bubble column
Slow reaction in liquid	0.02 < Ha < 0.3	$\beta k_2 C_{B0}/k_L a$ >>1	Stirred tank
Moderately fast reaction	0.3 < Ha < 3	-	Plate column
Fast reaction	Ha > 3	-	Packed column

Table 2-3 shows that bubble column reactors are preferred for reactions in which a large bulk liquid volume are required.

2.5.1) Superficial gas velocity

The superficial gas velocity is the most import design parameter. The gas throughput determines the hydrodynamic characteristics of the bubble column reactor.

Schumpe et al. (1979) have shown that the maximum gas velocity for a reaction occurring in a bubble column is given by:

$$u_{G\,max} = \frac{1}{\varepsilon_G^* \left(1 + \sqrt{\frac{k_L a^*}{k_2 C_B \varepsilon_G^*}}\right)} \qquad (2\text{-}3)$$

where a^* and ϵ^*_G are the interfacial area per unit volume and the average gas hold-up at $u_g = 1$ cm/s respectively. The authors have shown that the optimum superficial gas velocity for optimum space-time yield is approximately half the value of u_{Gmax}.

2.5.2) Pressure drop

The pressure drop due to friction at the reactor walls in bubble column reactors can be neglected. The pressure drop is composed of the drop exerted by the gas sparger and the hydrostatic head of the liquid. Therefore, the pressure profile within the column is given by:

$$P(z) = P_T\left(1 + \alpha(1 - z)\right) \tag{2-4}$$

where z is the dimensionless axial coordinate and, P_T the pressure at the top of the column, and α represents the ratio of the hydrostatic head to the pressure at the top of the column:

$$\alpha = \frac{\rho_L(1-\varepsilon_L)gL}{P_T} \tag{2-5}$$

where L is the dispersion height.

As the gas expands in the column, the axial variation in the pressure should be considered for the calculation of the local gas velocities, provided α is larger than 0.2 (Shah and Deckwer, 1983).

2.5.3) Bubble size and bubble distribution

The bubble size is important as it determines the mass transfer coefficient and the transfer area. Mashelkar (1970) states that for low gas velocities ($u_g < 0.5$ cm/s), the bubble diameter will be a strong function of the orifice diameter and a weak function of the gas velocity in the orifice. At gas velocities ranging from 0.5 to 10 cm/s the bubble diameter becomes a strong function of the gas velocity in the orifice. At higher gas velocities ($u_g > 10$ cm/s), both the orifice diameter and gas velocity will have a lesser effect on the bubble size. Bubble size is strongly affected by the surface tension of the liquid. It is well observed in the literature, that the presence of electrolytes in water results in the formation of smaller bubbles.

2.5.4) Gas hold-up and interfacial area

The gas hold-up ϵ_G is defined as the volume fraction of gas V_G present in the bubble column reactor. It is defined as:

$$\varepsilon_G = \frac{V_G}{V_G + V_L} \tag{2-6}$$

The gas hold-up provides an indication of the residence time and the effective interfacial area of the gas. Gas hold-up is not a constant quantity but varies locally in the axial and radial direction. In industry, the majority of reactors are operated under heterogeneous flow (Figure 2-2) conditions where the value of ϵ_G is typically in the range 0.1 to 0.4.

2.5.5) Mass transfer coefficients

Gas side resistances to inter-phase mass transfer are often negligible due to the slow reaction-absorption regime that bubble columns are often operated at. The liquid side volumetric mass transfer coefficient k_La is sufficient to describe the gas-liquid mass transfer rates (Deckwer and Schumpe, 1993). There have been many attempts to develop a theoretical prediction of liquid mass transfer coefficients in bubble columns; however they are of limited applicability. Figure 2-6 shows the how k_La values are affected by superficial gas velocity.

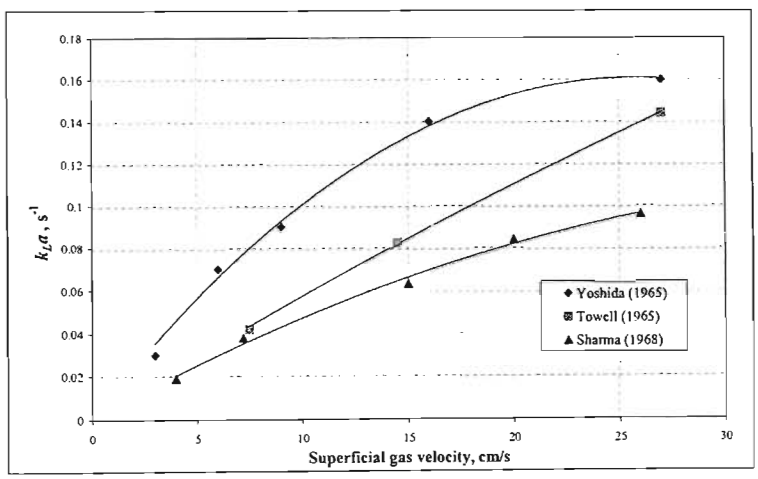

Figure 2-6: Liquid-side mass transfer coefficient in bubble columns as a function of superficial gas velocity

2.5.6) Heat transfer coefficients

A large number of the gas-liquid reactions are highly exothermic and hence heat removal becomes an important design feature. The well mixed nature of bubble columns results in a uniform temperature distribution throughout the reactor. The preferred means of heat removal is heat transfer through tubes within the reactor or through the walls of the reactor via a jacket. Deckwer (1992) reports that the heat transfer coefficients do not depend on the surface geometry of the heat transfer element. Mashelkar (1970) reports that the heat transfer rates in bubble columns compare well to those for mechanically agitated tanks.

2.5.7) Liquid mixing in bubble columns

Dispersion may be defined as the spreading of fluid particles as a result of departure from non-ideal flow. The fluid particles move forward in the direction of net flow, but at different speeds, thus resulting in the distribution of residence times. Dispersion occurring in a direction opposing the flow, such as that occurring in bubble columns is commonly known as back-mixing.

The back-mixing of the liquid phase in bubble columns has been the focus of many studies in literature and continues to be a subject under study. Back-mixing in bubble column reactors is affected both by the superficial gas velocity and the column diameter. Back–mixing influences the residence time distribution in the reactor and thus strongly influences the reaction yield and selectivity. Liquid back-mixing can be reduced by the incorporation of partition plates to sectionalise the column. It is common to make use of the axial dispersion model (ADM) to describe liquid phase mixing in bubble column reactors. In the ADM a lumped dispersion parameter E_L is used to represent the degree of back-mixing. The higher the value of E_L, the greater the degree of back-mixing in the reactor.

Mathematically, the axial dispersion model in the longitudinal z-direction is given by:

$$\frac{\partial C_B}{\partial t} = E_L \frac{\partial^2 C_B}{\partial z^2} - \frac{< u_L >}{1-\varepsilon_G} \frac{\partial C_B}{\partial z} + r_B \qquad (2\text{-}7)$$

with t as time, u_L, the superficial liquid velocity based on an empty reactor volume and E_L, the liquid back-mixing coefficient. E_L is an important design parameter and will be treated at length in Chapter 4.

The assumptions of the ADM are:

- negligible radial dispersion
- plug flow with constant velocity
- no stagnant pockets
- no bypassing or short-circuiting of fluid in the vessel

2.6) Scale-up considerations

Reactor performance is governed by the variables affecting the reaction and reactor specific quantities. The reaction specific data such as physical properties, stoichiometry, thermodynamics and kinetics are for the most part independent of reactor type and design.

In contrast, the reactor specific quantities are largely dependent on operating properties, physical properties, reactor geometry and type. It is the fluid dynamic phenomena and heat and mass transfer properties which cause the most difficulty in confident scale-up.

The fluid dynamics of the gas and liquid phases are often characterised by their respective residence time distributions (Chapter 3). A schematic drawing of the dependency of these phenomena is shown in Figure 2-7.

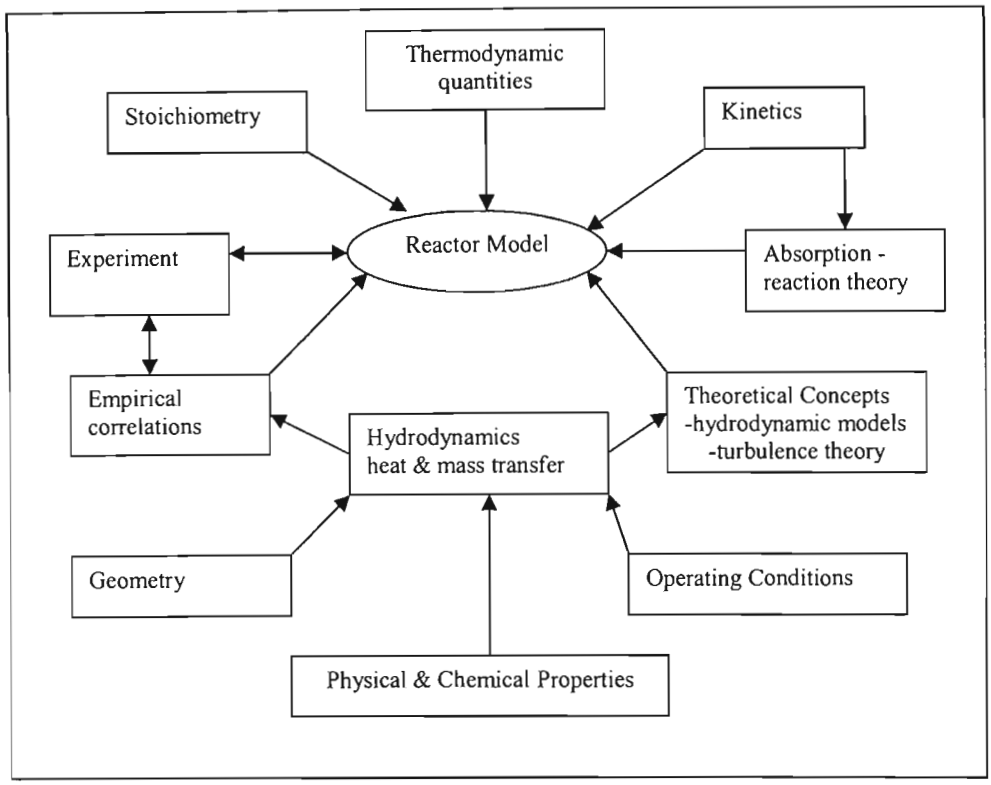

Figure 2-7: Design and modelling considerations for bubble column reactors

Correlations for parameter estimations are often developed under non-reactive conditions often referred to as "cold flow" measurements. Cold flow measurements are performed independently of a reaction in order to isolate the hydrodynamic phenomena. The subject of parameter estimation is covered in great depth in Chapter 4.

CHAPTER THREE

HYDRODYNAMICS OF BUBBLE COLUMN REACTORS: EXPERIMENTAL METHODS

The questions that reactor designers and engineers take into consideration can be categorised as follows:

1. What to measure?
2. Why to measure?
3. How to measure?

The answers to questions 1 and 2 have been outlined in Chapter 2. This chapter will focus primarily on experimental methods for measuring axial dispersion coefficients and gas hold-up in bubble column reactors. A brief description of experimental methods for measuring other hydrodynamic quantities will be provided as well as an account of current innovations in the measurement of bubble column hydrodynamics.

3.1) Measurement of liquid phase dispersion

Mechanisms responsible for the mixing in bubble columns are:

- turbulent eddies in the main liquid stream as well as eddies introduced by the movement of the dispersed gas phase relative to the continuous liquid phase
- liquid entrainment in the wakes of the bubbles combined with mass exchange between these wakes and the liquid phase
- molecular diffusion

It is difficult to deal with the analysis of the possible contribution from each individual mechanism. Instead, simplified models such as the one dimensional axial dispersion model are often assumed to represent the overall mixing phenomena. Dispersion may be defined as the spreading of fluid particles as a result of the departure from ideal plug and perfectly mixed flow conditions. The degree of dispersion may be obtained from tracer experiments such as residence time distribution studies and batch liquid mixing tests.

3.1.1) Residence time distribution theory

To predict the behaviour of a vessel as a chemical reactor, knowledge of the passage of the fluid through the vessel is required. Ideally, it would be required to tag and follow every molecule on the micro-scale to predict the exact behaviour of the fluid elements. The complexities of this approach make it impractical to implement experimentally. However, the distribution of residence times of molecules within the reactor can be determined by the stimulus-response technique. In this technique a quantity of tracer is injected into the inlet feed of the reactor and its resulting exit concentration profile is monitored with time.

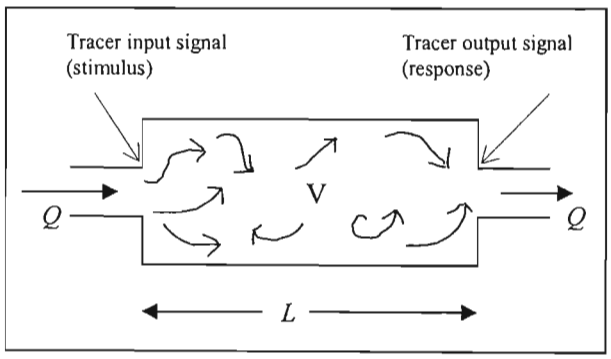

Figure 3-1: Schematic showing tracer input and signal response in a reactor vessel

The tracer input signal may be random, cyclic, a step or a pulse. The stimulus-response technique determines the form of the response of the tracer. Due to ease of analysis, step tracer and pulse (Dirac delta function) inputs are generally preferred over the other input signals. Analysing the response provides information on the behaviour of the system.

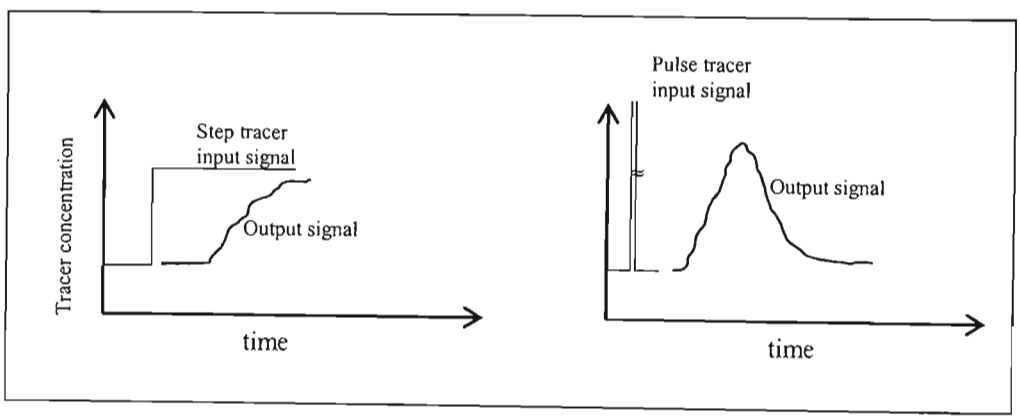

Figure 3-2: Stimulus-response signals to study the behaviour of flow systems

In general, different elements of fluid following different paths will take different periods of time to pass through the vessel. For a single fluid, under steady-state flow, without reaction and without density change, the average retention time (mean residence time) of the fluid in a vessel of volume V and length L is given by:

$$\bar{t} = \tau = \frac{V}{Q} = \frac{L}{u} \tag{3-1}$$

where Q is the volumetric flow-rate of the fluid under consideration.

Eq. 3-1 only holds for closed vessels and for the effective volume of the vessel. In the case of multiple phases and the presence of dead volume (due to internals or stagnant zones) the effective volume and flow rate of the phase under consideration must be used for V and Q respectively.

For a multi-phase system, the hold-up ϵ of phase P can be calculated from:

$$\varepsilon_P = \frac{u_P \bar{t}_P}{L} \tag{3-2}$$

A dimensionless time variable which measures time in units of mean residence time can be defined as:

$$\theta = \frac{t}{\bar{t}} \tag{3-3}$$

The exit age distribution $\boldsymbol{E}$ of a fluid leaving the reactor is a measure of the distribution of residence times of the fluid within the vessel. The age is measured from the time the fluid elements enter the vessel. A typical exit age distribution for a continuously stirred tank is shown in Figure 3-3.

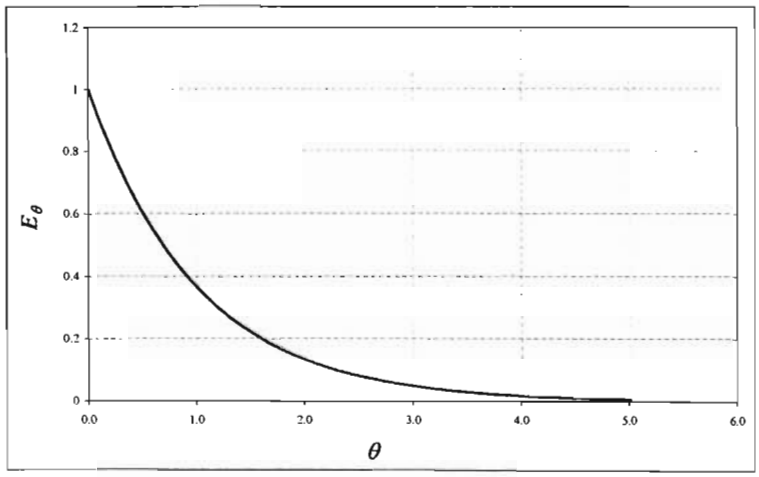

Figure 3-3: A typical exit age distribution for a CSTR

$\boldsymbol{E}$ is defined in such a way that $\boldsymbol{E}\ d\theta$ is the fraction of material in the exit stream with age between θ and $\theta + d\theta$. The area under an $\boldsymbol{E}$ versus θ curve is found to always be:

$$\int_0^\infty \boldsymbol{E} d\theta = 1 \tag{3-4}$$

Eq. 3-4 serves as a check on the mass balance of the tracer to determine that there are no errors in the tracer measurement.

To get to $\boldsymbol{E}$, a relationship between the concentration-time curve c and the exit age distribution must be used. Levenspiel (1962) shows that:

$$\boldsymbol{E}(t) = c(t) \times \frac{M}{Q} \tag{3-5}$$

with $\boldsymbol{E}(t)$ in units of s^{-1} and where M is the mass of tracer input into the system. $\boldsymbol{E}$ is related to $\boldsymbol{E}(t)$ by:

$$\boldsymbol{E} = \boldsymbol{E}(t) \times \tau \tag{3-6}$$

Associated with every age distribution, $y = f(x)$, are two sets of parameters called the moments of the distribution. The k^{th} moment about the origin is defined by:

$$M_k' = \frac{\int_0^\infty x^k f(x)\,dx}{\int_0^\infty f(x)\,dx} \tag{3-7}$$

and the k^{th} moment about the mean μ of the distribution is defined by:

$$M_k = \frac{\int_0^\infty (x-\mu)^k f(x)\,dx}{\int_0^\infty f(x)\,dx} \tag{3-8}$$

A particular distribution can be completely defined by its moments, and hence distributions can be compared by their moments without comparing the actual curves themselves (Levenspiel, 1962).

3.1.1.1) Determination of E, τ, μ *and* σ^2 from a concentration-time curve

From the concentration-time curve c:

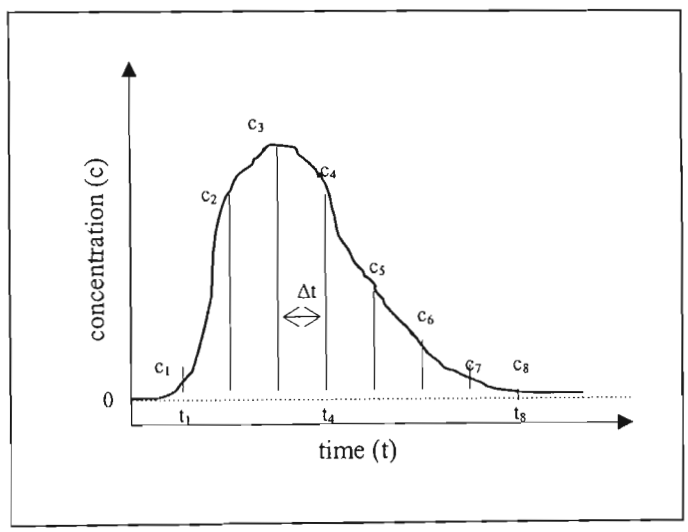

Figure 3-4: Concentration-time response to pulse input

the mean residence time can be found from:

$$\bar{t} = \frac{\int_o^\infty tcdt}{\int_o^\infty cdt} \approx \frac{\sum_i t_i c_i \Delta t_i}{\sum_i c_i \Delta t_i} = \frac{V}{Q} \tag{3-9}$$

The exit age distribution $E(t)$ is given by:

$$E_i(t_i) = \frac{c_i}{\sum_i c_i \Delta t_i} \tag{3-10}$$

The mean μ of the distribution is defined as:

$$\mu = M_1 = \frac{\int_0^\infty xf(x)dx}{\int_0^\infty f(x)dx} = \frac{\sum_i t_i c_i \Delta t_i}{\sum_i c_i \Delta t_i} = \bar{t} \tag{3-11}$$

The second moment about the mean, commonly called the variance σ^2, measures the spread of the distribution about the mean. It is defined as:

$$\sigma^2 = M_2 = \frac{\int_0^\infty (x-\mu)^2 f(x)dx}{\int_0^\infty f(x)dx} = \frac{\sum_i (t_i - \mu)^2 c_i \Delta t_i}{\sum_i c_i \Delta t_i} \tag{3-12}$$

For equidistant points, Eq. 3-12 reduces to:

$$\sigma^2 = \frac{\sum_i t_i^2 c_i}{\sum_i c_i} - \mu^2 \tag{3-13}$$

3.1.1.2) Methods of using age distribution information

Tracer information is used either directly or in conjunction with flow models to predict performance of real flow reactors, the method used depending in large part on whether the reactor can be considered a liner system or whether it must be treated as a non-linear system.

A process is linear if any change in stimulus results in a corresponding proportional change in response. That is:

$$\frac{\Delta(response)}{\Delta(stimulus)} = \frac{d(response)}{d(stimulus)} = \text{constant} = k \tag{3-14}$$

For linear systems where the tracer has no unusual behaviour but merely passes through the reactor and the kinetic reaction rate is also linear in concentration, a flow model is not required to determine the conversion. The tracer information together with the kinetic reaction data is sufficient to describe the behaviour of the vessel as a reactor. A variety of flow patterns can give the same tracer output curve. For linear processes, however, these all result in the same conversion (Levenspiel, 1962).

For reactions and processes which are not linear in concentration, conversion cannot be found using age distribution information directly. A flow model is required to determine the conversion in the reactor. Flow models are described by mathematical descriptions, boundary conditions and initial conditions.

3.1.2) Boundary conditions

The analysis and measurement of residence time distribution experiments are subject to many errors:

- experimental errors in the tracer measurements
- mathematical errors in the analysis of the tracer response measurements
- application of wrong boundary conditions

For example erroneous dispersion coefficients can be obtained if open-open boundary conditions are used when closed-closed boundary conditions are more representative of the system.

A closed vessel is defined as one in which material passes in and out by bulk flow only. Thus dispersion or diffusion is absent at the entrance and exit, so there is no movement of material upstream and out of the vessel by swirls or eddies. In contrast, an open vessel permits the movement of material across its boundaries as shown in Figure 3-5.

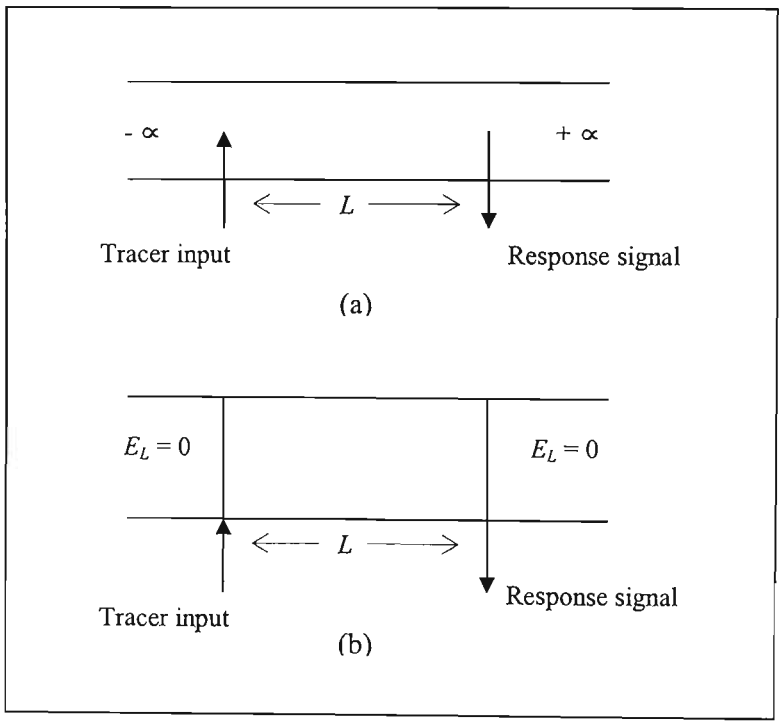

Figure 3-5: Boundary conditions (a) open-open (b) closed-closed

Levelspiel (1962) reports that for high values of *Pe* number [$(u_L L / E_L) > 78$] the effect of boundary conditions becomes negligible. However, this criteria is seldom achieved in bubble column experimental conditions and Ityokumbul et al. (1988) reports that many researchers prefer open-open boundary conditions since it yields a simpler analytical solution for mathematical flow models. They showed that the open-open Peclet number Pe_{oo} is related to the closed-closed Peclet number Pe_{cc} by:

$$\frac{Pe_{cc}}{Pe_{oo}} = 0.70 Pe_{oo}^{\,0.073} \tag{3-15}$$

It is recommended that closed-closed boundary conditions be used in the analysis of bubble columns (Deckwer, 1992).

3.1.3) Non-steady-state stimulus-response techniques for determining E_L

Non-steady state methods allow for a transient analysis of bubble column reactors.

3.1.3.1) Batch liquid measurements

This method has been utilised extensively in the literature. Ohki and Inoue (1970) is a well cited paper. Mixing time measurements, where the time required to reach a specific level of concentration uniformity $C_L/C_O < 1$, are used to obtain liquid dispersion coefficients. The term mixing is used here to denote movement, distribution, or diffusion of a component through a reaction vessel, tending to make fluid composition uniform throughout. Mixing eliminates concentration gradients in a reactor. In batch mixing experiments, tracer is injected as a pulse into the batch liquid phase and the resulting concentration is measured at a particular distance away from the feed point position (Figure 3-6).

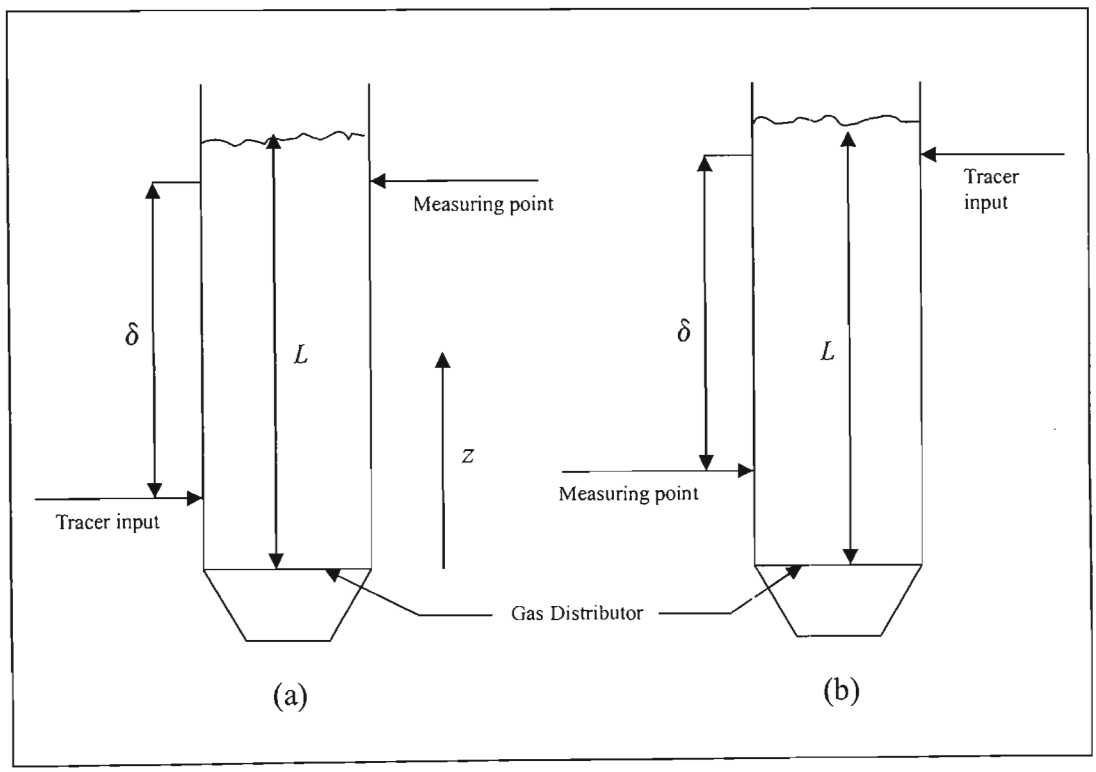

Figure 3-6: Tracer input and measurement points for batch liquid measurements

(a) input from bottom of reactor (b) input from top of reactor

The difference between the tracer inputs with respect to the top of the reactor is that this is a test for back-mixing. If no back-mixing occurred the tracer would not be detected upstream from the tracer input. Input from the bottom of the reactor, as in Figure 3-6(a), assumes that back-mixing occurs.

The one dimensional axial dispersion model (ADM) may be assumed when the distance between the injection point of tracer and the measuring point are sufficiently long. The longitudinal dispersion coefficient E_L is used to express the characteristics of the liquid mixing in bubble columns.

The mathematical description of the spreading of the tracer is described in an analogy to Fick's second law:

$$\frac{\partial C}{\partial t} = E_L \frac{\partial^2 C}{\partial z^2} \tag{3-16}$$

with closed-closed boundary conditions:

$$\frac{\partial C}{\partial z} = 0 \text{ at } z=0 \text{ and } z=L \tag{3-17}$$

The initial conditions are:

$$C(z,0) = C_i \text{ for } 0 \leq z \leq \lambda \tag{3-18}$$

$$C(z,0) = 0 \text{ for } z \geq \lambda \tag{3-19}$$

where λ is the height of the column corresponding to the volume of tracer injected.

Solution of Eqs. 3-16 to 3-19 gives:

$$\frac{C}{C_o} = 1 + 2\sum_{n=1}^{\infty}\left(\cos\frac{n\pi}{L}\delta\right)\exp\left(-\frac{n^2\pi^2}{L^2}E_L t\right) \tag{3-20}$$

Ohki and Inoue (1970) determined that six terms are sufficient to evaluate E_L with an error under one per cent.

Figure 3-7 shows C/C_o as a function of the dimensionless group $E_L t/L^2$ for various values of (δ/L). Deckwer (1992) reports that the measuring technique works best for (δ/L) values approximately equal to 0.8.

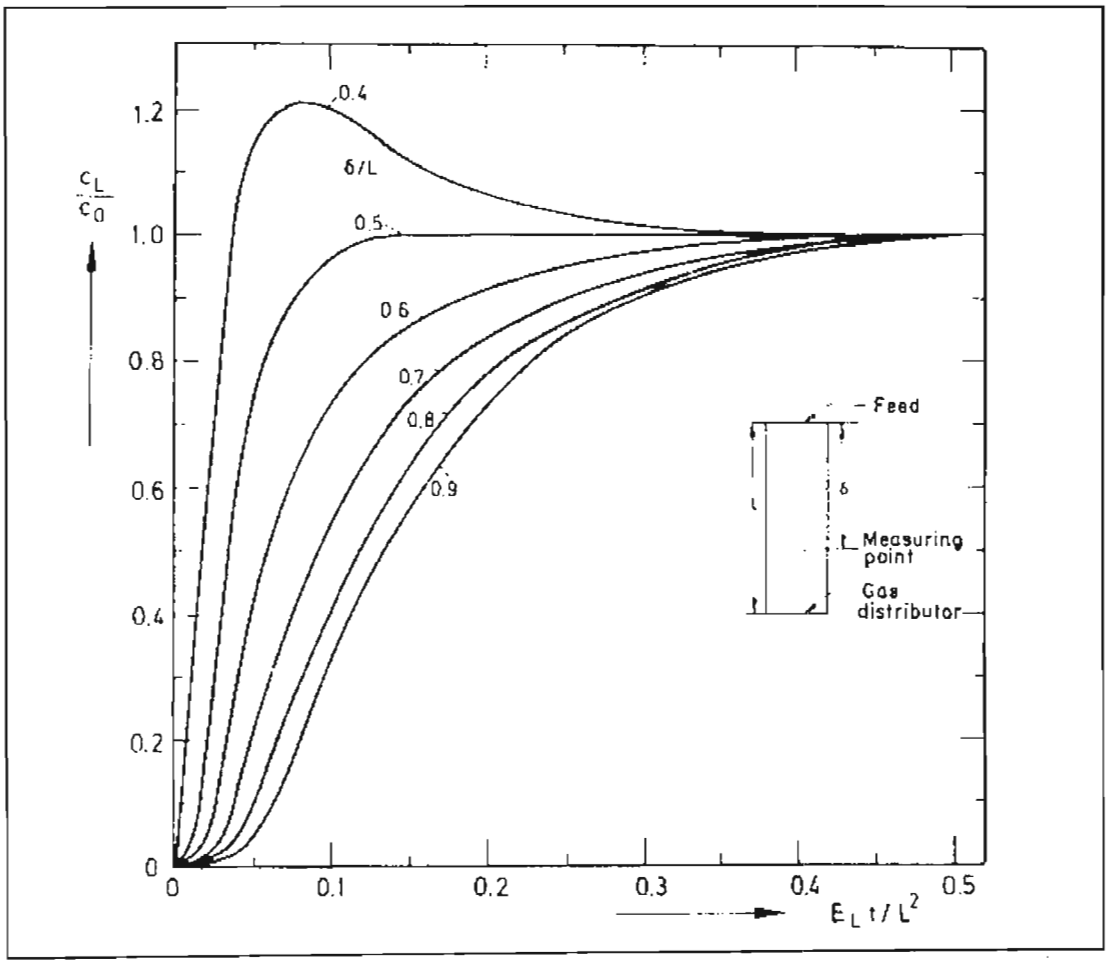

Figure 3-7: Dynamic concentration curves. Parameter: ratio of distance between feed and measuring point and reactor length (δ/L) (Deckwer, 1992)

Figure 3-7 can be used for the evaluation of E_L.

3.1.3.2) Continuous liquid RTD measurements

For a gas-liquid reaction, the chemical transformation takes place essentially in the liquid phase. Therefore, the residence time distribution (RTD) in this phase is of particular interest. The residence time distribution can be recorded when the liquid phase passes continuously through the reactor and from this the dispersion coefficient can then be calculated using an appropriate model for the liquid phase.

The one-dimensional axial dispersion equation for the system is (Levenspiel, 1962):

$$\frac{\partial c}{\partial t} = E_L \frac{\partial c^2}{\partial z^2} - \frac{u_L}{1-\varepsilon_g}\frac{\partial c}{\partial z} \tag{3-21}$$

Bischoff and Philips (1966) performed longitudinal mixing tests using the axial dispersion model. The authors note that there is the possibility of a "decay" in turbulence down stream from the gas distributor plate which means that the dispersion coefficient should properly vary with length. However, a proper account of this longitudinal dependency would severely complicate the model and it is common practice to use a constant liquid dispersion coefficient E_L. Baird and Rice (1975) showed that turbulence is isotropic in bubble column reactors and as such dispersion levels are approximately constant in the axial direction.

The closed-closed boundary condition at the entrance ($z = 0$) is:

$$c_{T0} = -\frac{E_L}{u_L}\left(\frac{\partial c}{\partial z}\right)_{z=0^+} + c\left(0^+, t\right) \tag{3-22}$$

and at the exit ($z = L$) is:

$$\frac{\partial c}{\partial z} = 0 \tag{3-23}$$

For a pulse tracer input the analytical solution, at $X = z/L$, to the governing equation is given by Field and Davidson (1980):

$$\frac{c_X}{C_0} = 2\exp\left[P\left(2X-\theta\right)\right]\sum_{k=i}^{\infty}\left[\lambda_k \exp\left(-\lambda_k^2/\theta\right)\frac{\lambda_k \cos\left(2\lambda_k X\right) + P\sin\left(2\lambda_k X\right)}{\lambda_k^2 + P^2 + P}\right] \tag{3-24}$$

where P is given by:

$$P = \frac{u_L L}{4E_L} \tag{3-25}$$

C_o is given by the concentration of the mass of tracer M in the bulk liquid volume V_L:

$$C_o = \frac{M}{V_L} \tag{3-26}$$

and λ_k are the roots of

$$\tan(2\lambda) = \frac{2\lambda P}{(\lambda^2 - P^2)} \tag{3-27}$$

and θ is given by Eq. 3-3.

Field and Davidson (1980) state that when $\theta = 0.1$ the first nine roots were used. The number of roots (λ_k) required decreases as T increases.

Eq. 3-24 can be used to fit experimental data in time and space. However dispersion coefficients can be calculated from the variance σ^2 and mean μ of measured RTD. It should be noted that the shape of the concentration-time curve as predicted by the ADM cannot be generated from these two parameters only.

It can be shown (Deckwer, 1992) that the variance of the RTD data can be related to the Peclet Number:

$$Pe_L = \frac{u_L L}{E_L} \tag{3-28}$$

For open-open boundary conditions (Figure 3-5a):

$$\sigma^2 = \frac{2}{Pe_L} + \frac{8}{Pe_L^2} \tag{3-29}$$

and for closed-closed boundary conditions (Figure 3-5b):

$$\sigma^2 = \frac{2}{Pe_L} - \frac{2}{Pe_L^2}(1 - e^{-Pe_L}) \tag{3-30}$$

where the variance σ^2 is given by Eq. 3-12.

Eqs. 3-29 or 3-30 can be solved for the Pe_L and E_L can be determined from Eq. 3-28 since u_L and L are known. This is much simpler than curve fitting in time-space.

3.1.4) Steady state method to determine liquid dispersion coefficients in bubble columns

The dispersion coefficient may be determined from steady-state measurements of axial concentrations in the reactor. The tracer is introduced from a continuous source and its concentrations are measured at different axial locations upstream of the source. The distribution of the tracer is measured either directly or by sampling as shown in Figure 3-8. The tracer should be added through a source uniformly over the cross-sectional area but can be just as effectively fed in through a distributor ring $0.707D_c$ in diameter (Deckwer, 1992).

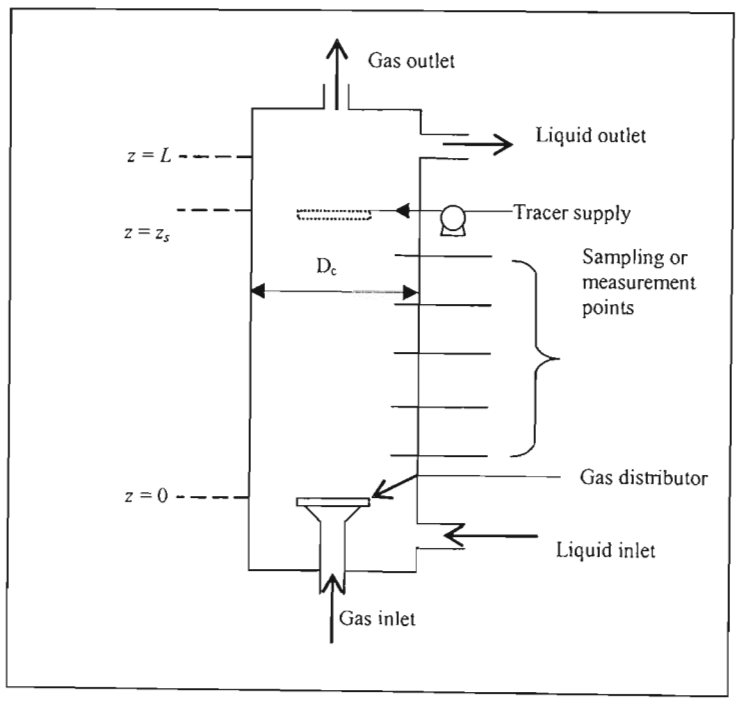

Figure 3-8: Experimental arrangement for recording concentration profiles based on the steady-state method

A mass balance of the tracer for co-current flow gives:

$$E_L \frac{\partial^2 c}{\partial z^2} - u_L \frac{\partial c}{\partial z} = 0 \qquad (3\text{-}31)$$

Subject to the boundary conditions:

$$c = \frac{E_L}{u_L}\frac{\partial c}{\partial z} \quad \text{at } z=0 \tag{3-32}$$

$$c = c_o \qquad \text{for } z_s \leq z \leq L \tag{3-33}$$

The solution of Eq. 3-31 is given by:

$$c = c_o.\exp\left[-\frac{E_L}{u_L}(x_s - x)\right] \tag{3-34}$$

A typical steady-state concentration profile is shown in Figure 3-9.

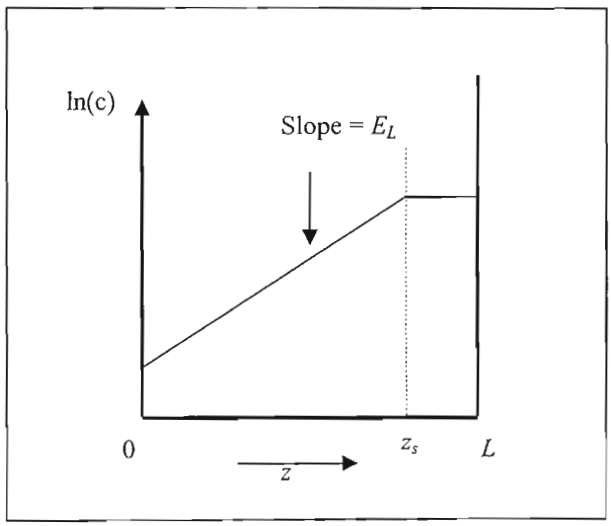

Figure 3-9: Typical steady-state concentration profile in a bubble column

E_L can be calculated from the slope of the straight line gradient of a plot of ln(c) against z.

3.1.5) Comparison of methods

Deckwer (1992) reports that although the steady-state method is expensive and time-consuming it produces the most reliable information on dispersion patterns in the liquid phase. The steady-state method also reveals information on the constancy of the dispersion coefficient in the axial direction. The non-steady state mixing test is easier to implement and Deckwer reports that there is very little variation in dispersion coefficient obtained via the two methods (Figure 3-10).

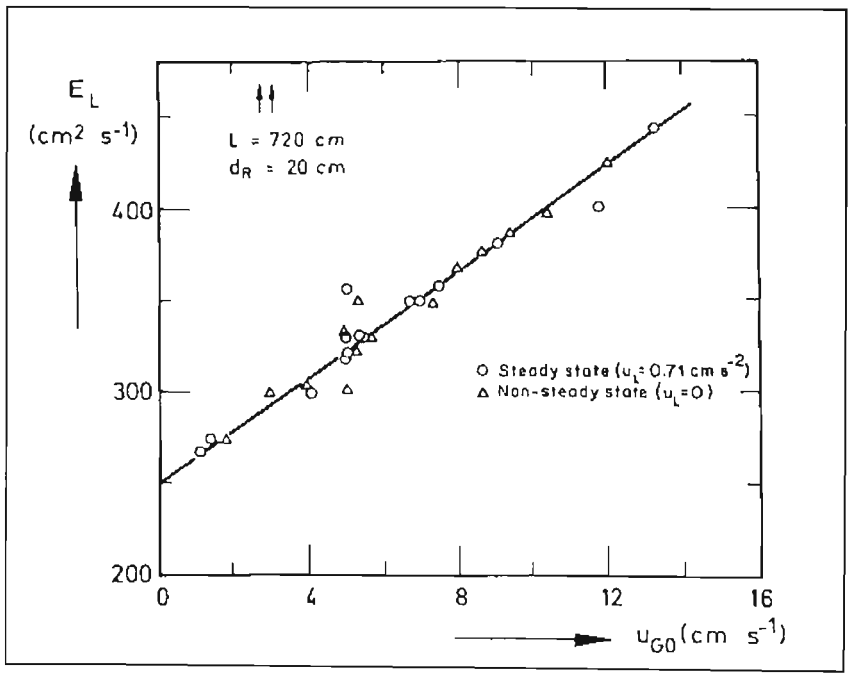

Figure 3-10: Comparison of dispersion coefficients as a function of gas velocity for steady-state and non-steady-state methods (Deckwer, 1992)

Deckwer also states that non-steady-state measurements with continuous flow do not reveal advantages in comparison with mixing time measurements for bubble columns. Continuous flow RTD measurements are recommended for bubble column cascades.

3.1.6) Choice of tracer for determination of E_L

It is well known that the selection of a tracer must meet the following specifications:

- have similar physical properties to the fluid of interest
- be easily detectable
- not change the hydrodynamics within the vessel
- no transfer of tracer between phases

Table 3-1 shows some tracers and detectors that are commonly used in bubble column research.

Table 3-1: Typical tracers and detectors for liquid phase experiments

Tracer	Example	Detector	Reference
Electrolyte	NaCl	Conductivity meter	Ohki and Inoue (1970)
Dye	$KMNO_4$	Spectrophotometer	Deckwer et al. (1974)
Concentrated acid	HCl	pH meter	Ityokumbul et al. (1974)
Heat		thermocouple	Kelkar et al. (1983)
Radioactive particle	Bromine 82	Scintillation counter	Field & Davidson (1980)

The mechanism of thermal dispersion is governed by liquid mixing and as such the transport of heat is used to determine liquid mixing coefficients. Ityokumbul et al. (1994) question the validity of this analogy as the transport of heat is effected by both the gas and liquid phases while the mass transport is effected by the liquid phase only. The use of heat as a tracer is particularly useful for liquid regeneration. Experimentally it is also difficult to implement as great care must be taken to ensure that the equipment is perfectly insulated and that the input flux is maintained at constant temperature.

Radioactive methods offer the benefit that detection may occur externally of the column as it is a non-intrusive measurement technique. However, the safety concerns far outweigh this advantage.

The use of absorption spectrophotometry is limited due to difficulty in calibration (usually non-linear) and the colour tainting of the columns and auxiliary equipment. Colour measurements are usually undertaken by sampling as it is extremely difficult to perform absorption spectrophotometry on a real-time basis.

For these reasons, conductivity and pH measurements are more common in the literature as there is ease in calibration (linear) and detection is relatively straight forward.

There does not appear to be any difference in the dispersion coefficient obtained by the various methods as Deckwer et al. (1974) reported that electrolyte, dye and heat were used as a tracer and each yielded identical dispersion coefficients.

3.2) Measurement of phase hold-up

The fraction of gas or liquid in a gas-liquid dispersion is referred to as the relative gas or liquid hold-up where the gas hold-up ϵ_G is given by Eq. 2-6 and the liquid hold-up ϵ_L by:

$$\varepsilon_L = \frac{V_L}{V_G + V_L} \tag{3-35}$$

For a gas-liquid system it is evident that:

$$\varepsilon_L + \varepsilon_G = 1 \tag{3-36}$$

The phase hold-ups represented by Eqs. 2-6 and 3-35 are representative of the average bulk phase hold-up across the reactor. Usually, these values are adequate to design the reactor as the average bulk hold-ups directly determine the total reactor volume required. In actuality the liquid and gas hold-ups are complex functions of both time and location (Deckwer, 1992).

There are many methods for measuring the fractional phase hold-ups in a bubble column reactor:

- physical methods
- optical methods
- radiation methods
- electrical methods

The most popular methods are via the measurement of bed expansion and the pressure drop measurement technique and will be discussed here. Details of the other methods can be found in Joshi et al. (1990).

3.2.1) Measurement of bed expansion

This is a simple method where measurements of the bed height are taken with the dispersed gas phase in the reactor H_D and measurements of the clear liquid height H_L are taken. The gas fraction being determined by:

$$\varepsilon_G = \frac{H_D - H_L}{H_D} \tag{3-37}$$

This allows for an average value of the fraction gas phase hold-up. The method makes no allowance for end effects such as the presence of a foam cap and is difficult to implement when the level continuously fluctuates.

3.2.2) Pressure drop measurement technique

The average gas hold-up is determined by measuring static pressures at several points along the column height. Neglecting pressure drop due to fluid friction and other losses, the difference in pressure between the column top P_T and at axial position $P(z)$ is given by:

$$P(z) - P_T = g\rho_L(H_D - z)[1 - \varepsilon_G(z)] \tag{3-38}$$

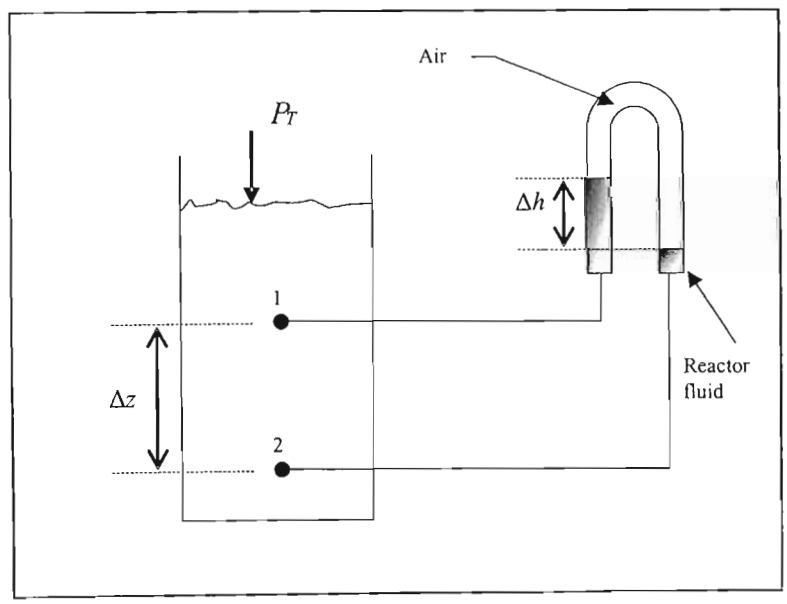

Figure 3-11: Pressure measurement in a bubble column with an inverted U-tube

The relative gas hold-up at position $z = (z_1+z_2) / 2$ between two points Δz apart results from the pressure difference $\Delta P = P(z_2) - P(z_1)$:

$$\varepsilon_G(x) = 1 - \frac{\Delta P}{\rho_L g \Delta z} = 1 - \left(\frac{\Delta h}{\Delta z}\right) \tag{3-39}$$

3.2.3) Determination of gas hold-up from RTD measurements

In two-phase systems the liquid residence time RTD will yield the liquid hold-up via Eq. 3-2. The gas hold-up can then be found by difference via Eq. 3-36.

3.3) Measurement of bubble size

The major characteristics of bubbles which are of vital importance from the design point of view are size, shape and terminal velocity. These parameters decide the interfacial areas and the residence time of the gas phase. There are various methods to determine the size and size distribution of bubbles:

- photographic methods
- impact methods
- thermal methods
- electrical methods
- optical methods
- residence time methods
- chemical methods

The principles and application of these methods are covered at great length by Joshi et al. (1990).

The photographic method is a relatively simple technique which generates reasonably accurate results. A major disadvantage of this method is that the curvature of cylindrical columns affects the size of the bubble in the photograph.

A popular method in the literature is based on resistivity or conductivity. Here, the difference in electrical properties of two different phases is used to measure the bubble diameter and its velocity of rise. Two or more needle electrodes (eg. platinum wire) are inserted into the column and the resulting conductivity-time profiles are analysed.

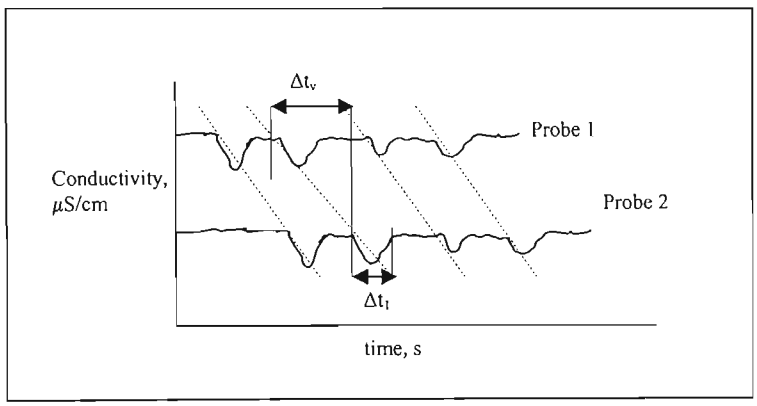

Figure 3-12: Illustrative recording of bubbles detected by electrodes

From conductivity-time measurements Ohki and Inoue (1970) showed that the mean rise velocity u_b of bubbles can be calculated from the average time of passage between the electrodes Δt_v:

$$v_b = \frac{\Delta l}{\Delta t_v} \tag{3-40}$$

where Δl is the space between probe 1 and probe 2.

The mean longitudinal length of the bubbles l_b is given by the average contact time of the bubbles with one electrode Δt_l and by v_b:

$$l_b = v_b . \Delta t_1 \tag{3-41}$$

This method suffers from the drawback that it is a flow intrusive measurement method and that in the case of ellipsoidal or spherical capped bubbles, the bubble diameter determined by this method is consistently small as only smaller axes are pierced (Joshi et al., 1990).

3.4) Measurement of velocity profiles

Essentially the main design parameters for bubble columns (phase hold-ups, mixing, RTD, mass and heat transfer coefficients) are all determined by the velocity field and the turbulence characteristics of the liquid phase.

The techniques for measurement of local velocity and turbulence include:

- pressure tube anemometers
- cross-correlation techniques
- thermal anemometers
- electrochemical method
- laser-Doppler anemometers (LDA)
- flow visualisation (eg. Particle Image Velocimetry, PIV)

Joshi et al. (1990) list the following characteristics for an ideal instrument to measure local velocity:

1. create minimum flow disturbance
2. small in size for essentially point measurement
3. minimal calibration requirements
4. measure a wide velocity range
5. work over a wide physical property range
6. high accuracy
7. high signal to noise ratio
8. ease of use
9. low cost

3.4.1) Pressure based measurements

The pressure exerted by a moving fluid on an open ended tube facing the direction of flow will be the sum of the static and dynamic pressures. It has been experimentally proven that the shape of the tube does not severely affect the observed total pressure (Joshi et al., 1990)

The tube is set along the flow direction so that the flow streamlines diverge around the tip. A static head probe can be a tube connected to the wall or in another location where the fluid velocity is zero. See Figure 3-13 for a schematic drawing of a pitot tube.

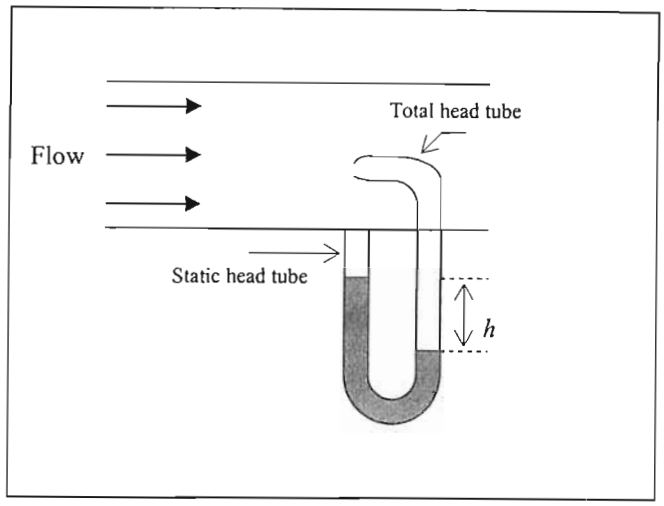

Figure 3-13: Schematic drawing of a pitot tube

Applying Bernoulli's equation and a force balance over the manometer yields:

$$u_{local} = K\sqrt{\frac{2gh(\rho_m - \rho_L)}{\rho_L}} \tag{3-42}$$

where K is a constant depending on the Reynolds number in the pitot tube. For Reynolds numbers greater than 100, based on the pitot tube diameter, K is unity and for lower Reynolds numbers a calibration for K in a known velocity field is required. ρ_m is the density of the manometer fluid.

Pressure based methods are often easier to use to estimate local liquid velocity but they suffer from a lack of accuracy and offer low resolution. They also cause flow disturbances and have a narrow application range for velocity measurement.

3.4.2) Thermal based measurements

Here the heat transfer rate from a small electrically heated sensor, which is proportional to the fluid velocity, is used to determine the fluid velocity.

The heat transfer from the sensor to the fluid depends upon:

- the fluid velocity
- the temperature difference between the sensor and the fluid
- physical properties of the fluid
- dimensions and physical properties of the probe\sensor

The only unknown is the fluid velocity as the other variables are known and constant.

The principle of hot wire and film anemometry is that the sensor of the wire is kept at a known temperature. Any rise in the fluid velocity increases the rate of heat transfer from the wire and causes the sensor to cool. A decrease in the resistance of the sensor is recorded due to the cooling. By measuring the voltage across the resistor, the fluid velocity can be determined. In practice an increase in fluid velocity in seen as an increase in the voltage across the resistor. It is necessary to calibrate the sensor in a velocity field and the sensor output is non-linear with respect to fluid velocity. When working properly, thermal methods offer good resolution and accuracy but are expensive and are not easy to implement.

3.4.3) Innovative experimental methods in bubble columns

3.4.3.1) Laser Doppler Anemometry (LDA)

In LDA the velocity of a tagged fluid element is determined by an optical method. Particles (dust or artificially added tracer) moving within the fluid are illuminated with a focussed laser beam. These particles scatter light in all directions. The frequency of the scattered light is detected and is 'Doppler shifted' because of the movement of the particles. The change in frequency (Doppler shift) is used to determine the velocity of these particles. The change in frequency is linearly proportional to the velocity of the particle.

LDA offers the following advantages:

- non-intrusive method so there are no flow disturbances
- requires no calibration
- precise measurement of velocity components

The drawbacks of LDA are that it is extremely costly and without the proper expertise it is difficult to use.

Kulkarni et al. (2001) used LDA to successfully measure gas and liquid velocities as well as fractional gas hold-up in a 15cm diameter column.

3.4.3.2) Particle Image Velocimetry (PIV)

LDA measurements are used to obtain local liquid velocities. In contrast, PIV is a whole field measurement. In PIV, a cross section of the flow is illuminated by a laser-sheet and the movement of fluid is visualised by the detection of small tracer particles in the flow. Two subsequent images of the cross section are recorded, with an exposure time delay of Δt. The displacement of the particles Δx between the two images is used to calculate the velocity u as:

$$u = \frac{\Delta x}{M \Delta t} \tag{3-43}$$

where M is the magnification of the camera. By performing these calculations the instantaneous velocity field for the entire cross section of flow can be obtained.

The data obtained by PIV and LDA are useful in validating theoretical concepts and for validation of computational fluid dynamic (CFD) simulations. PIV shares the same drawbacks as LDA.

Deen (2001) is an excellent reference on the use of PIV experiments for bubble column hydrodynamic studies.

CHAPTER ONE

INTRODUCTION

In the field of chemical reactor engineering, the study of multi-phase sparged reactors is of prime interest to chemical engineers. Although there have been extensive modeling and experimental efforts focused on understanding the behaviour of these reactors, there has still been a slow development of fundamental theories for their behaviour due to the complex physical phenomena occurring in these reactors.

Complete and well defined reactor models are required for the prediction of the fluid mechanics of these reactors. These models are needed for reliable designing and scale-up of sparged reactors. Due to the slow development of fundamental theories for multi-phase reactors, the design of these reactors is currently an art rather than a science. This present "state of art" requires that model parameters be obtained from experimental data. This method of design requires accurate experimental data for confident and optimum design.

In general, the following parameters are required for design of multi-phase sparged reactors:

- hydrodynamics and flow regime
- phase hold-ups
- dispersion and back-mixing phenomena
- interfacial area, mass and heat transfer resistances
- residence time distribution data

Sasol's Research and Development division have identified several gas-liquid reactions which they would like to perform on an industrial scale. Some of these reactions involve the use of a homogeneous liquid catalyst. The problem that Sasol is faced with is that the reacting component in the liquid phase is present in trace quantities, and as they would like to perform their reactions with a stoichiometric quantity of gas, this results in very low quantities of gas being required to obtain target conversions.

Bubble column reactors are effective vessels for contacting gas-liquid systems. The gas is sparged into the reactor and the equipment falls into the family of multi-phase sparged reactors. Traditionally bubble column reactors are operated at high gas throughputs ($u_g > 5$ cm/s) to ensure that there is adequate mass transfer and effective heat transfer due to the well mixed nature of bubble columns. Sasol have conducted kinetic studies and mass transfer studies for their systems and found the reactions to be reaction rate limited. An extensive literature review has shown that there is a dearth in the literature on information for the hydrodynamic behaviour of bubble column reactors in the superficial gas velocity range of Sasol's interest ($u_g < 0.8$ cm/s).

At high gas throughputs it is easy to understand that the liquid phase will be well mixed, however at such low gas flow-rates the possibility of a deviation from normal bubble column behaviour could exist. There is also the danger that extrapolation of correlations developed with data for higher gas flow-rates could yield erroneous design parameters at much lower flow-rates.

Furthermore, there is limited knowledge on the behaviour of bubble column reactors in South Africa. Hence the purpose of this study was two-fold. Firstly to address the issue of the measurement of hydrodynamic parameters at superficial gas velocities less than 0.8 cm/s and secondly to develop a bubble column research group at the University of KwaZulu-Natal – Howard College Campus.

With the advent of Sasol moving from coal based technology to that of natural gas, there will be continual interest in the behaviour of gas-liquid systems and the equipment could be used for further research at the University of KwaZulu-Natal as more questions and problems concerning bubble column reactors arise.

This dissertation serves as an introductory study on the hydrodynamic behaviour of two-phase gas-liquid co-current bubble column reactors. The format of the dissertation diverts from the traditional one. The chapters are presented in a manner such that the reader is always provided with the pertinent information that is required for the subsequent chapters to become more meaningful. The chapters are ordered in a manner such that there is always a smooth transition from one topic to the next.

CHAPTER TWO

BUBBLE COLUMN REACTORS – AN OVERVIEW

This chapter will provide a brief description of bubble columns and their applications in industry. A bubble column reactor is a vertical vessel in which a gas is bubbled through either a moving liquid or in a batch liquid. Prior to 1980 very little research was conducted in bubble column reactors. Interest in bubble column reactors grew quickly with the revival in interest of coal liquefaction and slurry phase Fisher-Tropsch synthesis. Bubble column reactors have also found extensive use in biotechnological applications.

Bubble column reactors are favoured for the following reasons:

- very simple structure resulting in low cost
- lack of moving parts
- good heat and mass transfer properties
- high thermal stability (uniform temperature profile)
- low energy input (only gas compression)
- high circulation rate resulting in excellent mixing
- high liquid phase residence time

The disadvantages of bubble columns are:

- complicated hydrodynamic flow patterns
- uncertainties in scale-up
- short residence time of gas (determined by bubble rise velocity)
- volume demand increased due to back-mixing

2.1) Industrial applications of bubble columns

Bubble columns have found diverse applications in chemical industries. Table 2-1 gives a list of two-phase gas-liquid reactions carried out in bubble columns.

Table 2-1: Industrial scale reactions in gas-liquid systems (Deckwer, 1992)

Reaction	Main Product
Partial oxidation of ethylene	Acetaldehyde
Cumene oxidation	Cumene hydroperoxide
Chlorination of aliphatic and aromatic compounds	Chloroparaffin
Ethylation of benzene	Ethylbenzene
Hydroformulation of ethylene	Aldehydes and Alcohols
Hydrogenation reactions	

2.2) Modes and range of operation

Bubble columns may by operated without any internals or they may be staged, packed or operated as a loop reactor.

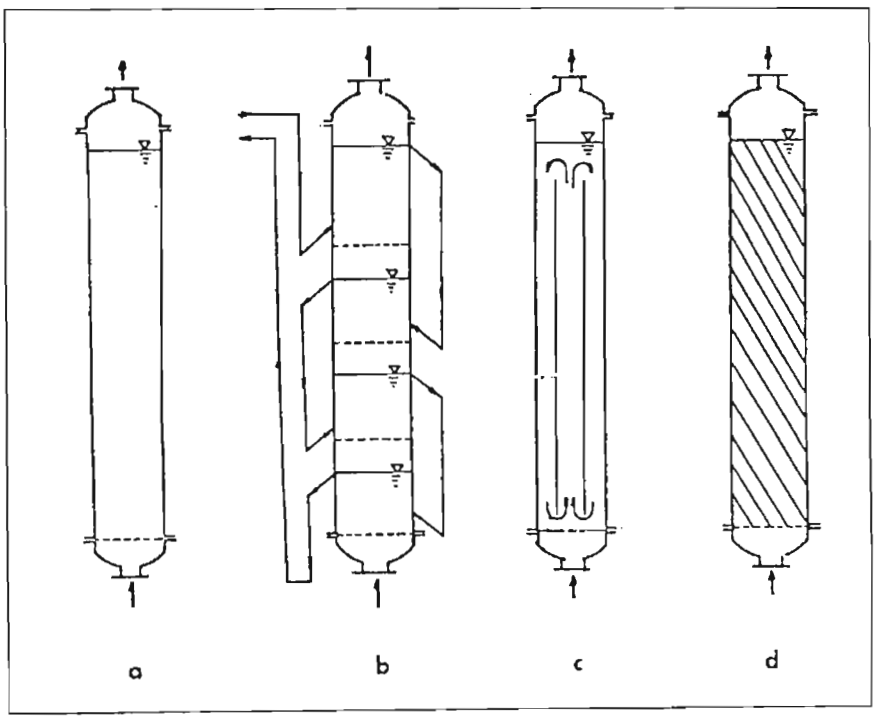

Figure 2-1: Types of gas-liquid bubble columns (Chen, 1986)

(a) simple (b) staged (c) loop-reactor (d) packed

The liquid phase has a much higher density than the gas phase, hence the liquid flow rate passing through a bubble column is low. The superficial gas velocity u_g based on empty reactor volume is typically in the range of 3-12 cm/s. The liquid and gas may be contacted in either a counter or co-current manner.

Table 2-2 summarizes the range of operating variables for bubble columns

Table 2-2: Range of operating variables for bubble columns (Shah and Deckwer, 1983)

Operating Variable	Size	Units
Volume: Chemical Process Industry	< 200	m^3
Volume: Biochemical Processes	< 3000	m^3
Diameter	0.2 – 20	m
Length to Diameter Ratio	3 – 10	
Superficial Gas Velocity	< 100	cm/s
Superficial liquid velocity	< 10	cm/s
Liquid Viscosities	0.5 – 100	mPa.s
Liquid Densities	0.6 – 2	g/cm^3
Liquid Surface Tensions	20 – 73	dyne/cm

2.3) Flow regimes and flow patterns

The phase hold-up, mixing and transport characteristics of a bubble column depend significantly on the prevailing flow regime in the column. Figure 2-2 shows the three observed flow regimes in bubble column reactors.

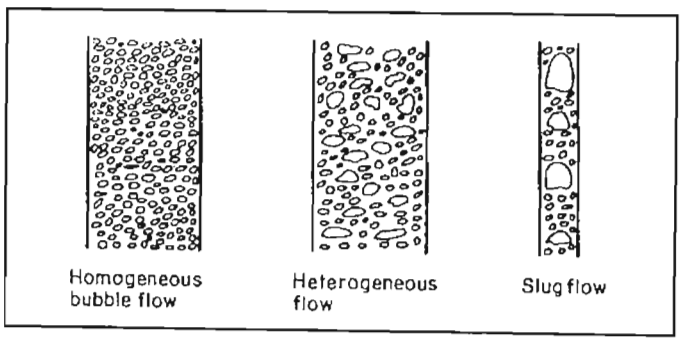

Figure 2-2: Flow regimes in bubble columns (Deckwer, 1992)

The three flow regimes shown above are normally observed as the gas flow rate increases (increasing flow rate from left to right in Figure 2-2).

The bubble flow regime occurs at low gas flows and is characterised by ordered chain bubbling. The churn-turbulent or heterogeneous regime is characterised by the onset of significant bubble coalescence and liquid circulation in the column. At very high gas flow rates, the gas bubbles coalesce to form large slugs.

The transition from one flow regime to another is not well defined. An approximate estimate of the boundaries can be obtained from Figure 2-3 for water and dilute aqueous solutions.

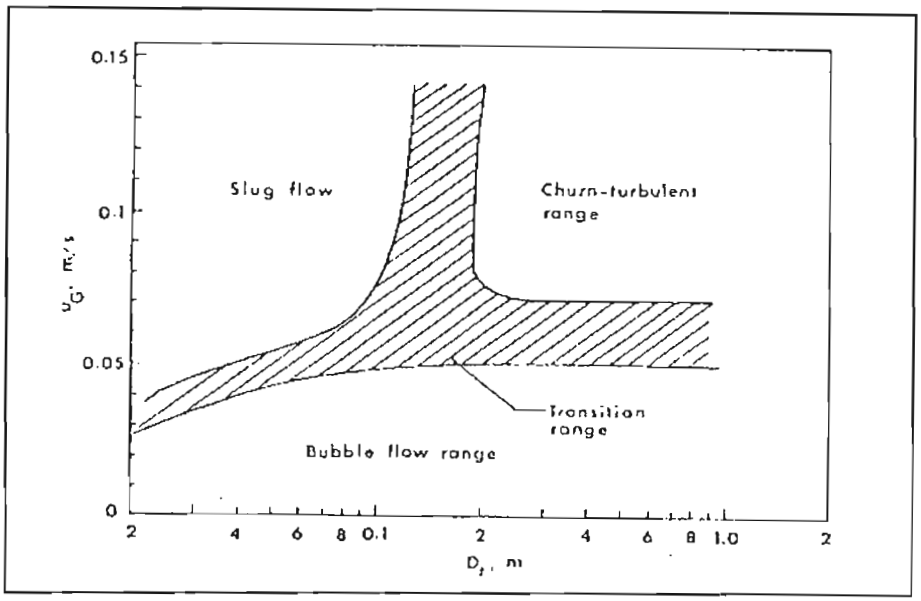

Figure 2-3: Approximate boundaries for flow regimes in gas-liquid bubble columns (Chen, 1986)

The detection of regime transition from homogeneous to churn-turbulent flow and the investigation of the transition regime are important. As the transition takes place, significant changes are observed in the hydrodynamic behaviour of the system.

The liquid flow patterns in bubble column reactors are complex. It is often assumed that large scale eddies with well defined circulation patterns are formed. The mechanism of liquid circulation is explained via the rising gas bubbles which entrain liquid with them, this amount of liquid being considerably greater in bubble column reactors than that corresponding to the liquid throughput (Deckwer, 1992). Continuity ensures that fluid returns down the column, producing a pronounced circulation pattern in which the central liquid is moving upwards and that next to the walls moves downwards (Figure 2-4).

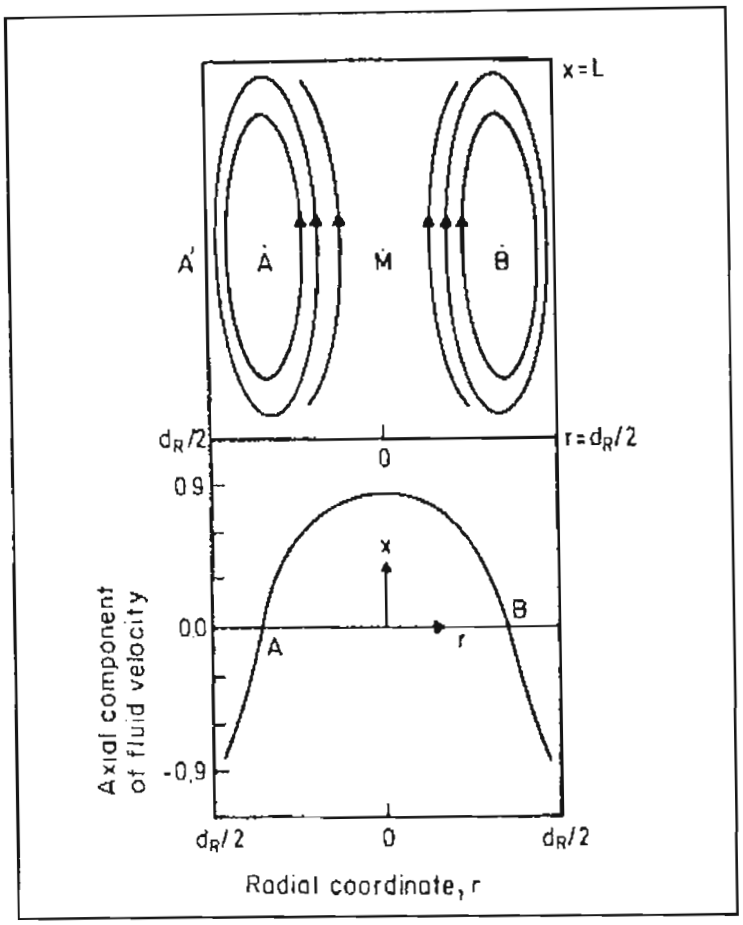

Figure 2-4: Liquid circulation velocity profile in an axial-symmetrical bubble column (Joshi and Sharma, 1979)

This circulatory flux is a function of gas flow-rate, column diameter, cross-sectional shape, gas hold-up, bubble diameter, bubble rise velocity and liquid viscosity (Deckwer, 1992). The zero-velocity point usually occurs at 0.7 of the column radius (Hills, 1974). Nottemkamper et al. (1983) performed velocity profile measurements which supported the findings of Hills (1974).

2.4) Gas distribution

The choice and design of the gas distributor influences the characteristics of the gas dispersion within the reactor. The gas distributor affects the hold-up, interfacial area and the mass transfer in bubble columns.

The gas may be dispersed through pores, holes, sintered plates, nozzles and perforated plates. Perforated plates and sieve plates are particularly useful for gas re-dispersion in cascade bubble columns. These dispersion methods are known as static gas distributors.

In contrast the dynamic twin jet variety of distributors such as an ejector jet, injector jet, venture jets and slit jets cause gas distribution by the kinetic energy generated by the liquid force.

Flexible spargers may also be used (Rice et al. 1980). For example a rubber plate will undergo a periodic deformation which aids in a uniform distribution of gas.

Deckwer (1992) asserts that there is no disadvantage in the gas distribution method used when the process taking place in the column is limited by the chemical reaction rate in the liquid phase. This is also indicative in the literature as the gas dispersion method has a very profound effect on the levels of mass transfer occurring in the column rather than on the dispersion levels.

Depending on the choice of distributor, gas distribution may occur in one of two ways. There may be even distribution of the gas across the reactor or distribution such that three easily identifiable zones may be observed as shown in Figure 2-5(b).

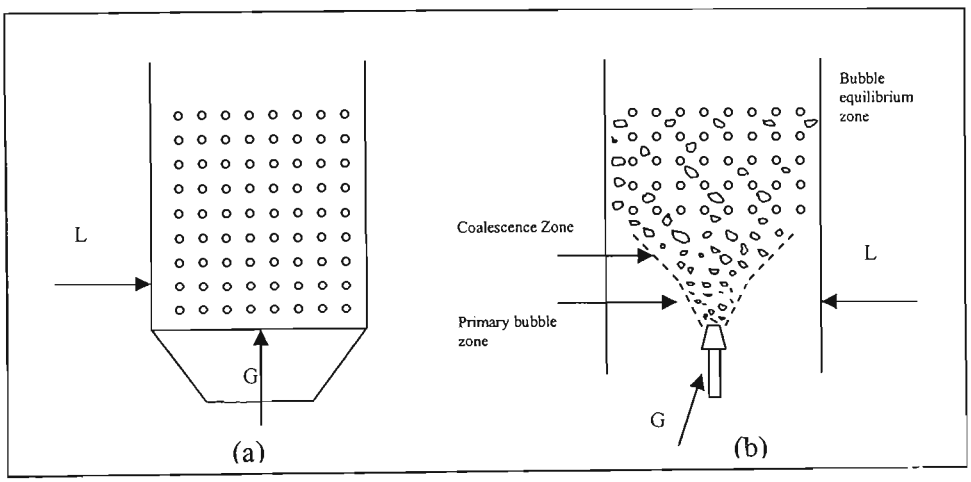

Figure 2-5: Gas distribution in bubble columns

(a) uniform distribution (b) distribution zones

2.5) Design parameters for bubble column reactors

The design, sizing and performance of bubble column reactors depend on the hydrodynamics, axial dispersion, mass and heat transfer and reaction kinetics.

Given the wide variety of gas-liquid reactions utilised in industry (Table 2-1) it becomes necessary to determine when a bubble column reactor will be the most effective means of contacting a gas with a liquid phase.

Other reactors in which a gas may be contacted with a liquid include:

- wetted or packed columns
- mechanically stirred vessels
- spray columns

Charpentier (1981) provides criteria for when the various reactors are suitable. To illustrate the choice of reactor consider a reaction in which a dissolved gas (component A) undergoes an irreversible second-order reaction with a reactant (component B) dissolved in the liquid. The stoichiometry of the reaction is given by

$$A + zB \xrightarrow{k_2} products$$

with the rate equation

$$r_A = k_2 C_A C_B = \frac{r_B}{z} \tag{2-1}$$

The ratio of the reaction rate to the mass transfer rate is represented by the dimensionless Hatta number:

$$Ha = \frac{\left(D_A k_2 C_{B0}\right)^{1/2}}{k_L} \tag{2-2}$$

with D_A, the diffusivity of A in the liquid, C_{B0}, the initial concentration of component B and k_L, the liquid mass transfer coefficient.

The value of the Hatta number provides an important indication of whether a large interfacial area a or a large liquid hold-up β is required for a particular reaction rate constant k_2. Table 2-3 summarises the criteria for selection of a gas-liquid reactor type.

Table 2-3: Selection of reactor for gas-liquid reactions

Reaction type	Ha range	Liquid hold-up	Reactor
Very slow reaction in liquid	Ha < 0.02	$\beta k_2 C_{B0}/k_L a \ll 1$	Bubble column
Slow reaction in liquid	0.02 < Ha < 0.3	$\beta k_2 C_{B0}/k_L a \gg 1$	Stirred tank
Moderately fast reaction	0.3 < Ha < 3	-	Plate column
Fast reaction	Ha > 3	-	Packed column

Table 2-3 shows that bubble column reactors are preferred for reactions in which a large bulk liquid volume are required.

2.5.1) Superficial gas velocity

The superficial gas velocity is the most import design parameter. The gas throughput determines the hydrodynamic characteristics of the bubble column reactor.

Schumpe et al. (1979) have shown that the maximum gas velocity for a reaction occurring in a bubble column is given by:

$$u_{G\,max} = \frac{1}{\varepsilon_G^{*}\left(1+\sqrt{\frac{k_L a^{*}}{k_2 C_B \varepsilon_G^{*}}}\right)} \qquad (2\text{-}3)$$

where a^{*} and ϵ^{*}_{G} are the interfacial area per unit volume and the average gas hold-up at $u_g = 1$ cm/s respectively. The authors have shown that the optimum superficial gas velocity for optimum space-time yield is approximately half the value of u_{Gmax}.

2.5.2) Pressure drop

The pressure drop due to friction at the reactor walls in bubble column reactors can be neglected. The pressure drop is composed of the drop exerted by the gas sparger and the hydrostatic head of the liquid. Therefore, the pressure profile within the column is given by:

$$P(z) = P_T\left(1 + \alpha(1 - z)\right) \tag{2-4}$$

where z is the dimensionless axial coordinate and, P_T the pressure at the top of the column, and α represents the ratio of the hydrostatic head to the pressure at the top of the column:

$$\alpha = \frac{\rho_L(1-\varepsilon_L)gL}{P_T} \tag{2-5}$$

where L is the dispersion height.

As the gas expands in the column, the axial variation in the pressure should be considered for the calculation of the local gas velocities, provided α is larger than 0.2 (Shah and Deckwer, 1983).

2.5.3) Bubble size and bubble distribution

The bubble size is important as it determines the mass transfer coefficient and the transfer area. Mashelkar (1970) states that for low gas velocities ($u_g < 0.5$ cm/s), the bubble diameter will be a strong function of the orifice diameter and a weak function of the gas velocity in the orifice. At gas velocities ranging from 0.5 to 10 cm/s the bubble diameter becomes a strong function of the gas velocity in the orifice. At higher gas velocities ($u_g > 10$ cm/s), both the orifice diameter and gas velocity will have a lesser effect on the bubble size. Bubble size is strongly affected by the surface tension of the liquid. It is well observed in the literature, that the presence of electrolytes in water results in the formation of smaller bubbles.

2.5.4) Gas hold-up and interfacial area

The gas hold-up ϵ_G is defined as the volume fraction of gas V_G present in the bubble column reactor. It is defined as:

$$\varepsilon_G = \frac{V_G}{V_G + V_L} \tag{2-6}$$

The gas hold-up provides an indication of the residence time and the effective interfacial area of the gas. Gas hold-up is not a constant quantity but varies locally in the axial and radial direction. In industry, the majority of reactors are operated under heterogeneous flow (Figure 2-2) conditions where the value of ϵ_G is typically in the range 0.1 to 0.4.

2.5.5) Mass transfer coefficients

Gas side resistances to inter-phase mass transfer are often negligible due to the slow reaction-absorption regime that bubble columns are often operated at. The liquid side volumetric mass transfer coefficient k_La is sufficient to describe the gas-liquid mass transfer rates (Deckwer and Schumpe, 1993). There have been many attempts to develop a theoretical prediction of liquid mass transfer coefficients in bubble columns; however they are of limited applicability. Figure 2-6 shows the how k_La values are affected by superficial gas velocity.

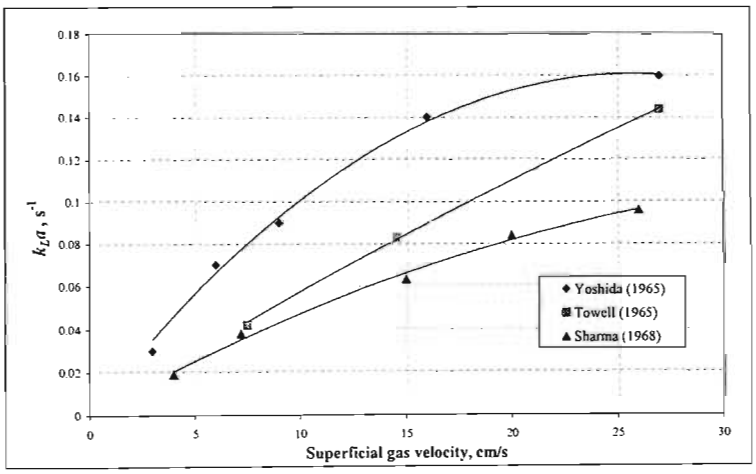

Figure 2-6: Liquid-side mass transfer coefficient in bubble columns as a function of superficial gas velocity

2.5.6) Heat transfer coefficients

A large number of the gas-liquid reactions are highly exothermic and hence heat removal becomes an important design feature. The well mixed nature of bubble columns results in a uniform temperature distribution throughout the reactor. The preferred means of heat removal is heat transfer through tubes within the reactor or through the walls of the reactor via a jacket. Deckwer (1992) reports that the heat transfer coefficients do not depend on the surface geometry of the heat transfer element. Mashelkar (1970) reports that the heat transfer rates in bubble columns compare well to those for mechanically agitated tanks.

2.5.7) Liquid mixing in bubble columns

Dispersion may be defined as the spreading of fluid particles as a result of departure from non-ideal flow. The fluid particles move forward in the direction of net flow, but at different speeds, thus resulting in the distribution of residence times. Dispersion occurring in a direction opposing the flow, such as that occurring in bubble columns is commonly known as back-mixing.

The back-mixing of the liquid phase in bubble columns has been the focus of many studies in literature and continues to be a subject under study. Back-mixing in bubble column reactors is affected both by the superficial gas velocity and the column diameter. Back–mixing influences the residence time distribution in the reactor and thus strongly influences the reaction yield and selectivity. Liquid back-mixing can be reduced by the incorporation of partition plates to sectionalise the column. It is common to make use of the axial dispersion model (ADM) to describe liquid phase mixing in bubble column reactors. In the ADM a lumped dispersion parameter E_L is used to represent the degree of back-mixing. The higher the value of E_L, the greater the degree of back-mixing in the reactor.

Mathematically, the axial dispersion model in the longitudinal z-direction is given by:

$$\frac{\partial C_B}{\partial t} = E_L \frac{\partial^2 C_B}{\partial z^2} - \frac{< u_L >}{1-\varepsilon_G} \frac{\partial C_B}{\partial z} + r_B \qquad (2\text{-}7)$$

with t as time, u_L, the superficial liquid velocity based on an empty reactor volume and E_L, the liquid back-mixing coefficient. E_L is an important design parameter and will be treated at length in Chapter 4.

The assumptions of the ADM are:

- negligible radial dispersion
- plug flow with constant velocity
- no stagnant pockets
- no bypassing or short-circuiting of fluid in the vessel

2.6) Scale-up considerations

Reactor performance is governed by the variables affecting the reaction and reactor specific quantities. The reaction specific data such as physical properties, stoichiometry, thermodynamics and kinetics are for the most part independent of reactor type and design.

In contrast, the reactor specific quantities are largely dependent on operating properties, physical properties, reactor geometry and type. It is the fluid dynamic phenomena and heat and mass transfer properties which cause the most difficulty in confident scale-up.

The fluid dynamics of the gas and liquid phases are often characterised by their respective residence time distributions (Chapter 3). A schematic drawing of the dependency of these phenomena is shown in Figure 2-7.

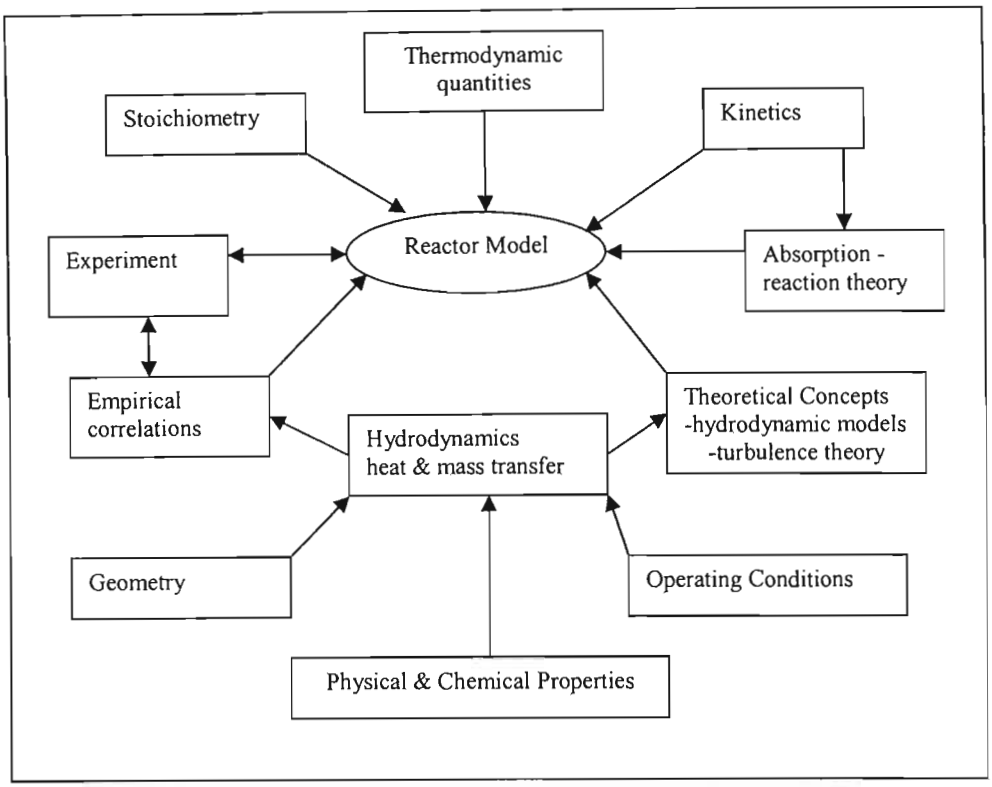

Figure 2-7: Design and modelling considerations for bubble column reactors

Correlations for parameter estimations are often developed under non-reactive conditions often referred to as "cold flow" measurements. Cold flow measurements are performed independently of a reaction in order to isolate the hydrodynamic phenomena. The subject of parameter estimation is covered in great depth in Chapter 4.

CHAPTER THREE

HYDRODYNAMICS OF BUBBLE COLUMN REACTORS: EXPERIMENTAL METHODS

The questions that reactor designers and engineers take into consideration can be categorised as follows:

1. What to measure?
2. Why to measure?
3. How to measure?

The answers to questions 1 and 2 have been outlined in Chapter 2. This chapter will focus primarily on experimental methods for measuring axial dispersion coefficients and gas hold-up in bubble column reactors. A brief description of experimental methods for measuring other hydrodynamic quantities will be provided as well as an account of current innovations in the measurement of bubble column hydrodynamics.

3.1) Measurement of liquid phase dispersion

Mechanisms responsible for the mixing in bubble columns are:

- turbulent eddies in the main liquid stream as well as eddies introduced by the movement of the dispersed gas phase relative to the continuous liquid phase
- liquid entrainment in the wakes of the bubbles combined with mass exchange between these wakes and the liquid phase
- molecular diffusion

It is difficult to deal with the analysis of the possible contribution from each individual mechanism. Instead, simplified models such as the one dimensional axial dispersion model are often assumed to represent the overall mixing phenomena. Dispersion may be defined as the spreading of fluid particles as a result of the departure from ideal plug and perfectly mixed flow conditions. The degree of dispersion may be obtained from tracer experiments such as residence time distribution studies and batch liquid mixing tests.

3.1.1) Residence time distribution theory

To predict the behaviour of a vessel as a chemical reactor, knowledge of the passage of the fluid through the vessel is required. Ideally, it would be required to tag and follow every molecule on the micro-scale to predict the exact behaviour of the fluid elements. The complexities of this approach make it impractical to implement experimentally. However, the distribution of residence times of molecules within the reactor can be determined by the stimulus-response technique. In this technique a quantity of tracer is injected into the inlet feed of the reactor and its resulting exit concentration profile is monitored with time.

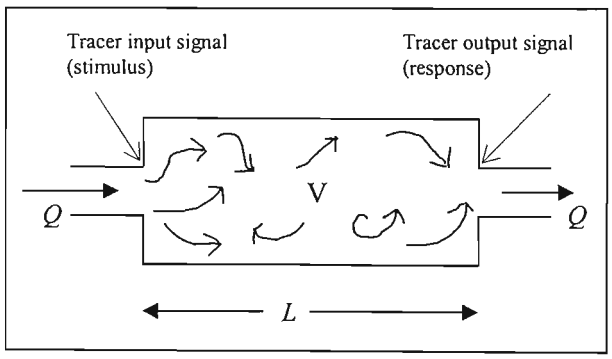

Figure 3-1: Schematic showing tracer input and signal response in a reactor vessel

The tracer input signal may be random, cyclic, a step or a pulse. The stimulus-response technique determines the form of the response of the tracer. Due to ease of analysis, step tracer and pulse (Dirac delta function) inputs are generally preferred over the other input signals. Analysing the response provides information on the behaviour of the system.

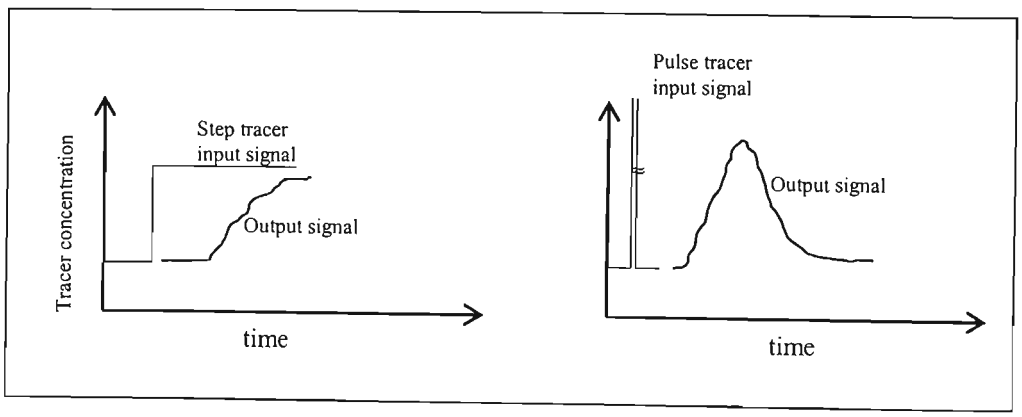

Figure 3-2: Stimulus-response signals to study the behaviour of flow systems

In general, different elements of fluid following different paths will take different periods of time to pass through the vessel. For a single fluid, under steady-state flow, without reaction and without density change, the average retention time (mean residence time) of the fluid in a vessel of volume V and length L is given by:

$$\bar{t} = \tau = \frac{V}{Q} = \frac{L}{u} \tag{3-1}$$

where Q is the volumetric flow-rate of the fluid under consideration.

Eq. 3-1 only holds for closed vessels and for the effective volume of the vessel. In the case of multiple phases and the presence of dead volume (due to internals or stagnant zones) the effective volume and flow rate of the phase under consideration must be used for V and Q respectively.

For a multi-phase system, the hold-up ϵ of phase P can be calculated from:

$$\varepsilon_P = \frac{u_P \bar{t}_P}{L} \tag{3-2}$$

A dimensionless time variable which measures time in units of mean residence time can be defined as:

$$\theta = \frac{t}{\bar{t}} \tag{3-3}$$

The exit age distribution $\boldsymbol{E}$ of a fluid leaving the reactor is a measure of the distribution of residence times of the fluid within the vessel. The age is measured from the time the fluid elements enter the vessel. A typical exit age distribution for a continuously stirred tank is shown in Figure 3-3.

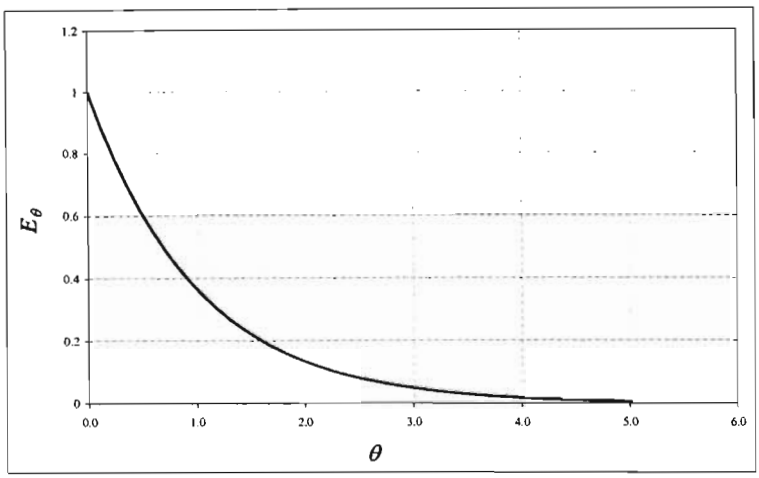

Figure 3-3: A typical exit age distribution for a CSTR

$\boldsymbol{E}$ is defined in such a way that $\boldsymbol{E}\, d\theta$ is the fraction of material in the exit stream with age between θ and $\theta + d\theta$. The area under an $\boldsymbol{E}$ versus θ curve is found to always be:

$$\int_0^\infty \boldsymbol{E} d\theta = 1 \tag{3-4}$$

Eq. 3-4 serves as a check on the mass balance of the tracer to determine that there are no errors in the tracer measurement.

To get to $\boldsymbol{E}$, a relationship between the concentration-time curve c and the exit age distribution must be used. Levenspiel (1962) shows that:

$$\boldsymbol{E}(t) = c(t) \times \frac{M}{Q} \tag{3-5}$$

with $\boldsymbol{E}(t)$ in units of s^{-1} and where M is the mass of tracer input into the system. $\boldsymbol{E}$ is related to $\boldsymbol{E}(t)$ by:

$$\boldsymbol{E} = \boldsymbol{E}(t) \times \tau \tag{3-6}$$

Associated with every age distribution, $y = f(x)$, are two sets of parameters called the moments of the distribution. The k^{th} moment about the origin is defined by:

$$M_k' = \frac{\int_0^\infty x^k f(x)\,dx}{\int_0^\infty f(x)\,dx} \tag{3-7}$$

and the k^{th} moment about the mean μ of the distribution is defined by:

$$M_k = \frac{\int_0^\infty (x-\mu)^k f(x)\,dx}{\int_0^\infty f(x)\,dx} \tag{3-8}$$

A particular distribution can be completely defined by its moments, and hence distributions can be compared by their moments without comparing the actual curves themselves (Levenspiel, 1962).

3.1.1.1) Determination of E, τ, μ *and* σ^2 from a concentration-time curve

From the concentration-time curve c:

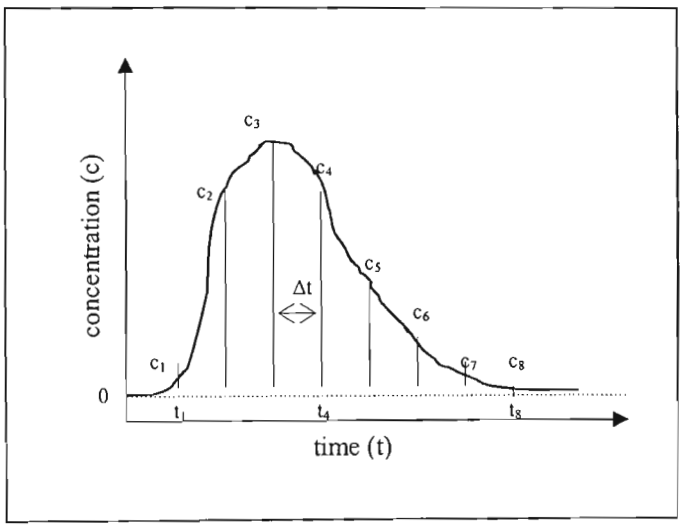

Figure 3-4: Concentration-time response to pulse input

the mean residence time can be found from:

$$\bar{t} = \frac{\int_o^\infty tcdt}{\int_o^\infty cdt} \approx \frac{\sum_i t_i c_i \Delta t_i}{\sum_i c_i \Delta t_i} = \frac{V}{Q} \tag{3-9}$$

The exit age distribution $\boldsymbol{E}(t)$ is given by:

$$\boldsymbol{E}_i(t_i) = \frac{c_i}{\sum_i c_i \Delta t_i} \tag{3-10}$$

The mean μ of the distribution is defined as:

$$\mu = M_1 = \frac{\int_0^\infty xf(x)dx}{\int_0^\infty f(x)dx} = \frac{\sum_i t_i c_i \Delta t_i}{\sum_i c_i \Delta t_i} = \bar{t} \tag{3-11}$$

The second moment about the mean, commonly called the variance σ^2, measures the spread of the distribution about the mean. It is defined as:

$$\sigma^2 = M_2 = \frac{\int_0^\infty (x-\mu)^2 f(x)dx}{\int_0^\infty f(x)dx} = \frac{\sum_i (t_i-\mu)^2 c_i \Delta t_i}{\sum_i c_i \Delta t_i} \tag{3-12}$$

For equidistant points, Eq. 3-12 reduces to:

$$\sigma^2 = \frac{\sum_i t_i^2 c_i}{\sum_i c_i} - \mu^2 \tag{3-13}$$

3.1.1.2) Methods of using age distribution information

Tracer information is used either directly or in conjunction with flow models to predict performance of real flow reactors, the method used depending in large part on whether the reactor can be considered a liner system or whether it must be treated as a non-linear system.

A process is linear if any change in stimulus results in a corresponding proportional change in response. That is:

$$\frac{\Delta(response)}{\Delta(stimulus)} = \frac{d(response)}{d(stimulus)} = \text{constant} = k \qquad (3\text{-}14)$$

For linear systems where the tracer has no unusual behaviour but merely passes through the reactor and the kinetic reaction rate is also linear in concentration, a flow model is not required to determine the conversion. The tracer information together with the kinetic reaction data is sufficient to describe the behaviour of the vessel as a reactor. A variety of flow patterns can give the same tracer output curve. For linear processes, however, these all result in the same conversion (Levenspiel, 1962).

For reactions and processes which are not linear in concentration, conversion cannot be found using age distribution information directly. A flow model is required to determine the conversion in the reactor. Flow models are described by mathematical descriptions, boundary conditions and initial conditions.

3.1.2) Boundary conditions

The analysis and measurement of residence time distribution experiments are subject to many errors:

- experimental errors in the tracer measurements
- mathematical errors in the analysis of the tracer response measurements
- application of wrong boundary conditions

For example erroneous dispersion coefficients can be obtained if open-open boundary conditions are used when closed-closed boundary conditions are more representative of the system.

A closed vessel is defined as one in which material passes in and out by bulk flow only. Thus dispersion or diffusion is absent at the entrance and exit, so there is no movement of material upstream and out of the vessel by swirls or eddies. In contrast, an open vessel permits the movement of material across its boundaries as shown in Figure 3-5.

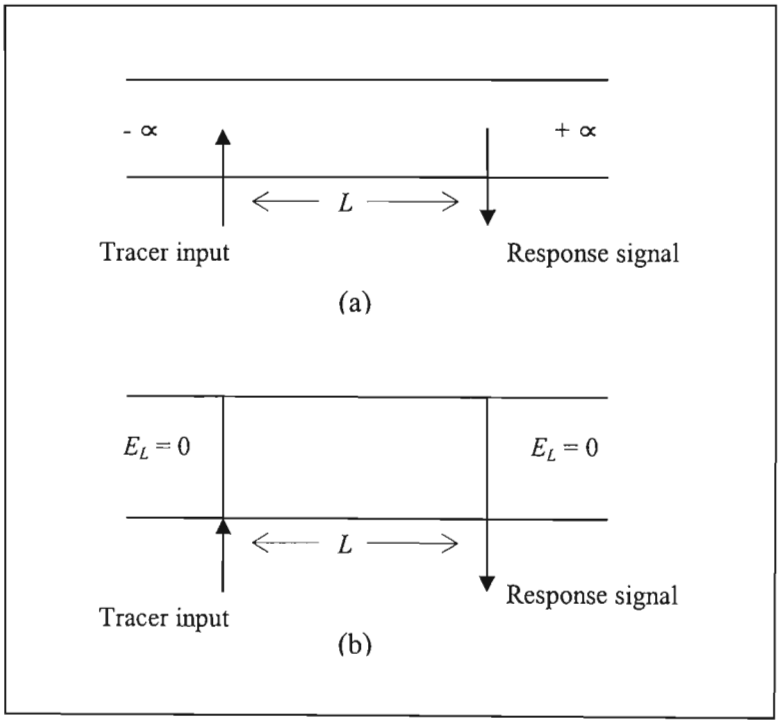

Figure 3-5: Boundary conditions (a) open-open (b) closed-closed

Levelspiel (1962) reports that for high values of *Pe* number [$(u_L L / E_L) > 78$] the effect of boundary conditions becomes negligible. However, this criteria is seldom achieved in bubble column experimental conditions and Ityokumbul et al. (1988) reports that many researchers prefer open-open boundary conditions since it yields a simpler analytical solution for mathematical flow models. They showed that the open-open Peclet number Pe_{oo} is related to the closed-closed Peclet number Pe_{cc} by:

$$\frac{Pe_{cc}}{Pe_{oo}} = 0.70 Pe_{oo}^{\,0.073} \tag{3-15}$$

It is recommended that closed-closed boundary conditions be used in the analysis of bubble columns (Deckwer, 1992).

3.1.3) Non-steady-state stimulus-response techniques for determining E_L

Non-steady state methods allow for a transient analysis of bubble column reactors.

3.1.3.1) Batch liquid measurements

This method has been utilised extensively in the literature. Ohki and Inoue (1970) is a well cited paper. Mixing time measurements, where the time required to reach a specific level of concentration uniformity $C_L/C_O < 1$, are used to obtain liquid dispersion coefficients. The term mixing is used here to denote movement, distribution, or diffusion of a component through a reaction vessel, tending to make fluid composition uniform throughout. Mixing eliminates concentration gradients in a reactor. In batch mixing experiments, tracer is injected as a pulse into the batch liquid phase and the resulting concentration is measured at a particular distance away from the feed point position (Figure 3-6).

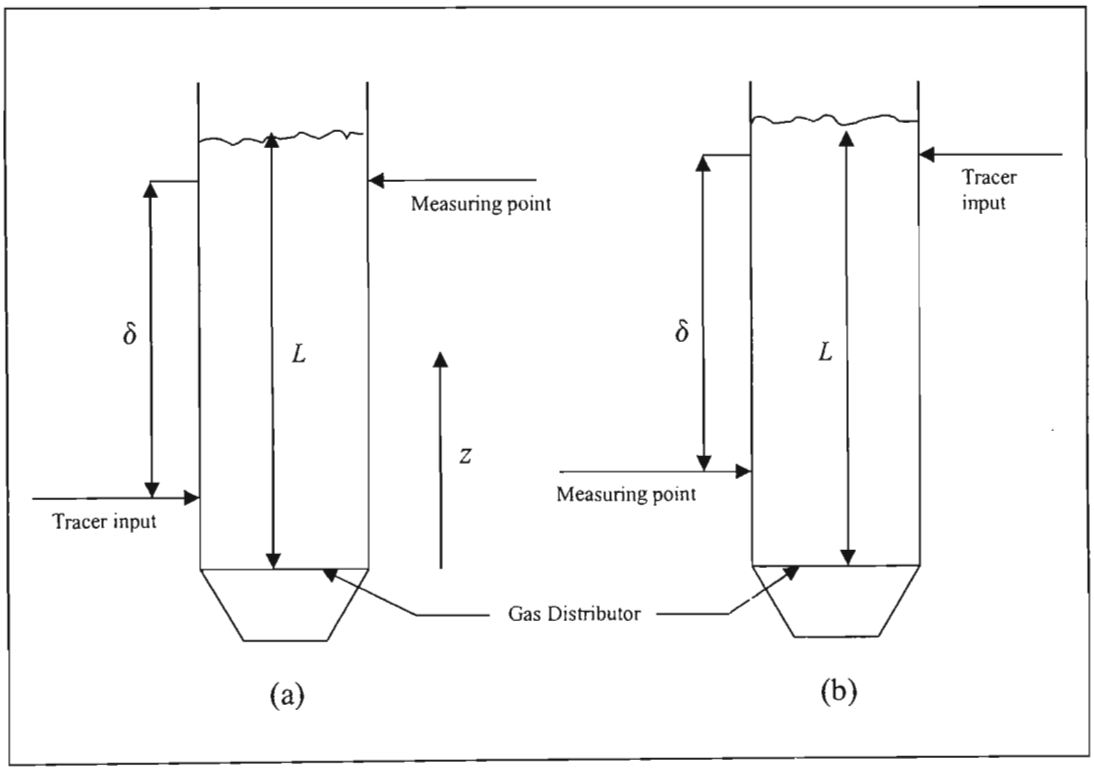

Figure 3-6: Tracer input and measurement points for batch liquid measurements

(a) input from bottom of reactor (b) input from top of reactor

The difference between the tracer inputs with respect to the top of the reactor is that this is a test for back-mixing. If no back-mixing occurred the tracer would not be detected upstream from the tracer input. Input from the bottom of the reactor, as in Figure 3-6(a), assumes that back-mixing occurs.

The one dimensional axial dispersion model (ADM) may be assumed when the distance between the injection point of tracer and the measuring point are sufficiently long. The longitudinal dispersion coefficient E_L is used to express the characteristics of the liquid mixing in bubble columns.

The mathematical description of the spreading of the tracer is described in an analogy to Fick's second law:

$$\frac{\partial C}{\partial t} = E_L \frac{\partial^2 C}{\partial z^2} \tag{3-16}$$

with closed-closed boundary conditions:

$$\frac{\partial C}{\partial z} = 0 \text{ at } z=0 \text{ and } z=L \tag{3-17}$$

The initial conditions are:

$$C(z,0) = C_i \text{ for } 0 \leq z \leq \lambda \tag{3-18}$$

$$C(z,0) = 0 \text{ for } z \geq \lambda \tag{3-19}$$

where λ is the height of the column corresponding to the volume of tracer injected.

Solution of Eqs. 3-16 to 3-19 gives:

$$\frac{C}{C_o} = 1 + 2\sum_{n=1}^{\infty}\left(\cos\frac{n\pi}{L}\delta\right)\exp\left(-\frac{n^2\pi^2}{L^2}E_L t\right) \tag{3-20}$$

Ohki and Inoue (1970) determined that six terms are sufficient to evaluate E_L with an error under one per cent.

Figure 3-7 shows C/C_o as a function of the dimensionless group $E_L t/L^2$ for various values of (δ/L). Deckwer (1992) reports that the measuring technique works best for (δ/L) values approximately equal to 0.8.

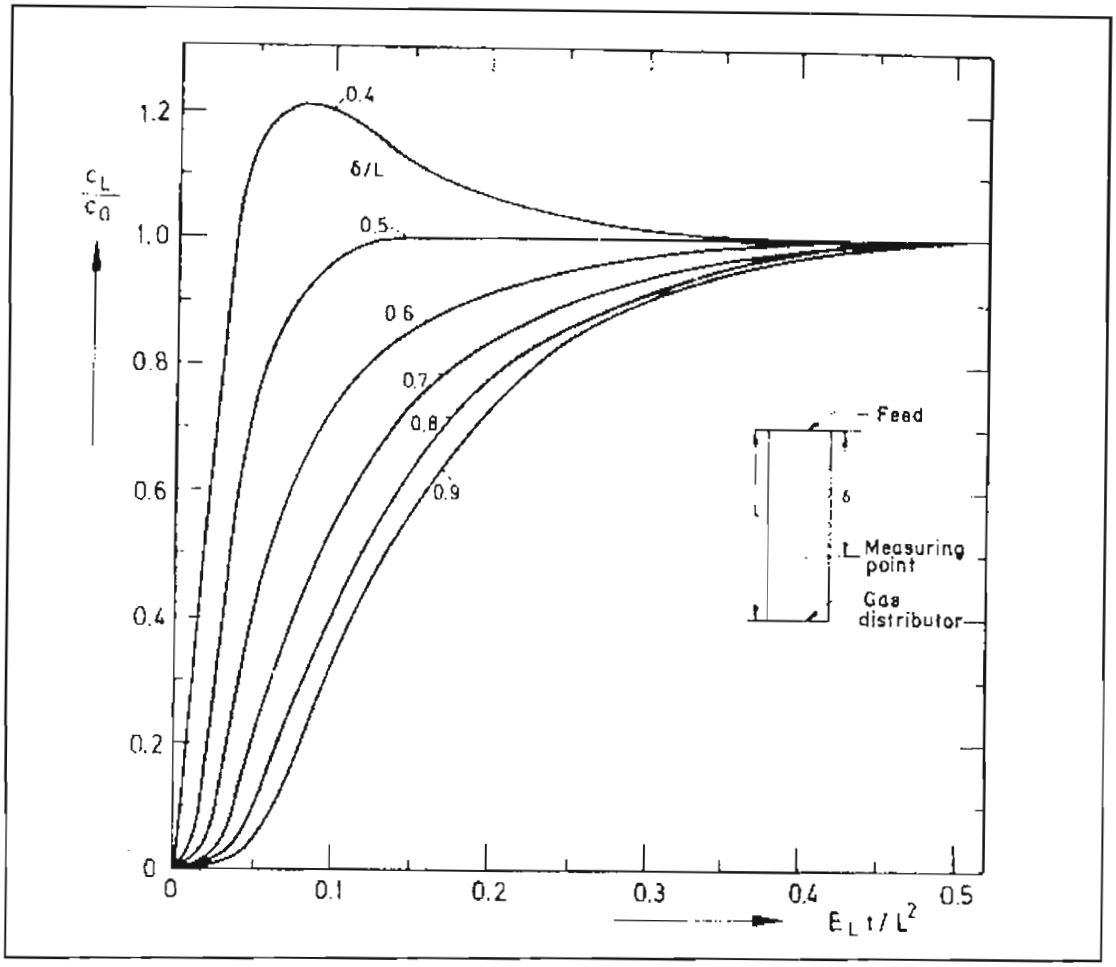

Figure 3-7: Dynamic concentration curves. Parameter: ratio of distance between feed and measuring point and reactor length (δ/L) (Deckwer, 1992)

Figure 3-7 can be used for the evaluation of E_L.

3.1.3.2) Continuous liquid RTD measurements

For a gas-liquid reaction, the chemical transformation takes place essentially in the liquid phase. Therefore, the residence time distribution (RTD) in this phase is of particular interest. The residence time distribution can be recorded when the liquid phase passes continuously through the reactor and from this the dispersion coefficient can then be calculated using an appropriate model for the liquid phase.

The one-dimensional axial dispersion equation for the system is (Levenspiel, 1962):

$$\frac{\partial c}{\partial t} = E_L \frac{\partial c^2}{\partial z^2} - \frac{u_L}{1-\varepsilon_g}\frac{\partial c}{\partial z} \tag{3-21}$$

Bischoff and Philips (1966) performed longitudinal mixing tests using the axial dispersion model. The authors note that there is the possibility of a "decay" in turbulence down stream from the gas distributor plate which means that the dispersion coefficient should properly vary with length. However, a proper account of this longitudinal dependency would severely complicate the model and it is common practice to use a constant liquid dispersion coefficient E_L. Baird and Rice (1975) showed that turbulence is isotropic in bubble column reactors and as such dispersion levels are approximately constant in the axial direction.

The closed-closed boundary condition at the entrance ($z = 0$) is:

$$c_{T0} = -\frac{E_L}{u_L}\left(\frac{\partial c}{\partial z}\right)_{z=0^+} + c\left(0^+, t\right) \tag{3-22}$$

and at the exit ($z = L$) is:

$$\frac{\partial c}{\partial z} = 0 \tag{3-23}$$

For a pulse tracer input the analytical solution, at $X = z/L$, to the governing equation is given by Field and Davidson (1980):

$$\frac{c_X}{C_0} = 2\exp\left[P(2X-\theta)\right]\sum_{k=i}^{\infty}\left[\lambda_k \exp\left(-\lambda_k^2/\theta\right)\frac{\lambda_k\cos(2\lambda_k X)+P\sin(2\lambda_k X)}{\lambda_k^2+P^2+P}\right] \tag{3-24}$$

where P is given by:

$$P = \frac{u_L L}{4E_L} \tag{3-25}$$

C_o is given by the concentration of the mass of tracer M in the bulk liquid volume V_L:

$$C_o = \frac{M}{V_L} \tag{3-26}$$

and λ_k are the roots of

$$\tan(2\lambda) = \frac{2\lambda P}{(\lambda^2 - P^2)} \tag{3-27}$$

and θ is given by Eq. 3-3.

Field and Davidson (1980) state that when $\theta = 0.1$ the first nine roots were used. The number of roots (λ_k) required decreases as T increases.

Eq. 3-24 can be used to fit experimental data in time and space. However dispersion coefficients can be calculated from the variance σ^2 and mean μ of measured RTD. It should be noted that the shape of the concentration-time curve as predicted by the ADM cannot be generated from these two parameters only.

It can be shown (Deckwer, 1992) that the variance of the RTD data can be related to the Peclet Number:

$$Pe_L = \frac{u_L L}{E_L} \tag{3-28}$$

For open-open boundary conditions (Figure 3-5a):

$$\sigma^2 = \frac{2}{Pe_L} + \frac{8}{Pe_L^2} \tag{3-29}$$

and for closed-closed boundary conditions (Figure 3-5b):

$$\sigma^2 = \frac{2}{Pe_L} - \frac{2}{Pe_L^2}(1 - e^{-Pe_L}) \tag{3-30}$$

where the variance σ^2 is given by Eq. 3-12.

Eqs. 3-29 or 3-30 can be solved for the Pe_L and E_L can be determined from Eq. 3-28 since u_L and L are known. This is much simpler than curve fitting in time-space.

3.1.4) Steady state method to determine liquid dispersion coefficients in bubble columns

The dispersion coefficient may be determined from steady-state measurements of axial concentrations in the reactor. The tracer is introduced from a continuous source and its concentrations are measured at different axial locations upstream of the source. The distribution of the tracer is measured either directly or by sampling as shown in Figure 3-8. The tracer should be added through a source uniformly over the cross-sectional area but can be just as effectively fed in through a distributor ring $0.707D_c$ in diameter (Deckwer, 1992).

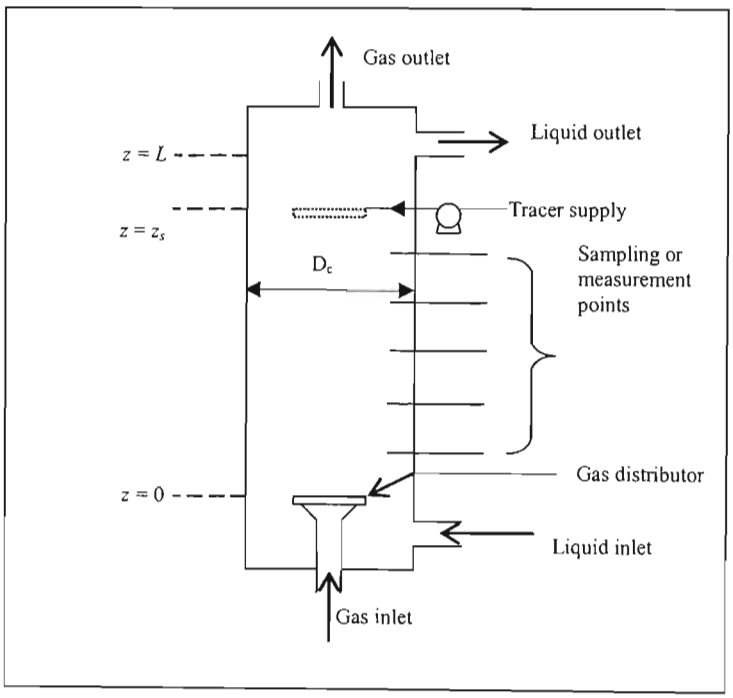

Figure 3-8: Experimental arrangement for recording concentration profiles based on the steady-state method

A mass balance of the tracer for co-current flow gives:

$$E_L \frac{\partial^2 c}{\partial z^2} - u_L \frac{\partial c}{\partial z} = 0 \qquad (3\text{-}31)$$

Subject to the boundary conditions:

$$c = \frac{E_L}{u_L}\frac{\partial c}{\partial z} \quad \text{at } z=0 \tag{3-32}$$

$$c = c_o \qquad \text{for } z_s \leq z \leq L \tag{3-33}$$

The solution of Eq. 3-31 is given by:

$$c = c_o.\exp\left[-\frac{E_L}{u_L}(x_s - x)\right] \tag{3-34}$$

A typical steady-state concentration profile is shown in Figure 3-9.

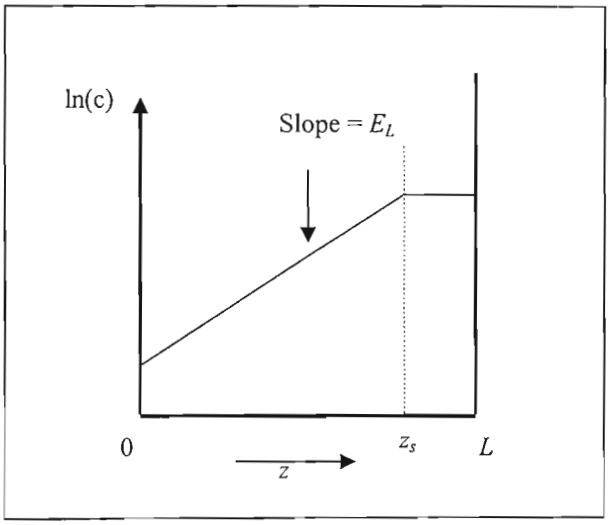

Figure 3-9: Typical steady-state concentration profile in a bubble column

E_L can be calculated from the slope of the straight line gradient of a plot of ln(c) against z.

3.1.5) Comparison of methods

Deckwer (1992) reports that although the steady-state method is expensive and time-consuming it produces the most reliable information on dispersion patterns in the liquid phase. The steady-state method also reveals information on the constancy of the dispersion coefficient in the axial direction. The non-steady state mixing test is easier to implement and Deckwer reports that there is very little variation in dispersion coefficient obtained via the two methods (Figure 3-10).

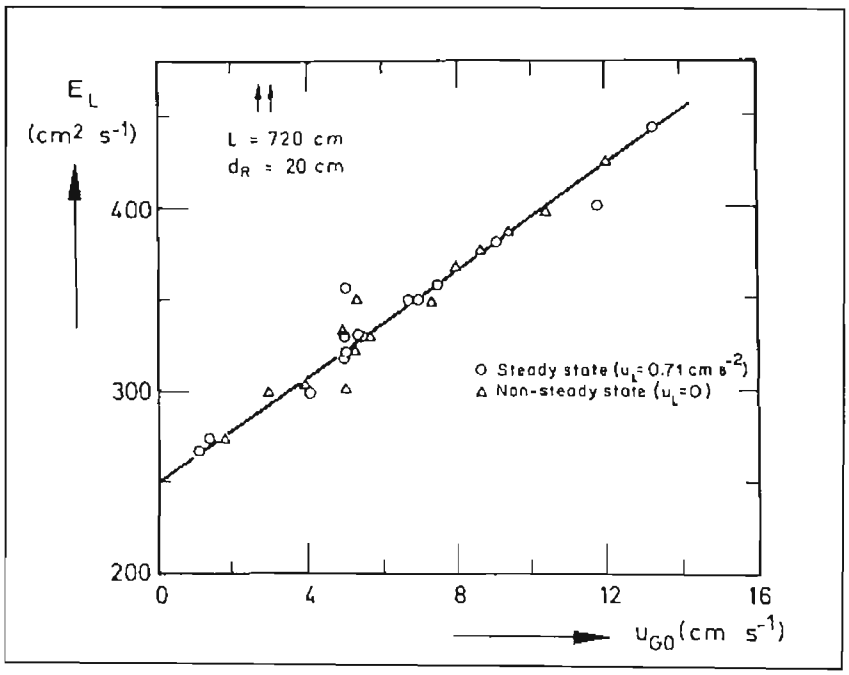

Figure 3-10: Comparison of dispersion coefficients as a function of gas velocity for steady-state and non-steady-state methods (Deckwer, 1992)

Deckwer also states that non-steady-state measurements with continuous flow do not reveal advantages in comparison with mixing time measurements for bubble columns. Continuous flow RTD measurements are recommended for bubble column cascades.

3.1.6) Choice of tracer for determination of E_L

It is well known that the selection of a tracer must meet the following specifications:

- have similar physical properties to the fluid of interest
- be easily detectable
- not change the hydrodynamics within the vessel
- no transfer of tracer between phases

Table 3-1 shows some tracers and detectors that are commonly used in bubble column research.

Table 3-1: Typical tracers and detectors for liquid phase experiments

Tracer	Example	Detector	Reference
Electrolyte	NaCl	Conductivity meter	Ohki and Inoue (1970)
Dye	$KMNO_4$	Spectrophotometer	Deckwer et al. (1974)
Concentrated acid	HCl	pH meter	Ityokumbul et al. (1974)
Heat		thermocouple	Kelkar et al. (1983)
Radioactive particle	Bromine 82	Scintillation counter	Field & Davidson (1980)

The mechanism of thermal dispersion is governed by liquid mixing and as such the transport of heat is used to determine liquid mixing coefficients. Ityokumbul et al. (1994) question the validity of this analogy as the transport of heat is effected by both the gas and liquid phases while the mass transport is effected by the liquid phase only. The use of heat as a tracer is particularly useful for liquid regeneration. Experimentally it is also difficult to implement as great care must be taken to ensure that the equipment is perfectly insulated and that the input flux is maintained at constant temperature.

Radioactive methods offer the benefit that detection may occur externally of the column as it is a non-intrusive measurement technique. However, the safety concerns far outweigh this advantage.

The use of absorption spectrophotometry is limited due to difficulty in calibration (usually non-linear) and the colour tainting of the columns and auxiliary equipment. Colour measurements are usually undertaken by sampling as it is extremely difficult to perform absorption spectrophotometry on a real-time basis.

For these reasons, conductivity and pH measurements are more common in the literature as there is ease in calibration (linear) and detection is relatively straight forward.

There does not appear to be any difference in the dispersion coefficient obtained by the various methods as Deckwer et al. (1974) reported that electrolyte, dye and heat were used as a tracer and each yielded identical dispersion coefficients.

3.2) Measurement of phase hold-up

The fraction of gas or liquid in a gas-liquid dispersion is referred to as the relative gas or liquid hold-up where the gas hold-up ϵ_G is given by Eq. 2-6 and the liquid hold-up ϵ_L by:

$$\varepsilon_L = \frac{V_L}{V_G + V_L} \tag{3-35}$$

For a gas-liquid system it is evident that:

$$\varepsilon_L + \varepsilon_G = 1 \tag{3-36}$$

The phase hold-ups represented by Eqs. 2-6 and 3-35 are representative of the average bulk phase hold-up across the reactor. Usually, these values are adequate to design the reactor as the average bulk hold-ups directly determine the total reactor volume required. In actuality the liquid and gas hold-ups are complex functions of both time and location (Deckwer, 1992).

There are many methods for measuring the fractional phase hold-ups in a bubble column reactor:

- physical methods
- optical methods
- radiation methods
- electrical methods

The most popular methods are via the measurement of bed expansion and the pressure drop measurement technique and will be discussed here. Details of the other methods can be found in Joshi et al. (1990).

3.2.1) Measurement of bed expansion

This is a simple method where measurements of the bed height are taken with the dispersed gas phase in the reactor H_D and measurements of the clear liquid height H_L are taken. The gas fraction being determined by:

$$\varepsilon_G = \frac{H_D - H_L}{H_D} \tag{3-37}$$

This allows for an average value of the fraction gas phase hold-up. The method makes no allowance for end effects such as the presence of a foam cap and is difficult to implement when the level continuously fluctuates.

3.2.2) Pressure drop measurement technique

The average gas hold-up is determined by measuring static pressures at several points along the column height. Neglecting pressure drop due to fluid friction and other losses, the difference in pressure between the column top P_T and at axial position $P(z)$ is given by:

$$P(z) - P_T = g\rho_L (H_D - z)[1 - \varepsilon_G(z)] \tag{3-38}$$

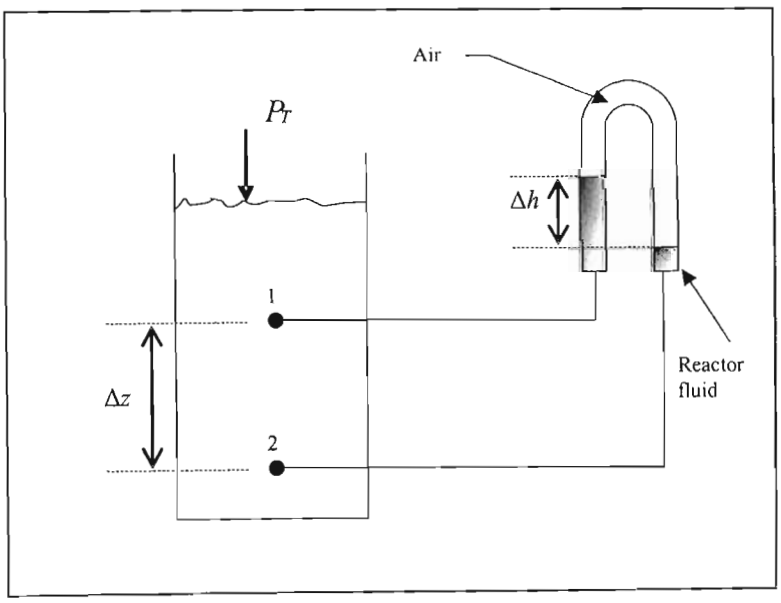

Figure 3-11: Pressure measurement in a bubble column with an inverted U-tube

The relative gas hold-up at position $z = (z_1+z_2) / 2$ between two points Δz apart results from the pressure difference $\Delta P = P(z_2) - P(z_1)$:

$$\varepsilon_G(x) = 1 - \frac{\Delta P}{\rho_L g \Delta z} = 1 - \left(\frac{\Delta h}{\Delta z}\right) \tag{3-39}$$

3.2.3) Determination of gas hold-up from RTD measurements

In two-phase systems the liquid residence time RTD will yield the liquid hold-up via Eq. 3-2. The gas hold-up can then be found by difference via Eq. 3-36.

3.3) Measurement of bubble size

The major characteristics of bubbles which are of vital importance from the design point of view are size, shape and terminal velocity. These parameters decide the interfacial areas and the residence time of the gas phase. There are various methods to determine the size and size distribution of bubbles:

- photographic methods
- impact methods
- thermal methods
- electrical methods
- optical methods
- residence time methods
- chemical methods

The principles and application of these methods are covered at great length by Joshi et al. (1990).

The photographic method is a relatively simple technique which generates reasonably accurate results. A major disadvantage of this method is that the curvature of cylindrical columns affects the size of the bubble in the photograph.

A popular method in the literature is based on resistivity or conductivity. Here, the difference in electrical properties of two different phases is used to measure the bubble diameter and its velocity of rise. Two or more needle electrodes (eg. platinum wire) are inserted into the column and the resulting conductivity-time profiles are analysed.

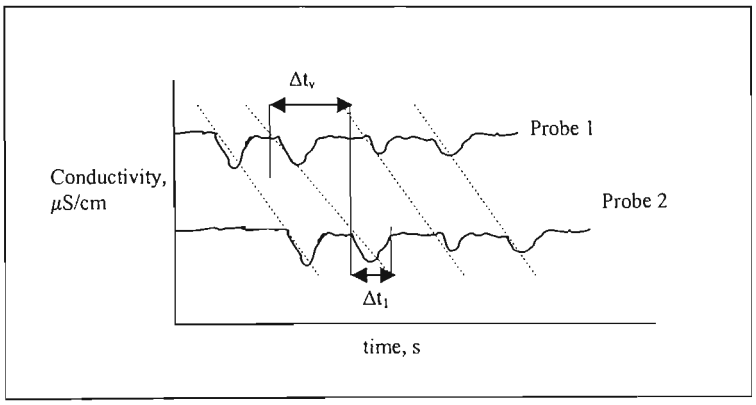

Figure 3-12: Illustrative recording of bubbles detected by electrodes

From conductivity-time measurements Ohki and Inoue (1970) showed that the mean rise velocity u_b of bubbles can be calculated from the average time of passage between the electrodes Δt_v:

$$v_b = \frac{\Delta l}{\Delta t_v} \tag{3-40}$$

where Δl is the space between probe 1 and probe 2.

The mean longitudinal length of the bubbles l_b is given by the average contact time of the bubbles with one electrode Δt_l and by v_b:

$$l_b = v_b . \Delta t_1 \tag{3-41}$$

This method suffers from the drawback that it is a flow intrusive measurement method and that in the case of ellipsoidal or spherical capped bubbles, the bubble diameter determined by this method is consistently small as only smaller axes are pierced (Joshi et al., 1990).

3.4) Measurement of velocity profiles

Essentially the main design parameters for bubble columns (phase hold-ups, mixing, RTD, mass and heat transfer coefficients) are all determined by the velocity field and the turbulence characteristics of the liquid phase.

The techniques for measurement of local velocity and turbulence include:

- pressure tube anemometers
- cross-correlation techniques
- thermal anemometers
- electrochemical method
- laser-Doppler anemometers (LDA)
- flow visualisation (eg. Particle Image Velocimetry, PIV)

Joshi et al. (1990) list the following characteristics for an ideal instrument to measure local velocity:

1. create minimum flow disturbance
2. small in size for essentially point measurement
3. minimal calibration requirements
4. measure a wide velocity range
5. work over a wide physical property range
6. high accuracy
7. high signal to noise ratio
8. ease of use
9. low cost

3.4.1) Pressure based measurements

The pressure exerted by a moving fluid on an open ended tube facing the direction of flow will be the sum of the static and dynamic pressures. It has been experimentally proven that the shape of the tube does not severely affect the observed total pressure (Joshi et al., 1990)

The tube is set along the flow direction so that the flow streamlines diverge around the tip. A static head probe can be a tube connected to the wall or in another location where the fluid velocity is zero. See Figure 3-13 for a schematic drawing of a pitot tube.

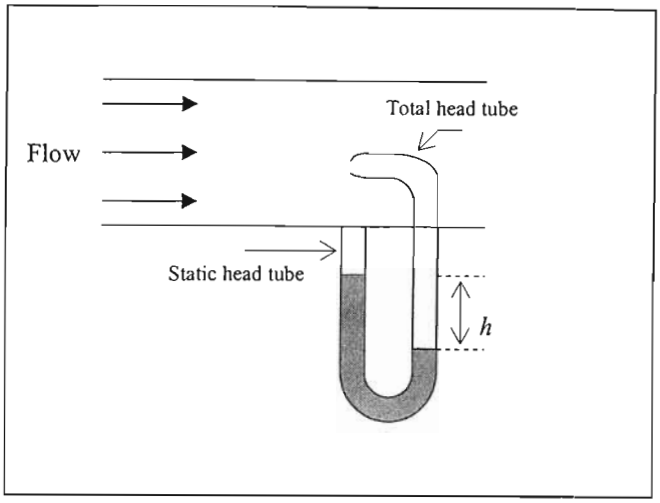

Figure 3-13: Schematic drawing of a pitot tube

Applying Bernoulli's equation and a force balance over the manometer yields:

$$u_{local} = K\sqrt{\frac{2gh(\rho_m - \rho_L)}{\rho_L}} \tag{3-42}$$

where K is a constant depending on the Reynolds number in the pitot tube. For Reynolds numbers greater than 100, based on the pitot tube diameter, K is unity and for lower Reynolds numbers a calibration for K in a known velocity field is required. ρ_m is the density of the manometer fluid.

Pressure based methods are often easier to use to estimate local liquid velocity but they suffer from a lack of accuracy and offer low resolution. They also cause flow disturbances and have a narrow application range for velocity measurement.

3.4.2) Thermal based measurements

Here the heat transfer rate from a small electrically heated sensor, which is proportional to the fluid velocity, is used to determine the fluid velocity.

The heat transfer from the sensor to the fluid depends upon:

- the fluid velocity
- the temperature difference between the sensor and the fluid
- physical properties of the fluid
- dimensions and physical properties of the probe\sensor

The only unknown is the fluid velocity as the other variables are known and constant.

The principle of hot wire and film anemometry is that the sensor of the wire is kept at a known temperature. Any rise in the fluid velocity increases the rate of heat transfer from the wire and causes the sensor to cool. A decrease in the resistance of the sensor is recorded due to the cooling. By measuring the voltage across the resistor, the fluid velocity can be determined. In practice an increase in fluid velocity in seen as an increase in the voltage across the resistor. It is necessary to calibrate the sensor in a velocity field and the sensor output is non-linear with respect to fluid velocity. When working properly, thermal methods offer good resolution and accuracy but are expensive and are not easy to implement.

3.4.3) Innovative experimental methods in bubble columns

3.4.3.1) Laser Doppler Anemometry (LDA)

In LDA the velocity of a tagged fluid element is determined by an optical method. Particles (dust or artificially added tracer) moving within the fluid are illuminated with a focussed laser beam. These particles scatter light in all directions. The frequency of the scattered light is detected and is 'Doppler shifted' because of the movement of the particles. The change in frequency (Doppler shift) is used to determine the velocity of these particles. The change in frequency is linearly proportional to the velocity of the particle.

LDA offers the following advantages:

- non-intrusive method so there are no flow disturbances
- requires no calibration
- precise measurement of velocity components

The drawbacks of LDA are that it is extremely costly and without the proper expertise it is difficult to use.

Kulkarni et al. (2001) used LDA to successfully measure gas and liquid velocities as well as fractional gas hold-up in a 15cm diameter column.

3.4.3.2) Particle Image Velocimetry (PIV)

LDA measurements are used to obtain local liquid velocities. In contrast, PIV is a whole field measurement. In PIV, a cross section of the flow is illuminated by a laser-sheet and the movement of fluid is visualised by the detection of small tracer particles in the flow. Two subsequent images of the cross section are recorded, with an exposure time delay of Δt. The displacement of the particles Δx between the two images is used to calculate the velocity u as:

$$u = \frac{\Delta x}{M \Delta t} \tag{3-43}$$

where M is the magnification of the camera. By performing these calculations the instantaneous velocity field for the entire cross section of flow can be obtained.

The data obtained by PIV and LDA are useful in validating theoretical concepts and for validation of computational fluid dynamic (CFD) simulations. PIV shares the same drawbacks as LDA.

Deen (2001) is an excellent reference on the use of PIV experiments for bubble column hydrodynamic studies.

CHAPTER FOUR

HYDRODYNAMICS: PARAMETER DEPENDENCY AND ESTIMATION

The design parameters for bubble column reactors can be divided into two categories. The non-adjustable parameters such as physical properties and column geometry; and operation sensitive parameters: dispersions coefficients, phase hold-ups etc. The interrelation between these parameters is complex and a simple schematic showing this interrelation is given in Figure 4-1.

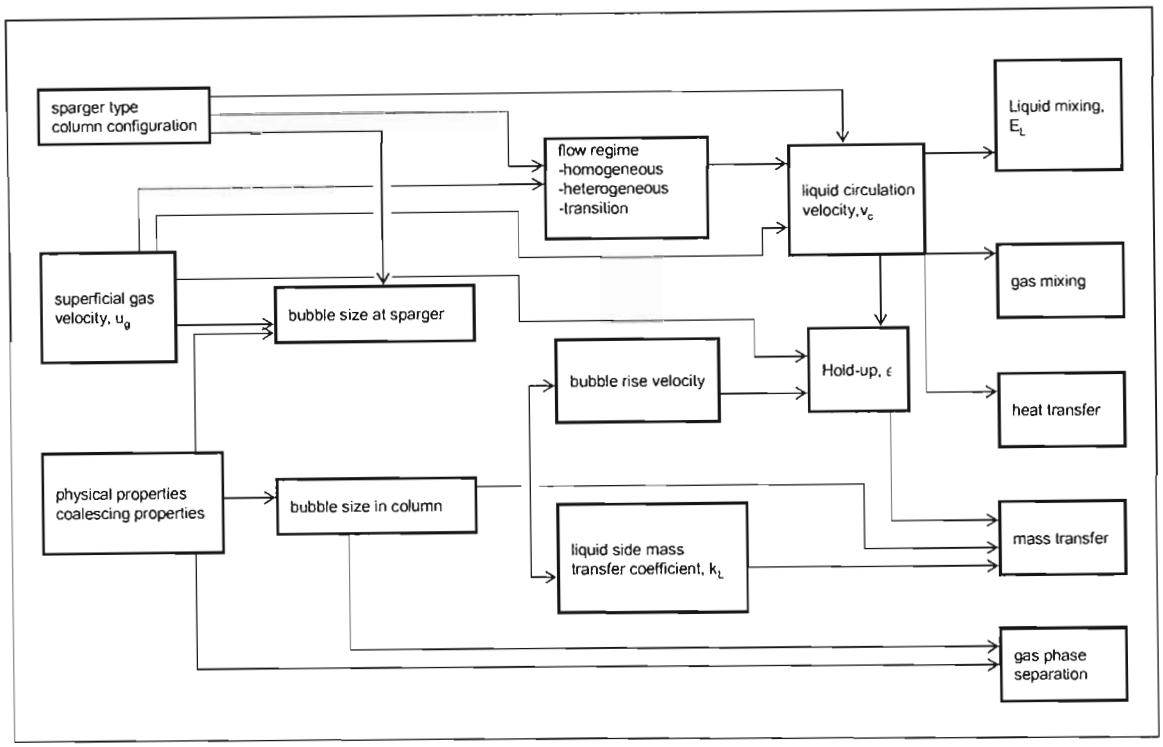

Figure 4-1: Interrelated design parameters for a bubble column reactor

There is a vast quantity of literature on the various aspects outlined in Figure 4-1. It would be impossible to provide a detailed account of the procedures for the estimation of all these parameters. In this chapter, various approaches for predicting liquid axial dispersion and gas hold-up are presented. In addition design considerations for the gas sparger and for partitioned bubble columns are discussed. For an in depth and complete treatment of the

work presented, the literature text of the various researchers should be consulted. In this chapter only the final results and pertinent findings of the researchers are provided in the proceeding sections.

4.1) Longitudinal mixing parameter estimation

Back-mixing is a flow pattern intermediate between the two limiting cases of plug flow and perfect mixing. A reactor with a finite amount of back-mixing would have a volume greater than with plug flow but less than for perfect mixing. In the case of back-mixing, a fluid element has an equal chance of moving forwards or backwards. This is analogous to Fick's law of diffusion which is therefore used to describe back-mixing. Under the influence of a net fluid flow, a fluid component will consist of a convective flow quantity and the back-mixed flow quantity. Ottmers and Rase (1966), suggested that the flow patterns in the orifice reactor can be made to approach plug flow rather than perfect mixing as found in stirred reactors. Generally, bubble column reactors are characterized by intense liquid recirculation levels.

4.1.1) Energy dissipation leading to liquid recirculation

The supply of energy in a bubble column is due to the introduction of the dispersed gas phase. The energy input E_i, can be represented by (Joshi, 1980):

$$E_i = \frac{1}{4}\pi D_c^{\,2} u_g (\rho_L - \rho_g) L (1-\varepsilon) g \qquad (4\text{-}1)$$

Energy is dissipated in the bubble column by frictional energy dissipation at the interface of the gas and liquid phase, E_s, and by the energy dissipation in the liquid motion, E_d:

$$E_d = E_i - E_s \qquad (4\text{-}2)$$

When the rate of energy input is higher than that dissipated at the gas-liquid interface recirculation of liquid occurs. In bubble columns, liquid recirculation causes the formation of circulation cells in the axial direction. The height of each circulation cell is roughly equal to the column diameter.

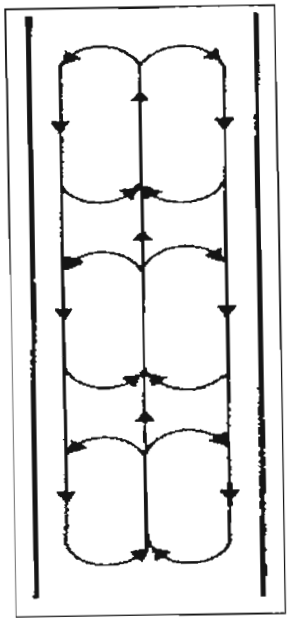

Figure 4-2: Multiple circulation cells in bubble columns (Deckwer, 1992)

The axial dispersion in the bubble column is strongly dependent on the level of liquid recirculation. It is evident from Eqs. 4-1 and 4-2 that the level of axial dispersion must depend on the gas throughput to the column and the diameter of the column. For this reason many correlations in the literature are of the form:

$$E_L = a u_g^{\ b} D_c^{\ c} \tag{4-3}$$

or some derivative of this form. The other parameters by which the axial dispersion coefficients are correlated are listed below:

- correlation with superficial gas velocity and diameter
- correlation with Peclet number
- correlation with liquid recirculation velocity
- correlation with centre-line liquid velocity

A major problem with a review of the correlations in the literature is that there is such a vast quantity of data and correlations. Many of these are purely empirical (based on experimental values), partly theoretical or analogous descriptions from single phase hydrodynamic theory. An extensive survey of the literature has shown that many of the existing correlations predict dispersion coefficients well. The recommended and most cited works are presented in Table 4-1.

Table 4-1: Literature liquid phase dispersion measurements

Author	System	Column diameters cm	Column height cm	Tracer [Steady (S) or transient (T) analysis]	Superficial liquid velocity cm/s	Superficial gas velocity cm/s	Hole diameters cm	Number of holes	Correlation
Bischoff & Philips (1966)	1	2.54	61	Potassium Chloride (T)	28.65	12.19 – 30.48	0.64, 0.16	1, 16	Eq. 4-12
Reith et al. (1968)	1	5.08, 14, 29	152 - 380	Sodium Chloride (S)	0.88 - 2.18	10 - 45	0.2	1	Eq. 4-13
Ohki & Inoue (1970)	1	4, 8, 16	200 - 300	Potassium Chloride (T)	Batch	2 - 25	0.04 - 0.3	2 - 91	Eq. 4-5
Kato & Nishiwaki (1972)	1	6.6, 12.2, 21.4	201 - 405	Potassium Chloride (T)	0.5, 1, 1.5	< 25	0.1 - 0.3	7 - 97	Eq. 4-16
Deckwer et al. (1973)	1	10,2 , 20	256, 222	Potassium Chloride (S)	0.17 - 0.74	0.15 – 7.7	No details	Glass-Sintered Plate	Eq. 4-37
Deckwer et al. (1974)	1	15, 20	440, 723	Electrolyte, Heat, Dye (S T)	Batch	< 5	150 μm	Glass-Sintered Plate	Eq. 4-6
Hikita & Kikukawa (1974)	2	19 , 10	240 , 150	Potassium Chloride (S)	Batch	4.3 – 33.8	1.31 - 3.62	1 Nozzle	Eq. 4-7
Eissa & Schuger I(1975)	1	15.9	390	Sodium Chloride (S)	0.35 - 1.40	0.35 - 6	0.2	200	
Kelkar et al. (1983)	3	15.4, 30	244, 335	Heat (S)	0 - 15	1 - 30	0.16, 0.1	Perforated plate	Eq. 4-8
Houzelot et al. (1985)	1	5	400	Sodium Chloride (T)	0.025 – 0.1	0.25 – 0.58	1	diffuser tube	Eq. 4-9
Ityokumbul et al. (1994)	1	6	106	Hydrochloric acid (T)	0.3 – 0.7	0.2 – 4	133 μm	Porous plate	Eq. 4-10
Krishna et al. (2000)	4	17.4, 38, 63	No details	Sodium Chloride (T)	Batch	5 - 35	50 μm	Sintered bronze plate	Eq. 4-28
Moustiri et al. (2001)	1	15, 20	425, 450	Sodium Chloride (T)	0.62 – 2.16	0.52 – 5.5	No details	Flexible membrane	-

1: air/water
2: air / aqueous methanol (8 – 53 wt %) & air/ aqueous eane sugar (35 – 50 wt %)
3: air/ aqueous aliphatic alchohols (0.5 – 2.5 wt % methanol, ethanol, n-propanol, i-propanol and butanol)
4: air/water & air/ Tellus oil

4.1.2) Correlation with superficial gas velocity and diameter

As shown in Figure 2-4, liquid flows in the vertical direction with a wide velocity distribution over the cross-section of the column. Ohki and Inoue (1970) made use of the velocity distribution model of Taylor. The authors report that according to Taylor, a general form of dispersion is given by:

$$E_L = \frac{D_c^{\,2} u_o^{\,2}}{\kappa D_m} + D_m \tag{4-4}$$

where D_m and u_o represent the molecular diffusion coefficient and the maximum velocity at the tube axis respectively. The constant κ is determined by the form of the velocity distribution and for a parabolic distribution, κ is equal to 768.

Based on this theoretical model and velocity profiles for the liquid phase, Ohki and Inoue showed that the axial dispersion coefficient for homogeneous bubble flow can be represented by the semi-theoretical equation:

$$E_L = 0.30 D_c^{\,2} u_g^{\,1.2} + 170 d_h \tag{4-5}$$

with E_L in cm^2/s, D_c in cm , u_g in cm/s and the plate hole diameter d_h in cm.

Deckwer et al. (1974) performed residence time distribution studies via the steady-state and non-steady state method and correlated the liquid dispersion coefficient as:

$$E_L = 2.7 D_c^{\,1.4} u_g^{\,0.3} \tag{4-6}$$

with E_L in cm^2/s, D_c in cm , u_g in cm/s.

Eq. 4-6 also considers the data of Ohki and Inoue (1970), Reith et al. (1968) and six other literature data sets.

A summary of the correlations based on superficial gas velocity and column diameter is given in Table 4-2.

Table 4-2: Literature correlations for axial dispersion coefficients as a function of superficial gas velocity and column diameter

Authors	Correlation	Avg. Deviation	Eq.
Ohki and Inoue (1970)	$E_L = 0.30 D_c^{\ 2} u_g^{\ 1.2} + 170 d_h$	Not reported	(4-5)
Deckwer et al. (1974)	$E_L = 2.7 D_c^{\ 1.4} u_g^{\ 0.3}$	30	(4-6)
Hikita & Kikukawa (1974)	$E_L = (0.15 + 0.69 u_G^{\ 0.77}) D_c^{\ 1.25}$	12	(4-7)
Kelkar et al. (1983)	$E_L \varepsilon_L = 1.42 D_c^{\ 1.33} \left[u_g - \frac{\varepsilon_g u_L}{(1-\varepsilon_g)} \right]^{0.73}$	14	(4-8)
Houzelot et al. (1985)	$E_L = 0.04 u_g^{\ 0.47}$	Not reported	(4-9)
Ityokumbul et al. (1994)	$E_L = 0.675 D_c^{\ 1.235} g^{0.235} u_g^{\ 0.53}$	Not reported	(4-10)

Eqs. 4-7 to 4-10 in Table 4-2 give E_L in m^2/s with u_g in m/s and D_c in m. The average deviation is the deviation of measured E_L data from the predicted dispersion coefficient via the empirical correlation.

4.1.3) Correlation with Peclet number and Froude number

The Peclet number Pe is a useful dimensionless parameter which indicates the ratio of transport due to dispersion E as compared to convective flow u for a characteristic length L_c:

$$Pe = \frac{uL_c}{E} = Bo \tag{4-11}$$

When the convective component is in the numerator, the Peclet number is referred to as the convective Peclet number or the Bodenstein number Bo, and when the dispersion coefficient is in the numerator of Eq. 4-11 the Peclet number is referred to as the dispersive Peclet number.

Many researchers correlate their experimental results in terms of the Peclet number or some modification of Eq. 4-11. There are many reports in the literature of constant Peclet numbers being achieved over a wide experimental range. In other cases, the Peclet number is correlated with superficial gas velocity or other dimensionless parameters such as the Froude number.

Bischoff and Philips (1966) found that:

$$Pe_L = \frac{u_L L}{E_L} \approx 4 \tag{4-12}$$

Reith et al. (1968) observed that the axial dispersion can be characterized by a nearly constant Peclet number based on the column diameter, D_C, and the relative gas velocity, u_r:

$$Pe_{Lm} = \frac{u_r D_c}{E_L} \approx 3.01 \pm 0.3 \tag{4-13}$$

where the relative gas velocity is given by :

$$u_r = 2u_g + u_b \tag{4-14}$$

with u_b the rise velocity of a single bubble. The authors suggest that a value of 30 cm/s be used for air bubbles in water with bubble diameters between 1 and 5 mm. It is assumed that the dispersion coefficient is proportional to the scale and to the velocity of the eddies in the column. Since the largest eddy which can exist in the column has a scale roughly equal to the column diameter, the authors have incorporated D_c as the characteristic length in the definition of the Peclet number. Figure 4-3 shows the results obtained by Reith et al. (1968).

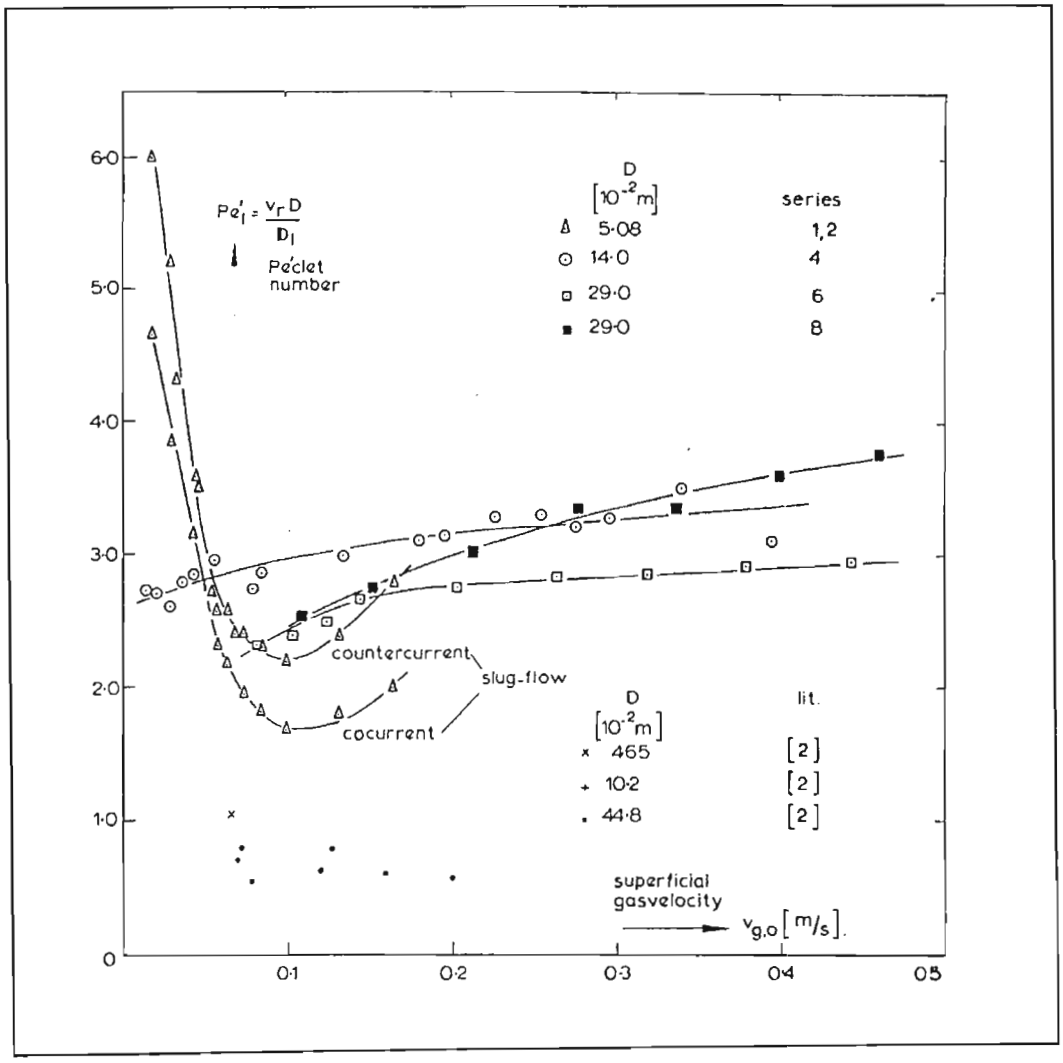

Figure 4-3: The Peclet number as a function of u_g (Reith et al. 1968)

Kato and Nishiwaki (1972) correlated E_L with a modified Peclet Number and the Froude number Fr which is the ratio of the inertia of the gas acting on the liquid to gravity g:

$$Fr = \frac{u_g}{(gD_c)^{1/2}} \tag{4-15}$$

Figure 4-4 shows the data and correlation of Kato and Nishiwaki (1972).

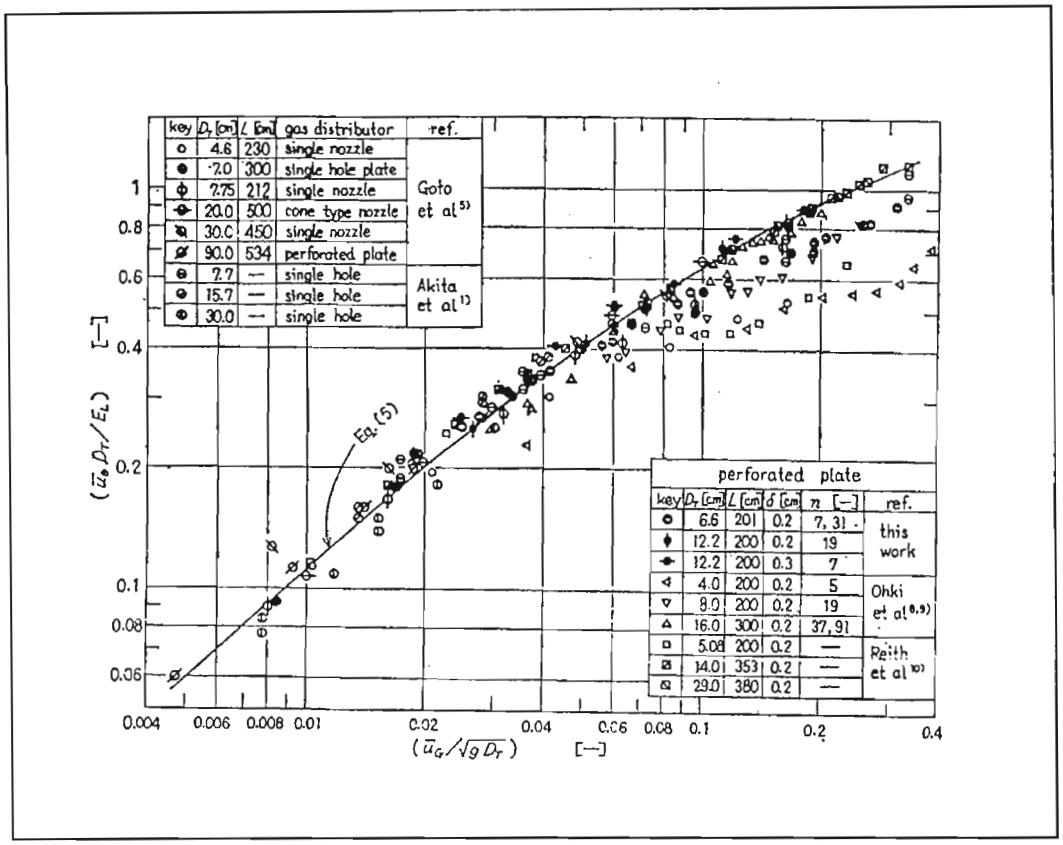

Figure 4-4: Relationship between Peclet number and Froude number

(Kato and Nishiwaki, 1972)

The data of Kato and Nishiwaki (1972) may be correlated by the following equation:

$$\frac{u_g D_c}{E_L} = \frac{13\left(\dfrac{u_g}{\sqrt{gD_c}}\right)}{1+6.5\left(\dfrac{u_g}{\sqrt{gD_c}}\right)^{0.8}} \tag{4-16}$$

or in terms of dimensionless parameters Pe_{Lm} and Fr:

$$Pe_{Lm} = \frac{13(Fr)}{1+6.5(Fr)^{0.8}} \tag{4-17}$$

Eissa and Schugerl (1975) performed back-mixing investigations in a 15.9 cm diameter column and analysed their data similarly to Reith et al. (1968). The results are shown in Figure 4-5.

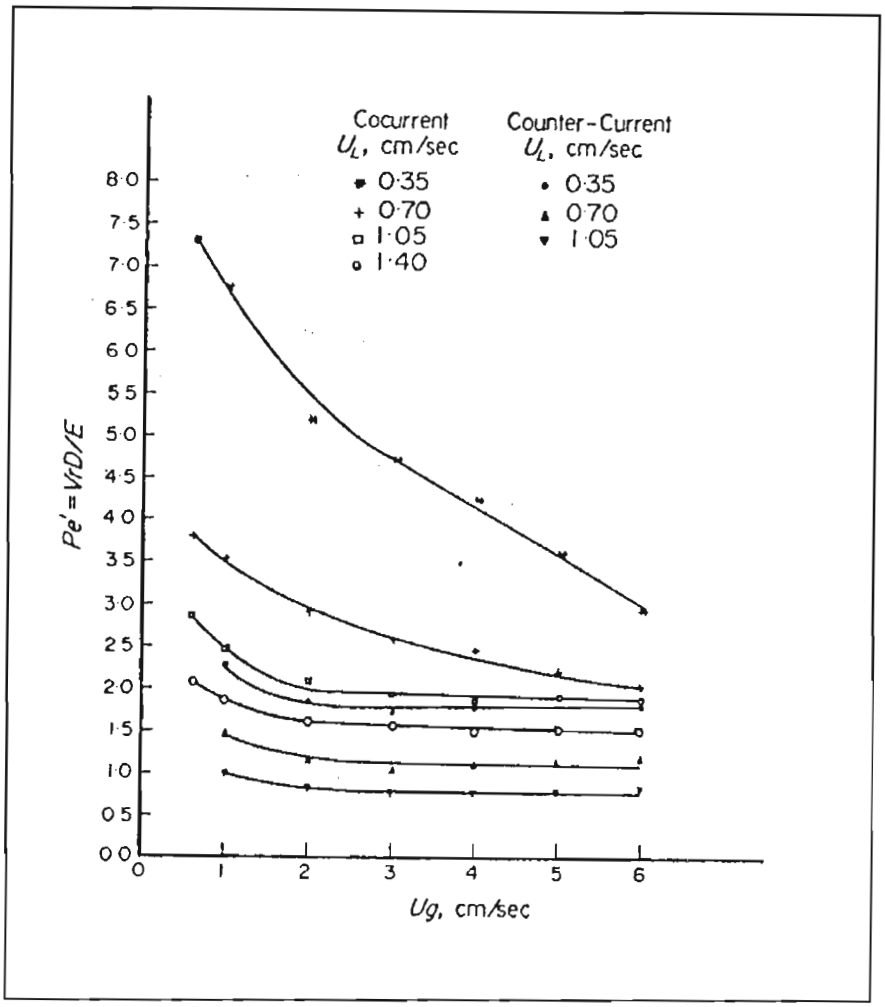

Figure 4-5: Variation of the modified Peclet number with gas velocity for both co-current and counter-current flow (Eissa and Schugerl, 1975)

Figure 4-5 shows that the modified Peclet number (Eq. 4-13) decreases with increasing gas velocity and increases with decreasing liquid velocity. The authors concluded that if the modified Peclet number was multiplied by the actual velocity of the liquid phase and plotted for different gas to liquid velocities, straight lines would be obtained. A reasonable correlation was obtained:

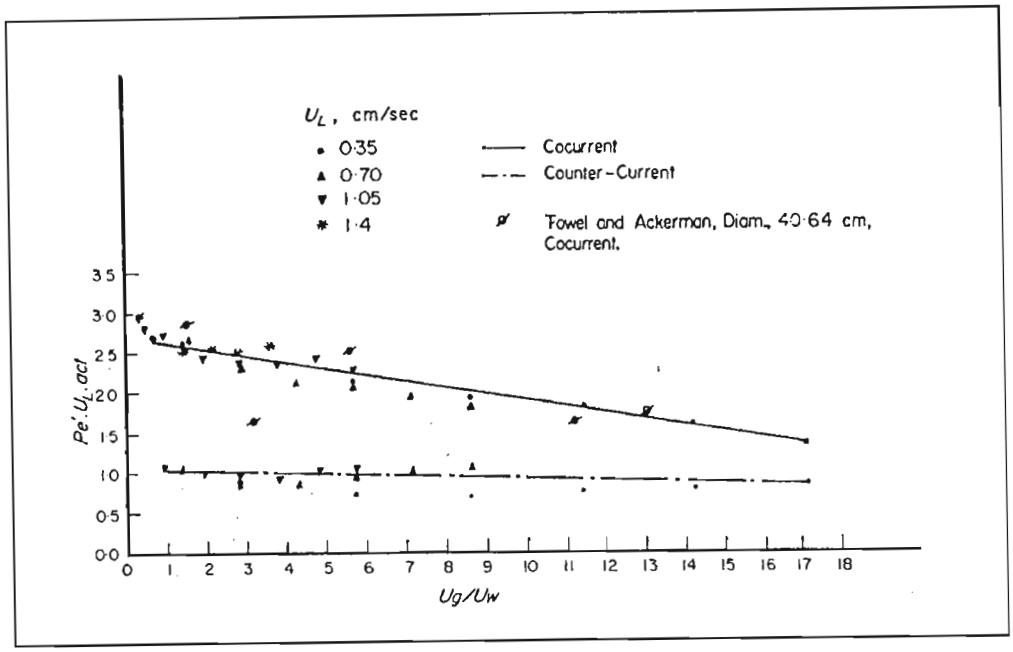

Figure 4-6: Correlation of $Pe_{Lm}.u_L$ with u_g/u_L (Eissa and Schugerl, 1975)

4.1.4) Effect of liquid velocity on axial dispersion

Bischoff and Philips (1966) reported that liquid velocities had no influence on the axial dispersion coefficient even if the liquid velocities were higher than the superficial gas velocity. Kato and Nishiwaki (1972), Deckwer et al. (1973), Ityokubul et al. (1994) also observed a similar result.

Moustiri et al. (2001) found that the dispersion coefficient increased with increasing liquid velocity. The range of superficial liquid velocities was 0.62 – 2.16 cm/s. No explanation was offered by the authors for this observation, except that increasing the liquid velocity caused the liquid to tend towards plug flow. Reith et al. (1968) offered the explanation that plug flow ($Pe_{Lm} > 3$) in the liquid phase of tall columns ($L/D_c >> 1$) can be assumed only if the fluid velocity is not too low $u_L / u_r > D_c / L$,where u_r is given by Eq. 4-14.

It is postulated that the range of liquid velocities considered by researchers is too small to affect dispersion. It is well known that air bubbles rise in water between 20-30 cm/s. Since it is the bubble rise velocity which causes liquid recirculation, net liquid flows lower than the bubble rise velocity would not considerably affect dispersion levels in bubble columns. Kastanek et al. (1993) report that when the actual liquid velocity in the column is less than 0.1 of the bubble rise velocity ($u_{Lactual} \leq 0.1\ u_b$), the effect of liquid velocity is negligible. It

should be remembered that bubble column reactors generally operate at low liquid throughputs (u_L < 1cm/s) and therefore this criteria is often satisfied in typical bubble column operation.

4.1.4.1) Correlation with liquid recirculation velocity

The average liquid recirculation velocity v_c causes an increase in dispersion. Mashelkar and Ramachandran (1975) report that under laminar conditions for circulation dominated bubble columns:

$$E_L \propto v_c^{\,2} \tag{4-18}$$

and that

$$v_c \propto u_g^{\,0.6} \tag{4-19}$$

The authors therefore suggested the following form for dispersion coefficients:

$$E_L \propto D_c^{\,2} u_g^{\,1.2} \tag{4-20}$$

From the energy balance (Eq. 4-1), Joshi and Sharma (1978) showed that:

$$E_L = 0.031 D_c^{\,1.5} v_c \tag{4-21}$$

with E_L in cm^2/s, D_c in cm and v_c in cm/s.

Joshi (1980) also suggests that the bubble column may be considered as N completely back mixed tanks in series with inter-stage recirculation. The value of N being given by:

$$N = \frac{L}{0.8 D_c} \tag{4-22}$$

Field and Davidson (1980) have shown that:

$$v_c = 1.47\left(\frac{E_d}{D_c^{\,2}\rho_L(1-\varepsilon_g)}\right)^{1/3} \tag{4-23}$$

with E_d the energy dissipated in liquid motion. The authors have shown that this can be further simplified to:

$$v_c = 1.36\left[Lg\left(u_g - \varepsilon_g u_s\right)\right]^{1/3} \tag{4-24}$$

with L in m, g in m/s^2; and v_c, u_g and u_s in m/s.

The slip velocity u_s between the gas and liquid phases is given by:

$$u_s = \frac{u_g}{\varepsilon_g} - \frac{u_L}{1-\varepsilon_g} \tag{4-25}$$

Lockett and Kirkpatrick (1975) provide an excellent review on the calculation of slip velocities for gas-liquid two phase flow.

Combing Equations 4-23 to 4-24 gives:

$$E_L = 0.9D_c^{\,1.5}\left[L\left(u_g - \varepsilon u_s\right)\right]^{1/3} \tag{4-26}$$

with E_L in m^2/s, D_c and L in m, u_g and u_s in m/s.

4.1.4.2) Correlation with centre-line liquid velocity

The upwardly directed axial-component of the liquid velocity at the centre of the column $V_L(0)$, can be taken as a measure of the liquid circulation velocity for bubble columns in which there is no net inflow or outflow of liquid.

Krishna et al. (2000) have verified experimentally that the centre-line velocity is estimated well by the following relation:

$$V_L(0) = 0.21(gD_c)^{1/2}\left(\frac{u_g^{\,3}}{gv_L}\right)^{1/8} \tag{4-27}$$

where υ_L is the kinematic viscosity of the liquid phase in m^2/s, D_c in m and u_g in m/s and $V_L(0)$ in m/s.

The authors have proposed the following relation between the centre-line liquid velocity and the axial dispersion coefficient:

$$E_L = 0.31 V_L(0) D_c \tag{4-28}$$

The authors performed experiments with Tellus oil which was 72 times more viscous than water. It was found that the liquid viscosity had a negligible influence on $V_L(0)$, however Eq. 4-26 may still be utilised with sufficient accuracy using the properties of water (i.e. $\upsilon_L = 10^{-6}$ m^2/s). Eulerian simulations were used to verify the applicability of Eq. 4-27 to diameters up to 6 m with good success. Ulbrecht and Baykara (1981) also successfully showed that the axial dispersion coefficients obtained in a 15 cm diameter column could be linearly correlated with the centre-line liquid velocity. The authors however did not determine the diameter dependency of $V_L(0)$.

4.1.5) Applications of Kolmogoroff's theory of isotropic turbulence

The liquid phase in bubble column reactors is very well mixed and the circulation flow patterns are similar to eddies that are formed in turbulent flow. The eddies in turbulent flow have a wide range of sizes. It has been found that the large scale eddies depend on the geometry of the flow while the small scale eddies appear to have a universal structure independent of the geometric configuration. Kolmogorov introduced the concept of the energy cascade where there is a transfer of kinetic energy from the larger eddies to the smaller ones. Kolmogorov proposed that the energy stored in small eddies is dissipated by viscosity υ. The end of the cascade is at the smallest length scale. From dimensional reasoning Kolmogoroff derived the order of length scale η for the smallest eddies to be given by:

$$\eta = \left(\frac{\upsilon^3}{r_d} \right)^{1/4} \tag{4-29}$$

with r_d the rate of energy dissipation per unit mass.

The isotropic turbulence model assumes that the turbulent intensity of a fluid is uniform and acts equally in all directions.

In a second hypothesis Kolmogoroff considered a sub-range in which viscous dissipation is unimportant. In this sub-range, if the Reynolds number is sufficiently large, the energy spectrum is independent of v and is determined solely from one parameter, r_d.

The velocity in this sub-range is given by:

$$u \approx (r_d l)^{1/3} \tag{4-30}$$

where u is the root-mean-square turbulence velocity between two points in the fluid a distance l apart.

The requirement for the validity of the isotropic turbulence theory is that the liquid Reynolds number should be sufficiently high. Kawase and Moo Young (1990) report that even when the flow-field is non-isotropic and far from homogeneous, isotropic turbulence theory has been used and has provided successful correlations. It is a very useful technique for engineering scale-up purposes. Shah and Deckwer (1983) used the isotropic turbulence theory to good effect in predicting wall-dispersion heat transfer coefficients and Calderbank (1967) used the theory to predict the maximum stable bubble diameter of a gas in a liquid. Deckwer (1992) reports that the success of correlations using Kolmogoroff's theory contributes to the conclusion that most of the energy input in a gas-liquid flow situation is dissipated by a mechanism which is the same as or very similar to that proposed by Kolmogoroff.

4.1.5.1) Correlation of axial dispersion via isotropic turbulence

Kolmogoroff's theory of isotropic turbulence suggests the following equation for the axial dispersion coefficient:

$$E_L \approx ul \tag{4-31}$$

Combining Eqs. 4-30 and 4-31 yields:

$$E_L \approx l^{4/3} r_d^{1/3} \tag{4-32}$$

Baird and Rice (1975) applied Eq. 4-32 to correlate the axial dispersion coefficient in bubble column reactors. They postulated that the length of the primary eddies is equal to the reactor diameter D_c and obtained the following relationship:

$$E_L = 0.35 D_c^{4/3} \left(u_g g\right)^{1/3} \tag{4-33}$$

The proportionality constant 0.35 was determined from experimental data in the literature with E_L in cm^2/s, D_c in cm, u_g in cm/s and g in cm/s^2.

Equation 4-33 considers the experimental data of Ohki and Inoue (1970), Reith et al. (1968), Deckwer et al. (1974) and four other researchers data.

It is interesting to note that most of the theoretical models for bubble column reactors based on other mathematical descriptions can by expressed in the same form as Eq. 4-33.

Kawase and Moo Young (1990) using an energy balance and mixing length theory showed that:

$$E_L = 0.343 D_c^{4/3} \left(u_g g\right)^{1/3} \tag{4-34}$$

which is nearly identical to Eq. 4-33. This further supports the supposition that energy in a bubble column is dissipated in a mechanism very similar to Kolmogoroff's theory of isotropic turbulence.

4.1.6) Zones of different mixing in the liquid phase of bubble columns

Deckwer et al. (1973) found that over a certain range of gas throughputs the mixing in the liquid phase of bubble columns is not uniform but splits into two zones of different mixing. The authors found that at superficial gas velocities between 0.4 and 6 cm/s two mixing regions existed with different back-mixing coefficients. It was determined that the point of separation between the two mixing zones was approximately in the middle of the bubble column. Figure 4-7 shows the results obtained by the authors.

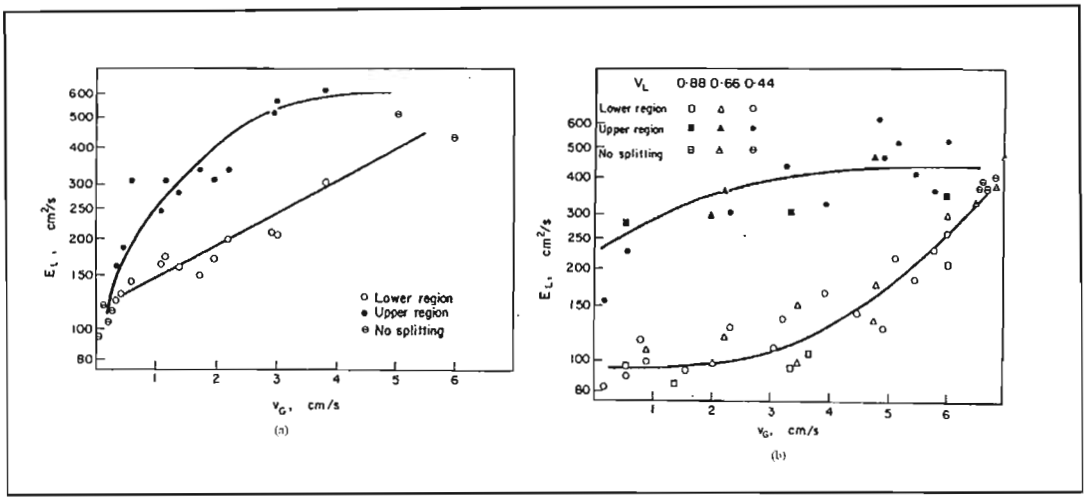

Figure 4-7: Back-mixing coefficients versus superficial gas velocity (Deckwer, 1973)

(a) 20 cm diameter column with $u_L = 0.74$ cm/s, co-current mode

(b) 20 cm diameter column at different liquid velocities, counter-current mode

No splitting occurred at superficial gas velocities of 0.15 and 0.24 cm/s. The authors suggest that the splitting of two zones between 0.4 and 6 cm/s is due to the transition from bubble flow to coalesced bubble flow.

The experimental data was correlated at a significance level of 95%. In the lower region of the column:

$$E_L = (1.2 \pm 0.12) D_c^{1.5} u_g^{0.5} \tag{4-35}$$

In the upper region:

$$E_L = (2.4 \pm 0.18) D_c^{1.5} u_g^{0.5} \tag{4-36}$$

and if no splitting into different back mixing zones occurs:

$$E_L = (2 \pm 0.15) D_c^{1.5} u_g^{0.5} \tag{4-37}$$

Eqs. 4-35 to 4-37 above apply to co-current as well as counter-current flow of the two phases.

It should be noted that the above experimental results were generated using a glass-sintered plate sparger. In a later paper Deckwer et al. (1974) report that the splitting into zones of

different mixing at gas velocities less than 5 cm/s are restricted only to bubble columns with porous gas spargers and attribute the splitting into mixing zones as an end effect of porous type spargers.

4.1.7) Effect of distributor geometry on E_L

Reith et al. (1968) observed that for superficial gas velocities less than 10 cm/s, the axial dispersion coefficients became more dependent on orifice geometry while for gas flow rates in excess of 10 cm/s the axial dispersion coefficient was unaffected. Kato and Nishiwaki (1972) and Ohki and Inoue (1970) reported no significant effect of the distributor geometry on E_L.

4.1.8) Counter-current and co-current operation

Reith et al. (1968) found no difference in axial dispersion for counter-current and co-current operation. Deckwer et al. (1973) also found no difference in dispersion coefficients for counter- and co-current operation.

4.1.9) Effect of radial dispersion

Due to the high height to diameter ratios in bubble columns, axial gradients are considered more important than radial gradients. Reith et al. (1968) found that radial concentration differences in their column were negligible. They found radial dispersion coefficients which were a factor 10 smaller than the axial dispersion coefficient at the same superficial gas velocity. This has implications on the validity of the isotropic model for bubble column reactors as the model assumes that dispersion is uniform within the reactor.

Deckwer (1992) states that radial dispersion phenomena only affect reactor conversion and selectivity under conditions of pronounced non-linearity (reaction order $\neq 1$ and heat effects). Deckwer asserts that the incorporation of radial dispersion coefficients in the modeling of the liquid phase is not necessary as the one dimensional model is adequate for characterising the mixing phenomena.

4.1.10) Effect of liquid physical properties

Cova (1974) measured axial dispersion coefficients in water, acetone, carbon tetrachloride, cyclohexanol, ethanol, 11% ethanol in water and 50% sugar in water. Nitrogen was used as the gas for all the liquids considered. Cova performed his measurements in a 4.6 cm diameter column which was 122 cm long. Of the liquid physical properties of surface tension, density and viscosity only density showed a slight effect on E_L. The author showed that E_L varied with liquid density ρ_L as:

$$E_L \propto \rho_L^{0.07} \tag{4-38}$$

where the range of densities covered was 0.79 – 1.59 g/cm^3.

Hikita and Kikukawa (1974) investigated aqueous cane-sugar and aqueous methanol systems with air as the gas. The authors found no effect of surface tension (28.2 – 74.2 dyne/cm) on the dispersion coefficient but found that the dispersion coefficient varied with liquid viscosity μ_L as:

$$E_L \propto \left(\frac{1}{\mu_L}\right)^{0.12} \tag{4-39}$$

where the range of liquid viscosity was 1.00 – 19.2 cP.

There have been many attempts at correlating the axial dispersion coefficient in bubble column reactors. However, there is little if any agreement between various research groups. This is due to the current state of bubble column knowledge. As shown in the preceding sections, good correlations have been obtained using various approaches. It is generally considered that the liquid recirculation approach to predicting dispersion coefficients is the most theoretically sound approach. However, the measurement of liquid recirculation velocities in bubble columns is subject to much difficulty as discussed in Chapter 3. The current state of bubble column knowledge is that axial dispersion cannot be predicted *a priori*. When dispersion levels are required at conditions similar to the empirical correlations in literature, the correlations are useful for obtaining order of magnitude dispersion levels. However, there is little agreement between the correlations when extrapolating the correlations to different conditions (Chapter 5). For this reason, laboratory scale measurements have to be undertaken at these new conditions and new correlations must be proposed.

4.2) Gas hold-up

Gas hold-up has been studied extensively in the literature. It has been shown that for dispersion coefficients, the most influential factors are gas velocity, column diameter and the recirculation velocity. The factors affecting gas hold-up are more numerous and complex:

- physical properties of gas and liquid phase
- distributor geometry
- operating conditions
- column geometry

As for axial dispersion coefficients, it is not possible for a single equation to incorporate all of these factors. As such there are many correlations in the literature. The factors affecting gas hold-up will be discussed here.

4.2.1) Effect of superficial gas velocity

Gas hold-up in bubble columns depends mainly on superficial gas velocity. Gas hold-up has been found to increase with increasing superficial gas velocity. The relationship between gas hold-up and gas velocity is usually of the form:

$$\varepsilon_G \propto u_g^{\,n} \tag{4-40}$$

The value of n is influenced by a number of factors. The flow regime has the most pronounced effect on n. Table 4-3 shows the typical values of n for air-water systems.

Table 4-3: Flow regime and flow index n for air-water systems

Flow index, n	Flow regime	u_g (cm/s)
1.00	Bubble flow	< 5
0.75	Transitional flow	5 - 20
0.55	Churn turbulent	20 - 40

Kantarci et al. (2005) offer an explanation for the dependency of gas hold-up on the flow regime. The gas fraction in bubble column reactors is considered to consist of two bubble groups: large bubbles and small bubbles. The small bubble fraction is higher in the bubbly

flow and the transitional flow regime and is more prone to coalesce than their large bubble counterparts.

In the bubbly flow regime, the gas hold-up is seen to increase proportionally to increasing gas velocity. This is due to the small bubble hold-up increasing, due to coalescence, as the superficial velocity is elevated.

In the churn turbulent regime, the gas hold-up does not increase as remarkably as the bubble flow regime with increasing gas velocity. This is due to the small bubble fraction remaining approximately constant (transition regime hold-up) and the large bubble hold-up increasing only.

4.2.2) Effect of liquid velocity

Several workers have found no effect of liquid rate on gas hold-up. A possible explanation for this is that they only investigated small liquid flows. Taking into consideration that bubbles rise at approximately 20-30 cm/s in water, the effect of small liquid velocities will be masked by the dominant liquid recirculation and bubble entrainment rates.

4.2.3) Effect of liquid and gas phase properties

The properties of the liquid phase has a large impact on bubble formation and/or coalescing tendencies and hence is an important factor affecting gas hold-up. Kumar and Kuloor (1970) provide a complete description of the impact of liquid and gas properties on the formation of bubbles.

The liquid viscosity and surface tension play a pivotal role in determining gas hold-up. An increase in liquid viscosity results in large bubbles and thus higher bubble rise velocities and lower gas hold-up. The influence of liquid surface tension is small and it is generally found that the gas hold-up increases with decreasing surface tension:

$$\varepsilon_G \propto \sigma^{-m} \tag{4-41}$$

with m varying between 0.1 and 0.2 (Chen, 1986)

It is widely reported that the presence of electrolyte or impurities also increases gas hold-up (Anderson and Quinn, 1970). Recently Tang and Heindel (2004) showed that tap water,

which is frequently used for bubble column gas hold-up studies, causes significant reproducibility problems due to the volatile substances present in tap water.

Ozturk et al. (1987) investigated the gas hold-ups in various organic liquids and reported that in several liquid mixtures, the gas hold-ups were higher as compared to pure liquids with the same properties (surface tension, density, viscosity). They also concluded that the gas hold-ups were higher with high gas densities. This finding is supported by Bhaga et al. (1971). In contrast, Akita and Yoshida (1973) showed that using air, oxygen and carbon dioxide as gases showed no effect on the gas hold-up.

It is evident that there is a great disparity on the effect of gas properties on gas hold-up and as such in pursuit of closure regarding the mechanism and prediction of gas hold-up, much research on the subject is on-going.

4.2.4) Effect of temperature and pressure

The effect of operating pressure and temperature on gas hold-up of bubble columns are the subject of many studies in the literature. It is commonly accepted that elevated pressures lead to higher gas hold-up (Kantarci et al., 2005).

Bhaga et al. (1971) showed that temperature had very little effect on the gas hold-up in pure liquids in the range 25–60°C. This suggests that the change in the physical properties (viscosity, density, surface tension) brought about by the increased temperature, did not play an important role in determining the gas hold-up.

4.2.5) Effect of column diameter

The effect of column diameter and height on hydrodynamics is widely investigated in literature. There has been conflicting reports in the literature on the existence of a critical diameter for gas hold-up. The critical diameter is defined as the diameter when gas hold-ups are no longer dependent on the column diameter. Mashelkar (1970) gave the critical diameter to be 7.5 cm. Yoshida and Akita (1973) showed a negligible effect of column diameter when the diameter is greater than 15cm and Kantarci et al. (2005) reported a value of 10 cm. Deckwer (1992) states that wall effects are negligible if the bubble diameter D_B is small in comparison with the column diameter, $D_B/D_c < 0.05$. There is better agreement in the effect of column height as it is well reported that the effect of column height is insignificant for height to diameter ratios between 3 and 12.

4.2.6) Effect of gas sparger

The gas sparger is critical in determining the gas hold-up as it is primarily the sparger which is responsible for the size of bubbles generated in bubble columns. For superficial gas velocities less than 6 cm/s the gas hold-up is more strongly affected by the sparger. At higher gas throughputs, the effect of the sparger is not as pronounced.

4.2.7) Empirical correlations

There are a large number of correlations available in the literature for gas hold-up. Only the recommended and proven correlations are presented here.

4.2.7.1) The correlation of Hughmark

Hughmark (1967) has performed the definitive work on bubble column gas hold-up studies. Hughmark measured gas hold-up over a wide range of variables and correlated his data with that of various other researchers to show that:

$$\varepsilon_G = \frac{1}{2 + \left(\frac{0.35}{u_g}\right)\left(\frac{\rho_L \sigma}{72}\right)^{1/3}} \qquad (4\text{-}42)$$

with u_g in m/s, ρ_L in g/cm^3 and σ in mN/m. Eq. 4-42 predicts gas hold-up with an average absolute deviation of 11 % from experimental hold-ups.

4.2.7.2) The correlation of Akita and Yoshida

Another well cited and supported gas hold-up correlation is given by Akita and Yoshida (1973). Their correlation is based on 13 different liquids and 3 gases in a 15 cm column. From dimensional analysis the authors showed that:

$$\frac{\varepsilon_G}{(1-\varepsilon_G)^4} = f_l\left(\frac{gD_c^{\,2}\rho_L}{\sigma}\right)^{1/8}\left(\frac{gD_c^{\,3}\rho_L^{\,2}}{\eta_L^{\,2}}\right)^{1/12}\left(\frac{u_g}{\sqrt{gD_c}}\right) \qquad (4\text{-}43)$$

where $f_l = 0.2$ for pure liquids and non-electrolytes

$f_l = 0.25$ for electrolytes

with u_g in cm/s and g in m/s^2. The authors provide no details on the maximum deviation of Eq. 4-43 from experimental data.

4.2.7.3) Range of applicability for correlations

The range of physical properties and operating conditions for which Eqs. 4-42 and 4-43 are valid is presented in Table 4-4.

Table 4-4: Range of applicability for gas hold-up correlations

Author	u_g cm/s	ρ_L g/cm^3	σ mN/m	η_L mPa.s	D_c cm	Gases	Liquids
Hughmark (1967)	0.4 – 45	0.78 – 1.7	25 – 76	0.9 – 152	≥10	Air only	H_2O, light oil, glycerol,
Akita & Yoshida (1973)	0.5 – 42	0.79– 1.59	22 - 74	0.58 – 21.1	15.2 - 60	Air, O_2, He, CO_2	H_2O, glycol, methanol

4.2.7.4) Comparison of correlations

Table 4.4 shows that the range of applicability for both correlations is very similar. Given that Hughmark's correlation is given by a standard deviation of 11 %, either equation is suitable to determine the gas hold-up. To illustrate, the correlations are compared for the conditions given below:

- $D_c = 30$ cm
- water-air system

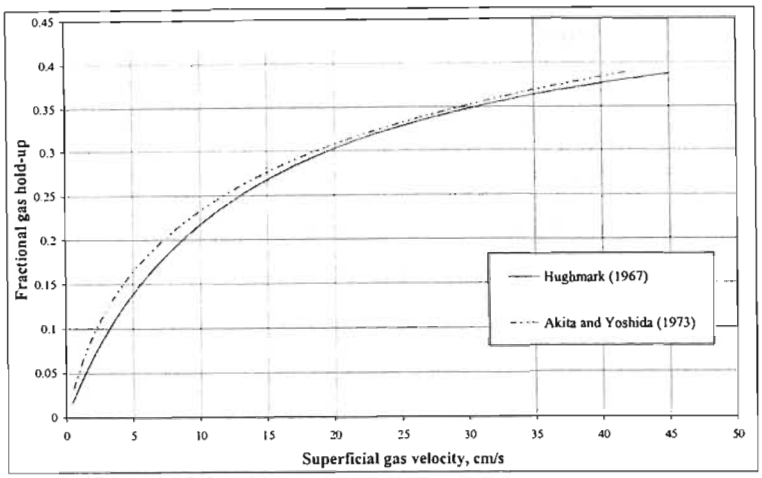

Figure 4-8: Comparison of gas hold-up correlations

Figure 4-8 illustrates that the two correlations compare well. It should be noted however, that the highly non-linear correlation of Akita and Yoshida (1973) requires more computational time than the correlation of Hughmark (1967).

There is very little consensus on the exact dependency of gas hold-up on the various operating parameters and physical properties. Many researchers have attempted to determine the dependency of liquid viscosity, liquid density, gas density and surface tension on gas hold-up. However, it is impossible to change only one of these properties as they are interdependent. This is one of the reasons why there is discrepancy in the literature. The net effect of moving from one liquid to another is observed in the gas hold-up measurements rather than the effect of the change in only one physical property. Also, many researchers tend to look at the properties of various phases independently rather than the interaction of the gas and liquid properties.

With the advent of computational fluid dynamics (CFD) being used to predict gas hold-up parameters (Thorat et al., 1998), the means to look at physical properties independently will become possible. However, without a fundamental theory and mechanism for bubble formation at the sparger and the resultant gas hold-up, the use of CFD will show no benefit.

For the moment, the use of empirical correlations based on experimental data must suffice. The concern being that the majority of gas hold-up data in the literature is for air-water systems which have little or no application in industry.

4.3) Sparger considerations

The gas sparger plays an important role in determining hydrodynamic parameters, such as gas hold-up, bubble size and bubble distribution. The formation of bubbles at the sparger has been the focus of many studies (Jamialahmadi et al., 2001). Many of these studies have focused on the formation of a single bubble at a single orifice. While the information obtained from models of this type are useful, they have little use for the formation of bubbles at multiple orifices and the interaction of the bubbles. For this reason, many studies have taken a brute force approach where many different spargers are designed and the effect of these spargers on gas hold-up, axial dispersion and other hydrodynamic parameters are examined experimentally.

Hebrard et al. (1996) attempted to perform a systematic study of the effect of the nature of the gas sparger on the hydrodynamics of bubble columns. The authors concluded that hydrodynamic parameters strongly depend on the type of sparger.

The design parameters considered for spargers are:

- type of sparger (perforated plate, porous diffuser, etc.)
- hole diameters, d_h
- free area of plate (number of holes), f
- sparger plate thickness, t
- hole geometry (square, triangular, random, etc.)
- pressure drop across sparger
- gas chamber volume, V_{ch}

It is difficult to examine the effect of each parameter independently as the effects cannot be looked at in isolation.

The most important criterion in the sparger design is the possibility of liquid weeping through the holes of the sparger. This will decrease the efficiency of the column. Thorat et al. (2001) performed an extensive study on the role of weeping in bubble columns. Weeping through perforated plates occurs when the pressure drop of the gas passing through the perforation is insufficient to support the liquid.

4.3.1) Weeping through sparger perforations

Thorat et al. (2001) provided criteria based on the dimensionless Weber number *We* for ensuring that a uniform gas load is achieved on all the holes of a perforated plate:

$$We_h = \frac{u_h^{\,2} d_h \rho_G}{\sigma} \geq 2.0 \tag{4-44}$$

where u_h is the hole velocity of the gas in a hole of diameter d_h.

Eq. 4-44 is valid provided that the modified Froude number *Fr'*:

$$Fr_h' = \frac{u_h^{\,2}}{d_h g}\left[\frac{\rho_G}{\rho_L - \rho_G}\right]^{1.25} \geq 0.37 \tag{4-45}$$

Equations 4-44 and 4-45 are obtained from a force balance incorporating the kinetic force of the gas and the pressure acting on the liquid film. When the forces acting on the liquid and gas are considered at equilibrium, the critical weep point criteria are obtained.

Another important design parameter is the gas chamber volume V_{ch} which plays a role in determining the extent of weeping. The dimensionless gas chamber number N_{ch} is defined as:

$$N_{ch} = \frac{4V_{ch}\rho_L g}{\left[\pi d_h^{\,2}\left(P_T + L\rho_L g\right)\right]} \tag{4-46}$$

where P_T is the pressure at the top of the column.

The authors state that the transition point from single bubbling to double bubbling at the sparger hole depends on the chamber volume N_{ch} and the Bond number B when $N_{ch} > 0.5$, and is independent of B and N_{ch} when $N_{ch} < 0.5$.

The Bond number B is given by:

$$B = \frac{(\rho_L - \rho_G) g d_h^{\,2}}{\sigma} \tag{4-47}$$

4.3.2) Partial bubbling from sparger holes

A further complication arises in the manner in which the gas is introduced into the gas chamber. The gas flow pattern in the gas chamber depends upon:

- the chamber diameter
- the inlet nozzle diameter
- shape of the chamber
- position of nozzle inlet

Figure 4-9 shows the possible flow patterns possible in gas chambers for side and bottom input of gas.

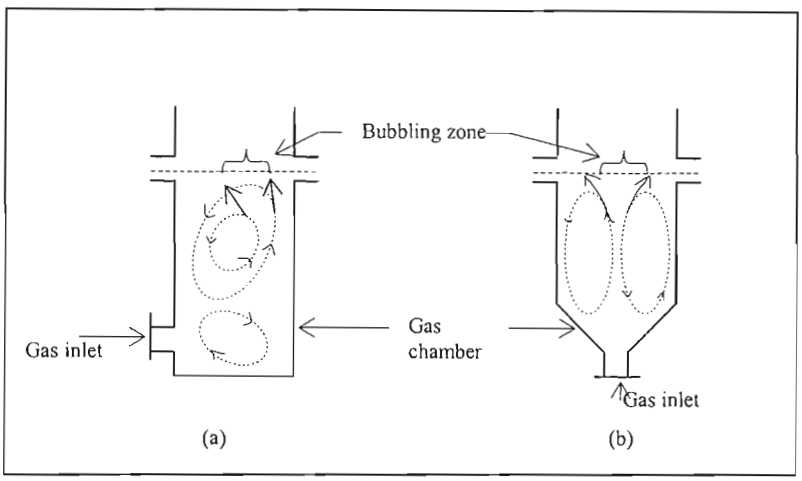

Figure 4-9: Flow pattern in gas distribution chamber

(a) side entry of gas and partial bubbling (b) central entry of gas and partial bubbling

Furthermore, Thorat et al. (2001) reported that at low gas velocities, only a few of the holes are fully active and gas-liquid dispersion prevails in one part of the column. Active holes are defined as holes in which no liquid film forms within the perforated hole as shown in Figure 4-10.

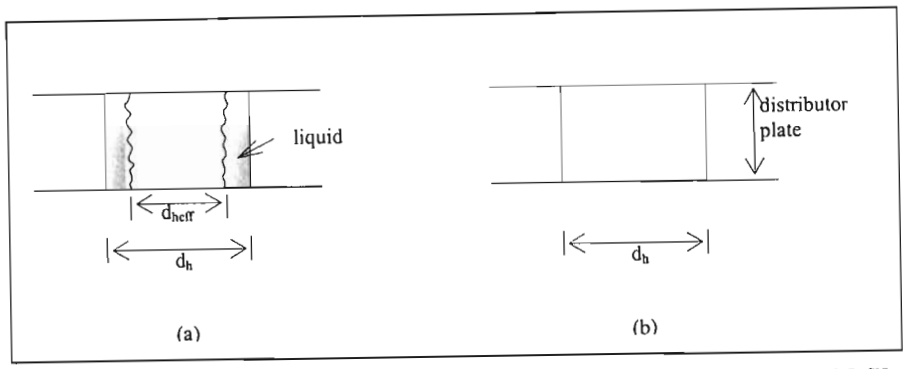

Figure 4-10: Distributor holes (a) partially open with an annular liquid film

(b) completely active hole

The authors observed that when partially active holes where predominant due to low gas flow-rates the bubble hose did not remain fixed at a single location but rotated in a random circular pattern, thus causing changes in the liquid circulation pattern according to the movement of the bubble hose as shown in Figure 4-11.

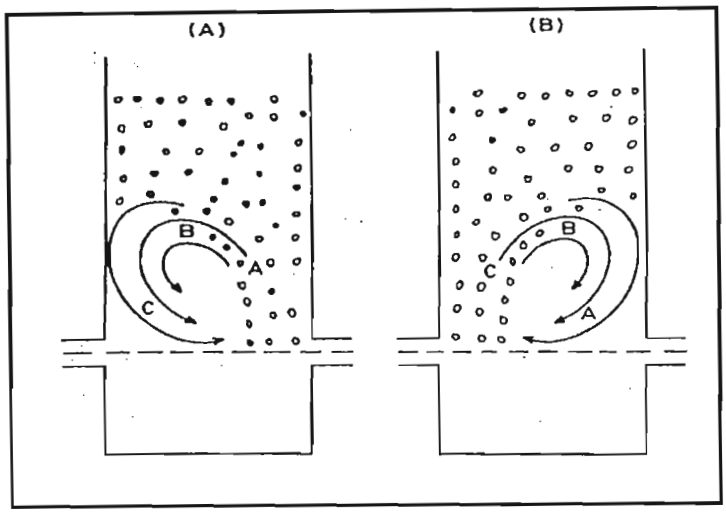

Figure 4-11: Bubble hose for partially active holes (Thorat et al, 2001)

(A) partially active (B) random switching of active holes

The sparger design and gas distribution chamber are important design parameters. Criteria for ensuring a uniform gas distribution across the gas sparger have been shown. The flow patterns at low gas throughputs in bubble columns are not uniform but exhibit dynamic swirling behaviour as described in the foregoing section. The sparger design is a critical design parameter for cascaded bubble columns and is treated in the next section.

4.4) Partitioned bubble columns

In order to improve the efficiency of continuous processes which occur in gas-liquid systems it is often desirable for the reactor to approach plug-flow behaviour. The behaviour of bubble column reactors in terms of hydrodynamic behaviour is better described by perfect mixing with high levels of axial liquid dispersion. The use of partition plates in bubble columns is often an effective and economical means of reducing dispersion. The resulting cascaded column is often used with co-current up-flow of the gas and liquid phases. A feature of partitioned bubble columns is the formation of a cushion of gas below the redistribution partition plates as shown in Figure 4-12.

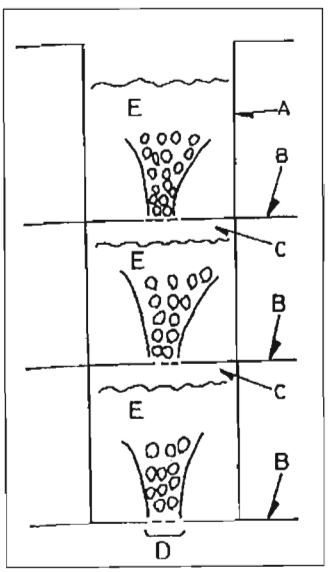

Figure 4-12: Bubble column with partition plates (Yamashita, 1994)

A=bubble column, B = partition plate, C=gas layer, D=bubbling layer

At low perforated cross-sectional areas of the partition plates, back-mixing may be eliminated completely and the bubble column cascade may be regarded as a series of continuously stirred vessels.

At higher perforated cross-sectional areas, the possibility of liquid exchange between neighbouring cells exists.

Deckwer (1992) reports that dispersion levels in a 45 cm diameter column can be reduced by as much as a factor of 10 for a partition plate spacing of 25 cm.

4.4.1) Models for partitioned columns

The models most commonly used for partitioned columns are the tanks in series model and the tanks in series with inter-stage mixing model.

4.4.1.1) Tanks in series model

The tanks in series model is given by:

$$E(\theta)\frac{N^N}{(N-1)!}\theta^{N-1}e^{-N\theta} \tag{4-48}$$

The graphical representation of Eq. 4-28 for various values of N is given in Figure 4-13.

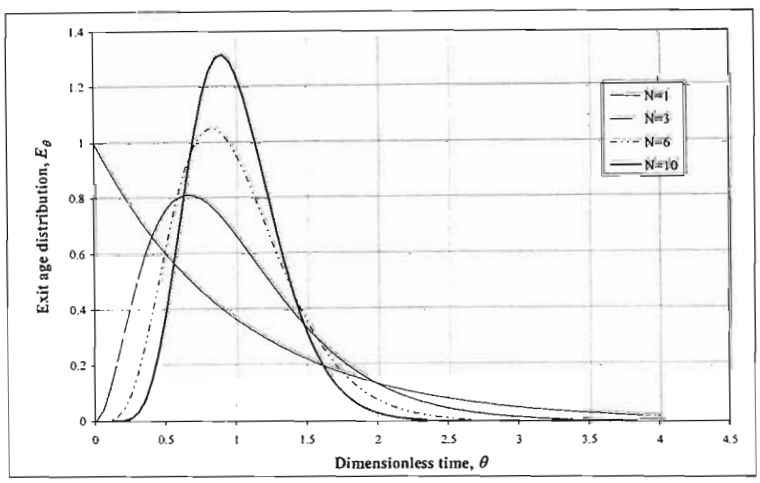

Figure 4-13: Theoretical age distribution curves for various tanks in series model

It is well known that plug-flow behaviour is approached when $N > 25$ (Levenspiel, 1962);

4.4.1.2) Tanks in series with inter-stage mixing model

A variation on the tanks in series model is the model of a cascade of perfectly mixed cells with mixing between the stages. The physical representation of the model is shown in Figure 4-14.

The parameters of the model are the number of physical stages N, the stage volume V_o and the ratio $K = (I/Q)$ with I the reverse flow and Q is the volumetric liquid flow rate.

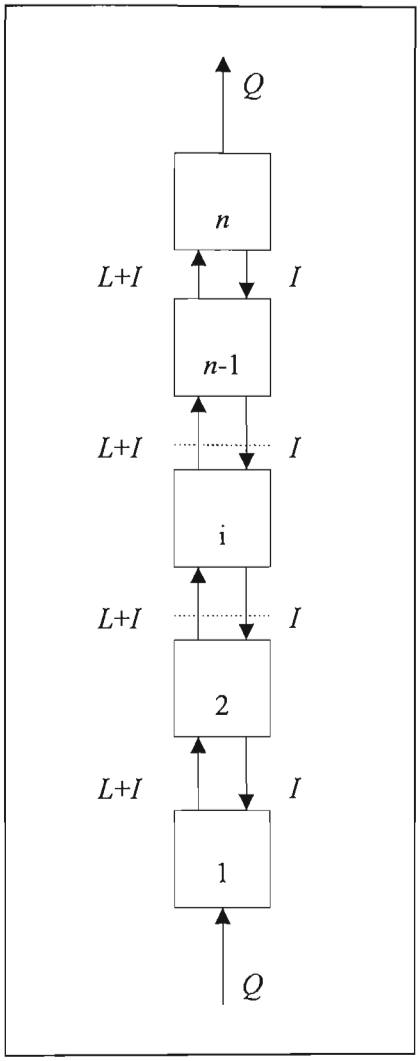

Figure 4-14: Model of a cascade of perfectly mixed units with mixing between stages

For a Dirac delta pulse the RTD of the system is given by (Kats and Genin, 1974):

$$E(\theta) = \frac{V}{Q} C_n(\theta) = \overline{C}_n(\theta) \tag{4-49}$$

with $C_n(\theta)$ given by the solution to the following differential equations:

$$\frac{d\overline{C}_n}{d\theta} = -(1+K)n\overline{C}_n + (1+K)n\overline{C}_{n-1} \tag{4-50}$$

$$\frac{d\overline{C}_i}{d\theta} = Kn\overline{C}_{i+1} - (1+2K)n\overline{C}_i + (1+K)n\overline{C}_{i-1} \tag{4-51}$$

$$\frac{d\overline{C}_1}{d\theta} = Kn\overline{C}_2 - (1+K)n\overline{C}_1 \tag{4-52}$$

The dimensionless time θ is given by:

$$\theta = \frac{\tau}{\tau_{avg}} = \frac{Q\tau}{NV_o} \tag{4-53}$$

The initial conditions for the model for tracer input are:

$$\overline{C}_1 = N \tag{4-54}$$

$$\overline{C}_1 = \overline{C}_2 = ... = \overline{C}_n = 0 \tag{4-55}$$

The solution to Eqs. 4-49 to 4-55 are generated via numerical methods. The function $E(\theta)$, calculated for N = 2 and various values of K is shown in Figure 4-15 and for N = 4 in Figure 4-16.

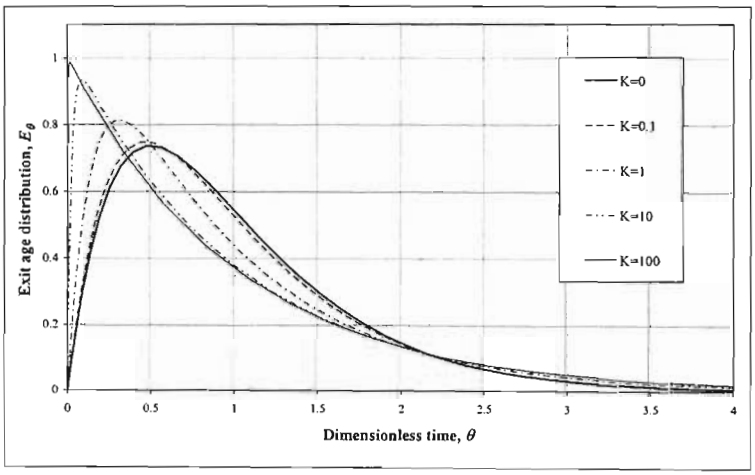

Figure 4-15:Theoretical RTD curves for N=2 and various values of K

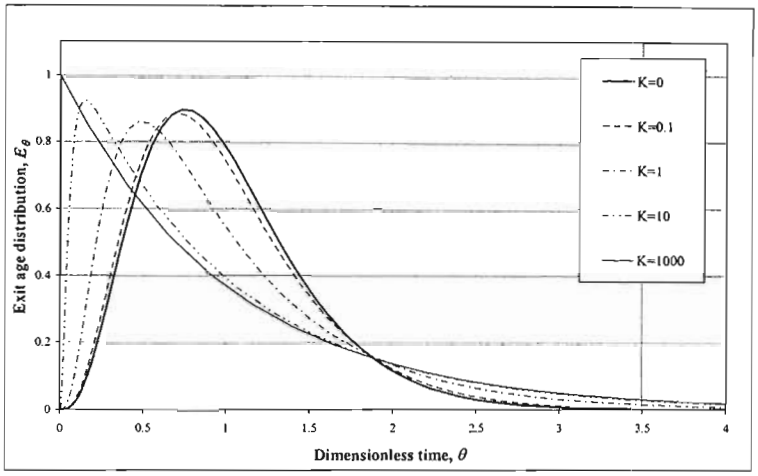

Figure 4-16: Theoretical RTD curves for N=4 and various values of K

The model presented above can be used to determine the parameter K by regression from experimental RTD curves. It is apparent that for $K = 0$ the model tends to the perfectly mixed tanks in series model and for a large K the model is well represented by a single perfectly mixed tank.

4.4.2) Partitioned bubble column studies: Literature

A summary of the experimental range covered by various researchers is provided in Table 4-5.

Table 4-5: Experimental conditions of partitioned bubble column studies in literature

Authors	D_C cm	L cm	L_{stage} cm	N -	u_g cm/s	u_L cm/s	f %
Kats and Genin (1974)	5.7, 9.5, 40	205, 600	20.5, 60	1, 10	0.01 - 100	0.08-0.8	0.68 – 26.5
Sekizawa & Kubota (1974)	5, 10, 20	100, 120, 200	10, 20, 40	3 - 10	0.36 – 9.3	0.116 – 0.450	0.07 – 0.202
Palaskar et al. (2000)	6.2, 20	77, 90	18, 20	4	0.017 – 1	0.038 – 0.2	0.5 – 10.8
Dreher & Krishna (2001)	10, 15, 38	270, 370, 289	68, 93, 72	4	5 - 40	0	18.6 – 30.7

The system considered was air/water in all cases.

4.4.2.1) Observations

Kats and Genin (1974) observed that superficial gas velocities greater than 1 cm/s together with liquid throughputs of up to 0.8 cm/s, that each stage in a partitioned column operates in the perfectly mixed regime. The authors also noted that for liquid throughputs less than 0.27 cm/s in a bubble column with no internals, the reactor operated for all practical purposes as a perfectly mixed unit. At low gas flow-rates and high open areas, back-flow of the liquid from stage to stage was observed. The authors state that for small open areas ($f < 1\%$), back-mixing in the complete range of gas and liquid flow-rates is negligibly low.

Sekizawa and Kubota (1974) observed that the back-flow rate was independent of the partition plate spacing and the column diameter. The authors found an influence of the gas velocity, the perforated area, the hole diameter, plate thickness and liquid viscosity on the rate of liquid back-flow in their experiments.

Palaskar et al. (2000), found that at lower gas superficial velocities (homogeneous regime) an increase in tray spacing reduced the level of liquid phase dispersion and that at higher gas velocities (heterogeneous regime) the effect is reversed ie. a decrease in tray spacing reduces the extent of back-mixing. The authors determined dispersion coefficients from RTD studies. They did not account for the possibility of back-flow of liquid between stages.

Dreher and Krishna (2001) measured the liquid back-flow and found it to be practically independent of column diameter. The authors worked in a batch liquid phase and described the variation of tracer concentration with time for any stage *i* as:

$$\frac{\partial C_i}{\partial t} = E_L \frac{\partial^2 Ci}{\partial z^2} \tag{4-56}$$

To determine the back-flow quantity the authors determined dispersion coefficients in an empty bubble column and assumed that these dispersion coefficients were representative of the dispersion in the partitioned column. This is contradictory to the fact that partitioning a bubble column causes a decrease in dispersion. A proper account would have been the determination of E_L and the liquid back-flow in the partitioned column. van Baten and Krishna (2003) ,with the aid of CFD simulations, showed the liquid back-flow rate to be independent of column diameter and a strong function of the open area of the partition plate, which supported the earlier experimental work of Dreher and Krishna (2001).

Recently, Pandit and Doshi (2005) showed that the mixing time in a partitioned 41 cm diameter column was an order of magnitude larger than that of the same column without partition plates.

The present state of art on bubble column design parameter estimation has been presented. It has been shown that although there are numerous methods available to determine design parameters for bubble columns, there is no clarity on the estimation and the effect of operating conditions on these parameters. For the present moment, the use of empirical correlations based on experimental observation must be used. Many authors have attempted a theoretical approach to predicting design parameters but the theory is often masked by empiricism and dimensional analysis.

Various macro-mixing models to correlate experimental RTDs have also been presented. These models are simple single-parameter models. It is possible to complicate the model, however, the parameters of complex models cannot be evaluated without sufficient and accurate experimental data which is often difficult to measure. Also, many researchers have shown good predictability with single parameter models. Shah et al. (1978) report that RTD models with more than two parameters would find very limited use for reactor design and modeling purposes.

For the estimation of other hydrodynamic design parameters such as liquid mass transfer coefficients and heat transfer coefficients the review articles by Shah et al. (1982), Deckwer and Schumpe (1993) and Kantarci et al. (2005) comprehensively cover the relevant literature.

CHAPTER FIVE

HYDRODYNAMICS AT LOW SUPERFICIAL GAS VELOCITIES:

ANALYSIS OF LITERATURE DATA

In the foregoing chapters the literature concerning axial dispersion coefficients and gas hold-up have been discussed. The term low superficial gas velocity must be viewed in a relative context. Most researchers would define low superficial gas velocities to be in the order of less than 5 cm/s as this is generally considered to be the transition zone from homogeneous bubbly flow to churn-turbulent flow. In the context of this study, low superficial gas velocities are less than 1 cm/s.

The questions that need to be considered for this flow regime are:

- Do correlations developed at higher superficial gas velocities apply at 1cm/s and less?
- Is the regime characterised by constant Peclet numbers?
- Does the theory of isotropic turbulence hold in this laminar flow regime?
- Is the behaviour of this regime inherently different from the churn-turbulent regime?

This chapter will deal with the relevant literature for studies in the superficial gas flow regime less than 1 cm/s. An extensive literature review has shown that hydrodynamic literature data is very sparse as compared to the literature at higher superficial gas velocities.

5.1) Axial dispersion coefficients

Table 5-1 lists the literature where the focus of study has been solely on axial dispersion at superficial gas velocities less than 1 cm/s.

In all the studies the system investigated was an air/water one. Apart from water, Ulbrecht and Baykara (1981) included three polymers in their experiments: carboxymethylcellulose, polyethleneoxide and polyacrylamid. The polymers were non-newtonian fluids. Only the air/water results of Ulbrecht and Baykara are presented.

Table 5-1: Literature studies at low superficial gas velocities

Author	D_c cm	u_g cm/s	u_L cm/s	Correlation	Eq.
Subramanian and Tien (1975)	10*	0.001 – 0.006	0	$E_L = 2.048 + 2039u_g$	(5-1)
Ulbrecht and Baykara (1981)	15.2	0.05 – 0.12	0	$E_L = 3.38V_L(0)$	(5-2)
Houzelot et al. (1985)	5	0.25 – 0.6	< 0.098	$E_L = 40u_g^{0.47}$	(5-3)

* square column with 10cm width

Eqs. 5-1 to 5-3 give E_L in cm^2/s with u_g and $V_L(0)$ in cm/s. None of the authors evaluated diameter effects in their studies.

Subramanian and Tien (1985) performed studies in a rectangular column. Anabtawi et al. (2003) who performed hydrodynamic studies in rectangular and cylindrical columns concluded that the hydrodynamic behaviour of these columns is markedly different. For this reason the work of Subramanian and Tien (1985) was not considered in the forthcoming analysis.

In addition to the works presented in Table 5-1 data points in the appropriate superficial gas regime were assimilated from various other authors. A summary of the points is given in Table 5-2.

Of the 60 data points only 29 correspond to dispersion coefficients obtained in columns of diameter 15 cm and greater. It is well reported in the literature that small diameter bubble columns exhibit different hydrodynamic behaviour due to wall effects and gas slugging due to coalescence. Therefore only the 30 data points obtained from columns with a diameter 15 cm or greater were considered. The relevant points and experimental conditions are given in Table 5.3.

Table 5-2: Summary of literature E_L data points for u_g ≤1cm/s

Author	D_c cm	Number of points	Source
Towell and Ackerman (1972)	107	1	Table
Kato and Nishiwaki (1972)	6.6	3	Figure
	12.2	2	Figure
	21.4	2	Figure
Deckwer et al. (1973)	20	4	Table
Eissa and Schugerl (1975)	15.9	8	Figure
Ulbrecht and Baykara (1981)	15	9	Figure
Kunigita et al. (1985)	5	4	Figure
Houzelot et al. (1985)	5	9	Table
Ityokumbul et al. (1994)	6	12	Figure
Moustiri et al. (2001)	15	3	Figure
	20	3	Figure

Values of dispersion coefficients were obtained either from tables in the referenced work or from figures presented by the authors. The values obtained from figures are subject to a slight error of no more than 3% of the actual experimental value.

Table 5-3: Literature data at low superficial gas velocities

Authors	Symbol	D_c cm	L cm	u_L cm/s	u_g cm/s	E_L cm^2/s
Deckwer et al. (1973)	▲	20	222	0.74	0.15	123
		20	222	0.74	0.24	118
		20	222	0.74	0.4	190
		20	222	0.44	0.56	230
Eissa and Schugerl (1975)	♦	15.9	390	0.35	0.35	40.0
		15.9	390	0.7	0.35	70.0
		15.9	390	1.05	0.35	105.0
		15.9	390	1.4	0.35	140.0
		15.9	390	0.35	1	44.0
		15.9	390	0.7	1	80.0
		15.9	390	1.05	1	118.0
		15.9	390	1.4	1	154.0
Kato and Nishiwaki (1972)	●	21.4	405	1.5	0.5	240.0
Moustiri et al. (2001)	■	15	425	0.62	0.54	30.9
		15	425	1.23	0.54	40.4
		15	425	1.86	0.54	42.9
	□	20	450	0.62	0.54	64.7
		20	450	1.23	0.54	89.7
		20	450	1.86	0.54	133.5
Towell and Ackermann (1972)	+	107	510	0.72	0.85	1900.0
Ulbrecht and Baykara (1981)	○	15.2	60.8	0	0.05	70.0
		15.2	60.8	0	0.05	80.0
		15.2	60.8	0	0.07	81.0
		15.2	60.8	0	0.085	98.0
		15.2	60.8	0	0.086	103.0
		15.2	60.8	0	0.092	118.0
		15.2	60.8	0	0.1	121.0
		15.2	60.8	0	0.1	130.0
		15.2	60.8	0	0.13	152.0

The results are plotted in Figure 5-1 below. The key for Figure 5-1 and all subsequent figures is given in Table 5-3.

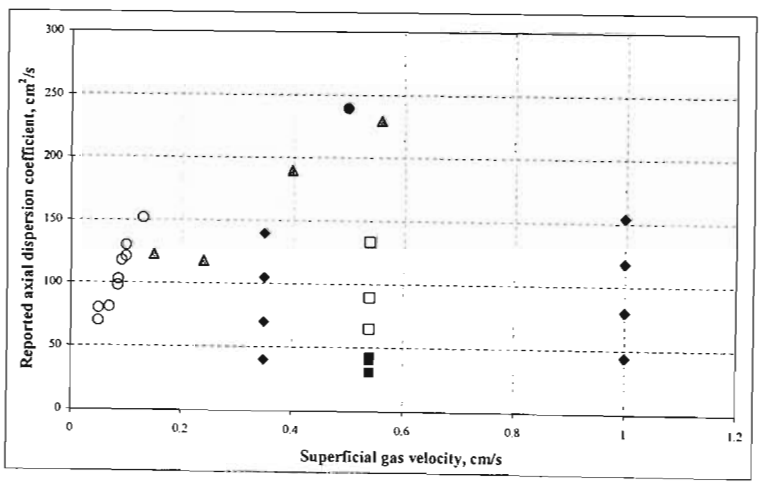

Figure 5-1: Plot to show reported literature dispersion coefficients as a function of superficial gas velocity

Moustiri et al. (2000) and Eissa and Schugerl (1975) both reported a liquid superficial velocity effect on E_L. Table 5-3 shows that the authors observed an increase in E_L for increasing superficial liquid velocity. Houzelot et al. (1985) also investigated the effect of liquid velocity and found no effect on the dispersion coefficient.

The validity of extrapolating literature correlations (Chapter 4) to low superficial gas velocities was determined using the literature data points shown in Table 5-3.

5.1.1) Prediction of E_L by superficial gas velocity and diameter correlations

The correlation of Deckwer et al. (1974) is well cited and recommended by many bubble column researchers. The results of the comparison between literature dispersion coefficients and predicted E_L values via the correlation of Deckwer et al. (1974), Eq. 4-6, is shown in Figure 5-2.

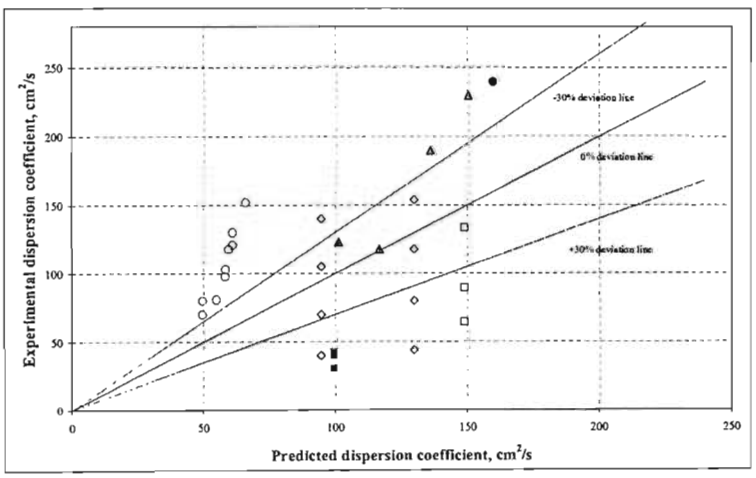

Figure 5-2: Comparison of literature dispersion coefficients to predicted E_L values via the correlation of Deckwer et al. (1974)

A small proportion of the literature data falls within a ± 30 % deviation from the prediction of Eq. 4-6. The data of Ulbrecht and Baykara (1981) is poorly estimated by the correlation of Deckwer et al. (1974). The comparison of Eq. 4-7 developed by Hikita and Kikukawa (1974) is shown in Figure 5-3.

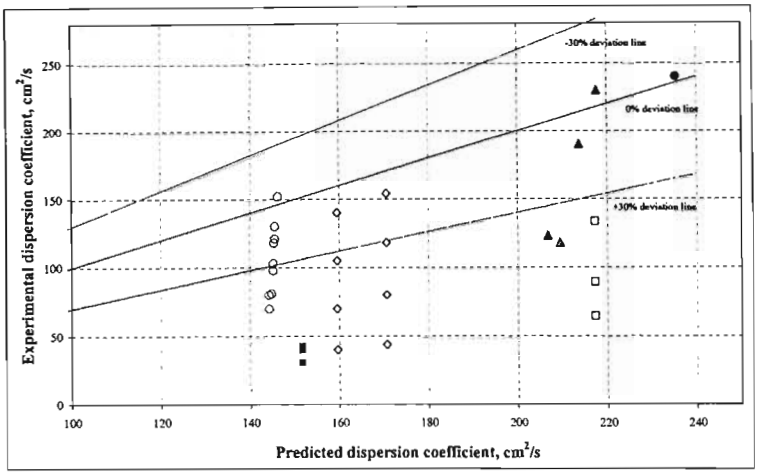

Figure 5-3: Comparison of literature dispersion coefficients to predicted E_L values via the correlation of Hikita and Kikukawa (1974)

The correlation of Hikita and Kikukawa (1974) satisfactorily estimates the largest proportion of literature data as compared to any of the other correlations considered from Table 4-2. The data that is not well predicted is observed to be over estimated by the correlation of Hikita and Kikukawa (1974).

The comparison of Eq. 4-10 developed by Ityokumbul et al. (1974) is shown in Figure 5-4 below.

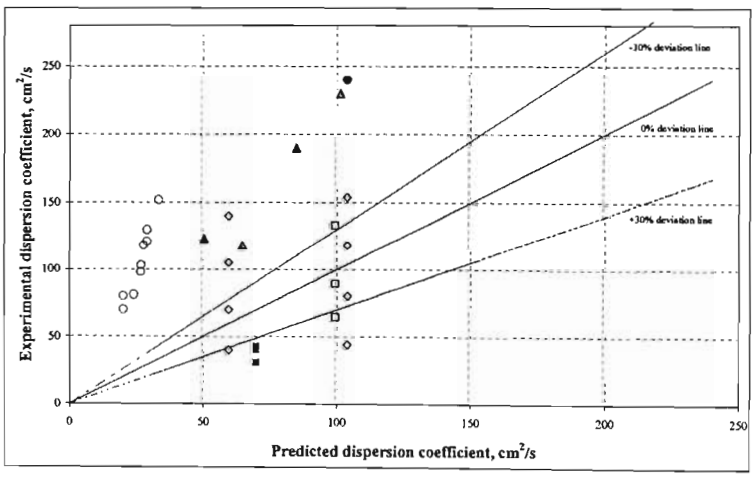

Figure 5-4: Comparison of literature dispersion coefficients to predicted E_L values via the correlation of Ityokumbul et al. (1994)

The correlation of Ityokumbul et al. (1994) tends to under-estimate the reported literature dispersion coefficients.

The comparison of Eq. 4-5 developed by Ohki and Inoue (1970) is shown in Figure 5-5 below.

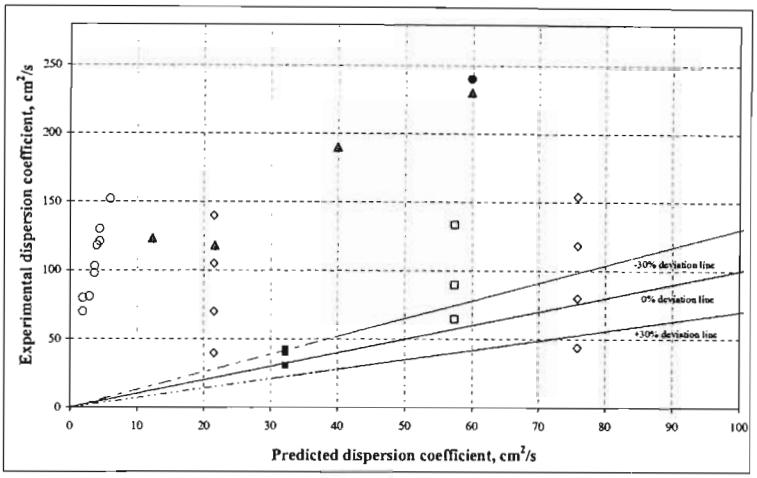

Figure 5-5: Comparison of literature dispersion coefficients to predicted E_L values via the correlation of Ohki and Inoue (1970)

As was the case for the correlation of Ityokumbul et al. (1994), the correlation of Ohki and Inoue (1970) is observed to greatly under-estimate the literature dispersion coefficients.

It is evident that there is a wide scatter in the prediction of literature dispersion coefficients. The literature correlations were found to either under-predict or over-estimate the measured literature dispersion coefficients.

In addition to this the literature data was correlated according to the form of Eq. 4-3. Initially the data point of Towel and Ackermann (1972) was not included in the regression. This was done to test the extrapolation of the correlation, developed from small diameter column data, to a larger diameter column. The regression gives:

$$E_L = 0.123 D_c^{2.39} \tag{5-4}$$

Regression of the data with Towel and Ackermann's data point yields:

$$E_L = 1.49 D_c^{1.53} \tag{5-5}$$

In both cases the superficial gas velocity dependency is negligible. A comparative analysis for Eq. 5-4 is shown in Figure 5-6.

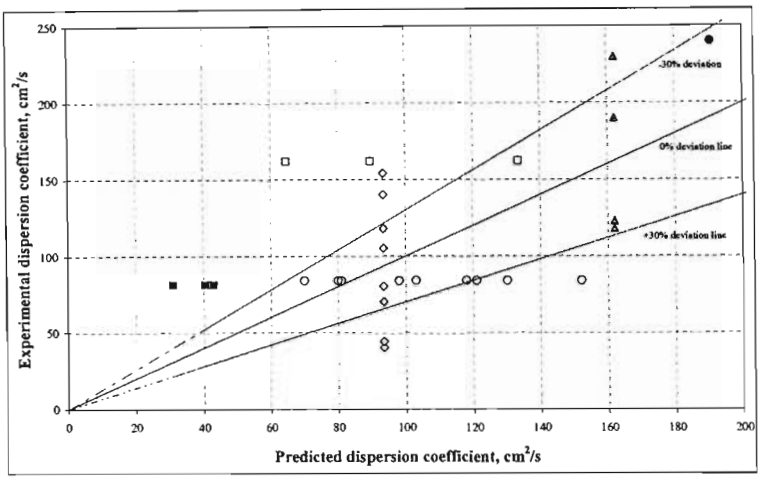

Figure 5-6: Comparison of literature dispersion coefficients to predicted Eq. 5-4 values

The correlation provides an improved estimation over existing literature correlations. However the effect of scaling to a large diameter column must be considered. A comparison is given in Table 5-4. Towell and Ackermann (1972) reported an E_L value of 1900 cm^2/s for a one meter diameter column.

Table 5-4: Prediction of Towell and Ackermann's dispersion coefficient data point

Author	E_L^{corr} cm^2/s	Eq.	Relative error %
Ohki and Inoue (1970)	2826.1	4-5	48.7
Deckwer et al. (1974)	1783.7	4-6	-6.1
Hikita and Kikukawa (1974)	1823.5	4-7	-4.0
Ityokumbul et al. (1974)	1002.8	4-10	-47.2
Regression (this work)	9031.4	5-4	375.3
	1900.3	5-5	0.0

The results are variant. The correlations of Deckwer et al. (1974) and Hikita and Kikukawa (1974) predict the dispersion coefficient very well. It should be noted that Towell and Ackermann worked at a u_g of 0.85 cm/s. It is possible that at lower gas flow rates literature correlations may not be valid. The prediction of Eq. 5-4 suitably highlights the danger in using empirical correlations for scale-up. If Eq. 5-4 was used to design a

commercial bubble column reactor it would result in tremendous over-design. This brings to bear the need for literature data at large column diameters.

The conclusion here is that the extrapolation of existing correlations based on diameter and superficial gas velocity is subject to large uncertainty at superficial gas velocities less than 0.8 cm/s. It must be emphasised that the error in the literature data is assumed to be negligible.

5.1.2) Prediction of E_L by analysis of Peclet number

Reith et al. (1968) reported that a constant Peclet number was achieved for high superficial gas velocities (Eq. 4-13). The literature data at low superficial gas velocities shows that no correlation can be determined from a similar analysis as Reith et al. (1968). The results shown in Figure 5-7 show no apparent trend. Figure 4-3 shows that the authors obtained complex behaviour of the Peclet number at superficial gas velocities less than 10 cm/s.

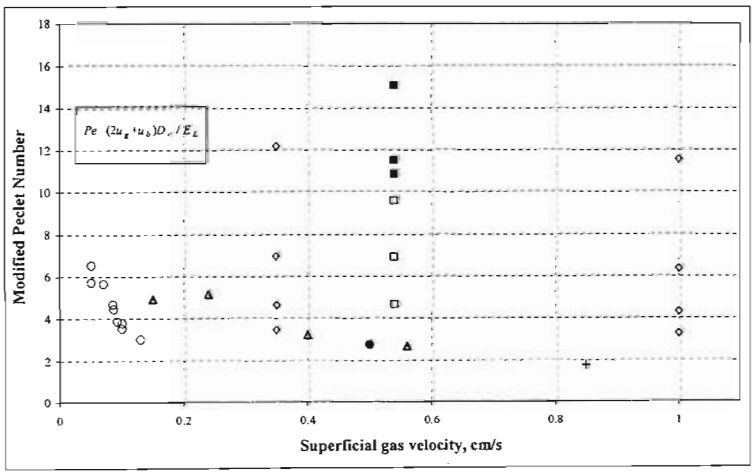

Figure 5-7: Literature data modified Peclet numbers versus superficial gas velocity

Eissa and Schugerl (1975) modified the analysis of Reith et al. (1968). A similar analysis was performed with the literature data. Eissa and Schugerl (1975) showed as per Figure 4-6 that the product of the modified Peclet number and the actual liquid velocity varied linearly with the ratio of the gas and liquid superficial velocities. For the literature data the value of actual liquid velocities was not reported and the superficial liquid velocity was used instead. The result is given in Figure 5-8.

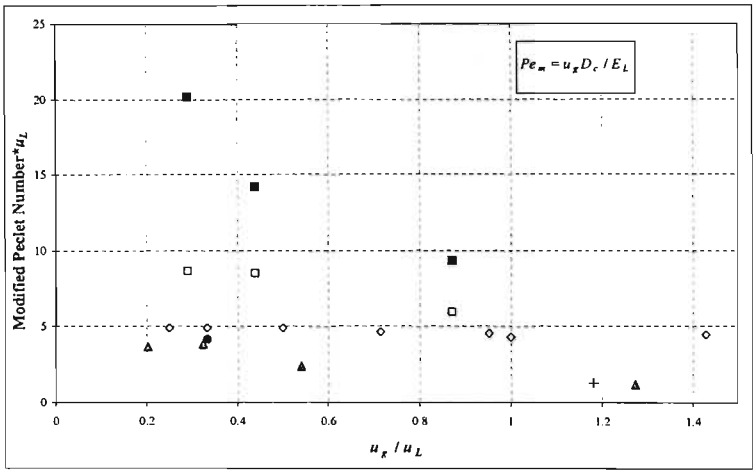

Figure 5-8: Literature Pe_m. u_L data versus dimensionless velocity as per Eissa and Schugerl (1975)

Figure 5-8 shows that data of Eissa and Schugerl (1975) settles about the value $Pe_m.u_L = 5$. No trend is apparent for the other literature data points.

Kato and Nishiwaki (1972) showed that the Peclet number can be correlated with the Froude number (Eq. 4-16). A comparison of their correlation to literature data is given in Figure 5-9.

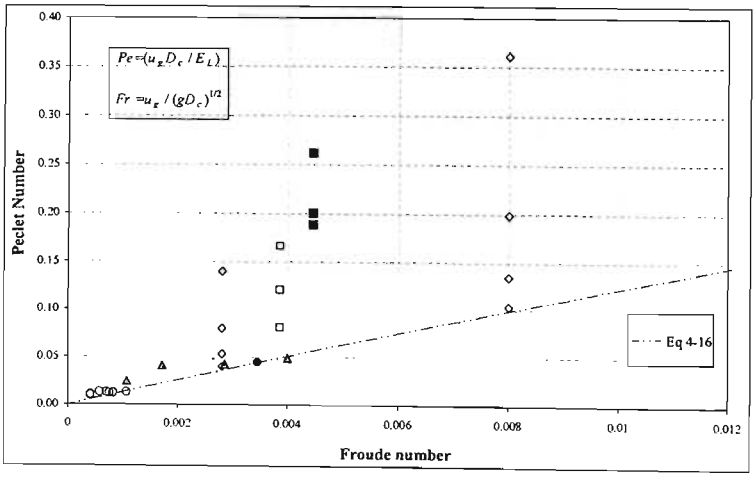

Figure 5-9: Plot of Peclet number against Froude number for literature data

Eq. 4-16 was solved for the axial dispersion coefficient. The results are shown in Figure 5.10.

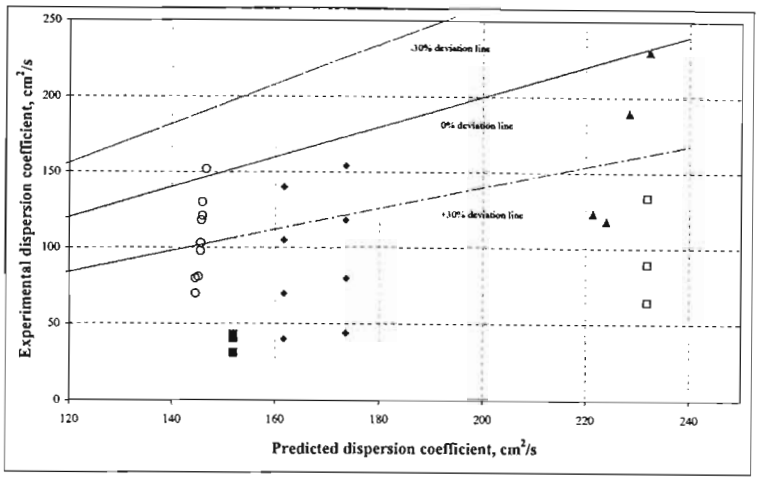

Figure 5-10: Comparison of literature data to Kato and Nishiwaki's (1972) correlation for predicting dispersion coefficients

The prediction of dispersion coefficients for Ulbrecht and Baykara's (1981) data is fair. Eq. 4-16 tends to over-estimate the reported literature data of the other authors.

5.1.3) Prediction of E_L by Kolmogoroff's theory of isotropic turbulence

Kolmogoroff's theory is only valid for high liquid Reynold numbers. It is questionable whether the assumptions made by Baird and Rice (1975) will hold in the bubbly flow regime where turbulence is not fully developed. The correlation predictions of Baird and Rice (1975) were compared to literature data as shown in Figure 5-11.

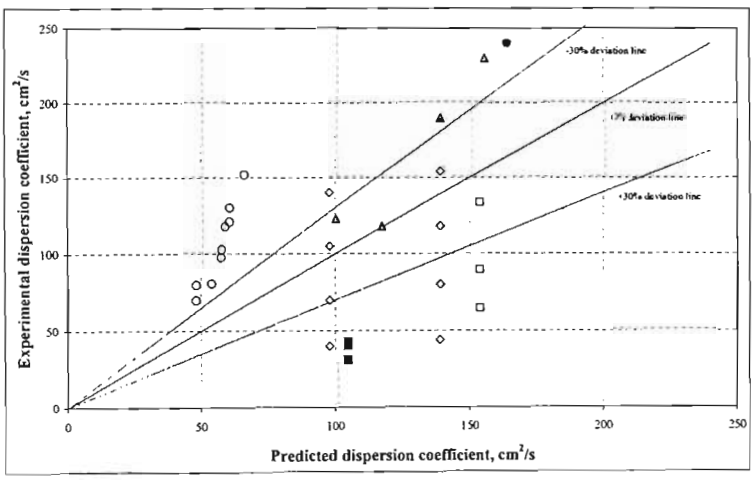

Figure 5-11: Comparison of literature data to Baird and Rice's (1975) correlation for predicting dispersion coefficients

The correlation of Baird and Rice (1975) does not yield an adequate estimation of the reported literature dispersion coefficients.

5.1.4) Prediction of E_L by recirculation and centre-line velocities

In order to analyse correlations of this nature experimental values for gas hold-up, centre-line liquid velocities, phase slip velocities and axial dispersion coefficients are required. Of the works cited in Table 5-2, only Ulbrecht and Baykura (1981) performed all the required measurements. The relevant data is provided in Table 5-5.

Table 5-5: Literature data of Ulbrecht and Baykura (1981)

u_g	$V_L(0)$	E_L	ϵ_g	u_b	u_s
cm/s	cm/s	cm^2/s	-	cm/s	cm/s
0.0500	25	70	0.0030	44	19
0.0500	25	80	0.0030	44	19
0.0700	29	81	0.0055	49	20
0.0850	33	98	0.0087	51	18
0.0860	33	103	0.0087	51	18
0.0920	34	118	0.0090	52	18
0.1000	38	121	0.0110	55	17
0.100	38	130	0.0110	55	17
0.1300	43	152	0.0140	64	21

In their studies Ulbrecht and Baykara (1981) correlated their measured dispersion coefficients with the centre-line liquid velocity. Krishna et al. (2000) reported that the centre-line liquid velocity was well represented by Eq. 4-27. A comparison of the measured centre-line velocities of Ulbrecht and Baykara as compared to Eq. 4-27 is shown in Figure 5-12.

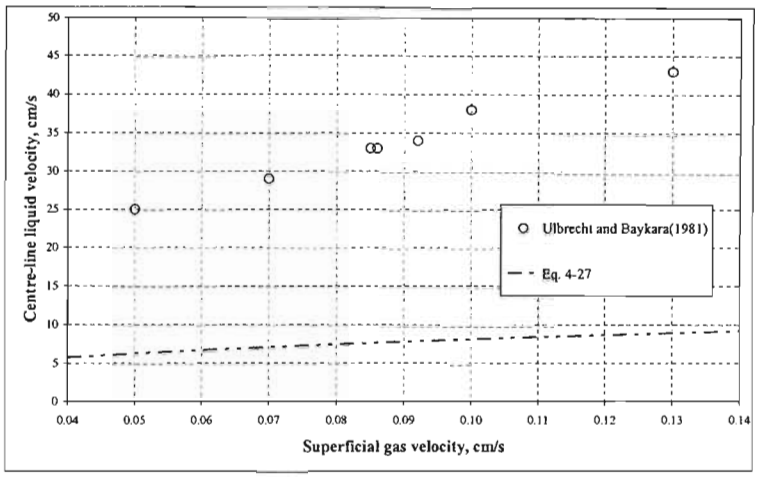

Figure 5-12: Comparison of Ulbrecht and Baykara's (1981) measured centre-line liquid velocities to predicted centre-line velocity via Eq. 4-27

It is evident that Eq. 4-27 severely under-predicts the measured values of Ulbrecht and Baykara.

Although other authors did not measure centre-line liquid velocities Eq. 4-28 and Eq. 4-27 were used to predict axial dispersion coefficients for the other works shown in Table 5-2. The comparison is given in Figure 5-13.

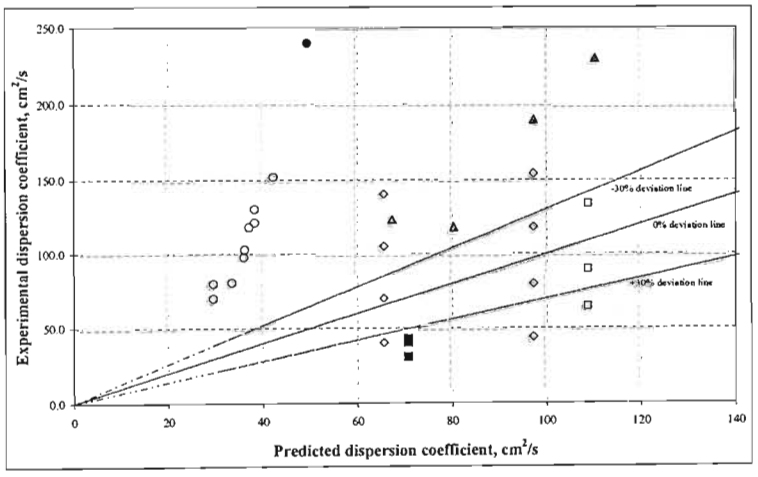

Figure 5-13: Comparison of literature data to correlation via centre-line velocity as per Krishna et al. (2000)

The prediction of axial dispersion coefficients as recommended by Krishna et al. (2000) does not satisfactorily describe the literature data. For the data of Ulbrecht and Baykara (1981) the dispersion coefficient is under-predicted as was the case with the majority of the literature data.

Correlation with centre-line liquid velocity is independent of knowledge of gas hold-up data. In the case of correlation via liquid recirculation velocity, accurate values of gas hold-up and slip velocities are required as per Eq. 4-26:

$$E_L = 0.9 D_c^{1.5} \left[L\left(u_g - \varepsilon u_s\right) \right]^{1/3} \tag{4-26}$$

It is clear that for positive dispersion coefficients $u_g - \epsilon_g . u_s \geq 0$.

For the data of Ulbrecht and Baykara (1981) this is not the case as shown in Table 5-6 below:

Table 5-6: Recirculation velocity values for Ulbrecht and Baykara's (1981) data

u_g cm/s	$\epsilon_g . u_s$ cm/s	$u_g - \epsilon_g . u_s$ cm/s
0.0500	0.0570	-0.0070
0.0500	0.0570	-0.0070
0.0700	0.110	-0.0400
0.0850	0.1566	-0.0716
0.0860	0.1566	-0.0706
0.0920	0.1620	-0.0700
0.1000	0.1870	-0.0870
0.100	0.1870	-0.0870
0.1300	0.2940	-0.1640

5.2) Gas hold-up

With respect to gas hold-up it would be folly to expect a single correlation to accurately predict hold-up at low superficial gas velocities. It was shown in Chapter 4 that gas hold-up is intricately dependent on operating conditions and sparger geometry. Gas hold-up has not been studied extensively at low superficial gas velocities.

There are two inter-related reasons for this:

i) gas hold-up is extremely low (negligible)

ii) it is difficult to accurately and precisely measure low gas hold-up values

Table 5-7 lists some reported gas hold-up values from literature sources and the predictions of Hughmark's (1967) correlation for these gas flow-rates.

Table 5-7: Comparison of reported literature gas hold-ups to Hughmark's (1967) correlation

Author	u_g	D_c	ϵ_g Reported	ϵ_g Hughmark (1967)
	cm/s	cm	-	Eq. 4-42
Towell and Ackermann (1972)	0.85	106	0.030	0.023
Deckwer et al. (1973)	0.15	20	0.010	0.004
	0.24	20	0.010	0.007
	0.4	20	0.020	0.011
Ulbrecht and Baykara (1981)	0.05	15.2	0.003	0.001
	0.07	15.2	0.006	0.002
	0.085	15.2	0.009	0.002
	0.092	15.2	0.009	0.003
	0.01	15.2	0.011	0.000
	0.013	15.2	0.014	0.000
Houzelot et al. (1985)	0.25	5	0.010	0.007
	0.6	5	0.020	0.017

Figure 5-14 shows that the correlation of Hughmark (1967) does not accurately predict gas hold-up values for literature sources. However the gas hold-up values are very small and hence the deviations are greatly exaggerated. For design purposes the correlation of Hughmark (1967) sufficiently describes gas hold-up at low superficial gas velocities.

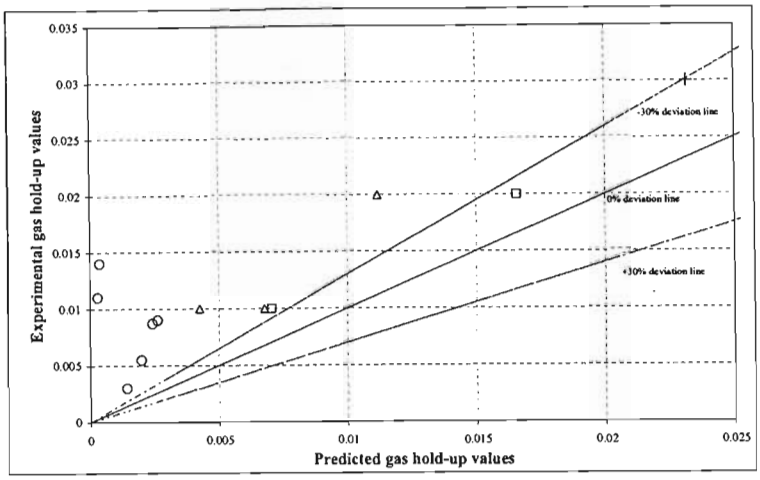

Figure 5-14: Comparison of literature gas hold-up values to Hughmark's (1967) correlation

The purpose of performing these computations with literature data has been:

i) to highlight the discrepancy in measured dispersion coefficients in the literature

ii) to extrapolate existing correlations to literature data at $u_g < 1$ cm/s

iii) show that a study at low superficial gas velocities is justified

iv) understand the mixing mechanism at low superficial gas velocities

It is evident from the foregoing analysis that existing correlations fail to accurately predict axial dispersion at low superficial gas velocities. This justifies and necessitates a study of axial mixing at these velocities. Also the need for data at high diameter columns is integral for the use of empirical correlations.

It is evident that there is a great discrepancy in the measured dispersion coefficients reported in the literature. This may be due to the method of data analysis used by the respective authors. In Chapter 7 the data analysis methods used to obtain axial dispersion coefficients are compared. The choice of data analysis method may explain why there is such a profound inconsistency in reported literature data.

CHAPTER SIX

APPARATUS AND EXPERIMENTAL PROCEDURE

The scope of this project included the design, construction and commissioning of suitable bubble column equipment for hydrodynamic studies. In the preceding chapters the critical design parameters and geometries were discussed. These aspects were taken into consideration in the designing of the bubble column apparatus. The specifications of the equipment assembled at the University of Kwa-Zulu Natal – Howard College Campus are comparable with bubble column vessels used by prominent international bubble column research groups (Table 4-1). The bubble columns specifications are given in Table 6-1.

Table 6-1: Bubble column apparatus for hydrodynamic studies

Column	Diameter (id) cm	Length cm	(L/D_c)	Material
BC1	22	195	0 - 8.8	QVF glass
BC2	30	200	0 – 6.7	304 Stainless-steel
BC3	30	80	0 – 2.7	QVF glass

This chapter will outline the process by which the final equipment and experimental procedure were obtained.

6.1) Preliminary equipment

In an attempt to practice and gain experience in hydrodynamic experiments trial runs were performed in a 14 cm inner diameter Perspex column. The column was salvaged from storage. The column had previously been used as a biochemical gas-liquid fermentor and had been tremendously stressed.

The following modifications were made to the equipment:

- a 6 mm hole was drilled into the column 5 cm above the distributor plate
- an injection port was installed at the point above
- a 12 mm hole was drilled into the column at 100 cm above the distributor plate to serve as a liquid outlet

The design of the column was such that the distributor plate could not be changed or modified as the gas chamber and plate were PVC welded together as a single unit. The distributor plate had 40 holes of 1 cm diameter. The column height was 110 cm. The column is shown in Figure 6-1 below.

Figure 6-1: Perspex column

The design of the column was such that the liquid and gas entered the PVC gas chamber and then into the Perspex section. A schematic representation is shown in Figure 6-2.

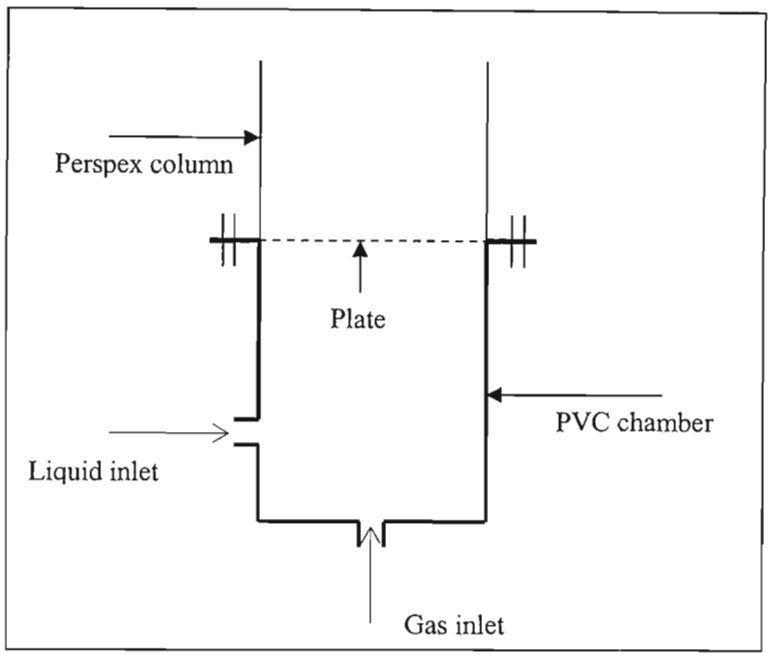

Figure 6-2: Schematic of gas and liquid inlets for Perspex column

The Perspex column was beleaguered by leaks and eventually had to be retired due to the propagation of cracks and plastic crazing resulting from the drilling of the holes into the column. However valuable insight on experimental method and an understanding of the mixing in bubble columns was achieved during the short life of this column.

6.2) Bubble column design specifications

The geometrical design parameters that required investigation can be summarised as follows:

- column diameter
- volume of gas distribution chamber
- aspect ratio (L/D_c)
- sparger geometry
- plate spacing for partitioned columns

The design of the bubble column vessels was performed with consideration of these parameters.

6.2.1) Choice of column diameter, height and material of construction

6.2.1.1) BC1 and BC3

The critical column diameter where hydrodynamic parameters become independent of diameter was shown to be 15 cm (Chapter 4). Any column diameter larger than 15 cm would be suitable for bubble column research. For BC1 and BC3 glass sections of inner diameter 30 cm and 22 cm respectively were chosen.

For the 30 cm diameter column two QVF glass sections were available as was the case for the 22 cm column. Table 6-2 gives the height of the sections.

Table 6-2: Heights of glass sections for bubble columns

Column	Height Section 1 cm	Height Section 2 cm
BC1	93	102
BC3	30	50

The sections would allow the incorporation of partition plates being installed between them. In terms of aspect ratios BC1 allowed for aspect ratios between 0-8.8. This was well representative of industrial column aspect ratios. In the case of BC3 the aspect ratio of 0-2.7 was very low. Both columns were transparent and would greatly assist in the qualitative analysis of bubble column behaviour.

6.2.1.2) BC2

The materials of construction considered for BC2 were:

- Perspex
- borosilicate glass
- stainless-steel
- various resins (eg. PVC, Nylon 12)

The materials were compared on the basis of cost, durability, transparency and solvent compatibility as shown in Table 6-3.

Table 6-3: Ranking of materials of construction

Material	Cost	Robustness	Transparent	Solvent compatibility
Perspex	High	Low	Yes	Very low
Glass	Very high	Medium	Yes	High
Steel	Low	High	No	High
PVC	High	Low	No	Low

All four options were explored extensively and eventually the choice of 304 stainless-steel was settled on for the following reasons:

- lowest cost
- good solvent compatibility for possible future work with organic solvents
- high strength for possible future work at higher pressures
- ease of modification
- supplied locally (no need to import as was the case for glass sections)

The only significant disadvantage was that a stainless-steel column would be opaque and the visual component of the experiments would have to be sacrificed. However the sparging mechanism in a 30 cm diameter column could easily be visualised in BC3. For this reason all spargers for BC2 were designed to be compatible with BC3.

The diameter was selected as 30 cm and the choice of height for BC3 was 200 cm. This allowed for aspect ratios in the range 0-6.7. In Figure 2-5 the distribution of bubble zones is shown. When the aspect ratio of the column is larger than the development region the circulation velocity in the column will be independent of the aspect ratio (Joshi, 2001). In this regard the height of 200 cm was sufficiently adequate. The wall thickness of the column as per supplier catalogue was 3 mm. The wall thickness offers sufficient strength for future work at pressures above atmospheric pressure.

The column was designed as four sections of 50 cm height. This would allow for various number of cells (1-4) in a partitioned column arrangement. The choice of section height for BC2 was chosen to be greater than the column diameter as many researchers suggest that the height of the circulation cells in bubble columns is approximately equal to the column diameter and therefore the height of the cell would not greatly influence the natural hydrodynamic circulation patterns.

All sections were electrochemically polished so as to ensure a smooth inner surface.

6.2.2) Arrangement of tappings

6.2.2.1) BC1

The 22 cm glass sections had no tappings fitted into them. The sections had to be modified to allow for injection port and liquid inlet/outlet points. The sections were too large for a glass-blower to handle and the modifications were therefore made in-house. The required holes were mechanically ground with a hollow stainless-steel tube. As glass is relatively fragile the size of the holes was restricted to 12 mm nominal diameter. As the modifications to the sections would be permanent only six tappings were made. Table 6-4 gives the chosen heights for the tappings. The tappings were chosen to give a wide range of operating aspect ratios for continuous runs.

Table 6-4: Tapping heights for BC1

Height above sparger	Aspect ratio
cm	-
19	0.86
44	2.00
66	3.00
108	4.90
141	6.40
176	8.00

A 316 stainless-steel bulk head fitting was installed into each tapping. Liquid seals were made with rubber rings and rubber septa were installed as shown in Figure 6-3.

Figure 6-3: Injection port for BC1

For use as a liquid inlet or outlet, 8 mm stainless-steel tubing with a nut and ferrule set was utilised.

6.2.2.2) BC3

The column was utilised primarily to visualise the sparging mechanism in a 30 cm column. The column was too short for quantitative experiments and as such no modifications were made to these sections.

6.2.2.3) BC2

Seven tappings were made in the stainless-steel sections. The choice of tappings for BC3 is given in Table 6-5.

For each of the tappings a ½" female socket was welded over the tapping. The socket allowed versatility of using a barbed hose fitting for liquid inlets/outlets or an arrangement as shown in Figure 6-3 for injection ports.

Table 6-5: Tapping heights for BC3

Section	Height above sparger	Aspect ratio
	cm	-
1	5	0.17
1	30	1.00
2	60	2.00
2	90	3.00
3	130	4.33
4	165	5.50
4	190	6.33

6.3) Gas chamber specifications

Thorat et al. (2001) used gas chambers of 6, 18 and 44.8 L and found no effect of the gas chamber volume in their studies for this range of volumes. In this study a single gas chamber was utilised for all three columns. A schematic for the gas chamber is given in Figure 6-4. A valve for draining the chamber was installed at the bottom. Air was fed from the side in the midst of the chamber.

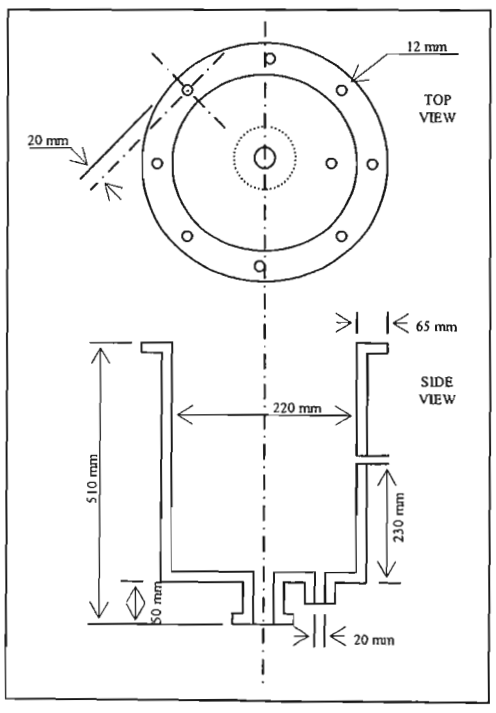

Figure 6-4: Schematic of primary gas distribution chamber

The gas chamber could be directly attached to BC1 with a suitable flange matching the bolt hole arrangement as shown in Figure 6-4.

For BC2 and BC3 an adaptor was designed to facilitate the use of the distribution chamber with the 30 cm diameter columns. The height of the adaptor was 22 cm. A schematic representation is shown in Figure 6-5.

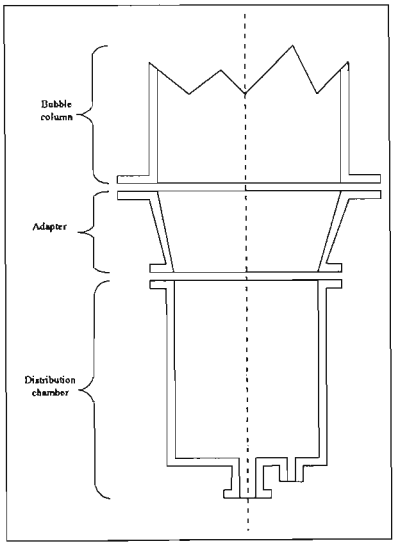

Figure 6-5: Schematic drawing of distribution chamber and adaptor

The adaptor acts as a flow expander. The design specifications of the gas chamber and adaptor are provided in Table 6-6.

Table 6-6: Design specifications for gas chamber and adaptor

	Inner flange diameter mm	Outer flange diameter mm	Number of bolt holes -	Nominal diameter of bolt holes mm	PCD of bolt holes mm	Volume L
Gas chamber	220	350	8	10	310	17.5
Adaptor bottom	220	350	8	12	310	7.8
Adaptor top	300	450	12	12	390	

6.4) Spargers

The specifications for the spargers used with BC1 are given in Table 6-7 and in Table 6-8 for BC2 and BC3.

- hole diameter d_h
- pitch of holes P
- plate thickness t
- percentage aerated area f

Table 6-7: Design details for BC1 sieve-plate spargers

Sparger	d_h	N_h	Geometry	P	t	t/d_h	f
-	mm	-	-	mm	mm	-	%
SP1	1.0	1	Orifice	90	2.0	2.00	0.0021
SP2	1.0	4	Square	80	3.0	3.00	0.0083
SP3	1.5	9	Square	45	1.5	1.00	0.0418
SP4	1.5	9	Triangular	60	1.5	1.00	0.0418
SP4	2.0	36	Square	30	2.0	1.00	0.2975
SP5	2.0	44	Square	65	1.5	0.75	0.3636
SP6	3.0	36	Square	30	2.0	0.67	0.6694
SP7	2.0	36	Square	30	2.0	1.00	0.2975

Table 6-8: Design details for BC2 and BC3 sieve-plate spargers

Sparger	d_h	N_h	Geometry	P	t	t/d_h	f
-	mm	-	-	mm	mm	-	%
SP8	1.0	1	Orifice	0	3.0	3.00	0.0011
SP9	1.0	4	Square	60	1.0	1.00	0.0044
SP10	1.0	4	Square	90	1.0	1.00	0.0044
SP11	1.5	9	Square	30	1.5	1.00	0.0225
SP12	1.5	9	Triangular	60	1.5	1.00	0.0225
SP13	2.0	36	Square	40	2.0	1.00	0.1600
SP14	4.0	36	Square	40	3.0	0.75	0.6400
SP15	4.0	36	Square	40	3.0	0.75	0.6400
SP16	4.0	36	Square	40	3.0	0.75	0.6400

6.5) Air supply

Air was supplied from a compressor and was available at a maximum of 7 bar gauge. For the experiments the supply pressure was regulated at 200 kPa and the gas flow rate was maintained with a calibrated gas rotameter.

6.5.1) Calibration of air rotameter

The gas rotameter was calibrated by measuring the displacement of water. The calibration was checked on a regular basis and remained constant over the entire experimental period. The calibration was non-linear and is shown in Figure 6-6.

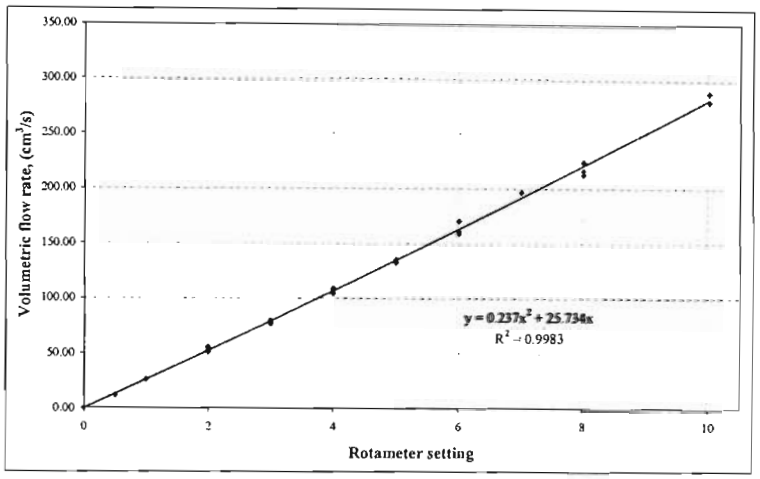

Figure 6-6: Plot of air volumetric gas flow rate versus air rotameter setting

6.6) Water supply

Municipality tap water was utilised for all experiments. For batch tests the column was filled directly with water from the mains.

Liquid flow rates were controlled with appropriate rotameters. Initially for the continuous liquid RTD measurements water was used directly from the mains. However the varying conductivity of the mains water during a run was a cause of immense experimental error. To circumvent this instability a 600 L plastic storage tank was installed. This allowed the use of a consistent batch of liquid for an experimental RTD run. The tank was always well mixed as a large liquid recycle from the pump created sufficient agitation. The liquid flow rate was

throttled by a valve and monitored with a rotameter. A schematic of the experimental setup is shown in Figure 6-7.

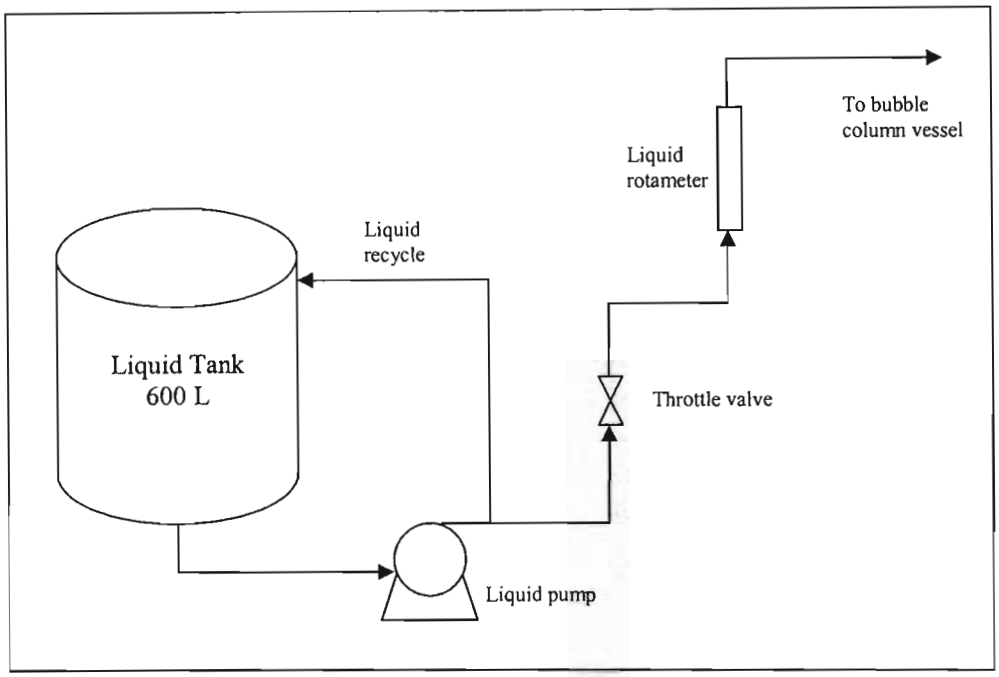

Figure 6-7: Schematic of liquid tank, pump and recycle

The pump was a three-phase KM Kolding pump which allowed a maximum liquid flow rate of 115 L/min. Two calibrated liquid rotameters were used. The range of flow rates for each rotameter is given in Table 6-9.

Table 6-9: Range of flow rates for liquid rotameters

Rotameter	Volumetric flow range L/min
LR1	0- 10
LR2	0 - 20

6.7) Conductivity meter and probe

A Jenway 4310 conductivity meter and probe was utilised for all experiments (Figure 6-8). The probe offered excellent dynamic response and the meter allowed logging to a computer via an RS 232 port. Software was written in Visual Basic® 6.0 to interface the meter with a computer. The software allowed for various time intervals at which readings could be recorded. Typically readings were recorded every second. The dynamic response of the probe and meter was determined to be in the order of nano seconds.

Figure 6-8: Jenway 4310 conductivity meter and probe

The probe is an immersion type probe and is designed primarily for use in the upright position. This limited the orientation of the probe for experiments. The probe recorded electrical conductivity as well as temperature.

6.7.1) Calibration of probe response to salt concentration

All experiments were performed with Lion brand table salt (NaCl). The reason for this was that the manufacturers do not add free-flowing agent to the salt. It was found that with other brands of table salt an aqueous milky emulsion formed due to the free-flowing agent.

After monitoring the temperature during continuous runs the temperature was found to increase gradually. An increase of approximately 3°C was observed from beginning to end. This was due to the energy input of the liquid pump.

After consultation with literature it was found that the conductivity of NaCl ions in water may change by as much as 2 % per degree Celsius rise in temperature (Talbot et al., 1990).

To this effect multiple calibrations of prepared standard salt solutions were performed in a fixed temperature water bath. Calibrations were performed at four temperatures for five different salt concentrations as shown in Figure 6-8.

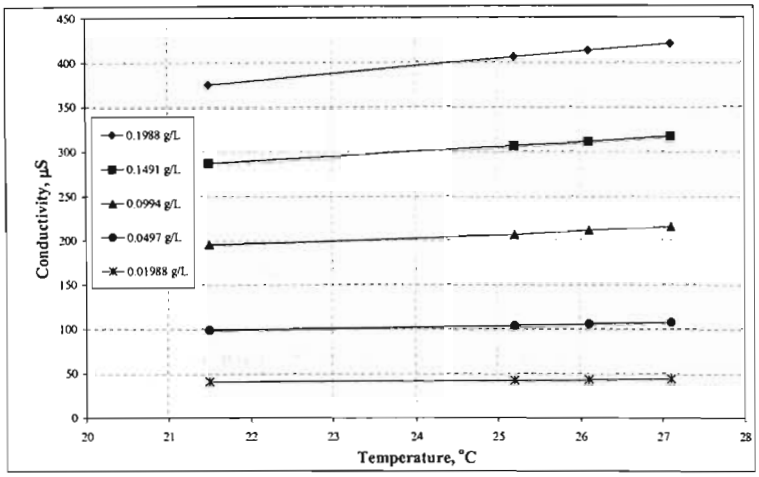

Figure 6-8: Plot to show variation of probe electrical conductivity response with temperature

The temperature effect was correlated via a relationship of the form (Talbot et al., 1990):

$$\kappa(25) = \kappa(T).\Psi^{(25-T)} \tag{6-1}$$

where κ is the electrical conductivity of NaCl ions, T is the temperature in degrees Celsius and Ψ is a constant.

The regression with 27.1°C as the reference temperature yielded:

$$\kappa(27.1) = \kappa(T).1.0197^{(27.1-T)} \tag{6-2}$$

From Eq. 6-2 it is evident that the conductivity of NaCl ions changed by 1.97 % per degree Celsius change in temperature. This is consistent with the findings of Talbot et al. (1990).

The calibration for salt conductivity with salt concentration is shown in Figure 6-9:

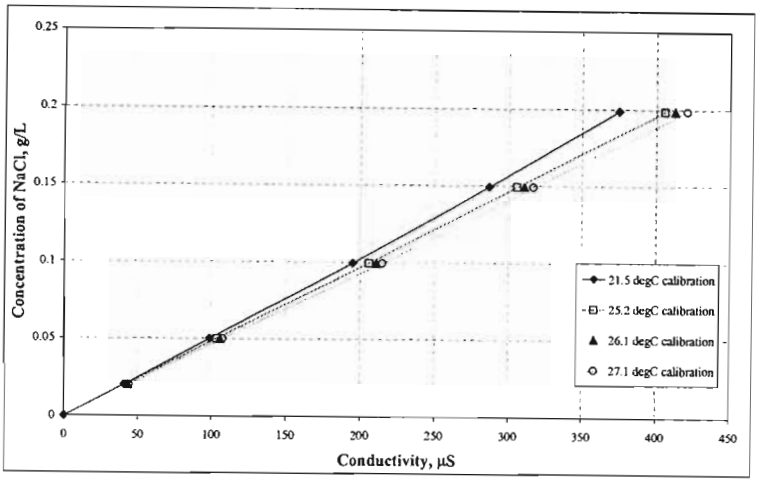

Figure 6-9: Calibration of probe conductivity response to salt concentration at various temperatures

The salt concentration c at 27.1°C is well represented by:

$$c(27.1) = \kappa(27.1) \times 4.3956 \times 10^{-4} \tag{6-3}$$

and $\kappa(27.1)$ is obtained from Eq. 6-2.

6.8) Auxiliary apparatus

Injections were performed with 10 mL and 50 mL plastic medical syringes.

Clear nylon tubing of various sizes was used to facilitate entry and exit of water into the columns.

Polyflow tubing was used to transport air from the regulator to the rotameter and into the gas chamber.

A one meter extension for the probe was constructed. This gave an effective length of 1.8 m of wire length from the probe to the meter. However the extension connections were not water tight. The extension did not affect the conductivity readings.

For BC1 a scissors jack was used to provide additional support at the base of the gas chamber (Figure 6-10).

A mild steel structure was designed and constructed to support the three columns. The final experimental set-up is shown in Figure 6-10.

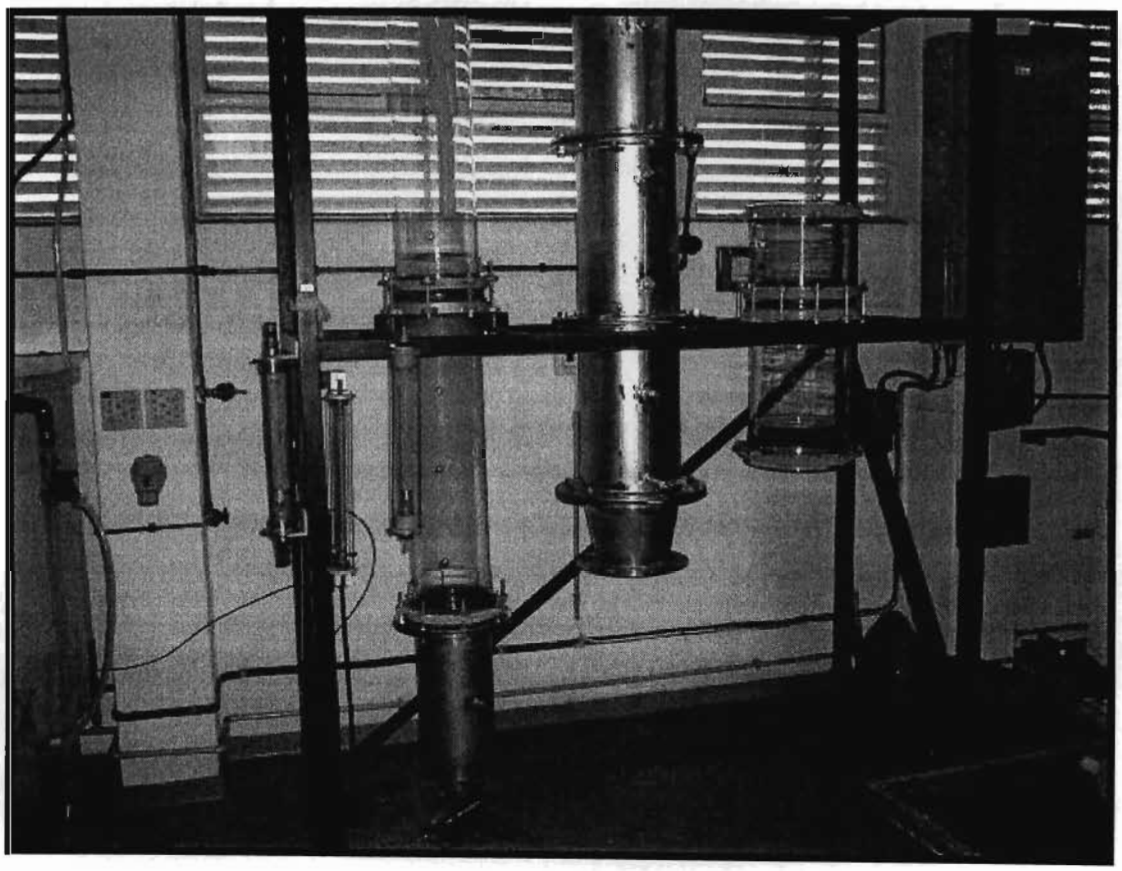

Figure 6-10: Photograph of bubble column apparatus

6.9) Procedure for batch mixing experiments

The following description applies to both BC1 and BC2 after installation of the desired sparger.

1. The water lines and nylon tubing are cleared by running water directly into the drain.
2. The main gas valve from the compressor line was opened and the regulator was set to 200 kPa.
3. Air was fed into the gas chamber before liquid was filled into the column. The pressure in the chamber prevented liquid from weeping through the holes into the distribution chamber.
4. The column was then filled with tap water to the desired level.
5. The probe was inserted from the top of the column to the desired height from the gas distributor plate.
6. The gas rotameter was set to the desired setting.
7. Sufficient time was allowed for the gas flow-rate to stabilise. The gas setting and regulator setting were monitored throughout the experiment to ensure that no fluctuations occurred.
8. Data logging was initiated simultaneously with salt tracer injection.
9. The salt tracer injection point was typically 19 cm and 30 cm above the distributor plate for BC1 and BC2 respectively.
10. After extensive investigation it was found that a tracer NaCl concentration of 250 g/L gave the best response. The volume of tracer varied between 10-20 mL depending on the liquid volume in the column.
11. The conductivity in the column was monitored until homogeneity was reached. This time period was typically less than 3 minutes.
12. To prevent gross wastage of water six injections were performed per batch of liquid. The amount of salt added was too minute to considerably affect the physical properties of the water.
13. After the six runs the air was shut off.
14. The column and chamber were left to drain.
15. The column was rinsed down with fresh mains water.
16. The top of the column was covered to prevent accumulation of dust and impurities.

6.10) Procedure for RTD experiments

The following description applies to both BC1 and BC2 after installation of the desired sparger and liquid rotameter.

1. The water lines and nylon tubing are cleared by running water directly into the drain.
2. The storage tank was filled with tap water.
3. The pump was started and the throttle valve was closed to allow total water recycle into the tank. This ensured that the liquid was well mixed and that ions did not settle.
4. Once the tank was filled the conductivity of the water in the tank was measured.
5. The main gas valve from the compressor line was opened and the regulator was set to 200 kPa.
6. Air was fed into the gas chamber before liquid was filled into the column. The pressure in the chamber prevented liquid from weeping through the holes in the distribution chamber.
7. The throttle valve was then opened to allow liquid to fill the column.
8. The valve was adjusted to obtain the desired liquid flow rate.
9. The air rotameter was set and monitored throughout the run.
10. The probe was inserted from the top of the column at a level close to the liquid outlet. The conductivity of the water in the column was compared to the conductivity of the water in the tank. It had been determined from investigations with the Perspex column that the RTD from a flow through cell installed in the exit line and the RTD from the probe in the column close to the exit yielded equivalent results.
11. The column was allowed to run for 5 minutes.
12. Outlet liquid was sent to the drain.
13. Data logging was initiated simultaneously with tracer injection.
14. Tracer was injected directly into the clear nylon tubing close to the column inlet. The syringe needle was adequately sharp to pierce the tubing. The friction on the plunger was sufficient to overcome the back pressure in the column.
15. The tracer volume was typically 20 and 50 mL for BC1 and BC2 respectively.
16. The conductivity was recorded until the conductivity in the column was within five per cent of the base liquid conductivity.
17. The pump and gas were shut down.
18. The column was drained and rinsed as described in Section 6.10.
19. The top of the column was covered.

6.11) Procedure for measuring gas hold-up

Gas hold-up was measured via the volume of bed expansion method. The low gas fractions were not detectable via pressure based measurements.

Measurements for gas hold-up were performed only in BC2:

1. The water lines and nylon tubing are cleared by running water directly into the drain.
2. The main gas valve from the compressor line was opened and the regulator was set to 200 kPa.
3. The column was filled with water to a suitable level.
4. The air rotameter was adjusted to obtain the desired air flow-rate.
5. Sufficient time was allowed for the gas flow rate to stabilise.
6. A measurement of the dispersion level was recorded.
7. The gas chamber was degassed rapidly by opening the draining valve on the chamber.
8. The air flow rate was stopped using the rotameter control valve.
9. When the last of the air bubbles broke the surface of the liquid a measurement of the clear liquid height was recorded.
10. The draining valve was closed.
11. Steps 4-10 were repeated to maximise the number of measurements from a single liquid batch.
12. The column was shut down as described previously.

6.12) Tracer concentration and volume for experiments

The tracer was made from distilled water and Lion brand table salt. For the batch tests the tracer was made on a mass/volume basis and for the RTD measurements on a mass/volume and mass/mass basis. The latter was done as a check to determine the exact amount of tracer injected into the column. The syringe was weighed before and after the injection to determine the mass of tracer input for the RTD.

Numerous experiments were performed with respect to tracer concentration and tracer volumes. This will be discussed in Chapter 8.

CHAPTER SEVEN

MODEL IMPLEMENTATION AND DATA REDUCTION

In Chapter 3 the errors that RTD measurements are often subjected to were discussed. In the pre-1980's, when the majority of bubble column research was undertaken, computers and software for curve fitting were not readily available. Therefore it is commonly found in the literature that dispersion coefficients were determined using nomographs and the method of moments (variances).

In this chapter the variance method will be compared to curve fitting approaches and the data reduction procedure used in this study for obtaining axial dispersion coefficients will be presented. Matlab 6.0® and Microsoft Excel® were used for all data handling and regression.

7.1) Batch liquid mixing model

7.1.1) Graphical approaches

The analytical solution for batch liquid measurements is given via Eq. 3-20:

$$\frac{C}{C_o} = 1 + 2\sum_{n=1}^{\infty}\left(\cos\frac{n\pi}{L}\delta\right)\exp\left(-\frac{n^2\pi^2}{L^2}E_L t\right) \qquad (3\text{-}20)$$

Ohki and Inoue (1970) reported that the first six terms in the infinite series were sufficient to evaluate E_L with an error under 1 per cent.

Eq. 3-20 was used to generate a theoretical batch mixing curve for the following conditions (Figure 7-1):

- E_L = 150 cm^2/s
- L = 185 cm
- δ = 185 cm ie. tracer input at boundary
- (δ/L) = 1

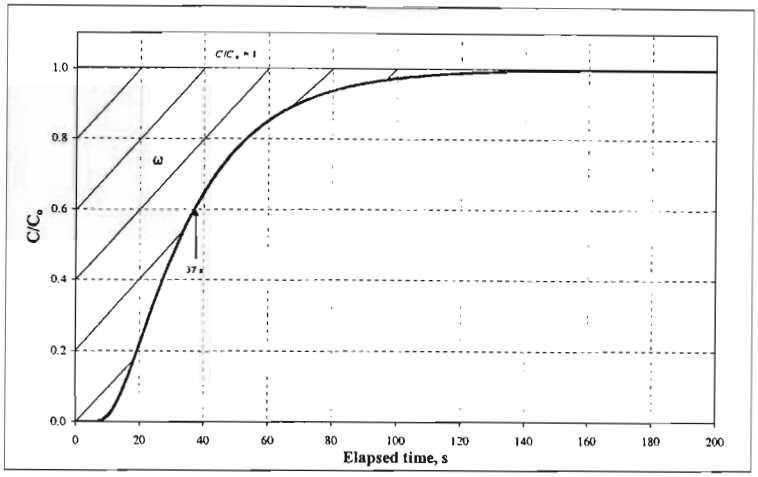

Figure 7-1: Theoretical batch mixing curve for E_L = 150 cm^2/s, L = 185 cm and δ =185 cm

It was common practice that a nomograph such as Figure 3-7 would be used to determine E_L. From Figure 3-7 the closest available ratio of measuring point to feed point (δ/L) is 0.9. From Figure 7-1 when C/C_o is 0.6 the elapsed time is 37 s and from Figure 3-7 the abissca value for C/C_o = 0.6 is 0.158. E_L is obtained from:

$$\frac{E_L t}{L^2} = 0.158 \Rightarrow E_L = \frac{0.158 \times (185\text{cm})^2}{37\text{s}} = 146.1 \text{ cm}^2/\text{s}$$

This compares well to the E_L value of 150 cm^2/s used to generate the theoretical curve.

Khang and Kothari (1980) developed a graphical method for determining axial dispersion coefficients. Their method based on the variance of the curve requires only the area above the time-concentration curve. The authors showed that the dispersion coefficient is related to the area ω between the tracer response curve and the horizontal line of unity (C/C_o = 1) as:

$$\omega = \frac{L^2}{6E_L} \tag{7-1}$$

Eq. 7-1 is valid only when (δ/L) = 1.

From Figure 7-1 the area ω = 38 s and E_L is determined from Eq. 7-1 as:

$$E_L = \frac{L^2}{6\omega} \Rightarrow E_L = \frac{(185\text{cm})^2}{6 \times 38\text{s}} = 150.1 \text{ cm}^2/\text{s}$$

This is exactly the dispersion coefficient that was used to generate the theoretical curve.

7.1.2) Curve fitting approach

The use of figures and variances are suitable when experimental data is smooth and free of scatter. However in practice this is seldom the case as measurements are often subject to fluctuations due to bubbles and probe dynamics. Measurements are also seldom performed at $(\delta/L) = 1$. A curve-fitting approach using regression algorithms offers an effective means of determining model parameters. However in order to extract meaningful model parameters accurate and precise experimental measurements are necessary.

In the case of electrical conductivity measurements bubbles are detected by the probe and cause low conductivity readings.

Figure 7-2 shows a typical experimental batch mixing test for BC1. The conditions for the experiment were:

- sparger: SP2
- u_g = 0.21 cm/s
- L = 170.0 cm
- δ = 142.9 cm
- (δ/L) = 0.84
- tracer input: 10 mL of 250 g/L aqueous NaCl tracer

The solid line in Figure 7-2 shows the theoretical model as predicted via Eq. 3-20. The regressed E_L value was determined by minimising the index of fitting parameter I using the Nelder-Mead simplex (direct search) method. I was defined as:

$$I = \sum_t (C_{model,t} - C_{experimental,t})^2 \qquad (7\text{-}2)$$

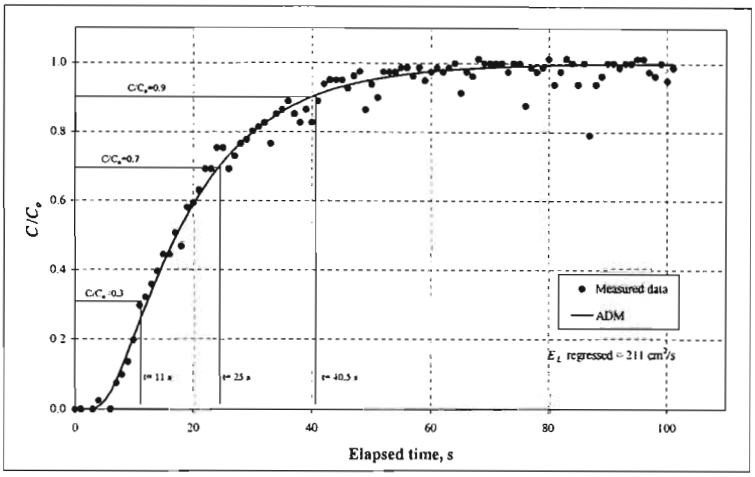

Figure 7-2: Typical batch mixing experimental curve and model fit with $E_L = 211$ cm^2/s

Data regression using the ADM yields an axial dispersion coefficient of 211 cm^2/s. To determine the quality of the prediction the relative percentage deviation between the experimental concentration data C_{exp} and the predicted ADM concentrations C_{model} as defined by Eq. 7-3 is plotted in Figure 7-3.

$$R = 100\frac{C_{\text{exp}} - C_{\text{model}}}{C_{\text{model}}} \tag{7-3}$$

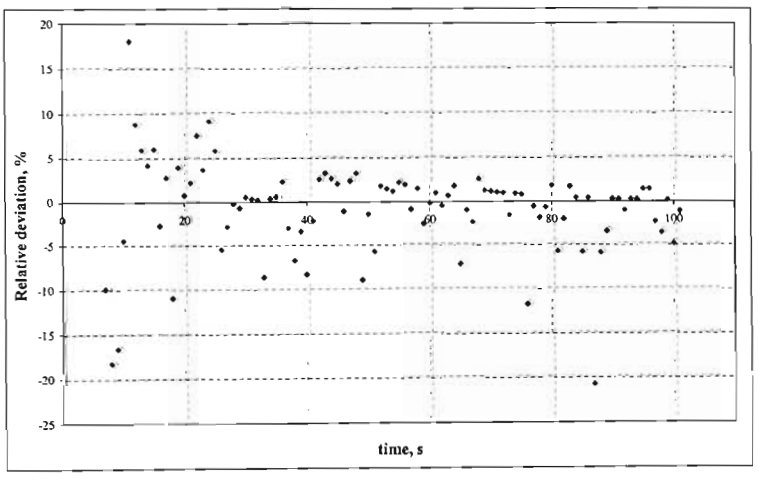

Figure 7-3: Plot of percentage relative deviation of experimental data to regressed model data versus time

70 % of the logged experimental data falls within the ± 5 % deviation limits and 86 % within the ± 10 % deviation limits. The relatively few outliers are due to abnormally low readings caused by bubbles reducing the observed conductivity and hence concentration and the deviation is also relatively higher in the initial period (t < 15 s) when the resolution in the conductivity readings was significantly lower than in the later time period. With increasing gas flow rate the quantity of experimental data falling within the ± 5 % deviation limits decreases due to increasing fluctuations in conductivity caused by the increased number of bubbles.

Various time segments of the experimental data were regressed independently of each other. The results are shown in Table 7-1 and indicate that the initial time period corresponding to $C/C_o \leq 0.3$ is not heavily weighted during the regression.

Table 7-1: Regressed E_L values for C/C_o ranges shown in Figure 7-2

C/C_o range	Regressed E_L value cm^2/s
0 - 0.3	207
0.3 - 0.7	218
0.7 - 0.9	204
0 - 1	211

Ohki and Inoue (1970) used only the 0.3 – 0.7 C/C_o range to determine E_L. However the authors utilised a graphical method rather than a curve fitting approach.

It is evident from Table 7-1 that the regression for the various C/C_o segments yields approximately identical dispersion coefficients. Therefore, for the purposes of this study the entire C/C_o range was used as the experimental regression range for determination of E_L.

7.2) Residence time distribution model

7.2.1) Determination of E_L by the variance method

The analytical solution for a pulse input RTD measurement is given by Eq. 3-24:

$$\frac{c_X}{C_0} = 2\exp[P(2X-\theta)]\sum_{k=i}^{\infty}\left[\lambda_k \exp\left(-\lambda_k^2/\theta\right)\frac{\lambda_k\cos(2\lambda_k X)+P\sin(2\lambda_k X)}{\lambda_k^2+P^2+P}\right] \qquad (3\text{-}24)$$

The solution to Eq. 3-27 for λ_k was performed using the Newton-Rhapson method. An algorithm to determine the first hundred unique roots of Eq. 3-27 was implemented. For the infinite series in Eq. 3-24 the first ten thousand terms were used.

Figure 7-4 below shows an RTD curve generated with Eq. 3-24 for the following conditions:

- mass of tracer input: 12.5 g
- column diameter: 30 cm
- superficial liquid velocity: 0.24 cm/s
- liquid height: 190 cm
- axial dispersion coefficient: 100 cm^2/s

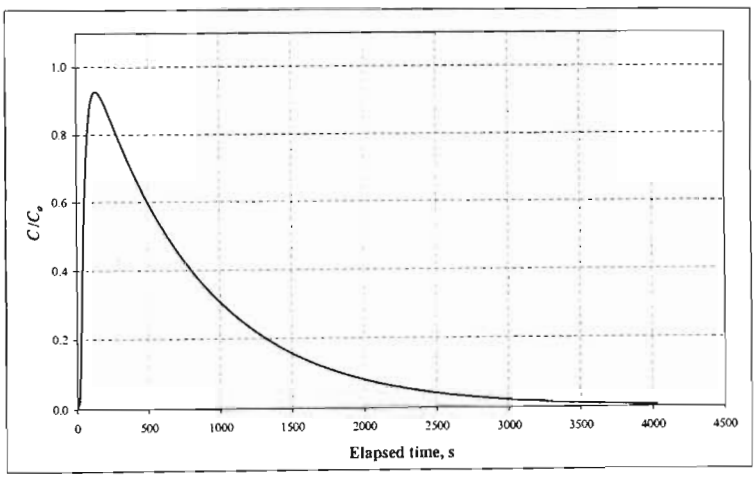

Figure 7-4: Theoretical ADM curve for E_L = 100 cm^2/s, D_C = 30 cm, L = 190 cm, C_o = 0.0931 g/L and u_L = 0.24 cm/s

From the concentration-time curve (Figure 7-4) μ and σ^2 are determined by numerical methods from Eq. 3-11 and Eq. 3-12 respectively.

Solution of Eq. 3-11 gives $\mu = 804.37$ s and solution of Eq. 3-12 yields $\sigma^2 = 0.8567$.

In Chapter 3 it was shown that the variance of an RTD curve can be used to solve for the Peclet number. From Eq. 3-30:

$$\sigma^2 = \frac{2}{Pe_L} - \frac{2}{Pe_L^2}(1 - e^{-Pe_L}) = 0.8567 \tag{7-4}$$

Solution of Eq. 7-4 by Newton's method gives $Pe_L = 0.463$

The axial dispersion coefficient E_L can be obtained from Eq. 3-28:

$$E_L = \frac{u_L L}{Pe_L} \Rightarrow E_L = \frac{0.24\text{cm/s} \times 190\text{cm}}{0.463} = 98.5\ \text{cm}^2/\text{s}$$

This compares well to the E_L value of 100 cm^2/s used to generate Figure 7-4. The slight discrepancy is most likely due to numerical diffusion occurring during the solution steps.

The variance method works well when the RTD curve is smooth and complete. When a single probe is used the variance method only yields representative E_L values when the tracer recovery is 100 %. Levenspiel (1962) reported that the tail of the RTD curve is heavily weighted for the variance method. Most often it is the tail of the RTD curve that is subject to error as it is the region of low concentration where there is large uncertainty in calibration. Levenspiel states that it is practically impossible to effect a 100 % recovery of salt during an RTD run. A common practice by researchers is to use the latter part of a CSTR model to predict the tailing of the ADM so that the variance method can be used (Figure 7-5).

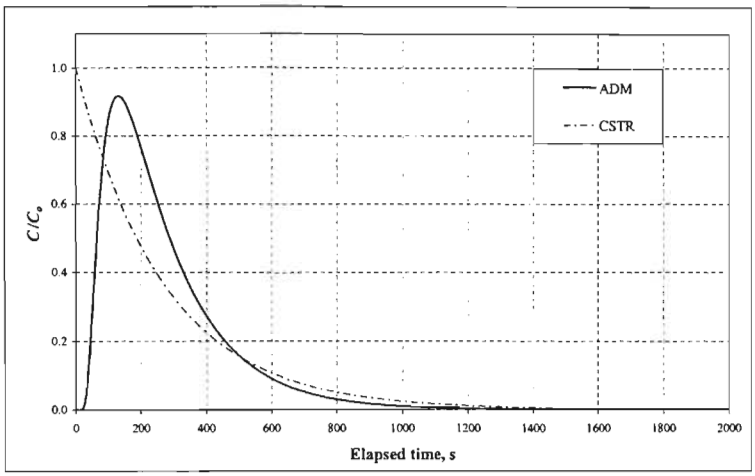

Figure 7-5: Plot to illustrate CSTR tailing and ADM tailing

7.2.2) Determination of E_L by curve fitting analysis

In the literature many researchers have used the variance method and graphical methods to determine E_L (Table 7-2).

Table 7-2: Literature references and method to determine E_L

Author	Type of measurement	Data analysis method
Bischoff & Philips (1966)	RTD	Variance
Ohki & Inoue (1970)	Batch	Nomograph
Kato & Nishiwaki (1972)	RTD	Nomograph
Deckwer et al. (1974)	Batch	Nomograph
Houzelot et al. (1985)	RTD	Variance
Ityokumbul et al. (1994)	RTD	Curve fitting
Krishna et al. (2000)	Batch	Curve fitting
Moustiri et al. (2001)	RTD	Variance

Clements (1969) reported that a least squares method for the estimation of Peclet number was less sensitive to errors occurring during variance computation. The author performed curve-fitting exercises using the least squares method in the time and frequency domain and reported that the choice was a matter of convenience. Clements stated that the most attractive feature of the least squares procedure was that it weighted the tail of an experimental RTD curve no more heavily than the rest of the curve.

These findings were supported by Fahim and Wakao (1982) who compared the moment method, weighted moment method, Fourier analysis and time-domain analysis techniques for parameter estimation. The authors concluded that the time-domain analysis yielded the most reliable parameter values. The methods were ranked in decreasing order of reliability as time-domain analysis, Fourier analysis, weighted moment and moment analysis.

The variance method does not reveal whether the determined model parameters are representative of the data while with curve fitting methods a numerical estimate of the quality of the fit is obtainable. In this study time-domain analysis was accomplished by minimising the index of fitting parameter I (Eq. 7-2) between the experimental data and model data (Eq. 3-24) by regression of model parameter E_L.

A flowchart for the regression procedure is provided in Figure 7-6. The regression technique was tested by using various theoretical RTD curves generated via Eq. 3-24 as experimental data curves. The developed regression algorithms were then used to determine E_L from the pseudo-experimental curves. In all instances the exact dispersion coefficient used to generate the pseudo-experimental curves was obtained by the regression analysis.

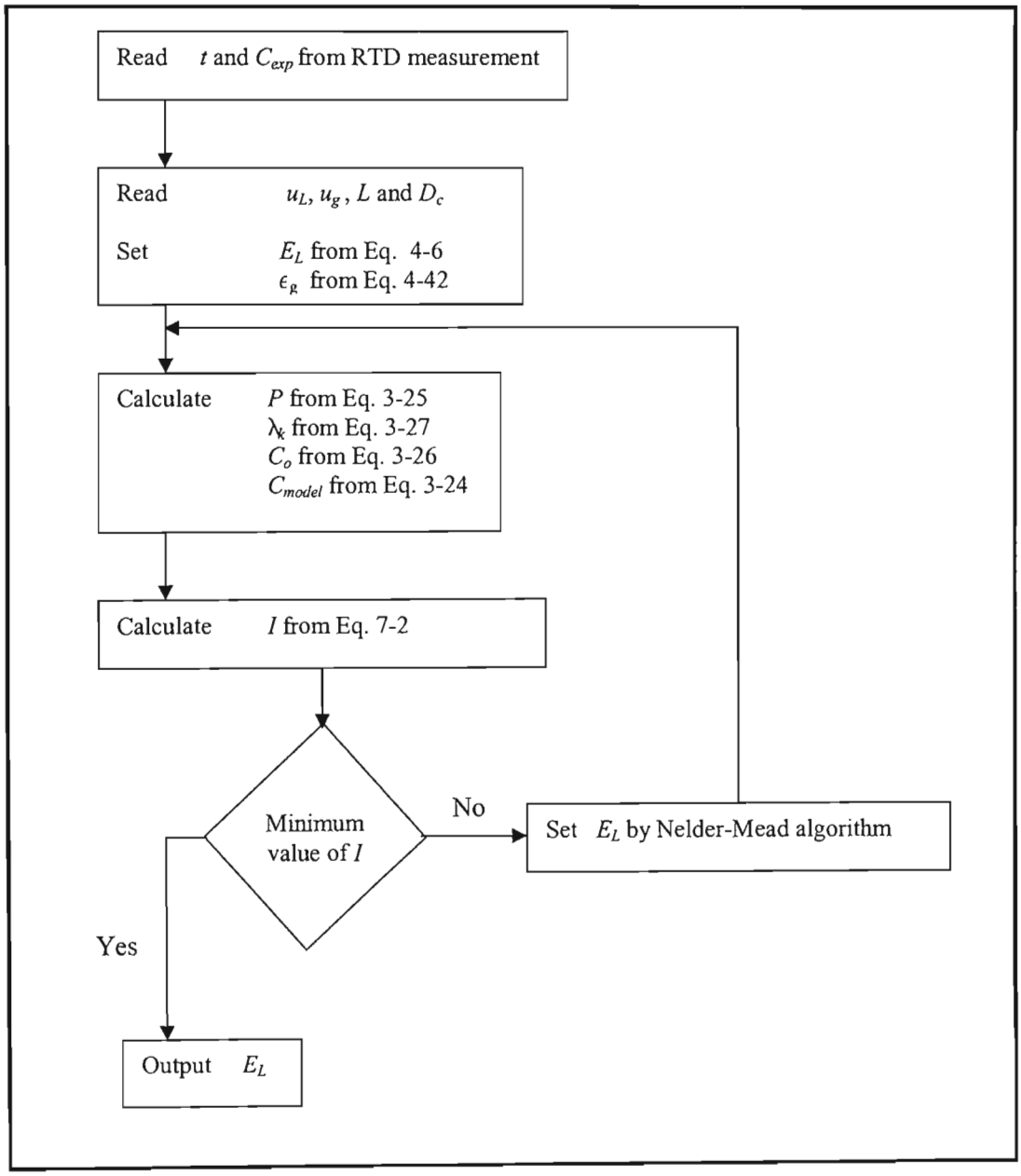

Figure 7-6: Block diagram to show determination of E_L from RTD data

7.3) Numerical solutions versus analytical solutions

In addition to the analytical solutions presented numerical solutions were also utilised. The solutions compared very well. The analytical solutions were easier to implement and converged faster than their numerical counter-parts. The only significant downfall of the analytical solutions is that they are based on idealised tracer inputs (Dirac delta pulse). In practice it is extremely difficult to implement such an idealised input. Numerical solutions allow for tracer input functions to be utilised which are more representative of the actual tracer input.

However it is well known (Levenspiel, 1962) that the tracer input can be assumed to be a pulse if the tracer injection time t_{inj} and the mean residence time of the phase of interest τ satisfy:

$$\frac{t_{inj}}{\tau} \leq 0.05 \tag{7-5}$$

For the RTD measurements in this study the criterion was always met.

In this chapter it was shown that curve fitting analysis is the best method for determining model parameters. In the literature the variance method and graphical method were and still remain widely used for determining model parameters. The disadvantages and potential erroneous model parameters that can be achieved by these methods has been highlighted.

In addition theoretical curves have been generated using analytical solutions. The variance method and graphical method have been used to demonstrate that the implementation of the models has been performed accurately. This together with numerical solution verification shows that the models have not been implemented erroneously.

The data reduction techniques used to determine E_L from experimental data has been presented. The results presented in the proceeding chapter have been obtained by the methods outlined here.

CHAPTER EIGHT

RESULTS AND DISCUSSION

The experimental measurements undertaken in this study were primarily that of axial dispersion coefficients. These measurements were performed under a variety of experimental conditions.

The variables considered for measurements were:

- the effect of superficial gas velocity
- the effect of column diameter
- the effect of probe orientation and probe position
- the effect of volume and concentration of salt tracer
- the effect of liquid level
- the effect of liquid flow rate
- the effect of sparger geometry

Axial dispersion coefficients were measured using the transient batch liquid mixing method and the RTD method as described in Chapter 3. The experimental data was analysed as presented in Chapter 7.

In addition to axial dispersion measurements attempts were made to measure gas hold-up in BC2. The measurement of the low gas fractions proved to be difficult.

RTD measurements were also undertaken in various cascaded column configurations.

In this chapter the experimental results obtained will be presented and discussed.

8.1) Gas hold-up

Gas hold-up was measured via the volume of bed expansion method. The low gas fractions were not detectable via pressure based methods. The measured gas hold-up in BC2 as a function of superficial gas velocity is shown in Figure 8-1 below.

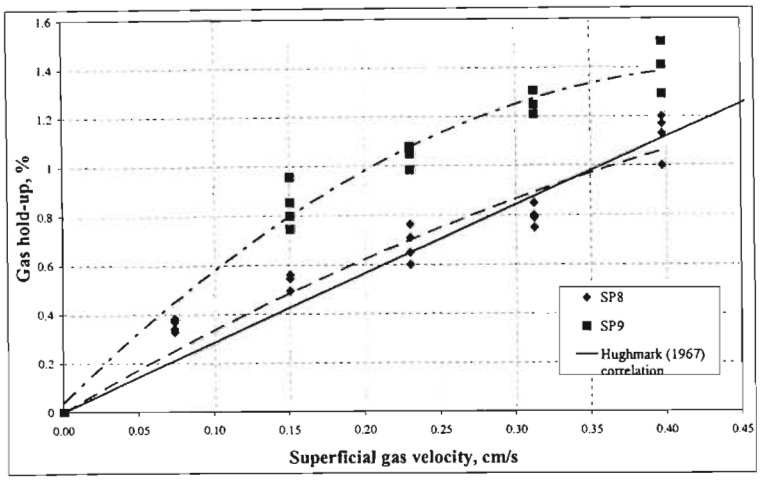

Figure 8-1: Plot to show variation of measured gas hold-up with Sparger 8 and Sparger 9 for BC2 as compared to gas hold-up prediction of Hughmark (1967)

Figure 8-1 shows that the gas hold-up using a four hole sparger is higher than that using a single orifice sparger. However the experimental error in obtaining the gas hold-up measurements must be brought to bear.

Take into consideration that when the pressure in the gas chamber subsides weeping of liquid will occur. It is obvious that this rate of liquid weeping will be much more significant in a four hole plate than for a single orifice sparger. The experimental method involved taking a height reading while the gas was flowing, H_D, and a reading when the gas was shut off, H_L. This process was far from instantaneous and a finite time of approximately one minute was the norm in reading the dispersed liquid level to that of the clear liquid level.

The experimental method did not take into consideration the amount of liquid that weeped and/or drained through the sparger from the column into the de-pressurised gas chamber. Given the small scale of gas hold-up fractions this small amount of liquid greatly exaggerates the gas hold-up. Table 8-1 provides an example of typical measurements for SP8 and SP9.

Table 8-1: Typical clear and dispersed liquid levels for SP8 and SP9

Sparger	H_D	H_L	Gas hold-up Eq. 3-37	H_D-H_L
	cm	cm	%	cm
SP8	183.4	182.4	0.55	1.0
SP9	182.9	181.1	0.98	1.8

These measurements are subject to precision errors in measurement and even a small amount of liquid weeping through SP9 would greatly exaggerate the gas hold-up as the H_L measurement would be lower than if no weeping occurred.

For instance if 8 mm of liquid were to weep through SP9 during the time it took to take the H_D and H_L reading then a more representative H_L value would have been 181.8 cm. This reading would have given an overall gas hold-up of 0.60 % as compared to the 0.98 % shown in Table 8-1.

For these reasons gas hold-up was not measured with the other spargers as a procedure to properly account for the weeping rate could not be established.

The measurements using a single 1 mm orifice sparger would give the most representative overall gas hold-up values. This is also evident in Figure 8-1 as the correlation of Hughmark (1967) provides an excellent prediction of overall gas hold-up in BC2 as measured with the single orifice.

Intimate knowledge of gas hold-up is required when mass transfer measurements are undertaken. For the purposes of this study only an estimate of overall gas hold-up was required and as such an extensive study on gas hold-up was not warranted.

The correlation of Hughmark (1967) is recommended for predicting gas hold-up at low superficial gas velocities.

8.2) Longitudinal axial dispersion coefficients via batch mixing tests

8.2.1) The effect of liquid level

In the literature axial dispersion coefficients are generally measured in tall bubble columns ($L/D_c > 4$). BC1 and BC2 allowed for study of axial dispersion in a wide range of aspect ratios (Table 6-1).

It was found that tracer mal-distribution occurred when the liquid level was equal to or lower than 110 cm. The tracer mal-distribution as shown in Figure 8-2 and Figure 8-3 is attributed to gross bypassing of tracer during the experiment.

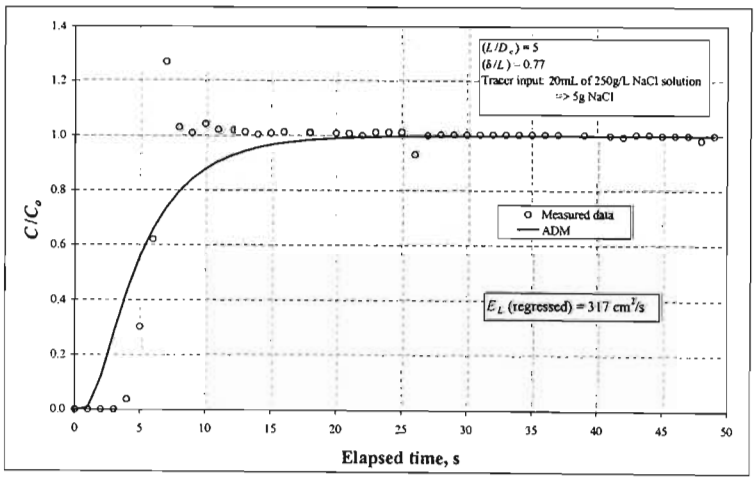

Figure 8-2: Plot to show tracer bypassing in BC1 at $u_g = 0.28$ cm/s

for $L = 110$ cm and $\delta = 85$ cm

In Figure 8-2 it is evident that the ADM model with a regressed E_L parameter is not representative of the experimental data. This too is the case for batch tests in the 30 cm column at a liquid height of 110 cm (Figure 8-3). This behaviour was typical for all superficial gas flow rates considered at a liquid height of 110 cm in both BC1 and BC2.

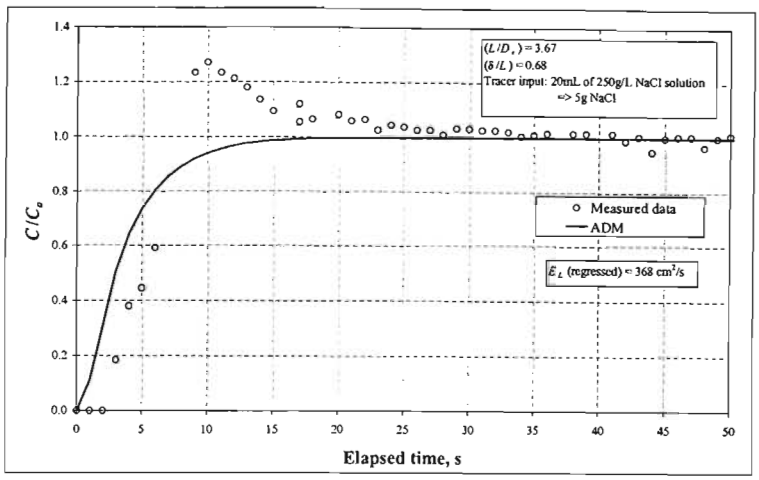

Figure 8-3: Plot to show tracer bypassing in BC2 at u_g = 0.074 cm/s

for L = 110 cm and δ = 75 cm

In BC1 two more liquid heights were investigated. At a liquid height of 150 cm the experimental data begins to be more representative of axially dispersed tracer as per the ADM. At a liquid height of 170 cm the experimental data is well represented by the ADM.

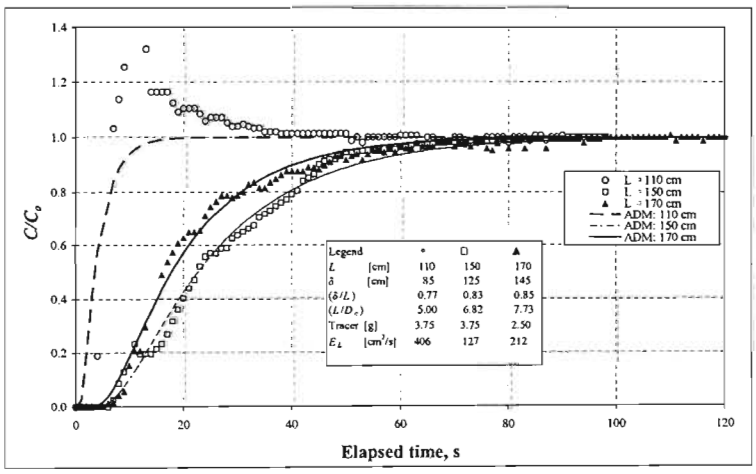

Figure 8-4: Measured batch mixing data in BC1 at u_g = 0.28 cm/s

for L = 110, 150 and 170 cm

In BC2 liquid heights of 150 and 190 cm were investigated. The results are similar to that observed for BC1. The data is well represented by the ADM as shown in Figure 8-5.

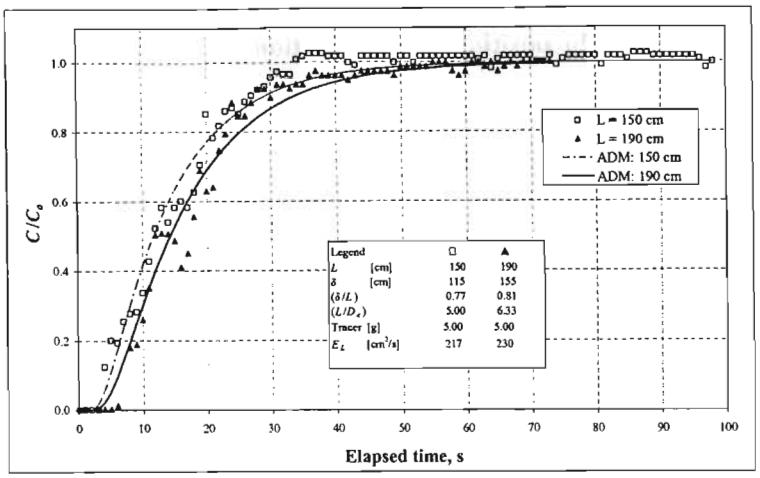

Figure 8-5: Measured batch mixing data in BC2 at u_g = 0.074 cm/s

for L = 150 and 190 cm

The anomalous results at liquid heights of 110 cm may be due to the shallow bed height propagating gross bypassing of tracer or that simply the detector is too close to the tracer input. There is no indication in the literature on the existence of a critical length for batch mixing experiments. However one of the assumptions of the ADM is that there must be no bypassing or short-circuiting of fluid in the vessel (Chapter 2). Given that the time taken to reach uniform concentration (C/C_o = 1) for a 110 cm liquid height is typically much less than 15 s it is understandable that erratic results are obtained as a pocket of injected tracer may mix faster than the bulk injection and is consequently detected as the observed spikes shown in Figures 8-2 and 8-3.

For the higher liquid heights the mixing time is in excess of 45 s. This allows sufficient time for the tracer to distribute uniformly and hence acceptable results are obtained.

For these reasons the majority of batch mixing tests were undertaken at the highest workable liquid height.

8.2.2) The effect of probe position and orientation

For the batch mixing tests the effect of probe position was investigated. The probe was inserted through the top of the column at various liquid depths and radial positions.

The radial positions, as shown in Figure 8-6, considered were:

- at the column centre
- at the column wall
- at $0.7D_C$
- random position

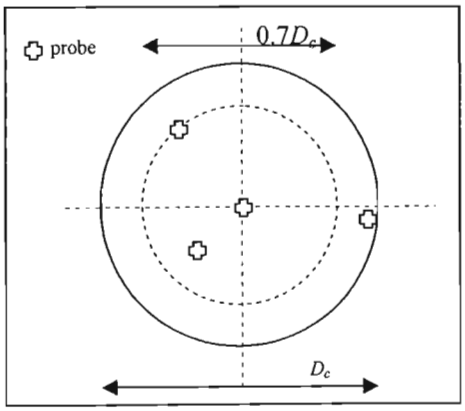

Figure 8-6: Illustration to show radial probe positions considered for batch mixing tests

No discernable effect of the radial position of the probe was observed.

The probe orientation was also tested. Batch mixing tests were considered with the probe in a vertical and horizontal orientation as shown in Figure 8-7.

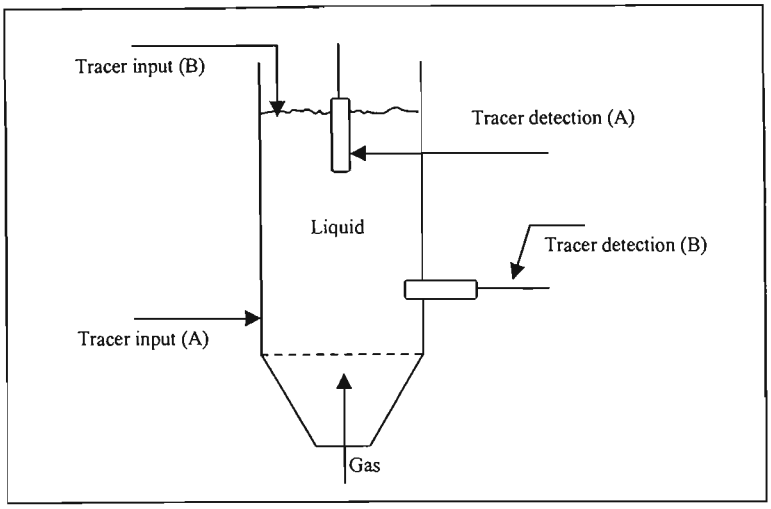

Figure 8-7: Illustration to show probe arrangements considered for batch mixing tests

(A) vertical probe orientation (B) horizontal probe orientation

The orientation as shown in Figure 8-7(B) offered no significant advantage. It should be noted that tracer was not injected but was poured uniformly on the top of the liquid surface. Results similar to those observed with the vertical probe arrangement were also obtained with the horizontal probe arrangement. The spiking phenomenon was also observed at a liquid height of 110 cm with the horizontal probe arrangement.

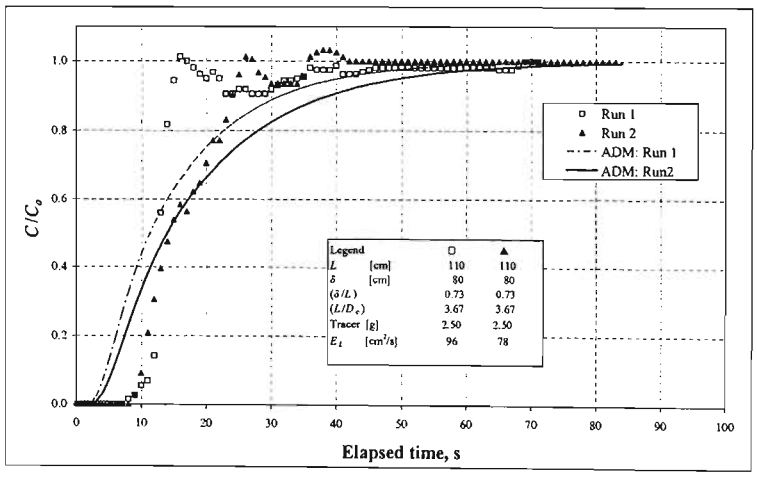

Figure 8-8: Measured batch mixing data in BC2 at u_g = 0.074 cm/s

for L = 110 cm with probe in horizontal orientation

It was difficult to install the probe in the horizontal arrangement and maintain a liquid seal. The possibility of damage to the glass probe was of grave concern and consequently for ease of experimentation the vertical probe orientation was utilised for batch mixing experiments. Hebrard et al. (1996) and Subramanian and Tien (1975) also performed their batch mixing experiments with tracer injection at the bottom and detection at the column top.

8.2.3) The effect of tracer concentration and volume

For a batch liquid volume, V_L, and mass of tracer input, M, the equilibrium tracer concentration in the liquid, C_E, is given by:

$$C_E = \frac{M}{V_L} \tag{8-1}$$

The smaller the value of M the lower the rise in conductivity will be. This is not desirable as the small conductivity rise amounts to low resolution in the conductivity probe response. Ideally a large quantity of salt should be used as the tracer input so that the resulting resolution would be high. However, if a large quantity of salt is injected then the injection time t_{inj} is also increased. In Chapter 7 the practical issues of injecting an ideal Dirac delta pulse were discussed. For continuous RTD experiments where the mean residence time is much larger than t_{inj} the injection can be considered for all practical purposes as a Dirac delta pulse. In the case of batch mixing tests however where the mixing time is often less than one minute the time taken to inject the tracer becomes more significant. It is evident that a balance between conductivity resolution and tracer injection time must be realized.

The tracer concentrations considered were in the range 100 – 300 g/L. The quantity of tracer injections investigated was between 5 and 25 mL. In effect the tracer concentration and volume determines M and the volume of tracer injected was an indication of the injection time.

After numerous batch mixing experiments using various tracer concentrations and input volumes the optimum tracer concentration was established to be 250 g (NaCl) / L (water). It was found that a suitable probe resolution was achieved when the amount of tracer was adjusted such that the equilibrium concentration in the batch liquid was 0.038 g/L.

For a 250 g/L tracer concentration the mass of tracer M and tracer injection volume can be determined from Figure 8-9.

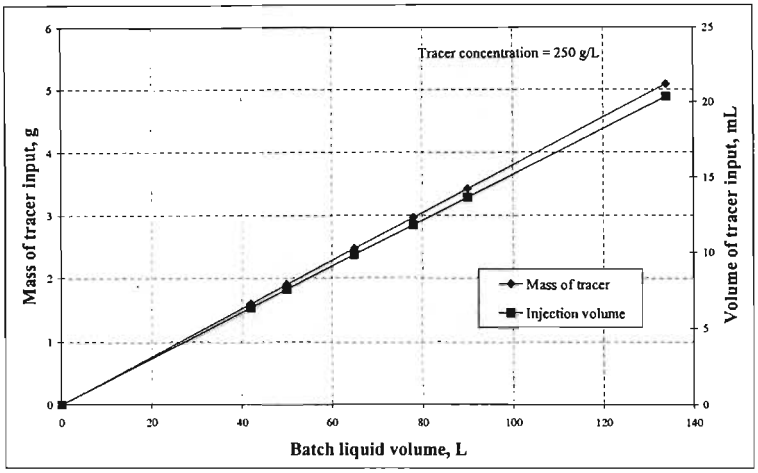

Figure 8-9: Plot to show mass of tracer injected and injection volume for a specified batch liquid volume

For batch mixing experiments the tracer quantity *M* used was determined from Figure 8-9.

Once the optimum amount of tracer had been determined the effect of the radial injection position was investigated. This was achieved by using needles of various lengths and injecting coloured tracer at various radial positions. The qualitative and quantitative results suggested that the radial position of tracer injection would not significantly affect the measured dispersion levels.

8.2.4) Results

A vast number of mixing experiments were undertaken. A large quantity of these experiments had been performed as preliminary runs to perfect the experimental technique as described previously.

The results presented in Figure 8-10 are the overall axial dispersion coefficients obtained by regression of multiple experimental data sets at common experimental conditions for BC1 and BC2.

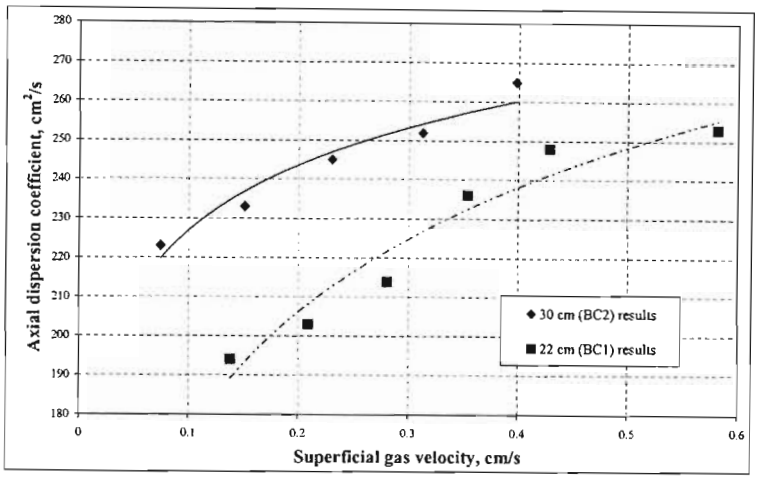

Figure 8-10: Axial dispersion coefficients obtained via batch mixing experiments for BC1 and BC2

The results show that the dispersion coefficient increases with increasing superficial gas velocity in both BC1 and BC2. The dispersion levels are slightly higher in BC2 than in BC1. These trends are as expected.

8.2.4.1) Quality and reproducibility of experimental data

Typical plots of experimental results obtained for BC1 and BC2 are provided in Appendix A. The experimental data was well represented by the ADM. At higher superficial gas velocities ($u_g > 0.3$ cm/s) the measured conductivity data was subject to a relatively higher conductivity measurement fluctuation. This was due to the increased frequency of bubble detection by the conductivity probe. A sample experimental curve is shown in Figure 8-11.

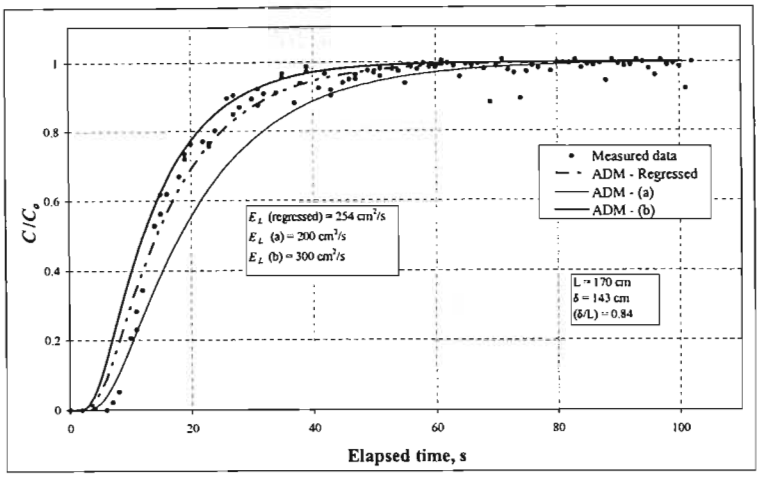

Figure 8-11: Plot to show typical fluctuations in measured batch mixing data in BC1 at u_g = 0.58 cm/s

It should be stressed however that the batch mixing experiments are based simply on the period of the time taken to go from one steady state concentration to another. The manner in which this change occurs is modelled in terms of axial diffusion in the longitudinal direction as described via Eq. 3-16. This period is termed the mixing time π and is typically defined as the time taken to effect a concentration change from C/C_o = 0 to C/C_o = 0.99. In Figure 8-12 the mixing time is clearly identifiable.

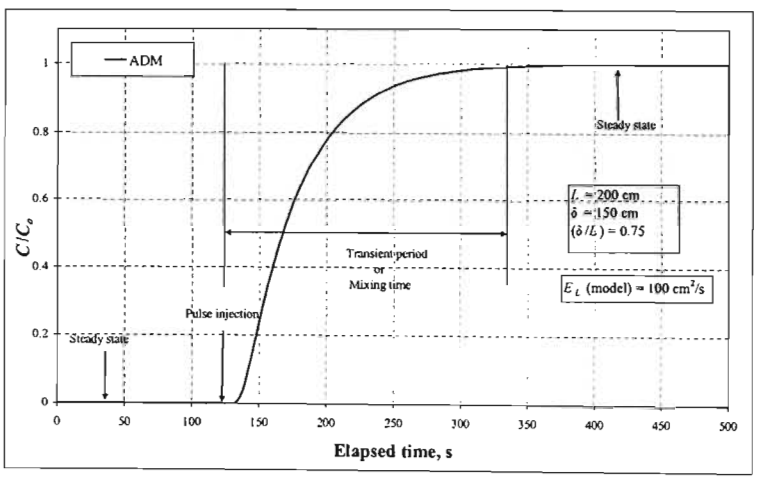

Figure 8-12: Plot to show mixing period for transient analysis

In Figure 8-11 the transient behaviour was described via the theoretical ADM. When the ADM is used to describe the transient period the following can be deduced:

$$\pi \propto \frac{L^2}{E_L} \tag{8-2}$$

When the scatter in the experimental data was significant due to conductivity measurement fluctuations the experimental run was still considered as the transient period was qualitatively described by the ADM as shown in Figure 8-11. To ensure that a representative overall dispersion coefficient was obtained multiple experiments were performed at the desired superficial gas flow rates. These experimental data sets were regressed as a single data set to obtain the representative dispersion coefficients shown in Figure 8-10.

In addition to this time shifting analysis on the experimental data was performed. The analysis showed that the experimental data was not particularly sensitive to time shifting in either the positive or negative direction.

With respect to reproducibility the nature of the experiment and the measured quantity must first be considered. In the fields of for example reaction kinetics and thermodynamics where the physical mechanisms are governed by strict fundamental laws it is understandable that repeat experiments will yield very reproducible results. In the case of bubble column hydrodynamics where there is complex random intrinsic behaviour it becomes understandable that high precision in reproducibility of experiments will not be achieved.

There are two major reasons for this:

1. The complex hydrodynamic behaviour is described by the relatively simple single parameter axial dispersion model.
2. The lumped dispersion parameter E_L will not remain constant from one experiment to the next as it incorporates various hydrodynamic quantities that are very transient and random in behaviour.

The quantities affecting E_L have been discussed previously. In this study partial bubbling from sparger holes (Figure 4-10) has been observed as well as the swirling bubble hose (Figure 4-11) which will obviously affect the measured E_L value from one experiment to another.

Other researchers such as Rubio et al. (2004) reported an error in replicate measurements of 10 %. The authors however did not perform large quantities of replicate measurements. Subramanian and Tien (1975) who performed many replicate measurements reported a deviation of 15 % in their measured E_L values. Other researchers do not report details of the reproducibility of their measured data and more often is the case than not that only a single dispersion coefficient is measured per superficial gas velocity.

In this study where large population sets (> 20 experimental runs) were measured for each superficial gas velocity the deviation increased from 12 % at a u_g of 0.0743 cm/s to 18 % at a u_g of 0.5814 cm/s. The increase in deviation with increasing gas velocity is attributed to probe effects due to increased gas bubble detection.

For the experiments in this study a local concentration measurement was used to evaluate E_L. It would have been preferable to perform concentration measurements along the reactor length however since only a single probe was available this was not possible.

The option of taking samples along the reactor length for batch tests proved to be difficult. Complete mixing of the injected tracer was achieved in too short a period of time (< 60 s) to draw an appropriate number of samples.

8.2.4.2) Effect of sparger

Given the low resolution in the dispersion coefficients with superficial gas velocity and the deviation associated with the measurements it was difficult to ascertain an effect of the sparger on E_L. Therefore various runs were performed with the spargers listed in Tables 6-7 and 6-8 and these data sets were included in the population set for data reduction used to obtain the results in Figure 8-10. In the literature the influence of the sparger geometry on axial dispersion levels is reported to be minimal and is evident in the correlated expressions (Chapter 4) where the sparger geometry is not taken into consideration.

8.3) Longitudinal axial dispersion coefficients via RTD measurements

8.3.1) Results

Over 60 RTD measurements were undertaken in BC2 and BC1 under various experimental conditions. The range of experimental conditions considered is given in Table 8-2:

Table 8-2: Range of experimental conditions for RTD measurements

Quantity	Units	BC1	BC2
Liquid level	cm	110 – 170	120 – 190
Volumetric liquid flow rate	L/min	4	5 – 13
Superficial liquid velocity	cm/s	0.17	0.12 – 0.31
Superficial gas velocity	cm/s	0.1381 – 0.2807	0.074 – 0.398

The RTD results are given in Figure 8-13 below.

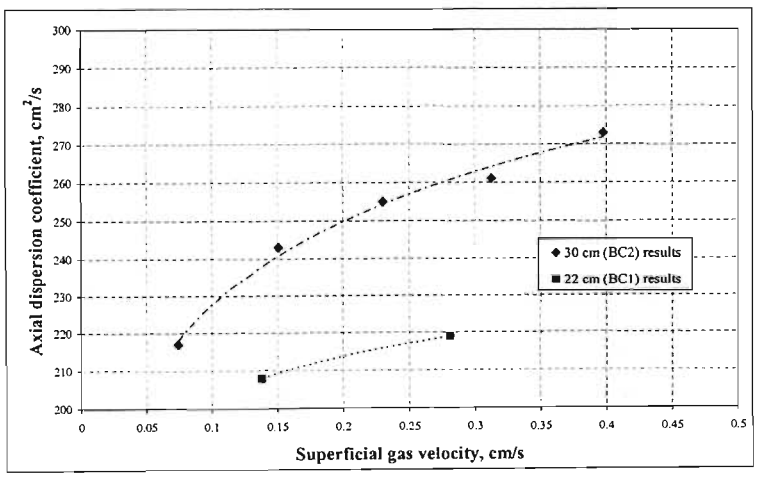

Figure 8-13: Axial dispersion coefficients for BC2 and BC1 obtained via RTD experiments

The results shown in Figure 8-13 above are the result of regression of multiple data sets at common experimental conditions.

8.3.2) Comparison of RTD measurements to batch measurements

The results compare very well as shown in Figure 8-14.

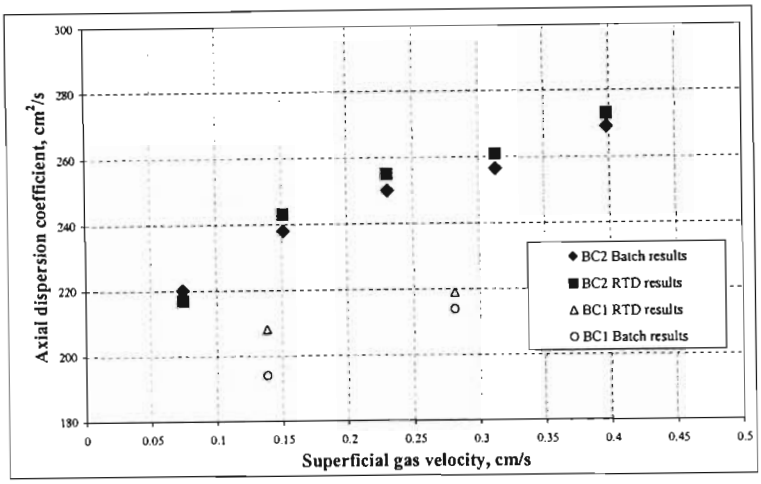

Figure 8-14: Plot to show comparison of axial dispersion coefficients obtained in BC2 via RTD and batch mixing measurements

8.3.3) Effect of Peclet number on RTD measurements

The dispersive Peclet number has a profound effect on the shape of the RTD:

$$Pe_L = \frac{E_L}{u_L L} \tag{8-3}$$

For large Peclet numbers the ADM tends towards CSTR behaviour. This made it difficult to regress meaningful dispersion coefficients especially in BC1 where the volumetric liquid flow rate was limited to 4 L/min as the liquid outlets in BC1 could only handle small liquid flow rates. It was not possible to widen the outlets as the glass sections had already been tremendously stressed. Neither was it possible to implement a liquid overflow arrangement as one of the glass sections had a radial baffle moulded on to the section.

Figures 8-15 and 8-16 show typical measured RTD data in BC1 and BC2 respectively.

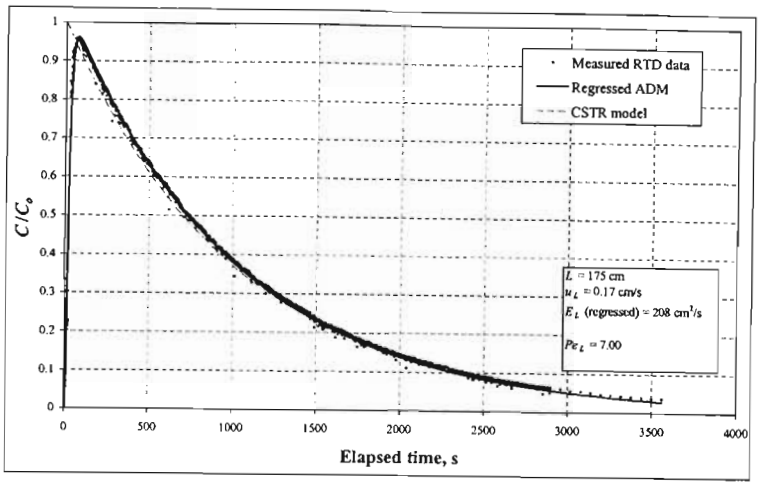

Figure 8-15: Measured RTD data in BC1 at u_g = 0.1381 cm/s with SP1

It is evident from Figure 8-15 that with a Peclet number of 7.00 there is very little difference between the measured RTD data and a CSTR model. For all practical purposes the experimental data is very well represented by a single well mixed tank. For this reason RTD measurements were not pursued extensively in BC1.

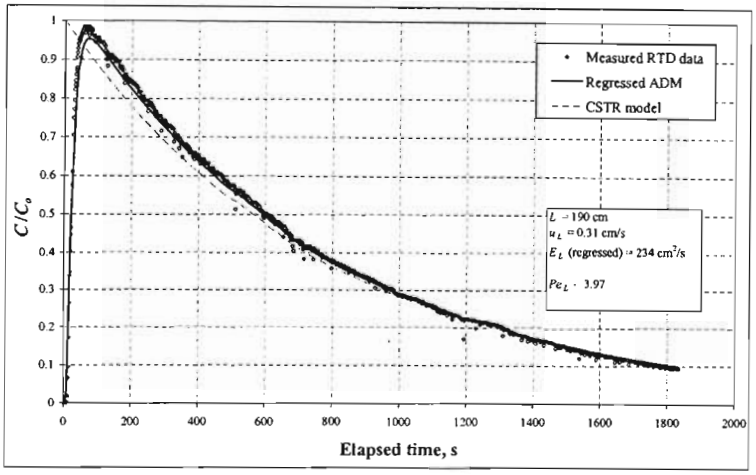

Figure 8-16: Measured RTD data in BC2 at u_g = 0.0793 cm/s with SP10

In the case of BC2 where smaller Peclet numbers ($Pe_L < 5$) were achievable it is more apparent that the bubble column is well represented by the ADM as shown in Figure 8-16. Many RTD measurements were undertaken in BC2 and typical sample plots are provided in Appendix B. For BC2 at high Peclet numbers ($Pe_L > 5$) the RTD was also well represented by the CSTR model as was the case for BC1.

8.3.4) Quality and reproducibility of experimental RTD data

The RTD measurements exhibited better reproducibility than batch mixing tests. The deviation was always less than 14 %. However the RTD measurements were time consuming and the volume of solvent used was much greater than for the batch mixing experiments. Fluctuations in conductivity measurement were experienced as for the batch mixing tests.

8.4) Cascaded column results

RTD measurements were undertaken in BC1 and BC2 using various configurations. In all instances the RTD measurements were well represented by the tanks in series model (Chapter 4).

An investigation of the sparger geometry was not undertaken. Palaskar et al. (2000) extensively investigated sectionalised columns at superficial gas velocities of 0.0166 – 0.2 cm/s. The results of this study are consistent with the findings of Palaskar et al. (2000).

8.4.1) BC1

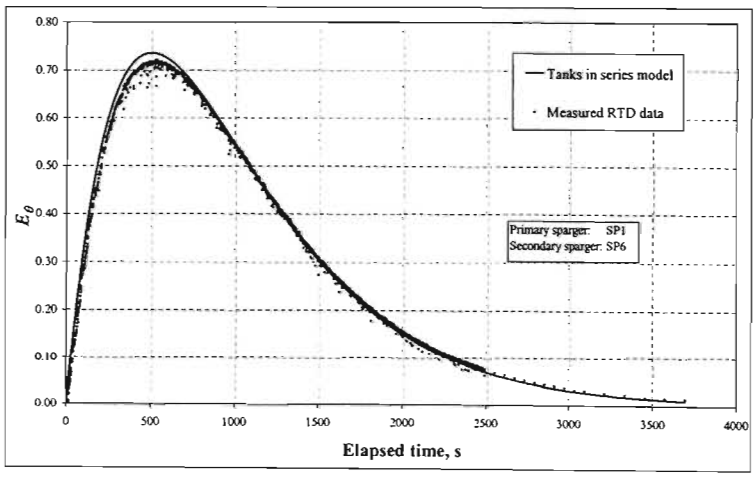

Figure 8-17: Measured RTD data in BC1 with cascaded column arrangement (N=2) at u_g = 0.1381 cm/s and u_L = 0.17 cm/s with L_1 = 93 cm and L_2 = 84 cm

In Figure 8-17 it is clearly evident that the measured RTD is well represented by two perfectly mixed tanks in series. The slight discrepancy between the measured RTD data and the model is that the two sections were not identical in size.

8.4.2) BC2

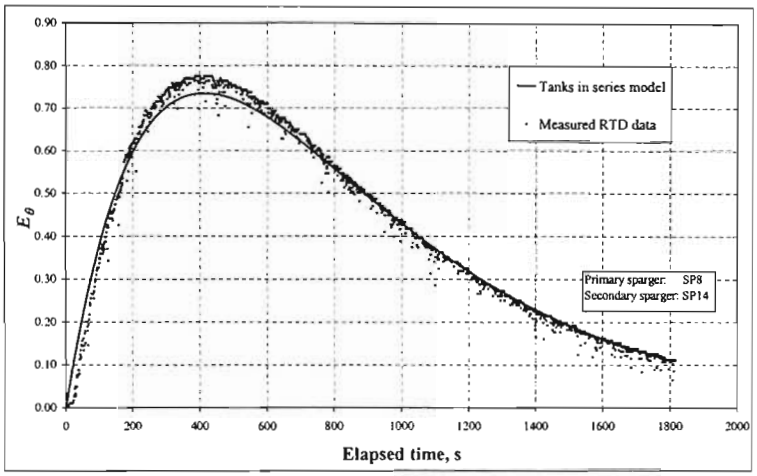

Figure 8-18: Measured RTD data in BC2 with cascaded column arrangement (N=2)

at u_g = 0.15 cm/s and u_L = 0.24 cm/s with L_1 = 100 cm and L_2 = 92 cm

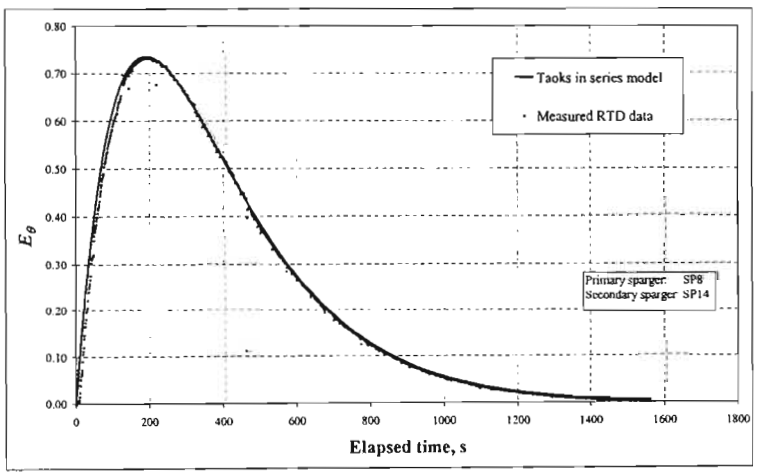

Figure 8-19: Measured RTD data in BC2 with cascaded column arrangement (N=2)

at u_g = 0.15 cm/s and u_L = 0.24 cm/s with L_1 = 50 cm and L_2 = 42 cm

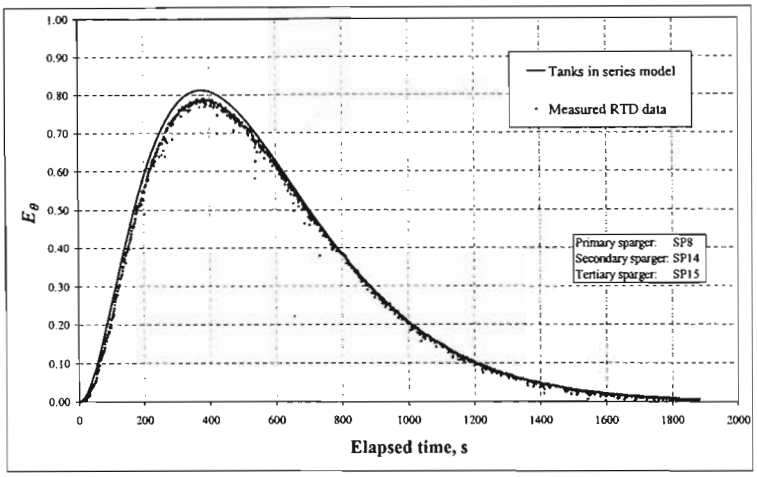

Figure 8-20: Measured RTD data in BC2 with cascaded column arrangement (N=3) at u_g = 0.15 cm/s and u_L = 0.24 cm/s with L_1 = 50 cm, L_2 = 50 cm and L_3 = 42 cm

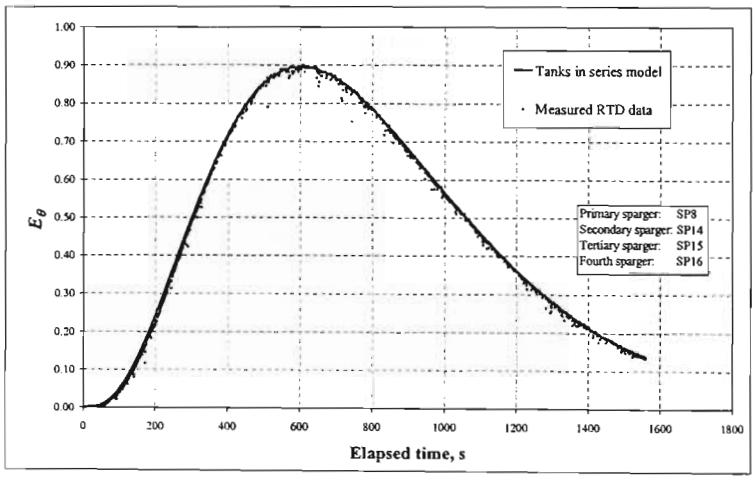

Figure 8-21: Measured RTD data in BC2 with cascaded column arrangement (N=4) at u_g = 0.15 cm/s and u_L = 0.24 cm/s with L_1= L_2=L_3= 50 cm and L_4 = 42 cm

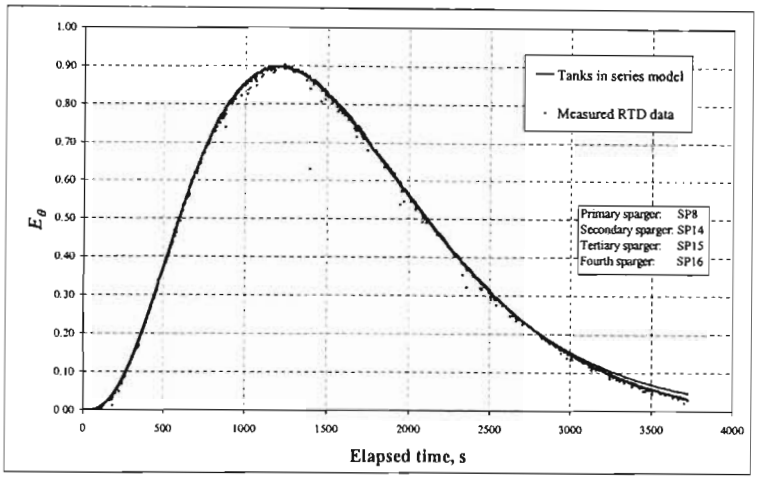

Figure 8-22: Measured RTD data in BC2 with cascaded column arrangement (N=4)

at u_g = 0.15 cm/s and u_L = 0.12 cm/s with L_1= L_2=L_3= 50 cm and L_4 = 42 cm

In all instances for replicate measurements with varying superficial gas velocity the measured RTD data corresponded to the tanks in series model. The energy input even at low superficial gas velocities is sufficient to prevent substantial back flow of liquid from one cell to another.

For reactions where plug flow conditions are preferable a bubble column reactor can be made to approach plug flow like behaviour with the incorporation of additional partition plates.

In industry the choice of partition plate geometry is based on the resultant pressure drop across the plates and also that the column should be a free draining system for ease of maintenance. In this study only partition plates with a perforated area of 0.64 % were considered.

8.5) Comparison of experimental results to literature correlations

The final results for axial dispersion coefficients in BC1 and BC2 are given in Table 8-3. The average results for RTD measurements and batch measurements were used for BC2 and only the batch measurements for BC1.

Table 8-3: Axial dispersion coefficients for BC1 and BC2

BC1		BC2	
u_g cm/s	E_L cm^2/s	u_g cm/s	E_L cm^2/s
0.1381	194	0.0743	220
0.2088	203	0.1509	238
0.2807	214	0.2304	250
0.3539	236	0.3127	257
0.4284	248	0.3978	269
0.5814	253		

The results are plotted in Figure 8-23 below.

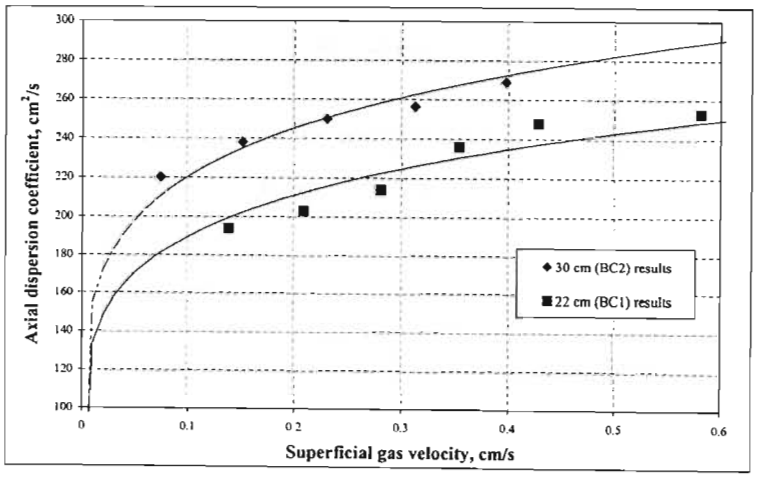

Figure 8-23: Axial dispersion coefficients versus superficial gas velocity for BC1 and BC2

In Chapter 5, literature data at low superficial gas velocities was analysed using literature correlations. The measured data obtained in this study was subjected to a similar analysis.

8.5.1) Prediction of E_L via superficial gas velocity and column diameter correlations

The measured data from this study was compared to the literature correlations shown in Table 4-2. Most authors report that their measured data at higher superficial gas velocities is well represented by the correlation of Deckwer (1974).

8.5.1.1) BC2 (30 cm diameter column)

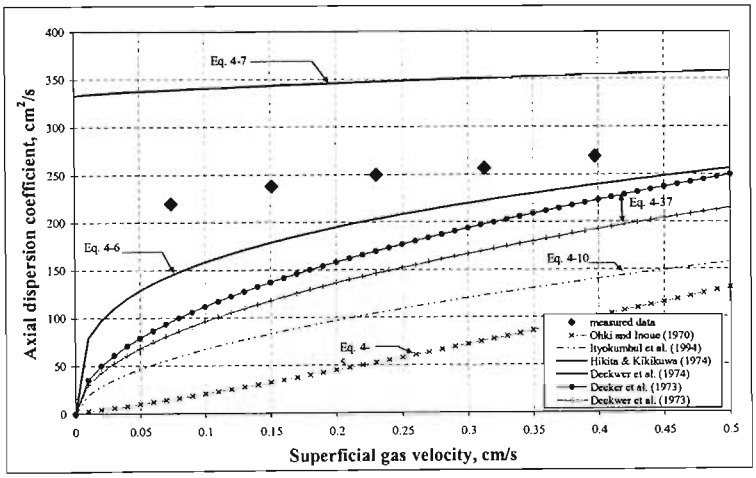

Figure 8-24: Comparison of measured data in BC2 to literature correlations based on diameter and superficial gas velocity

It is noticeable that the correlations of Deckwer et al. (1973) and Deckwer et al. (1974) tend to under predict the measured dispersion coefficients at superficial gas velocities less than 0.3 cm/s. As the superficial gas velocity increases the two correlations achieve a better approximation of the measured E_L values. The other correlations do not compare well to the measured data in BC2.

8.5.1.2) BC1 (22 cm diameter column)

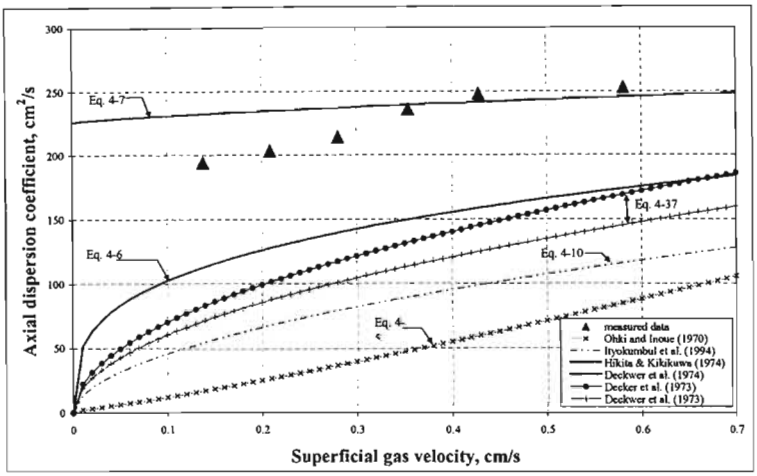

Figure 8-25: Comparison of measured data in BC1 to literature correlations based on diameter and superficial gas velocity

In BC2 it was ascertained that the measured dispersion coefficients were relatively well described by the correlation of Deckwer et al. (1974). In the case of BC1 all the considered correlations except that of Hikita and Kikukawa (1974) severely under predict the measured dispersion coefficients obtained in BC1. In fact the correlation of Hikita and Kikukawa (1974) very accurately approximates the dispersion coefficient in BC1 at superficial gas velocities higher than 0.35 cm/s.

8.5.1.3) Correlation of measured data with u_g and D_c dependency

In Chapter 5 literature data at low superficial gas velocities was correlated as per Eq. 5-5.

$$E_L = 1.49 D_c^{1.53} \tag{5-5}$$

Table 8-4 shows the predicted E_L value for the bubble column diameters used in this study.

Table 8-4: Predicted dispersion coefficients as per Eq. 5-5

D_c	E_L
Cm	cm^2/s
22	169
30	271

The results obtained in this study show a slight dependence on superficial gas velocity (Eq. 8-3) and as such it is difficult to extract a comparison. Suffice to say the use of Eq. 5-5 is not recommended for predicting dispersion coefficients at low superficial gas velocities.

The experimental results obtained in this study for BC1 and BC2 were also correlated according to the form of Eq. 4-3. The measured data is well represented by:

$$E_L = 60.6 u_g^{0.153} D_c^{0.483} \tag{8-4}$$

with E_L in cm^2/s, u_g in cm/s and D_c in cm. Eq. 8-4 correlates the experimental data with an average absolute deviation of 2.7 %.

Eq. 8-4 shows that the measured data in this study has a much lower diameter dependency than that of typical literature correlations. In the literature E_L is usually dependent on column diameter D_c as:

$$E_L \propto D_c^{1.1-1.5}$$

Eq. 8-4 shows that for the measured data in this study:

$$E_L \propto D_c^{0.483}$$

The literature data of Table 5-3 is compared to the prediction of Eq. 8-4. It is evident from Figure 8-26 that existing literature data is not accurately described by Eq. 8-4.

For the data point of Towell and Ackermann (1972) Eq. 8-4 predicts an E_L value of 565 cm^2/s. Towell and Ackermann reported a dispersion coefficient of 1900 cm^2/s in their one meter diameter column. The legend for Figure 8-26 is provided in Table 5-3.

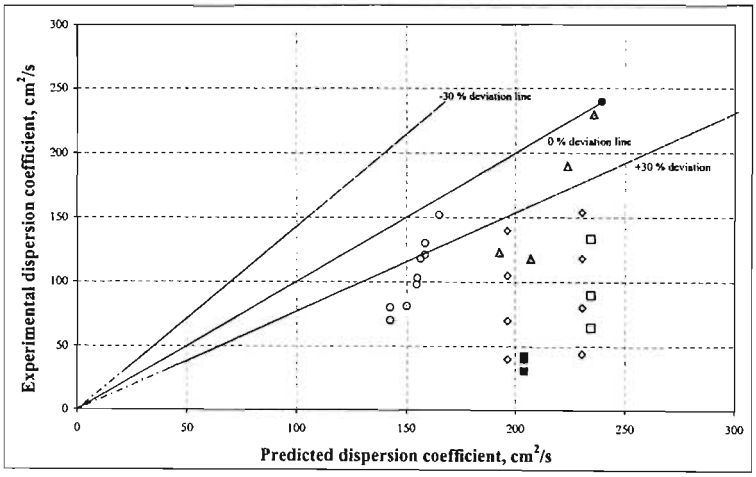

Figure 8-26: Comparison of literature dispersion coefficients to predicted Eq. 8-4 values

Very few of the literature data points fall within a ± 30 % deviation from the prediction of Eq. 8-4.

8.5.2) Correlation of measured data with Peclet number

Many researchers have reported constancy of Peclet number with superficial gas velocity (Chapter 4). A similar approach as other researchers was implemented with the measured data obtained in this study.

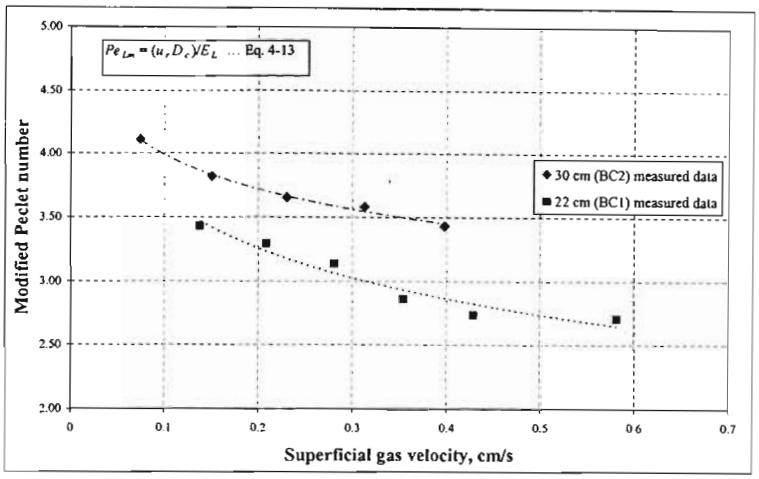

Figure 8-27: Modified Peclet number as per Reith et al. (1968) versus u_g for measured data

From Figure 8-27 it is evident that the measured data displays no trend with the Peclet number as defined by Reith et al. (1968). The analysis method of Eissa and Schugerl (1975) also yielded results with no apparent trend.

With the following modified Peclet number *Pe'* (Eq. 8-5) a trend for the measured data was observed as shown in Figure 8-28.

$$Pe' = \frac{E_L}{u_g D_c} \tag{8-5}$$

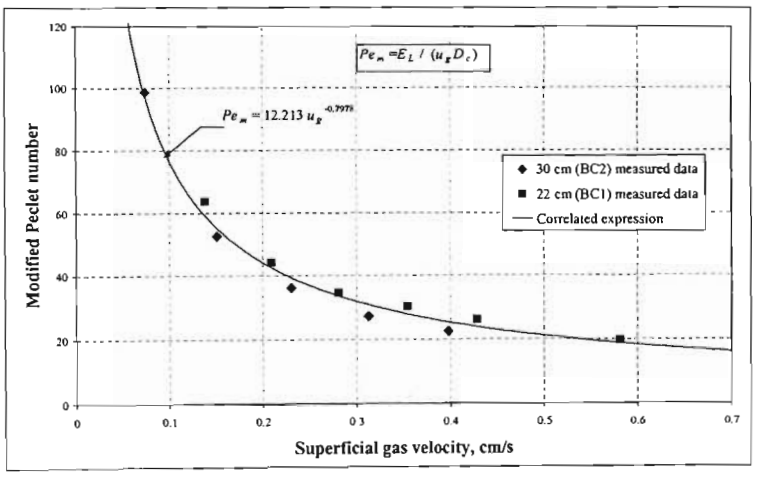

Figure 8-28: Modified Peclet number as per Eq. 8-5 versus u_g for measured data

The measured data is correlated by:

$$Pe' = \frac{E_L}{u_g D_c} = 12.212 u_g^{-0.7978} \qquad (8\text{-}6)$$

Eq. 8-6 correlates the experimental data with an average absolute deviation of 6.9 %.

The literature data as per Table 5-3 was compared to predicted E_L values by Eq. 8-6. The comparison is given in Figure 8-29. The legend for Figure 8-29 is given in Table 5-3.

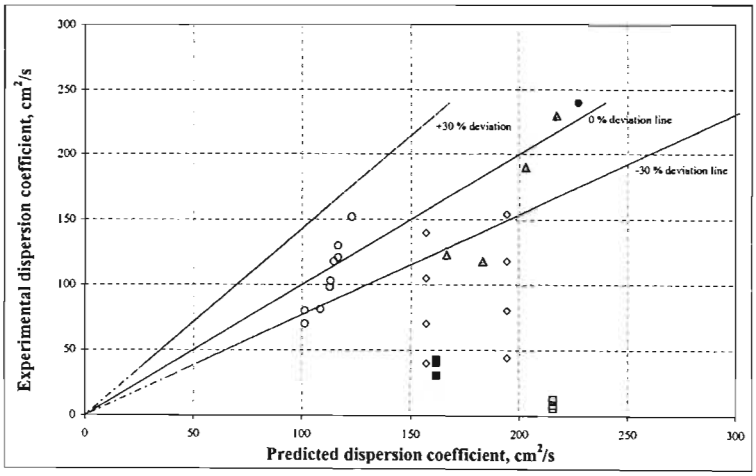

Figure 8-29: Comparison of literature dispersion coefficients to predicted Eq. 8-6 values

For the data point of Towell and Ackermann (1972) Eq. 8-6 predicts an E_L value of 1265 cm^2/s. Towell and Ackermann reported a dispersion coefficient of 1900 cm^2/s.

The majority of the literature data falls outside of the ± 30 % deviation limits of the predicted E_L values. Interestingly the data of Ulbrecht and Baykara (1981) is well predicted by Eq. 8-6 whereas the data of other authors is observed to be over estimated. The prediction of literature data via Eq. 8-6 is an improvement over Eq. 8-4.

8.5.2.1) Prediction of E_L via correlation with Peclet and Froude number

Kato and Nishiwaki (1972) reported that axial dispersion coefficients could be predicted by correlation with Peclet number and Froude number (Eq. 4-17). The measured data obtained in this study shows that the modified Peclet numbers for BC1 and BC2's measured data

varied linearly with the Froude number (Figure 8-30). However the data sets could not be correlated via a single equation.

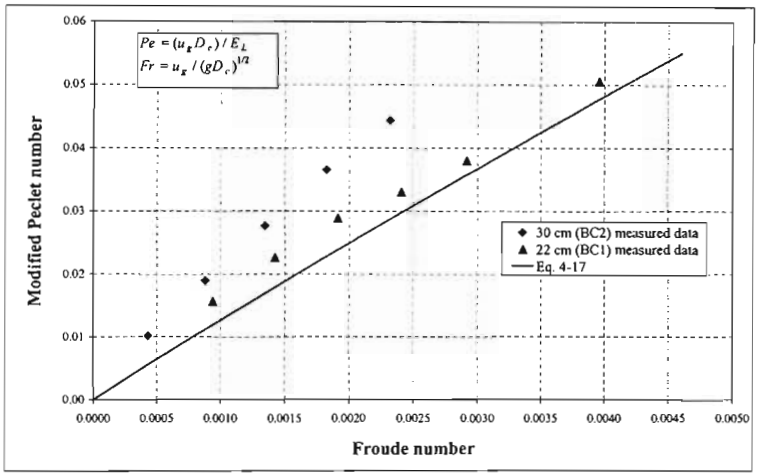

Figure 8-30: Comparison of experimental data to Kato and Nishiwaki's (1972) correlation for predicting Peclet numbers

The comparison of Kato and Nishiwaki's (1972) predicted dispersion coefficients are provided in Figure 8-31. The prediction is poor.

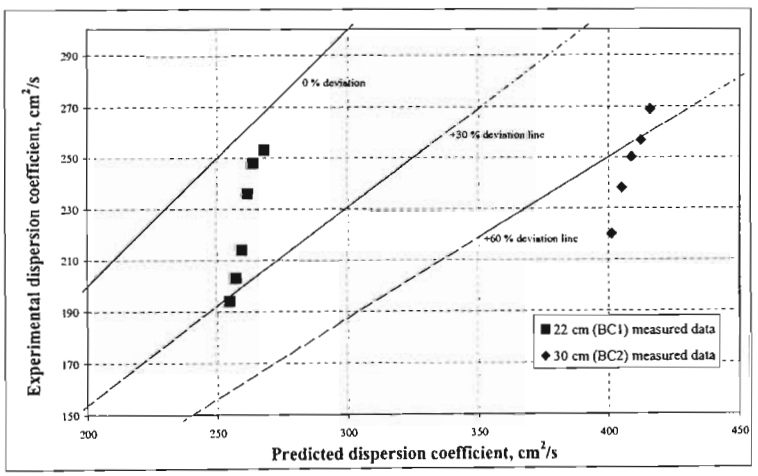

Figure 8-31: Comparison of experimental data to Kato and Nishiwaki's (1972) correlation for predicting dispersion coefficients

8.5.3) Prediction of E_L by Kolmogoroff's theory of isotropic turbulence

The correlation of Baird and Rice (1975) was used to predict dispersion coefficients in BC1 and BC2. It is evident from Figure 8-32 that the correlation under predicts the measured dispersion coefficients. In fact the prediction of dispersion coefficients for a 30 cm column via Eq. 4-33 coincides with the measured data in a 22 cm column.

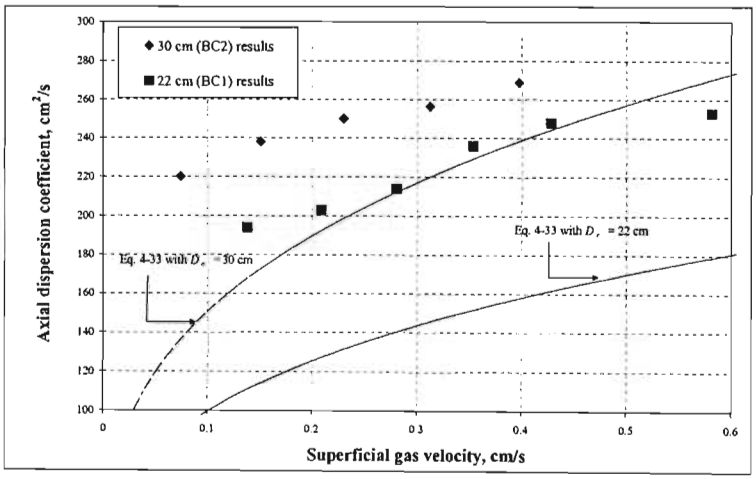

Figure 8-32: Comparison of experimental data to Baird and Rice's (1975) correlation for prediction dispersion coefficients

8.5.4) Prediction of E_L by recirculation velocity

Joshi and Sharma (1978) showed that dispersion coefficients can be predicted with column recirculation velocity as per Eq. 4-21. Recirculation liquid velocity measurements were not undertaken in this study however the correlations recommended by the authors were utilised to predict dispersion coefficients as shown in Table 8-5 and Table 8-6.

Table 8-5: Predicted E_L values for 22 cm column via Eq. 4-21

u_g	ϵ_g	v_c	E_L (predicted)	E_L (observed)
	Eq. 4-42	Eq. 4-24	Eq. 4-21	
cm/s	[-]	cm/s	cm^2/s	cm^2/s
0.1381	0.0039	6.54	21	194
0.2088	0.0058	7.51	24	203
0.2807	0.0078	8.28	26	214
0.3539	0.0099	8.94	29	236
0.4284	0.0119	9.52	30	248
0.5814	0.0160	10.52	34	253

Table 8-6: Predicted E_L values for 30 cm column via Eq. 4-21

u_g	ϵ_g	v_c	E_L (predicted)	E_L (observed)
	Eq. 4-42	Eq. 4-24	Eq. 4-21	
cm/s	[-]	cm/s	cm^2/s	cm^2/s
0.0743	0.0021	6.75	34	220
0.1509	0.0042	8.55	44	238
0.2304	0.0064	9.83	50	250
0.3127	0.0087	10.88	55	257
0.3978	0.0111	11.78	60	269

The correlation of Joshi and Sharma (1978) severely under predicts dispersion coefficients at low superficial gas velocities.

8.5.5) Prediction of E_L by centre-line liquid velocity

Krishna et al. (2000) showed that the centre-line liquid velocity in a bubble column can be used to predict dispersion coefficients as per Eq. 4-28.

Table 8-7: Predicted E_L values for 22 cm column via Eq. 4-28

u_g	$V_L(0)$ Eq. 4-27	E_L (predicted) Eq. 4-28	E_L (observed)
cm/s	cm/s	cm^2/s	cm^2/s
0.1381	11.04	75	194
0.2088	12.89	88	203
0.2807	14.40	98	214
0.3539	15.71	107	236
0.4284	16.88	115	248
0.5814	18.92	129	253

Table 8-8: Predicted E_L values for 30 cm column via Eq. 4-28

u_g	$V_L(0)$ Eq. 4-27	E_L (predicted) Eq. 4-28	E_L (observed)
cm/s	cm/s	cm^2/s	cm^2/s
0.0743	10.22	95	220
0.1509	13.32	124	238
0.2304	15.62	145	250
0.3127	17.51	163	257
0.3978	19.17	178	269

The recommended correlations of Krishna et al. (2000) under predict the observed dispersion coefficients obtained in this study. Since centre-line liquid velocities were not measured the correlation predicted values of Eq. 4-27 cannot be commented on.

8.6) E_L correlations for bubble column scale up at low superficial gas velocities

The measured experimental data has been rigorously compared to existing literature correlations. Literature data at low superficial gas velocities has been similarly analysed and no consensus for prediction of dispersion coefficients at low superficial gas velocities could be reached.

At this point a hypothetical case study will be considered. Ultimately the purpose of correlations is for use in scale-up to pilot and commercial sized bubble columns. The literature correlations as well as correlations developed in this study will be used to illustrate the dangers in using incorrect empirical correlations and/or extrapolating empirical correlations. Before the case study is performed a few aspects must be considered.

8.6.1) Conversion for axially dispersed type flow

According to Chisti (1989) the one dimensional axial dispersion model is applicable for a slow first order chemical reaction with reaction constant k_r when:

$$\frac{k_r D_c^{\,2}}{E_L} \leq 40 \tag{8-7}$$

Levenspiel (1962) showed that when the axial dispersed plug flow model is assumed, then for a first order reaction the concentration at the exit C_L is related to the inlet concentration C_{in} as:

$$\frac{C_L}{C_{in}} = \frac{4a \times \exp\left(\frac{Pe}{2}\right)}{(1+a)^2 \exp\left(\frac{aPe}{2}\right) - (1-a)^2 \exp\left(-\frac{aPe}{2}\right)} \tag{8-8}$$

where

$$a = \sqrt{1 + \frac{4k_r \tau}{Pe}} \tag{8-9}$$

and

$$Pe = \frac{u_L L}{E_L} \tag{8-10}$$

Conversion is defined as:

$$X = \frac{C_{in} - C_L}{C_{in}} = 1 - \frac{C_L}{C_{in}} \tag{8-11}$$

A nomograph of conversion for various Peclet numbers against the product of reactor liquid residence time τ and reaction rate constant k_r is shown in Figure 8-33.

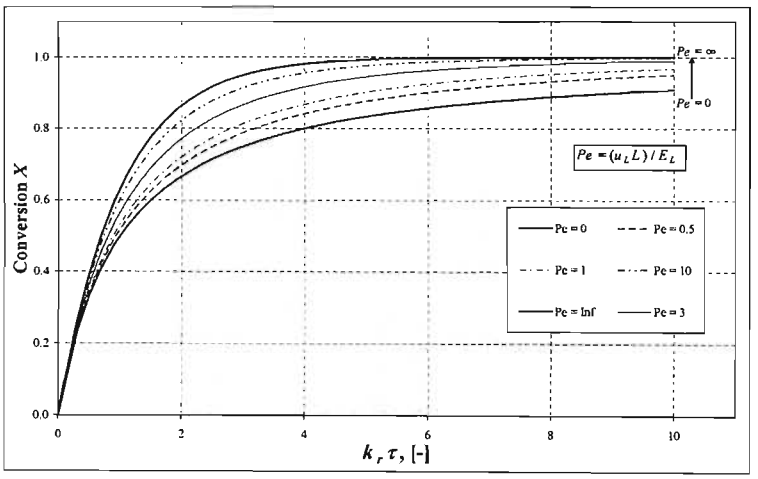

Figure 8-33: Conversion for a first order reaction with axially dispersed flow

Levenspiel (1962) showed that the volume of a reactor V_r with axially dispersed flow is related to a reactor with plug flow according to Figures 8-34 and 8-35.

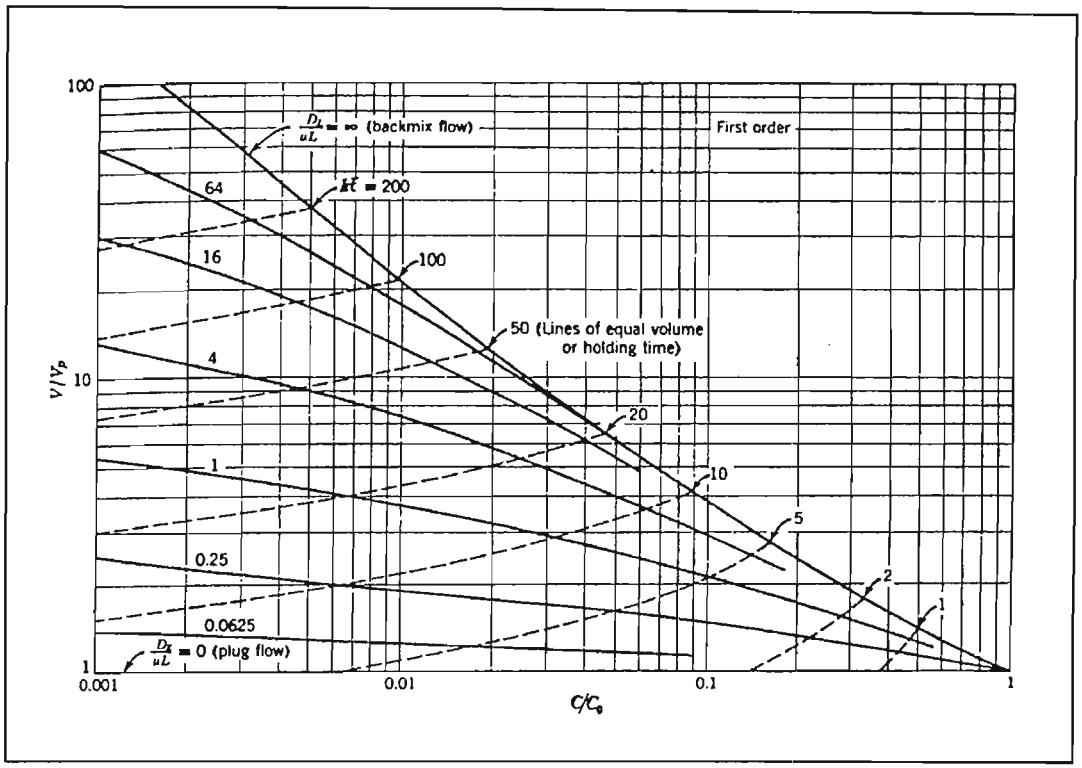

Figure 8-34: Plot to show reactor size versus conversion levels for axially dispersed type flow, Levenspiel (1962)

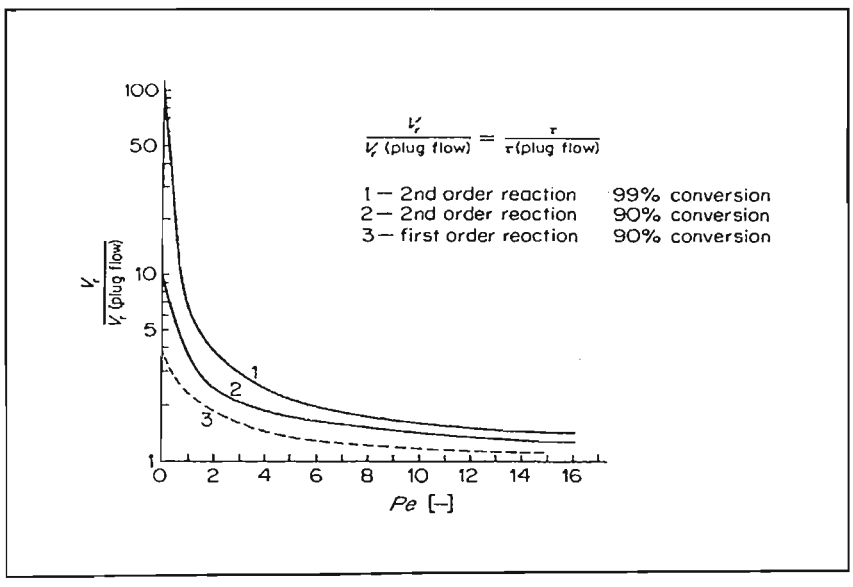

Figure 8-35: Reactor volume or residence time ratio for an axially dispersed flow reactor as compared to a plug flow reactor, Levenspiel (1962)

8.6.2) Case scenario

Consider the following scenario. The first order reaction constant k_r is 1 hr^{-1} and the desired conversion X is 90 %. The volumetric flow rate of reactant liquid is 125 m^3/h. For illustrative purposes column diameters in the range 1-6 m will be considered. The superficial gas velocity is determined to be 0.2 cm/s.

For u_g = 0.2 cm/s predicted dispersion coefficients via literature correlations and correlations developed in this study are shown in Table 8-9.

Table 8-9: Predicted axial dispersion coefficients for various column diameters at u_g = 0.2 cm/s

Author		E_L, cm^2/s			
		1 m	2 m	3 m	6 m
Deckwer et al. (1974)	Eq. 4-6	1051	2774	4894	12915
Hikita and Kikukawa (1974)	Eq. 4-7	1558	3705	6150	14627
Kato and Nishiwaki (1972)	Eq. 4-17	2453	6908	12665	35722
Baird and Rice (1975)	Eq. 4-33	944	2379	4084	10292
Krishna et al. (2000)	Eq. 4-28	838	2371	4355	12319
This work	Eq. 8-4	438	612	745	1041
This work	Eq. 8-6	882	1764	2646	5292

The predicted dispersion coefficients are used to calculate the required reactor volume needed to effect a 90 % conversion. These calculated volumes are given in Table 8-10.

Table 8-10: Required reactor volume for 90 % conversion (scenario case) using predicted dispersion coefficients

	Reactor volume, m^3			
	1 m	2 m	3 m	6 m
Deckwer et al. (1974)	293	398	639	1075
Hikita and Kikukawa (1974)	295	421	672	1081
Kato and Nishiwaki (1972)	299	479	779	1109
Baird and Rice (1975)	293	387	614	1063
Krishna et al. (2000)	293	387	622	1073
This work (Eq. 8-4)	291	323	422	820
This work (Eq. 8-6)	293	368	556	1015

Peclet numbers can be computed from Eq. 8-10 using the calculated reactor volume and the column diameter to determine *L*. The Peclet numbers are provided in Table 8-11.

Table 8-11: Peclet numbers for scenario case

	Peclet number			
	1 m	2 m	3 m	6 m
Deckwer et al. (1974)	156.90	5.0475	0.9074	0.03615
Hikita and Kikukawa (1974)	106.61	3.9980	0.0594	0.03210
Kato and Nishiwaki (1972)	68.62	2.4395	0.4065	0.01348
Baird and Rice (1975)	174.71	5.7237	0.0705	0.04486
Krishna et al. (2000)	196.77	5.7429	1.1973	0.03783
This work (Eq. 8-4)	373.93	18.5602	0.2622	0.34218
This work (Eq. 8-6)	187.00	7.3396	2.5967	0.08331

The required reactor volumes are plotted against the predicted dispersion coefficients in Figure 8-36.

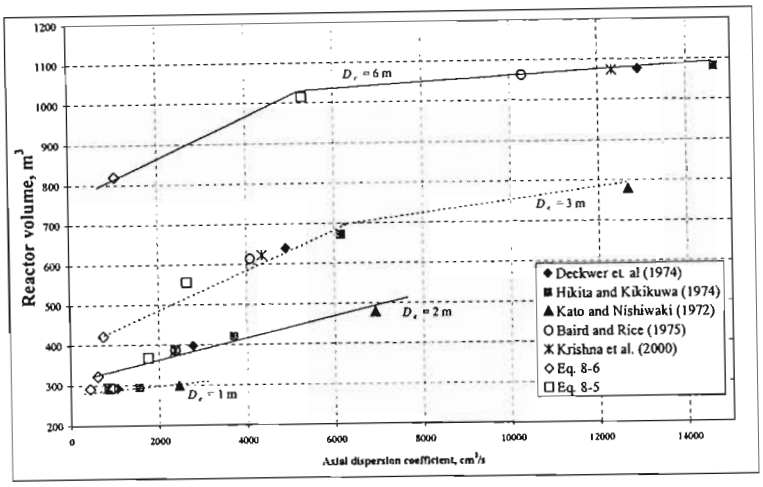

Figure 8-36: Reactor volumes for 90 % conversion as per case scenario

The required volume is plotted against the Peclet number in Figure 8-37 below.

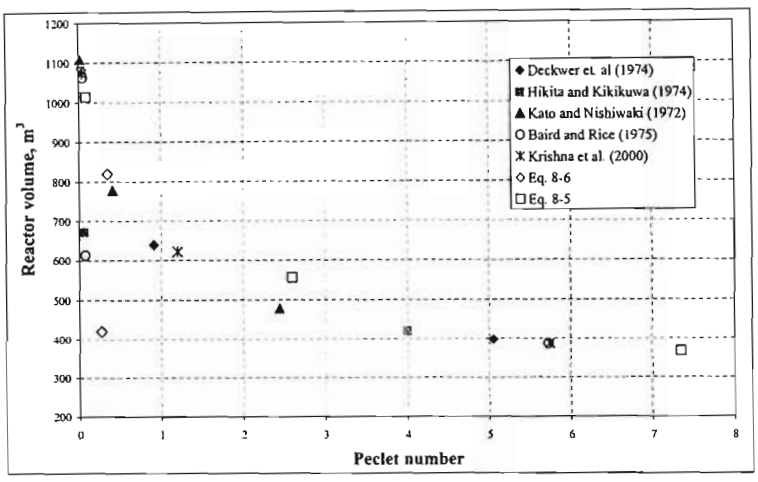

Figure 8-37: Reactor volumes versus Peclet number for case scenario

The required reactor volume is minimal when the Peclet number is large ($Pe > 15$). This corresponds to plug flow like behaviour where the convective mass transport component is dominant over the dispersive component (Figure 8-33). For small Peclet numbers the largest required reactor volume is approached. This corresponds to complete back mixing in the bubble column and CSTR type behaviour and reactor sizes are approached.

The grey area for optimum bubble column design is when the convective Peclet number falls in the range 0.02 – 6. This is evident in Figure 8-37 where the required reactor volume is a strong function of the Peclet number. In this range accurate estimates of dispersion coefficients are required for confident design. For example in the case scenario problem for column diameters of 3 and 6 m the use of Eq. 8-4, developed in this study, for predicting dispersion coefficients resulted in significantly lower required reactor volumes. On the other extreme the dispersion coefficient predicted by Kato and Nishiwaki (1972) resulted in significantly higher reactor volumes (Table 8-10). It is evident that the choice of correlation for the prediction of E_L has a significant effect on the required reactor volume. The danger of extrapolating correlations has also been highlighted. The principle danger is that of over or under design which affects conversion and operating costs. The difficulty lies in that once the column is operational it is extremely difficult to implement control strategies to overcome the design flaws.

The objective of this study has been primarily to:

1. investigate the behaviour of bubble column reactors at low superficial gas velocities
2. establish whether existing literature correlations are valid in this flow regime
3. develop applicable correlations at low superficial gas velocities
4. investigate the effect of scale up

These issues will be addressed here and in Chapter 9.

With respect to the first objective this has been adequately accomplished. It has been found that bubble column reactors are very well mixed at low superficial gas velocities and the quality of mixing is comparable to that at higher superficial gas velocities. Dispersion coefficients have been measured by two methods and the results compare well.

With respect to the validity of whether existing correlations are applicable at low superficial gas velocities, the analysis of existing literature data as well as the data measured in this study lends to the conclusion that the considered literature correlations tend to under-predict or over-estimate the tested data. The reason for this is that these correlations have been developed at high superficial gas velocities where churn-turbulent behaviour in the liquid is prevalent. Also in Chapter 5 the dearth of data at low superficial gas velocities was exposed. Also the relatively few researchers who have undertaken work at low superficial gas velocities have used either very small columns or did not investigate the influence of scale on their measurements. It is therefore not surprising that literature correlations fail to adequately describe dispersion coefficients at low superficial gas velocities.

Two correlations have been developed in this study. However there is an inconsistency in the two correlations.

Eq 8-6 essentially has the form:

$$E_L = 12.212 u_g^{0.202} D_c \qquad (8\text{-}12)$$

Eq. 8-12 exhibits a stronger column diameter dependency than Eq. 8-4 which was regressed using the same data used to correlate Eq. 8-12.

$$E_L = 60.6 u_g^{0.153} D_c^{0.483} \qquad (8\text{-}4)$$

This brings to bear the danger in method of correlation. Eq. 8-4 shows a diameter dependency approximately half that of Eq. 8-12. In the case scenario Eq. 8-12 resulted in reactor volumes which compared well to reactor volumes obtained using the correlations of Baird and Rice (1975), Deckwer et al. (1974) and Krishna et al. (2000).

The issue of scale-up is a complex one. It is unfortunate that more column diameters could not be investigated in this study. Any conclusion on the influence of column diameter at low superficial gas velocities will be purely speculative. This issue can only be satisfactorily addressed with the integration of more data especially at larger column diameters. This information will steadily become available as Sasol develops pilot plant bubble column reactors operating at low superficial gas velocities. The results of this study and that of existing literature data lead to the conclusion that the column diameter effect is not as pronounced in bubble column reactors of diameter 30 cm and less. It is clear that more data at larger column diameters is necessary.

CHAPTER NINE

CONCLUSION

The behaviour of bubble column reactors at low superficial gas velocities has been investigated.

The essential questions that required answers were:

- Do existing literature correlations apply at low superficial gas velocities?
- How does column diameter affect hydrodynamic quantities at low superficial gas velocities?

The answer to the issue on the validity of existing correlations is that they do not accurately describe dispersion levels at low superficial gas velocities. The reason for this is simply that these empirical correlations do no incorporate data at low superficial gas velocities and the extrapolation does not work satisfactorily.

With respect to column diameter, analysis of literature data and the measured data in this study lends to the conclusion that the issue of scale-up at low superficial gas velocities is extremely complex. The results obtained in this study are inconsistent with respect to column diameter.

At then end of any study a critical examination of what has been accomplished must be undertaken.

The following has been achieved:

1. The development of suitable bubble column apparatus at the University of Kwa-Zulu Natal - Howard College Campus which will be used for further research.

2. The foundation for a bubble column research group at the above mentioned university has been established.
3. An extensive literature review on bubble column hydrodynamics has been performed.

4. The lack of data at low superficial gas velocities has been demonstrated. Furthermore analysis of this data has been undertaken and there are significant deviations in the published data.

5. Measurements of gas hold-up, and axial dispersion coefficients at low superficial gas velocities (u_g < 0.8 cm/s) have been undertaken. RTD measurements in cascaded bubble column arrangements were performed.

6. The measured results have been compared to literature predictions and the comparison was found to be poor.

7. The analysis method used by previous researchers has been criticised. The graphical and variance method have been shown to be liable to error in estimating dispersion coefficients. To this extent the method of curve-fitting was implemented in this study for obtaining dispersion coefficients. Also the erroneous dispersion coefficients obtained via the use of incorrect boundary conditions has been highlighted.

8. Data measured in this study has been correlated and the results show a weaker diameter dependency than existing literature correlations. In the absence of further data it can only be speculated that the diameter effect at low superficial gas velocities is not as pronounced as that at higher superficial gas velocities.

9. Areas for further research have been identified and are presented in Chapter 10.

CHAPTER TEN

RECOMMENDATIONS

When research is first started in a new field, as was the case in this study, it is understandable that it will be difficult to perform cutting edge work. In this study the majority of funds were utilised for development of equipment. It is regrettable that in any study the quality of measurements and type of measurements must be governed by economic constraints. Ideally all bubble column research groups would prefer to work with PIV and LDA equipment. Measurements of these types provide a better understanding of fundamental hydrodynamic interactions in bubble column reactors.

The ADM has proven to be adequate for rudimentary modelling purposes and the use of Computational Fluid Dynamics (CFD) is being used by leading bubble column research groups to good effect. With CFD type approaches the interaction between the liquid and gas can be modelled in great detail. However in most studies the focus is orientated on one phase, i.e. either liquid or gas. The focus of study should ideally be on the interaction of the gas and liquid phase which are intimately linked.

PIV, LDA and CFD experiments would be a quantum leap away from the type of measurements undertaken in this study. However before the necessary and required experience is achieved to perform high end measurements and analysis the following areas need to be addressed and investigated:

- the design and commissioning of a large diameter column ($D_c > 60$ cm)
- the incorporation of pilot plant data ($D_c > 2$ m) for empirical correlations
- the procurement of multiple conductivity probes so that concentration profiles along the reactor length can be measured. In this study only a local conductivity measurement was performed.
- the measurement of liquid recirculation velocities and centre-line velocities at low superficial gas velocities. Existing correlations have been found to severely under predict these hydrodynamic quantities at low superficial gas velocities

There is little doubt that there is tremendous scope for Master's level and undergraduate laboratory projects for bubble column research. With each investigation valuable experience and knowledge of bubble column reactors will be acquired and contributions to the field of bubble column research will be made.

Data at low superficial gas velocities may prove to be highly valuable for CFD type modelling. The present state of technology does not allow for intimate tracking of individual bubbles in a bulk liquid. For high gas fractions the tracking of individual bubbles is nearly impossible. As CFD methods grow and technology progresses for hydrodynamic measurements at low superficial gas velocities, it may be possible to track individual bubbles for validating CFD modelling.

REFERENCES

Alexander BF and Shah TY, (1976), "Axial Dispersion in bubble columns," *The Chemical Engineering Journal*, Vol. 11, Pg. 153-156

Anabtawi MZA, Abu-Eishah SI, Hilal N and Nabhan MBW, (2003), "Hydrodynamic studies in both bi-dimensional and three-dimensional bubble columns with a single sparger," *Chemical Engineering and Processing*, Vol. 42, Pg. 403-408

Anderson JA and Quinn JL, (1970), "Bubble columns: flow transitions in the presence of trace contaminants," *Chemical Engineering Science*, Vol. 25, Pg. 373–380

Baird MHI and Rice RG, (1975), "Axial dispersion in large unbaffled columns," *The Chemical Engineering Journal*, Vol. 9, Pg. 171-174

Bhaga D, Pruden BB and Weber ME, (1971), "Gas hold-up in bubble column containing organic liquid mixtures," *The Canadian Journal of Chemical Engineering*, Vol. 49, Pg. 417-419

Bischoff KB and Philips JB, (1966), "Longitudinal mixing in orifice plate gas-liquid reactors," *I&EC Process Design and Development*, Vol. 5 No. 4, Pg. 416-421

Charpentier JC, (1981), "Mass-transfer rates in gas-liquid absorbers and reactors," *Advances in Chemical Engineering*, Vol. 11, Pg. 1-93

Chen BH, (1986), " Handbook of Heat and Mass Transfer Volume 2: Mass Transfer and Reactor Design," Editor: Cheremisinoff NP, Gulf Publishing Company Houston Texas, Pg. 1005-1028

Clements WC, (1969), "A note on determination of the parameters of the longitudinal dispersion model from experimental data," *Chemical Engineering Science*, Vol. 24, Pg. 957-963

Cova DR, (1974), "Axial mixing in the liquid phase in gas-sparged columns," *Ind. Eng. Chem. Process Des. Development*, Vol. 13, No. 3, Pg. 292-296

Deckwer W, Graesar U, Langemann H and Serpemen Y, (1973), "Zones of different mixing in the liquid phase of bubble columns," *Chemical Engineering Science*, Vol. 28, Pg. 1223-1225

Deckwer, W D, (1992), "Bubble Column Reactors", John Wiley & Sons, New York

Deckwer WD and Schumpe A, (1993), "Improved tools for bubble column reactor design and scale-up," *Chemical Engineering Science*, Vol. 48, No. 5, Pg. 889-911

Deckwer WD, Burckhart R and Zoll G, (1974), "Mixing and mass transfer in tall bubble columns," *Chemical Engineering Science*, Vol. 29, Pg. 2177-2188

Deen NG, (2001), "An experimental and computational study of fluid dynamics in gas-liquid chemical reactors," PhD thesis, Aalborg University

Dreher AJ and Krishna R, (2001), "Liquid-phase backmixing in bubble columns, structured by introduction of partition plates," *Catalysis Today*, Vol. 69, Pg. 165-170

Eissa SH and Schugerl K, (1975), "Holdup and backmixing investigations in cocurrent and countercurrent bubble columns," *Chemical Engineering Science*, Vol. 30, Pg. 1251-1256

Fahim MA and Wakao N, (1982), "Parameter estimation from tracer response methods," *The Chemical Engineering Journal*, Vol. 25, Pg. 1-8

Field RW and Davidson FJ, (1980), "Axial dispersion in bubble columns," *Transactions of the Institution of Chemical Engineers*, Vol. 58, Pg. 228-236

Hebrard G, Bastoul D and Roustan M, (1996), "Influence of gas sparger on the hydrodynamic behaviour of bubble columns," *Transactions of the Institute of Chemical Engineers*, Vol. 74, Pg. 406-414

Hikita H and Kikukaw H, (1974), "Liquid-phase mixing in bubble columns: Effect of liquid properties," *Chemical Engineering Journal*, Vol. 8, Pg. 191-197

Hills JH, (1974), "Radial non-uniformity of velocity and voidage in a bubble column," *Transactions of the Institution of Chemical Engineers*, Vol. 52, Pg. 1-9

Houzelot JL, Thiebaut MF, Charpentier JC, Schiber J, (1985), "Contribution to the hydrodynamic study of bubble columns," *International Chemical Engineering*, Vol. 25, No. 4, Pg. 645-650

Hughmark GA, (1967), "Holdup and mass transfer in bubble columns," *I&EC Process Design and Development*, Vol. 6, No. 2, Pg. 218-220

Ityokumbul MT, Kosaric N and Bulani W, (1988), "Parameter estimation with simplified boundary conditions," *Chemical Engineering Science*, Vol. 43, No. 9, Pg. 2457-2462

Ityokumbul MT, Kosaric N and Bulani W, (1994), "Gas hold-up and liquid mixing at low and intermediate gas velocities I. Air-water system," *The Chemical Engineering Journal*, Vol. 53, Pg. 167-172

Jamihlahmadi M, Zehtaban MR, Muller-Steinhagen H, Sarrafi A and Smith JM, (2001), "Study of bubble formation under constant flow conditions," *Transactions of the Institute of Chemical Engineers*, Vol. 79, Pg. 523-532

Joshi JB and Sharma MM, (1978), "A unified correlation for gas-liquid contactors," *Canadian Journal of Chemical Engineering*, Vol. 56, Pg. 116-124

Joshi JB and Sharma MM, (1979), "A circulation cell model for bubble columns," *Transactions of the Institution of Chemical Engineers*, Vol. 57, Pg. 244-251

Joshi JB, (1980), "Axial mixing in multiphase contactors - A unified correlation," *Transactions of the Institution of Chemical Engineers*, Vol. 58, Pg. 155-165

Joshi JB, Patil TA, Ranada VV and Shah YT, "Measurement of hydrodynamic parameters in multiphase sparged reactors," *Reviews in Chemical Engineering*, Vol. 6, Nos. 2-3, Pg. 73-227

Kantarcia N, Borakb F and Ulgena KO, (2005), "Bubble Column Reactors-Review Article," Article in Press, *Process Biochemistry*

Kastanek F, Zahradnik J, Kratochvil and Cermak J, (1993), "Chemical reactors for gas-liquid system," Ellis Horwood Publishers

Kato Y and Nishiwaki A, (1972), "Longitudinal dispersion coefficient of a liquid in a bubble column," *International Chemical Engineering*, Vol. 12, No. 1, Pg. 182-187

Kats MB and Genin LS, (1974), "Study of longitudinal mixing of liquid in cocurrent sparged reactors sectionilized with sieve trays," *International Chemical Engineering*, Vol. 7, No. 2, Pg. 246-252

Kawase Y and Moo-Young M, (1990), "Mathematical models for design of bioreactors: Applications of Kolmogoroff's Theory of Isotropic Turbulence," *The Chemical Engineering Journal*, Vol. 43, Pg. B19-B41

Kelkar BG, Godbole SP, Honath MF, Shah YT, Carr NL and Deckwer WD, (1983), "Effect of addition of alcohols on gas hold-up and backmixing in bubble columns," *AIChE Journal*, Vol. 29, No. 3, Pg. 361-369

Khang SJ and Kothari SP, (1980), "Experimental determination of axial dispersion coefficient in a bubble column," *Chemical Engineering Science*, Vol. 35, Pg. 2203-2205

Krishna R, Urseanu MI, van Baten JM and Ellenberger J, (2000), "Liquid phase dispersion in bubble columns operating in the churn-turbulent flow regime," *Chemical Engineering Journal*, Vol. 78, Pg. 43-51

Kulkarni AA, Joshi JB, Kumar VR and Kulkarni BD, (2001), "Application of multiresolution analysis for simultaneous measurement of gas and liquid velocities and fractional gas hold-up in bubble column using LDA," *Chemical Engineering Science*, Vol. 56, Pg. 5037-5048

Kumar R and Kuloor NR, (1970), "The formation of bubbles and drops," *Advances in Chemical Engineering*, Vol. 8, Pg. 228-368

Kunugita E, Ikuri M and Otake T, (1970), "Liquid behaviour in bubble column," *Journal of Chemical Engineering of Japan*, Vol. 3, No. 1, Pg. 24-29

Levenspiel O, (1962), "Chemical Reaction Engineering An introduction to the design of chemical reactors," John Wiley and Sons

Lockett MJ and Kirkpatrick RT, (1975), "Ideal bubbly flow and actual flow in bubble columns," *Transactions of the Institution of Chemical Engineers*, Vol. 53, Pg. 267-273

Mashelkar RA and Ramachandran PA, (1975), "Longitudinal dispersion in circulation dominated bubble columns," *Transactions of the Institution of Chemical Engineers*, Vol. 53, Pg. 274-277

Mecklenburg JC, (1974), "Backmixing and design: A Review," *Transactions of the Institution of Chemical Engineers*, Vol. 53, Pg. 180-192

Moustiri S, Hebrard G, Thakre SS and Roustan M, (2001), "A unified correlation for predicting liquid axial dispersion coefficient in bubble columns," *Chemical Engineering Science*, Vol. 56, Pg. 1041-1047

Nottemkamper R, Steiff A and Weinspach PM, (1983), "Experimental investigation of hydrodynamics of bubble columns," *German Chemical Engineering*, Vol. 6, Pg 147-155

Ohki Y and Inoue H, (1970), "Longitudinal mixing of the liquid phase in bubble columns," *Chemical Engineering Science*, Vol. 25, Pg. 1-16.

Ottmers Dm and Rase HF, (1964), "Characteristics of singe- and multiple-hole orifice plates for gas-liquid reactions," *I&EC Fundamentals*, Vol. 3, No. 2, Pg. 106-110

Ozturk SS, Schumpe A, Deckwer WD, (1987),"Organic liquids in a bubble column: holdups and mass transfer coefficient," *AICHE Journal*, Vol. 33, No. 9, Pg. 1473-1480

Palaskar SN, De JK and Pandit AB, (2000), "Liquid phase RTD studies in sectionilized bubble column," *Chemical Engineering Technology*, Vol. 23, Pg. 61-68

Pandit AB and Doshi YK, (2005), "Mixing Time Studies in Bubble Column Reactor with and without Internals," *International Journal of Chemical Reactor Engineering*, Vol. 3, Pg. A22

Reith T, Renken S and Israel BA, (1968), "Gas hold-up and axial mixing in the fluid phase of bubble columns," *Chemical Engineering Science*, Vol. 23, Pg. 619-629

Rice RG, Tupperainen JMI and Hedge RM, (1981), "Dispersion and hold-up in bubble columns - Comparison of Rigid and Flexible Spargers," *Transactions of the Institution of Chemical Engineers*, Vol. 59, Pg. 677-687

Rubio FC, Miron AS, Garcia MCC, Camacho FG, Grima EM and Chisti Y, (2004), "Mixing in bubble columns: a new approach for characterising dispersion coefficients," *Chemical Engineering Science*, Vol. 59, Pg. 4369-4376

Sekizawa T and Kubota H, (1974), "Liquid mixing in multistage bubble columns," *Journal of Chemical Engineering of Japan*, Vol. 7, No. 6, Pg. 441-446

Shah YT and Deckwer WD, (1983), "Handbook of Fluids in Motion", Editors: Cheremisinoff NP and Gupta R, Ann Arbor Science, Pg. 583-620

Shah YT, Kelkar BG, Godbole SP and Deckwer WD, (1982), "Design parameter estimations for bubble column reactors," *AIChE Journal*, Vol. 28, No. 3, Pg. 353-379

Shah YT, Stiegel GJ and Sharma MM, (1978), "Backmixing in gas-liquid reactors," *AIChE Journal*, Vol. 24, No. 3, Pg. 369-300

Subramanian G and Tien C, (1975), "Induced liquid phase mixing due to bubble motion at low gas velocity," *The Canadian Journal of Chemical Engineering*, Vol. 53, Pg. 611-620

Talbot JDR, House WA and Pethybridge AD, "Prediction of temperature dependence of electrical conductance for river waters," *Water Research*, Vol. 24, No. 10, Pg. 1295-1304

Tang C and Heindel TJ, (2004), "Time dependent gas-holdup variation in air-water bubble column," *Chemical Engineering Science*, Vol. 59, Pg. 623-632

Thorat BN, Kulkarni AV and Joshi JB, (2001), "Design of sieve plate spargers for bubble columns: Role of Weeping," *Chemical Engineering Technology*, Vol. 24, No. 8, Pg. 815-828

Thorat BN, Shevade AV and Joshi JB, (1998), "Effect of sparger design and height to diameter ratio on fractional gas hold-up in bubble columns," *Transactions of the Institute of Chemical Engineers*, Vol. 76, Pg. 823-834

Ulbrecht JJ and Baykara ZS, (1981), "Significance of the central plume velocity for the correlation of liquid phase mixing in bubble columns," *Chemical Engineering Communications*, Vol. 10, Pg. 168-185

van Baten JM and Krishna R, (2003), "Scale up studies on partitioned bubble column reactors with the aid of CFD simulations," *Catalysis today*, Vol. 79-80, Pg. 219-227

Wilkinson PM and Dierendonck LL, (1994), "A theoretical model for the influence of gas properties and pressure on single-bubble formation at an orifice," *Chemical Engineering Science*, Vol. 49, No. 9, Pg. 1429-1438

APPENDIX A

SAMPLE PLOTS OF MEASURED DATA AND MODEL FITS FOR BATCH MIXING EXPERIMENTS

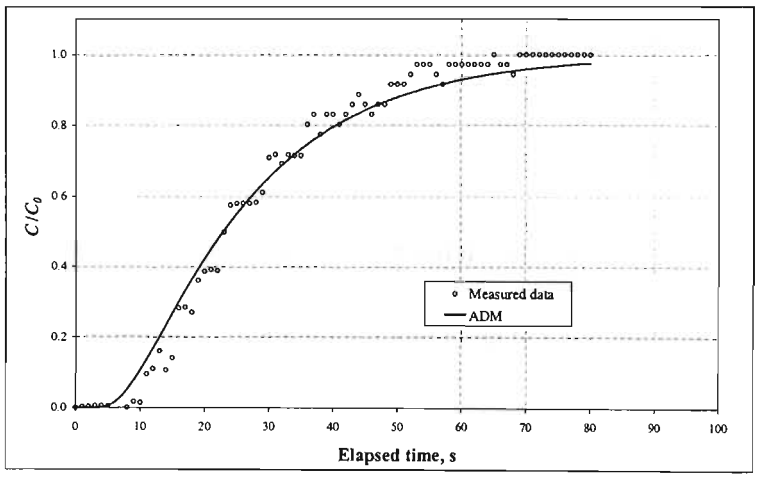

Figure A-1: Measured batch mixing data with SP10 in BC2 at u_g = 0.0743 cm/s, L = 188.6 cm, δ = 151.5 cm and ADM fit with a regressed E_L = 191 cm^2/s

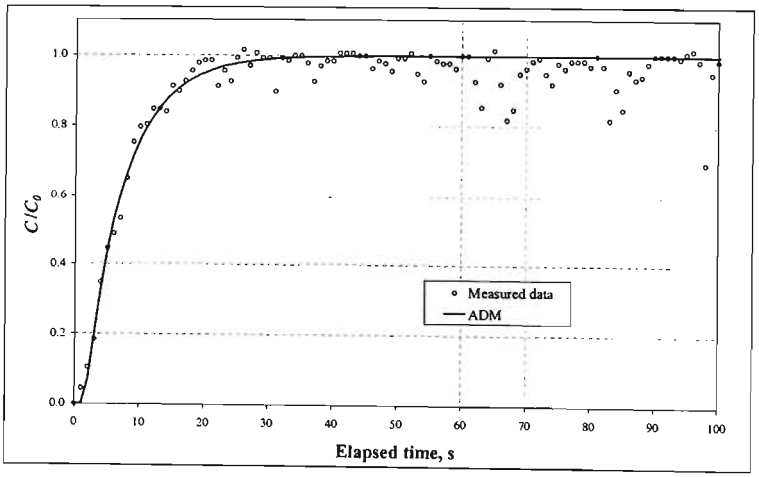

Figure A-2: Measured batch mixing data with SP8 in BC2 at u_g = 0.0743 cm/s, L = 110 cm, δ = 88 cm and ADM fit with a regressed E_L = 194 cm^2/s

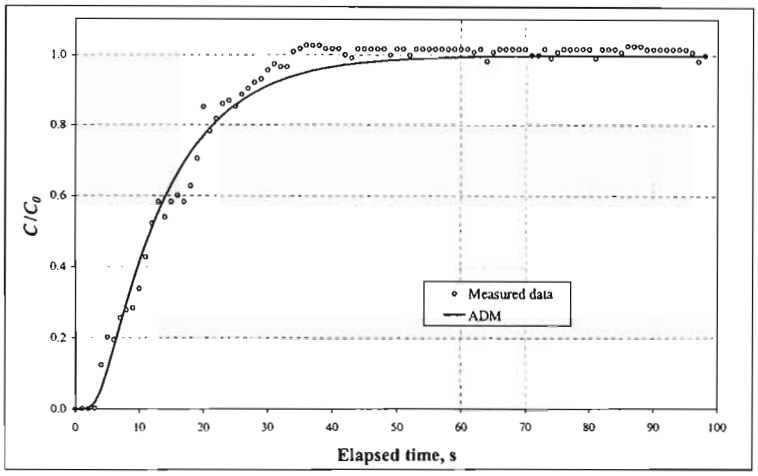

Figure A-3: Measured batch mixing data with SP8 in BC2 at u_g = 0.0743 cm/s, L = 150 cm, δ = 120 cm and ADM fit with a regressed E_L = 217 cm^2/s

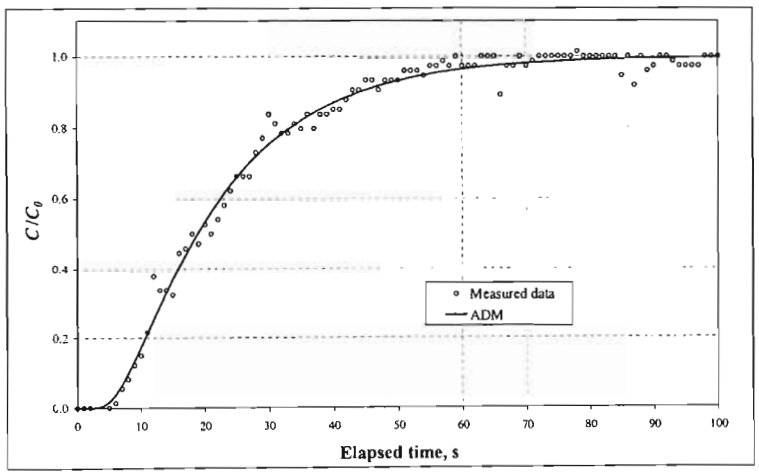

Figure A-4: Measured batch mixing data with SP10 in BC2 at u_g = 0.1509 cm/s, L = 188.6 cm, δ = 151.50 cm and ADM fit with a regressed E_L = 232 cm^2/s

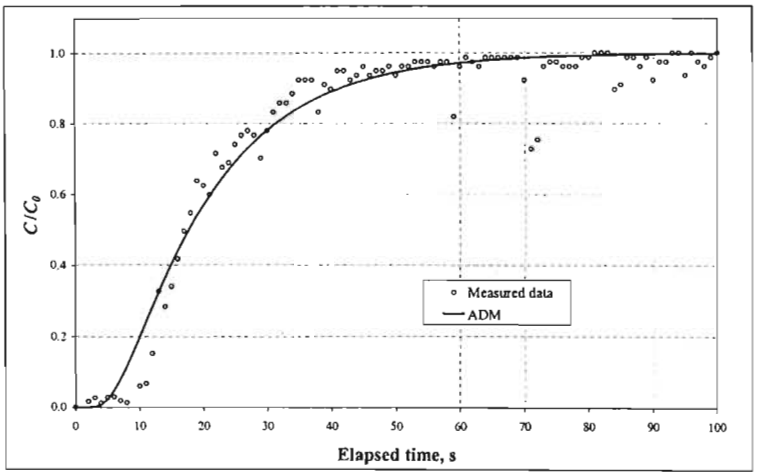

Figure A-5: Measured batch mixing data with SP10 in BC2 at u_g = 0.2304 cm/s, L = 189.2 cm, δ = 154.50 cm and ADM fit with a regressed E_L = 248 cm^2/s

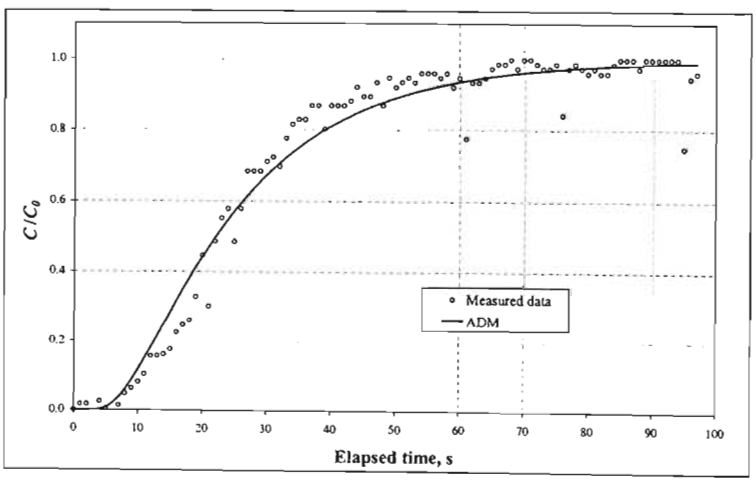

Figure A-6: Measured batch mixing data with SP10 in BC2 at u_g = 0.3127 cm/s, L = 188.3 cm, δ = 153.50 cm and ADM fit with a regressed E_L = 255 cm^2/s

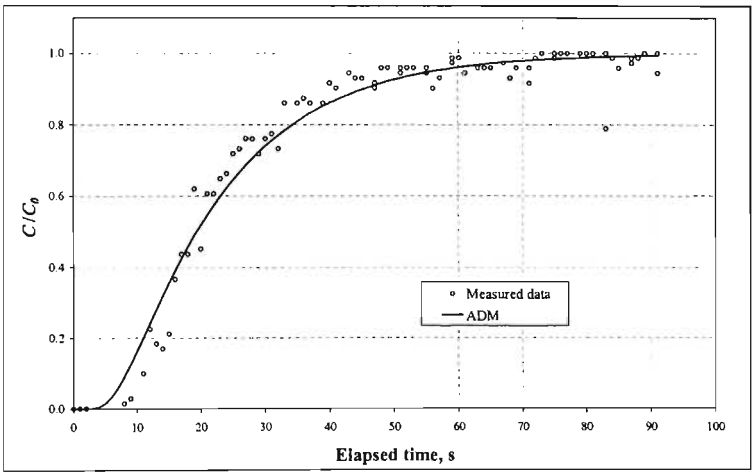

Figure A-7: Measured batch mixing data with SP10 in BC2 at u_g = 0.1509 cm/s, L = 189.1 cm, δ = 152.1 cm and ADM fit with a regressed E_L = 227 cm^2/s

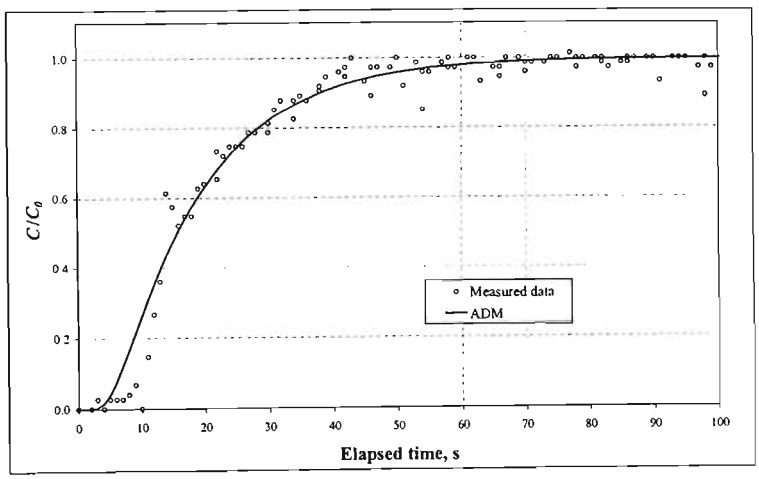

Figure A-8: Measured batch mixing data with SP10 in BC2 at u_g = 0.2304 cm/s, L = 189.0 cm, δ = 152 cm and ADM fit with a regressed E_L = 266 cm^2/s

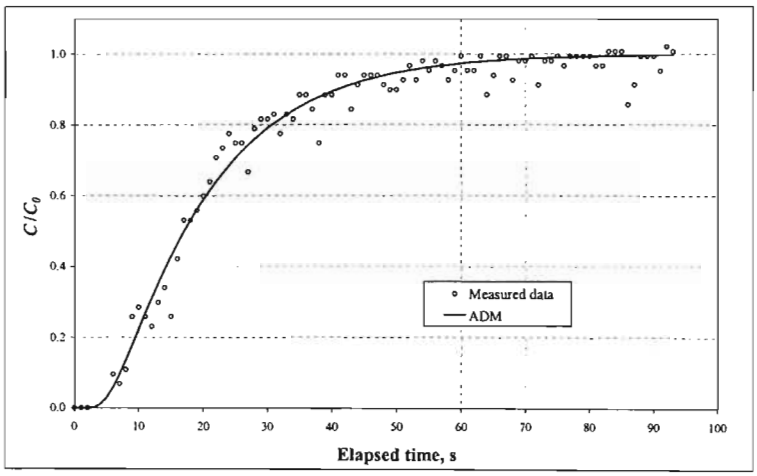

Figure A-9: Measured batch mixing data with SP10 in BC2 at u_g = 0.3127 cm/s, L = 188.2 cm, δ = 151.2 cm and ADM fit with a regressed E_L = 244 cm^2/s

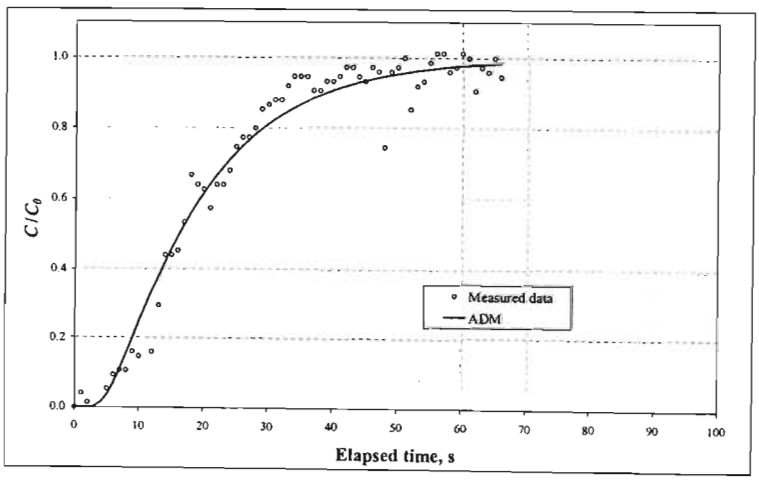

Figure A-10: Measured batch mixing data with SP10 in BC2 at u_g = 0.3978 cm/s, L = 188.0 cm, δ = 151.0 cm and ADM fit with a regressed E_L = 256 cm^2/s

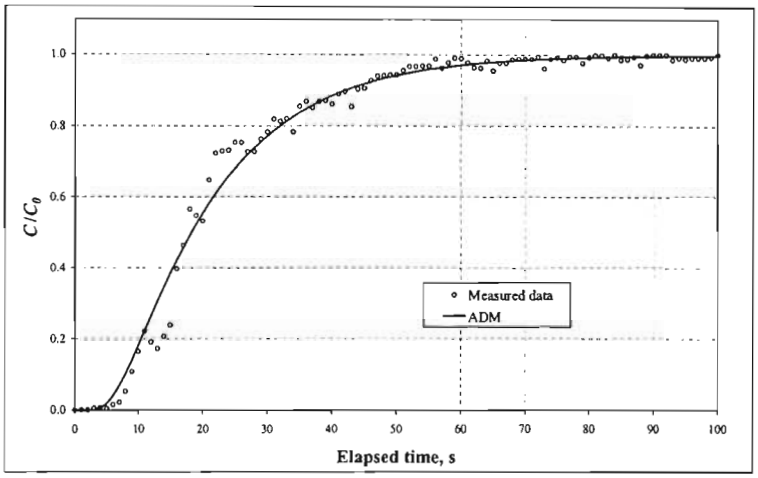

Figure A-11: Measured batch mixing data with SP2 in BC1 at u_g = 0.1381 cm/s, L = 170 cm, δ = 145 cm and ADM fit with a regressed E_L = 199 cm^2/s

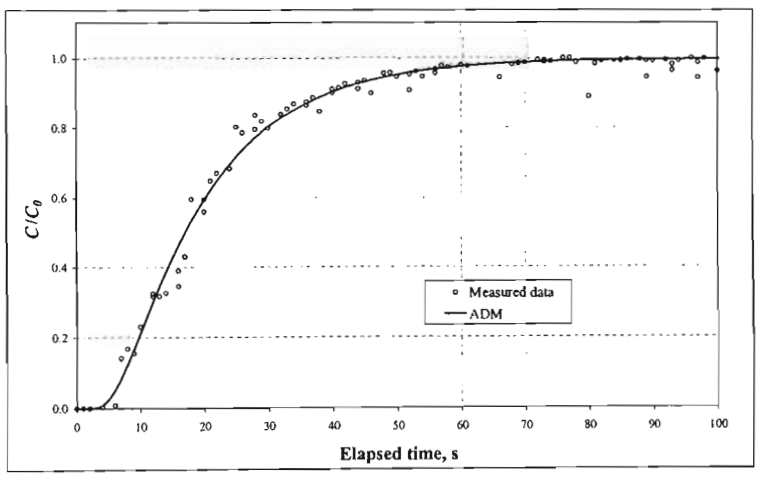

Figure A-12: Measured batch mixing data with SP2 in BC1 at u_g = 0.2807 cm/s, L = 170 cm, δ = 145 cm and ADM fit with a regressed E_L = 216 cm^2/s

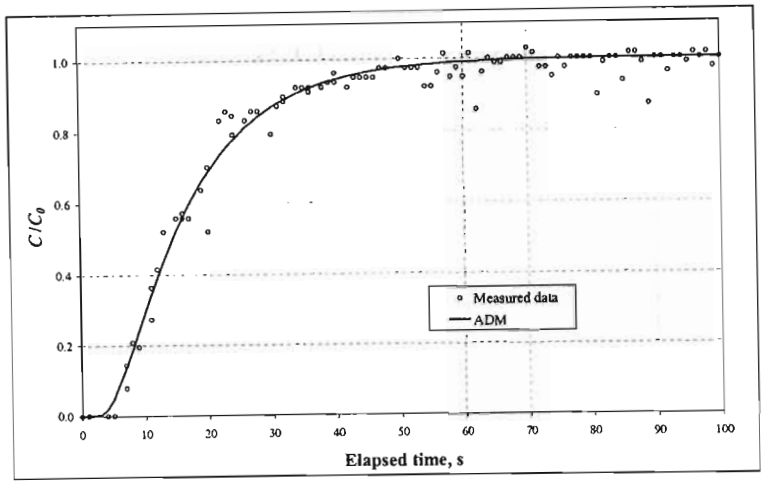

Figure A-13: Measured batch mixing data with SP2 in BC1 at u_g = 0.4284 cm/s, L = 170 cm, δ = 145 cm and ADM fit with a regressed E_L = 229 cm^2/s

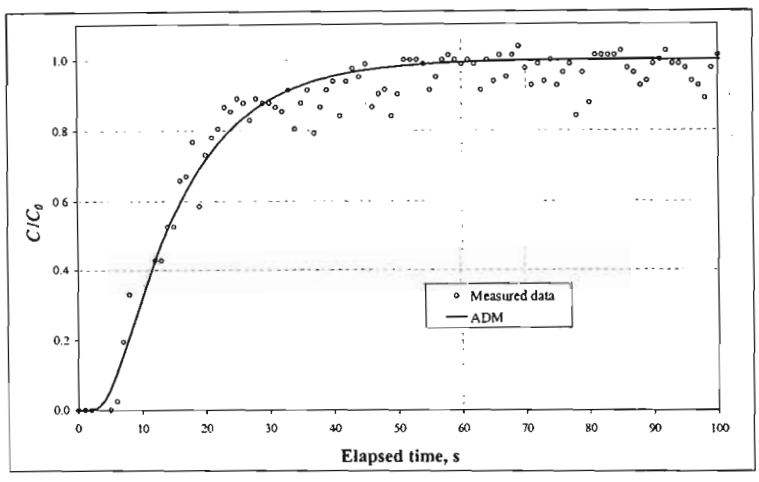

Figure A-14: Measured batch mixing data with SP2 in BC1 at u_g = 0.5814 cm/s, L = 170 cm, δ = 145 cm and ADM fit with a regressed E_L = 254 cm^2/s

APPENDIX B

SAMPLE PLOTS OF MEASURED DATA AND MODEL FITS FOR RTD EXPERIMENTS

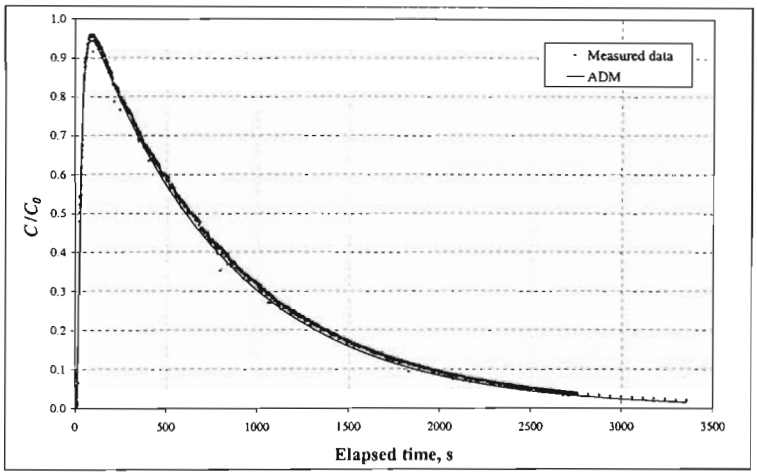

Figure B-1: Measured data with SP1 in BC1 at u_g = 0.1381cm/s, Q = 4 L/min, L = 170 cm and ADM fit with E_L = 146 cm^2/s

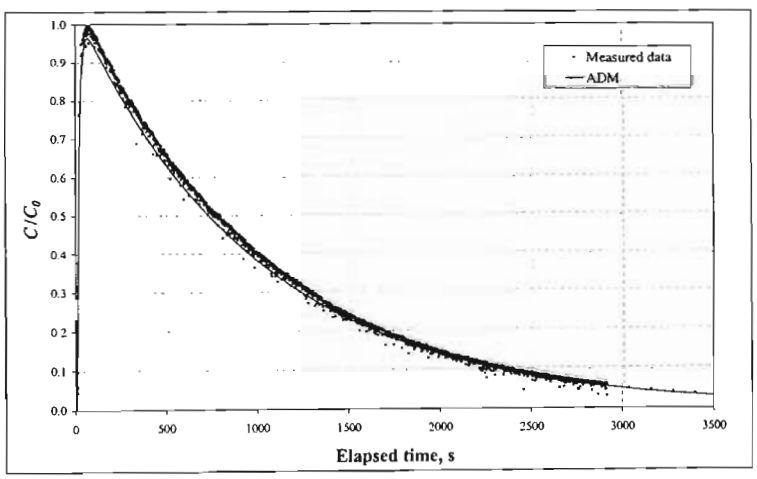

Figure B-2: Measured data with SP1 in BC1 at u_g = 0.2807 cm/s, Q = 4 L/min, L = 170 cm and ADM fit with E_L = 232 cm^2/s

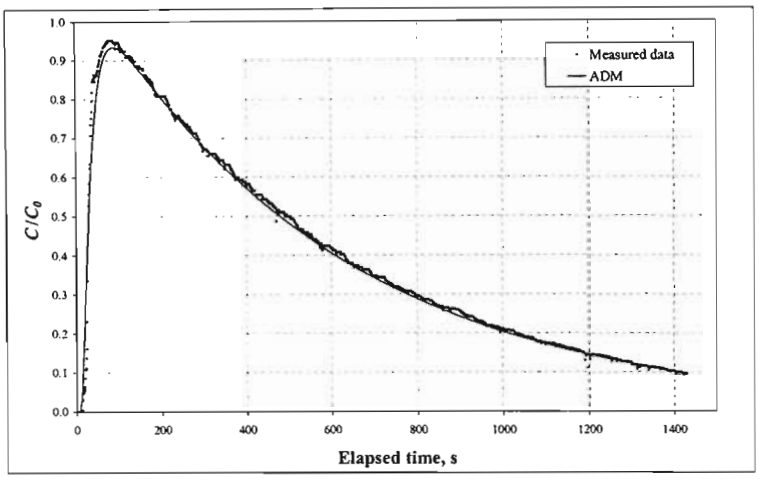

Figure B-3: Measured data with SP10 in BC2 at u_g = 0.0743 cm/s, Q = 13 L/min, L = 190 cm and ADM fit with E_L = 200 cm^2/s

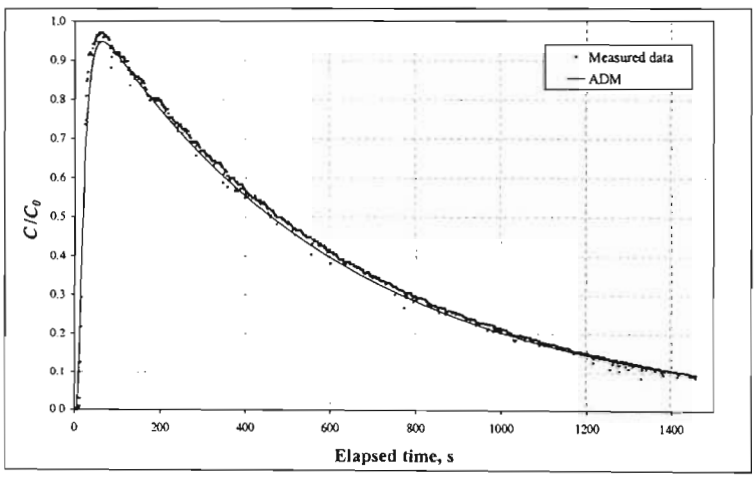

Figure B-4: Measured data with SP10 in BC2 at u_g = 0.1509 cm/s, Q = 13 L/min, L = 190 cm and ADM fit with E_L = 244 cm^2/s

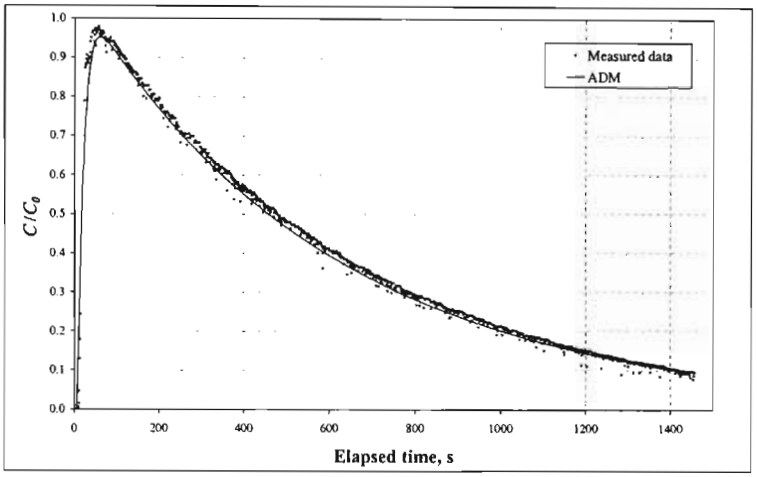

Figure B-5: Measured data with SP10 in BC2 at u_g = 0.2304 cm/s, Q = 13 L/min, L = 190 cm and ADM fit with E_L = 256 cm^2/s

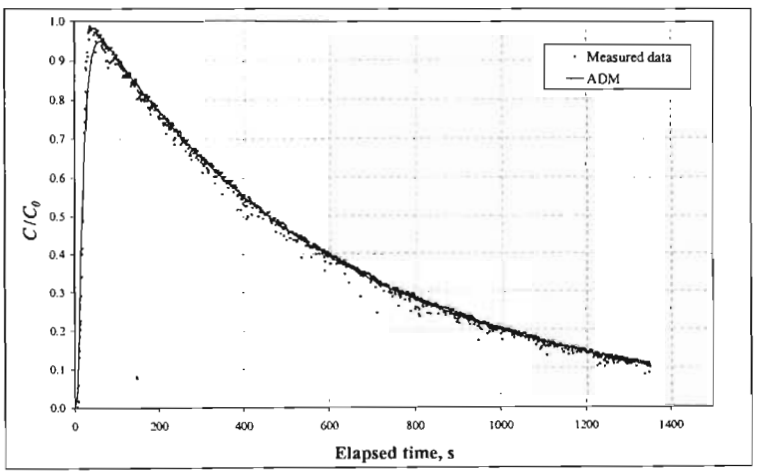

Figure B-6: Measured data with SP10 in BC2 at u_g = 0.3127 cm/s, Q = 13 L/min, L = 190 cm and ADM fit with E_L = 270 cm^2/s